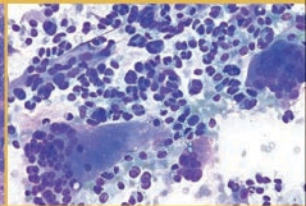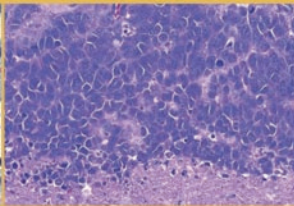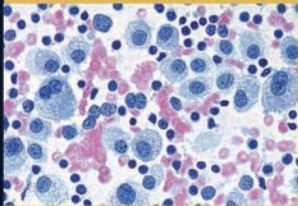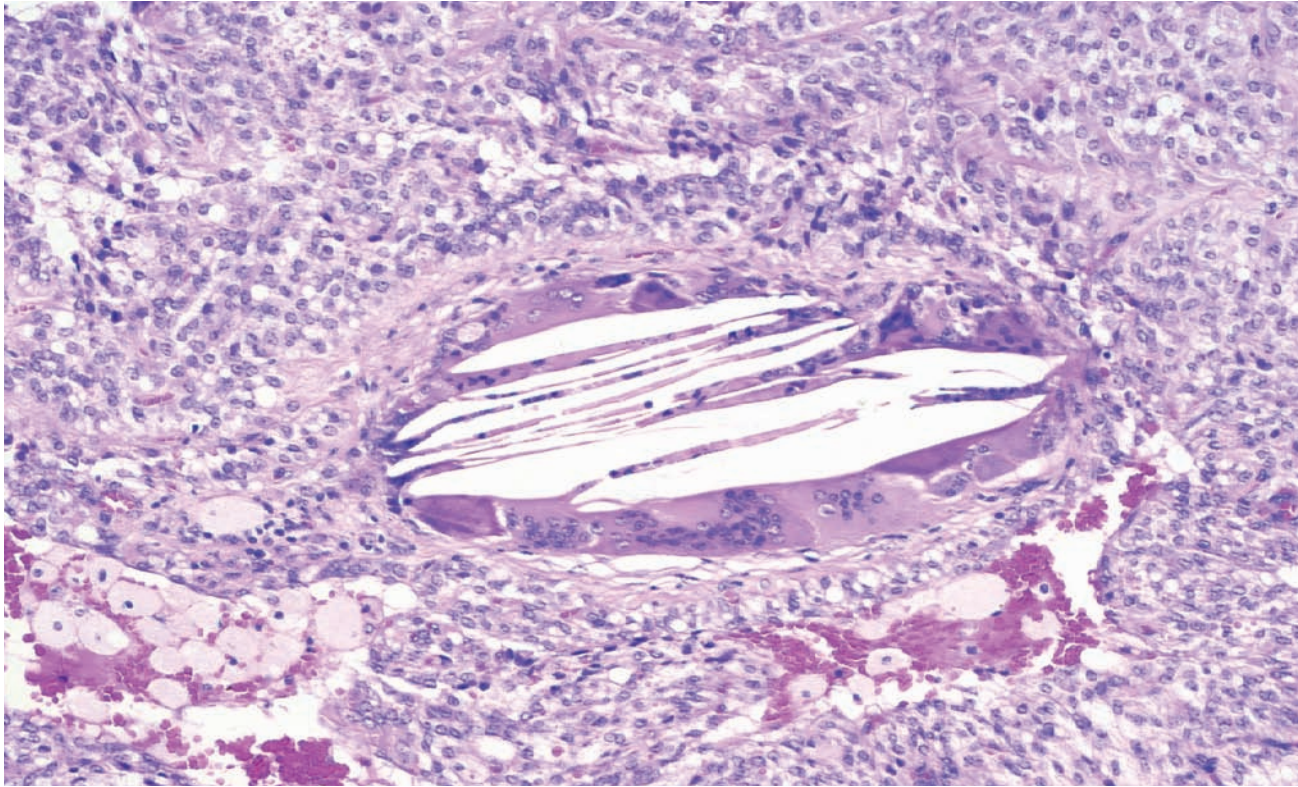# ATLAS OF

PANCREATIC CYTOPATHOLOGY

WITH HISTOPATHOLOGIC CORRELATIONS

SYED Z. ALI • YENER S. EROZAN • RALPH H. HRUBAN

demosMEDICAL

Atlas of Pancreatic Cytopathology

Syed Z. Ali, MD
Associate Professor of Pathology and Radiology
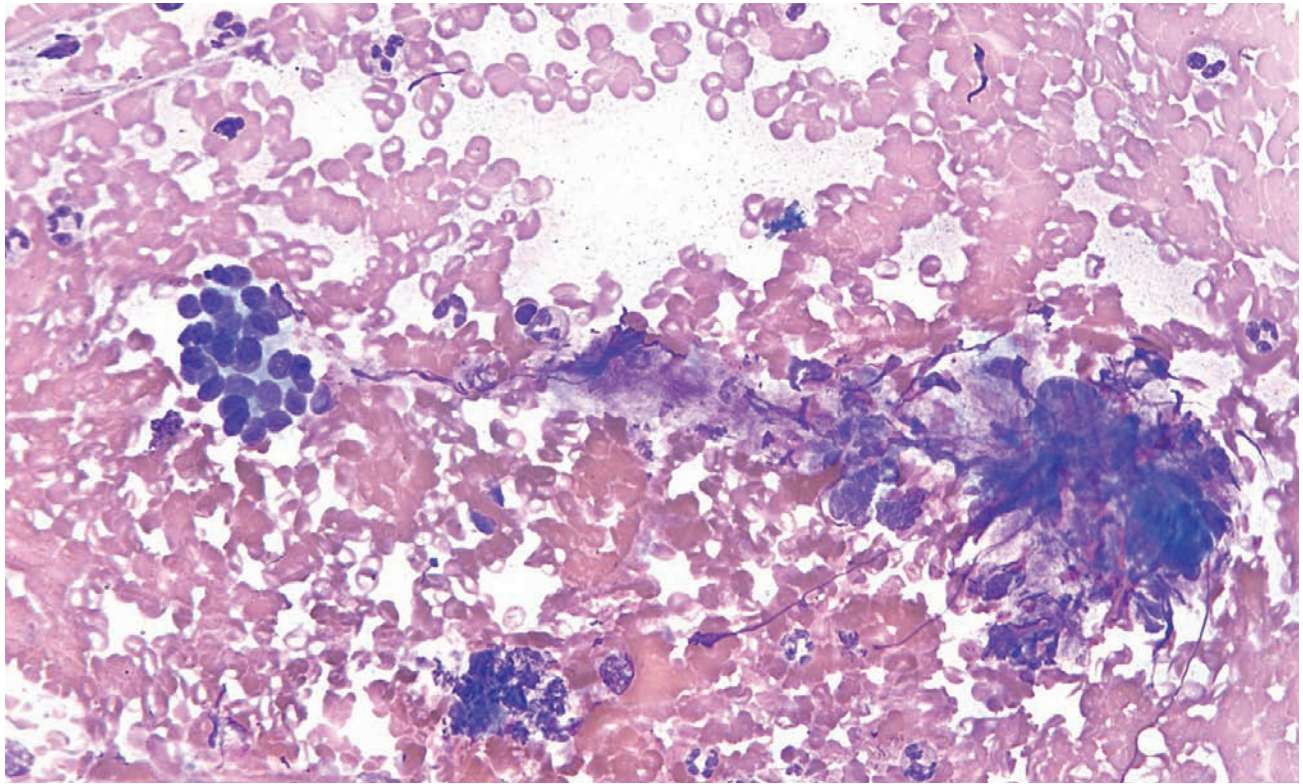The Sol Goldman Pancreatic Cancer Research Center

Yener S. Erozan, MD
Professor of Pathology
The Sol Goldman Pancreatic Cancer Research Center

Ralph H. Hruban, MD
Professor of Pathology and Oncology
The Sol Goldman Pancreatic Cancer Research Center

Department of Pathology
The Johns Hopkins University School of Medicine
Baltimore, Maryland

Atlas of Pancreatic Cytopathology

With Histopathologic Correlations

demosMEDICAL

Medicine is an ever-changing science. Research and clinical experience are continually expanding our knowledge, in particular our understanding of proper treatment and drug therapy. The authors, editors, and publisher have made every effort to ensure that all information in this book is in accordance with the state of knowledge at the time of production of the book. Nevertheless, the authors, editors, and publisher are not responsible for errors or omissions or for any consequences from application of the information in this book and make no warranty, express or implied, with respect to the contents of the publication. Every reader should examine carefully the package inserts accompanying each drug and should carefully check whether the dosage schedules mentioned therein or the contraindications stated by the manufacturer differ from the statements made in this book. Such examination is particularly important with drugs that are either rarely used or have been newly released on the market.

To our trainees—past and present.

Contents

Foreword

Diagnostic pathology, in general, and cytopathology, in particular, is in the process of rapid change as advances in technology have provided new tools to the clinician and the pathologist. These advances have significantly enhanced our ability to obtain and evaluate tissue and cellular specimens for the diagnosis and sub-classification of diseases. Nowhere has this been more evident than in the evaluation of patients with potential neoplastic entities. An obvious example of the contributions made by technological advances is in the area of fine needle aspiration biopsy. This technique has been used as a routine diagnostic modality since the 1970s. In recent years, however, its role has markedly expanded as advanced imaging technology and new instrumentation for obtaining samples has made virtually any body site accessible through minimally invasive methodologies. The significant increase in fine needle aspiration samples from the pancreas that has been experienced in most medical centers is a well-recognized example of this trend. Virtually all pancreatic mass lesions are sampled prior to definitive treatment. Although in the past such tumors were often sampled intra-operatively, biopsies are now usually obtained trans-abdominally utilizing ultrasound or computed tomography (CT) guidance. More recently endoscopic ultrasound guided needle biopsy has become the method of choice for many pancreatic lesions in numerous medical centers because it

offers some advantages over other techniques. These advantages include the ability to find and sample small lesions, which may be difficult to otherwise address as well as the opportunity to evaluate potentially, involved lymph nodes. In addition, the technique provides the means to visualize and guide the sampling in real-time under direct observation.

While these techniques have significantly improved the ability to obtain diagnostic material they present pathologists with new challenges and complexities in their quest for accurate interpretations. Differential diagnoses can be complicated by such issues as contaminating cells and mucus from the gastrointestinal tract or by cells obtained inadvertently from adjacent tissues. Well differentiated neoplasms, particularly low-grade mucinous lesions of the pancreas, can be very difficult to distinguish from contaminating material from the gastrointestinal tract in these types of samples. In addition, unusual neoplasms that many pathologists may have had little or no experience with in cytologic samples because they previously were rarely sampled are now diagnostic considerations.

Fortunately, this well written and superbly illustrated atlas provides a welcome solution to many of these and related issues. Drs. Ali, Erozan, and Hruban present a comprehensive and detailed, yet succinct, summary of pancreatic cytopathology and its histopathology correlates. A nicely prepared,

informative overview of the radiologic features of pancreatic disease contributed by Dr. Sheth provides a worthy complement to the comprehensive coverage of the pathology. The heart of this text consists of outstanding, well chosen illustrations depicting the cytologic features and the histologic correlates of the spectrum of pancreatic lesions. These are accompanied by excellent discussions of the cytologic characteristics emphasizing the diagnostic criteria and potential pitfalls associated these entities. Drs. Ali, Erozan, and Hruban share their wealth of experience and widely recognized expertise with the reader in a manner that is both educational and enjoyable. Virtually all of the entities one is likely to encounter are covered in a well-arranged presentation that

readers will find to be both practical and easy to use in their day-to-day work. Although there are other excellent references available on the topic I do not know of any that will better fulfill the needs of both pathologists who are experienced with pancreatic cytopathology and those who are new to the field. The reader will be very appreciative of being able to learn from the extensive experience of these expert pathologists and the wealth of material from the Johns Hopkins Department of Pathology that they share with us in this work.

Thomas A. Bonfiglio, MD
Professor, Pathology and Laboratory Medicine
University of Rochester Medical Center

Preface

Cytopathology enjoys a unique position in diagnostic medicine; it interacts closely with all major areas of clinical medicine early in the course of a patient's disease. Diseases of the pancreas are no exception. Although pancreatic cytopathology is fraught with diagnostic pitfalls, an integrated approach to establishing a diagnosis, incorporating an understanding of cytopathology, surgical pathology, and radiology, paves the road to the correct diagnosis. The gross and radiologic characteristics of the lesion help the cytopathologist narrow the differential diagnosis, and a sound knowledge of the histopathologic features is needed to appreciate the full spectrum of changes that can be seen in fine needle aspirations of the pancreas.

This atlas presents an integrated multidisciplinary approach to diagnostic cytopathology. Experts from cytopathology, radiology, and surgical pathology provide a wealth of diagnostic information for a wide audience. Cytotechnologists, increasingly involved in on-site evaluation of pancreatic fine needle aspiration, as well as pathology trainees, general and surgical pathologists, and the most seasoned of cytopathologists, will all benefit from this atlas.

This publication is not intended to replace a good general textbook, but to supplement theoretical knowledge by presenting visual images of the characteristic features of the various diseases discussed. The book begins with a chapter on the normal pancreas, followed by a chapter on radiologic images. This later chapter illustrates salient features of selected lesions without added mundane information for the nonradiology reader. Each subsequent chapter is introduced by gross and histopathologic images, enabling the reader to adequately appreciate tissue architectural features in a fine needle aspiration specimen.

Over 450 high-resolution images were selected from the authors' practice at The Johns Hopkins Hospital. "Classic" features and diagnostic clues are illustrated with image and text legend, paying special attention to cyto-histologic correlation of the various entities. Carefully worded, detailed figure legends describe the most important features presented by the images and elaborate on the differential diagnoses and potential pitfalls.

The authors would like to acknowledge the contributions of several individuals in the preparation of this book. Dr. Sheila Sheth condensed
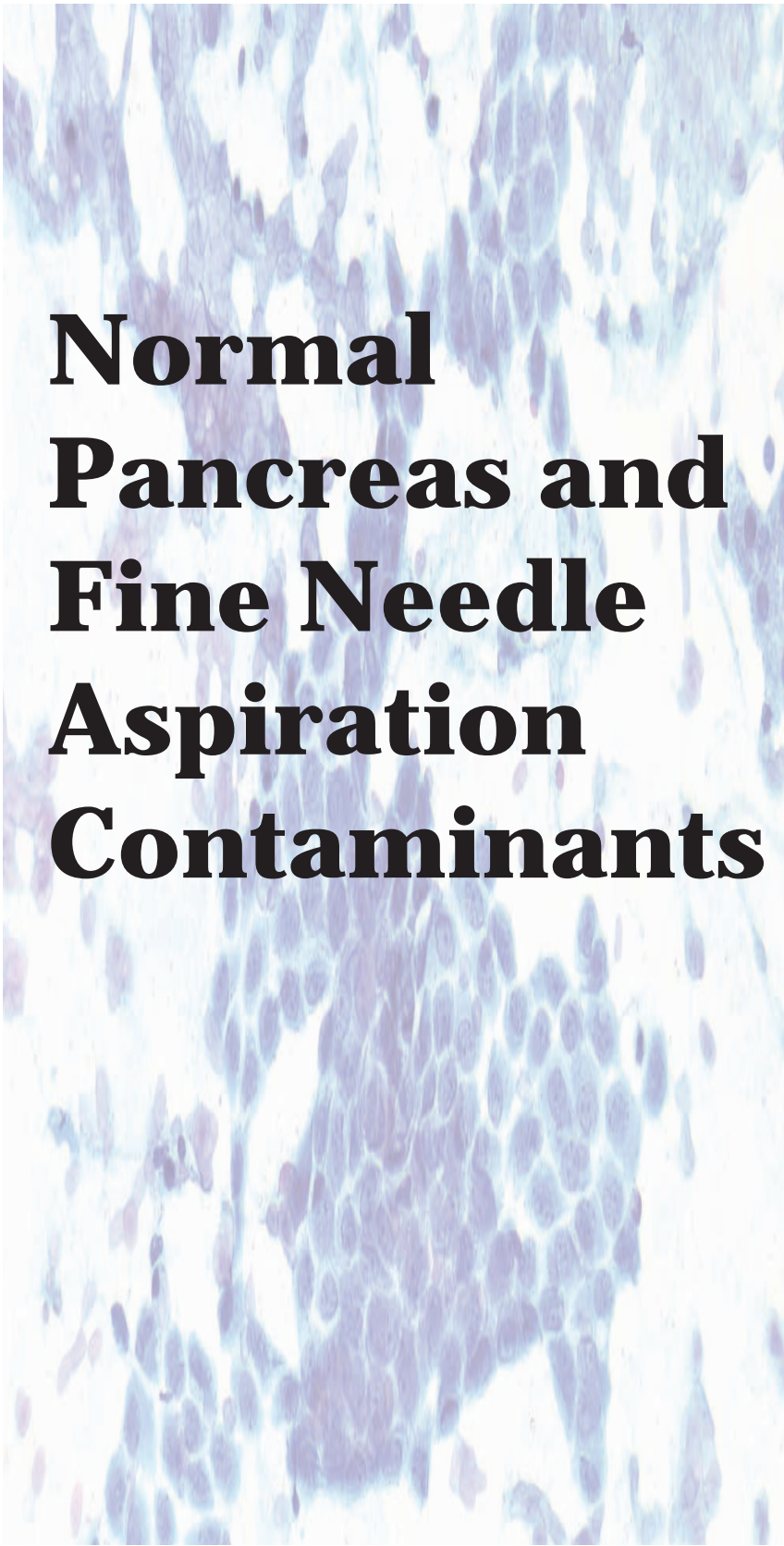
a large amount of information into a small, easily readable chapter on radiologic characteristics. Fran Burroughs, SCT (ASCP), coordinated retrieval of the cytopathology materials used for illustration and Ms. Sandra Markowitz provided excellent secretarial help. The faculty, technical staff, and residents/fellows in pathology were all instrumental in case identification. Finally, we would like to extend our appreciation to Richard Winters, senior medical editor at Demos Medical Publishing, whose guidance, encouragement, and patience helped us successfully complete the book.

The authors acknowledge the family of Sol and Lillian Goldman for their clear-sighted vision and philanthropy.

It is our hope that the users of this atlas will develop a visual understanding of pancreatic pathology as viewed through a number of different lenses—CT, gross, histopathologic and cytopathologic.

Syed Z. Ali
Yener S. Erozan
Ralph H. Hruban

Atlas of Pancreatic Cytopathology

Normal Pancreas and Fine Needle Aspiration Contaminants

1

Normal Pancreatic Tissue

Figure 1.1 — Normal pancreatic tissue—ductal epithelium. This monolayered epithelial tissue fragment has the "honeycomb" appearance characteristic of nonneoplastic glandular/ductal-type epithelium. Some peripheral palisading of the nuclei is evident at the top and the bottom of the fragment. (Papanicolaou stain, low power)
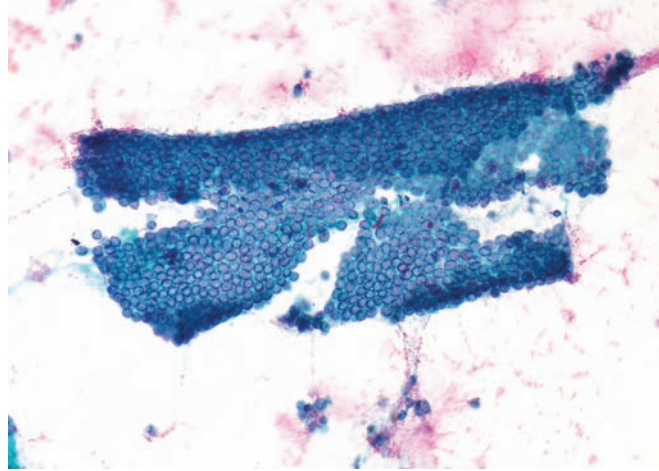

Figure 1.2 — Normal pancreatic tissue—ductal epithelium. The tissue fragment is similar to that depicted above. Note the uniform round-to-oval nuclei with fine chromatin and smooth nuclear membrane. There is minimal overlapping of the nuclei. The smear background is clean and no single dispersed cells are noted. (Papanicolaou stain, low power)
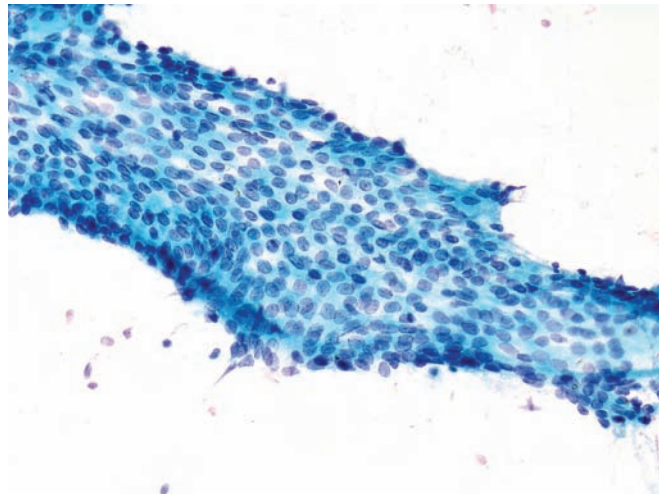
Figure 1.3 — Normal pancreatic tissue—ductal epithelium. Cells display minimal nuclear enlargement with inconspicuous nucleoli. Occasional nuclei are elongated and focally stratified, which is entirely normal and should not be labeled "atypical." (Papanicolaou stain, medium power)
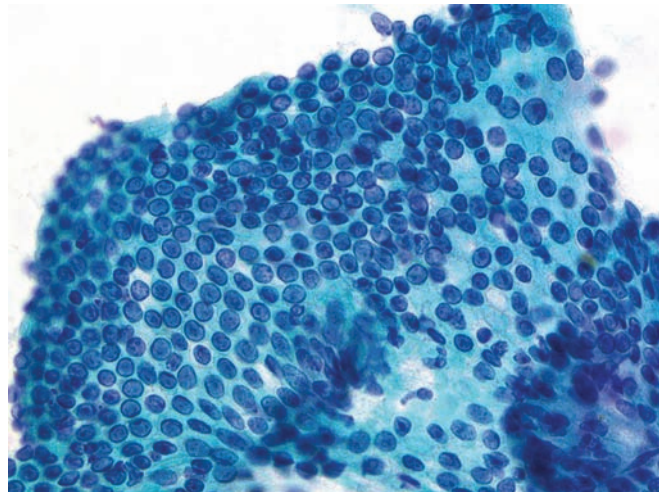
Normal Pancreatic Tissue
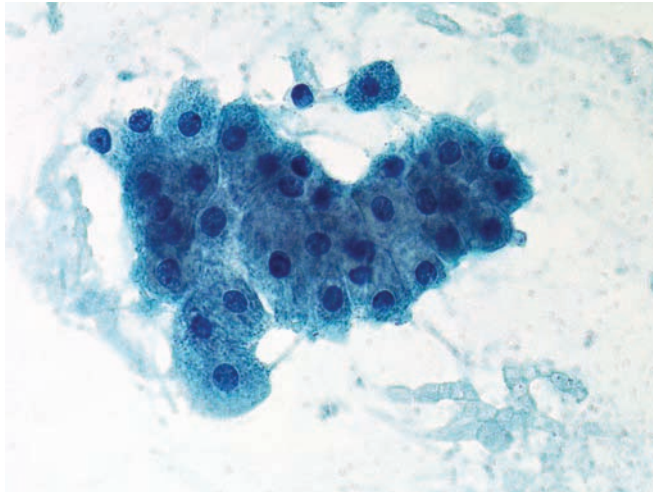
Figure 1.4 — Normal pancreatic tissue—acinar epithelium. Acinar cells have uniform, round nuclei with occasional single prominent nucleoli and moderate to abundant granular cytoplasm. Note the relatively larger cell size compared to ductal epithelium. The nuclear to cytoplasmic (N/C) ratio remains low. (Papanicolaou stain, high power)
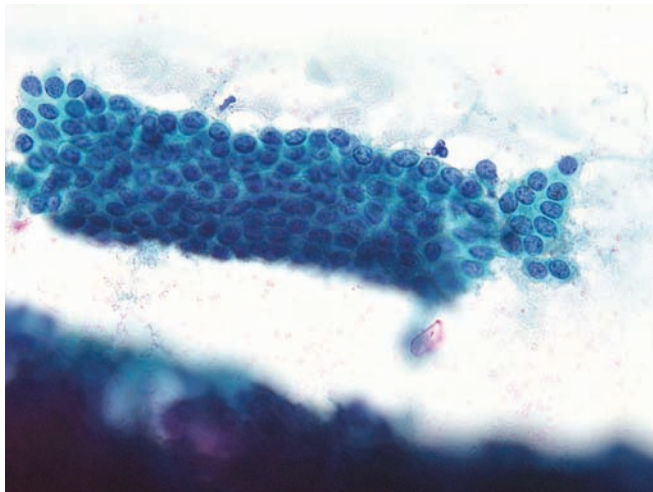

Figure 1.5 — Normal pancreatic tissue—ductal epithelium. This monolayer tissue fragment with a tubular "duct-like" architecture composed of uniform epithelial cells is organized in an orderly fashion (honeycomb pattern). The N/C ratio is relatively increased but still well within normal limits. (Papanicolaou stain, high power)
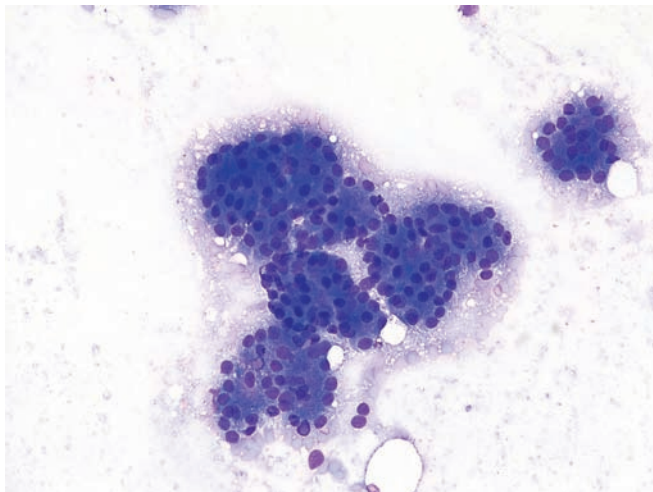
Figure 1.6 — Normal pancreatic tissue—acinar epithelium. These uniform acinar formations are lined with uniform cells with monotonous round nuclei and moderate amounts of densely granular, basophilic cytoplasm. The typical "bunches of grape-like" appearance, a hallmark of normal acinar differentiation, is retained. The differential diagnosis, in addition to a well-differentiated acinar cell carcinoma, would include normal pancreatic islets of Langerhans and a well-differentiated endocrine neoplasm (islet cell tumor). (Diff Quik stain, medium power)

Normal Pancreatic Tissue

Figure 1.7 — Normal pancreatic tissue—acinar epithelium. These acinar cells arranged singly and in small groups. The cells have uniform, round to ovoid nuclei with delicate, finely vacuolated cytoplasm. Because the cell membranes are often disrupted when these cells are smeared, the smear background often assumes a fine, bubbly appearance. These cells should not be confused with a "clear cell" neoplasm or a well-differentiated acinar cell carcinoma as the "bunches of grape-like" appearance is focally retained (at 3 and 9 o'clock). (Diff Quik stain, medium power)
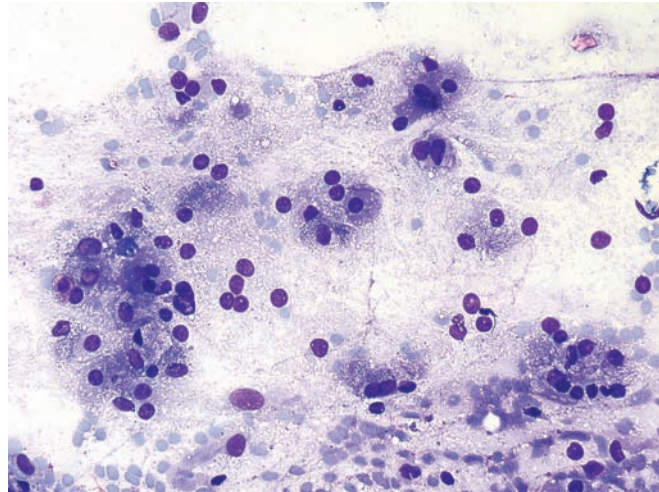
Figure 1.8 — Normal pancreatic tissue—acinar epithelium. Large tissue fragments are composed of small uniform acini. The cytoplasm is densely granular, and numerous "naked" or "stripped-off" nuclei are visible in the smear background. (Diff Quik stain, low power)
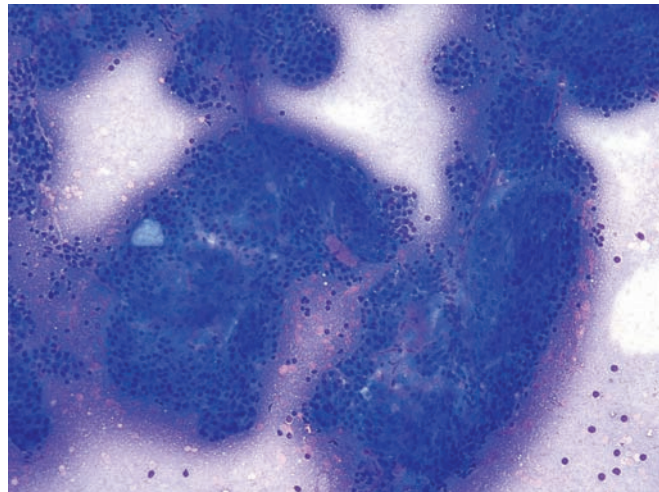
Figure 1.9 — Normal pancreatic tissue—acinar epithelium. A large tissue fragment similar to that in the previous image is seen. The smear shows abundant blood and a small fragment of nerve tissue at 1 o'clock. Large acinar tissue framents are not unusual in a pancreatic aspirate and should not be confused with a well-differentiated acinar cell carcinoma. The presence of distinct lobules (as opposed to solid sheets) helps in the diagnosis of benign pancreatic acinar tissue. (Papanicolaou stain, low power)
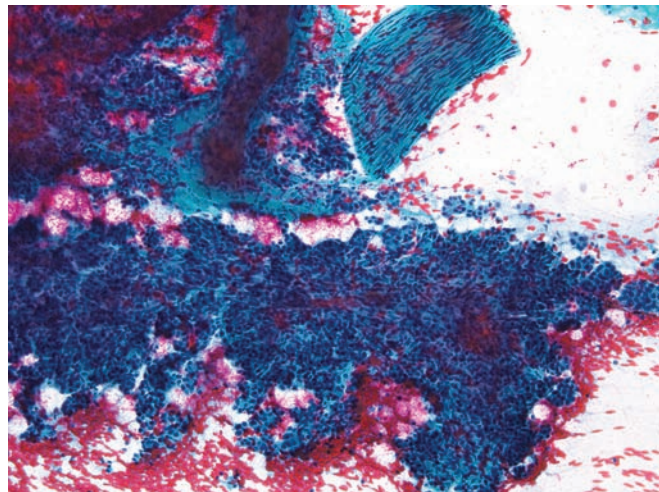
Normal Pancreatic Tissue
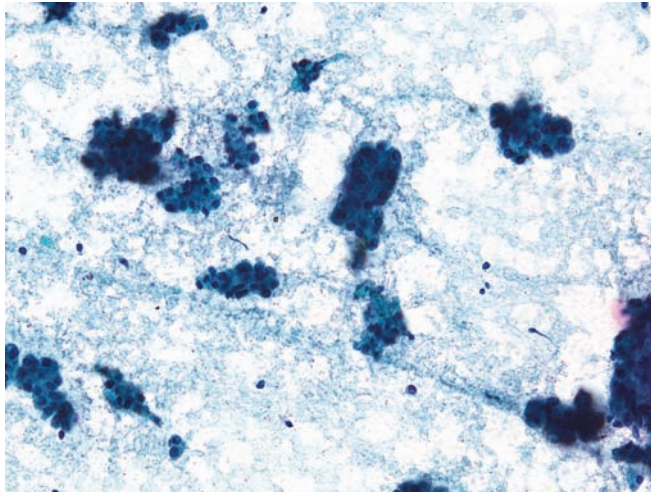
Figure 1.10 — Normal pancreatic tissue—serous acinar epithelium. These almost equi-sized acinar structures are formed by uniform cuboidal cells with basally located, round nuclei. A well-differentiated pancreatic endocrine neoplasm typically shows more dyshesion with single cells. (Papanicolaou stain, medium power)
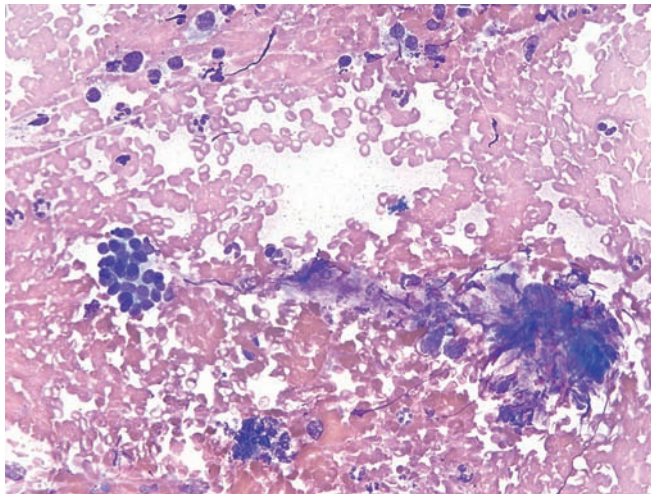

Figure 1.11 — Normal pancreatic tissue—islet of Langerhans. This aspirate from a patient with chronic pancreatitis contains a small partially intact islet (9 o'clock) associated with focal fibrosis. Normal islets are rarely seen in pancreatic aspirates except in cases of chronic pancreatitis where the endocrine cells aggregate. (Diff Quik stain, low power)

Normal Gastrointestinal Tract Contamination

Figure 1.12 — Normal gastrointestinal tract contamination (transduodenal EUS-guided FNA)— duodenal epithelium and mucin. This cellular smear is composed of a monolayer fragments of columnar epithelium and background mucinous material. Numerous stripped nuclei give this smear a "busy" look. The differential diagnosis includes intraductal papillary mucinous neoplasm and cystic mucinous neoplasm of the pancreas. (Papanicolaou stain, low power)
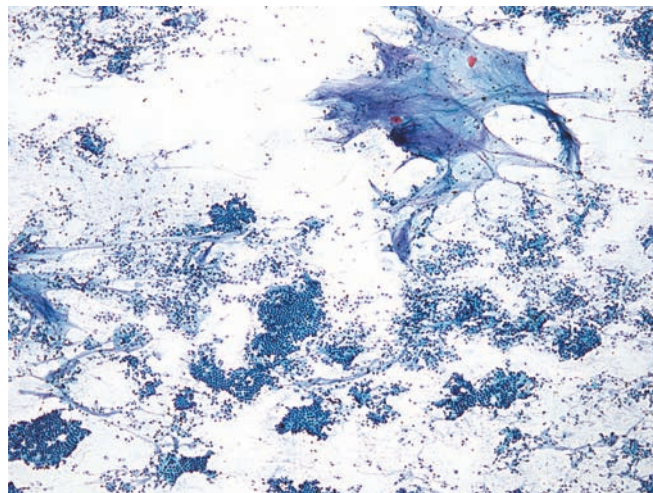
Figure 1.13 — Normal gastrointestinal tract contamination (transduodenal EUS-guided FNA). A large enface tissue fragment is composed of intestinal-type epithelium with monolayered columnar cells and interspersed goblet cells. An FNA comprised solely of such contaminating cells should be called "nondiagnostic" or "insufficient." Correlation with radiologic findings should be advised particularly if a neoplastic process is still suspected after the procedure. (Papanicolaou stain, low power)
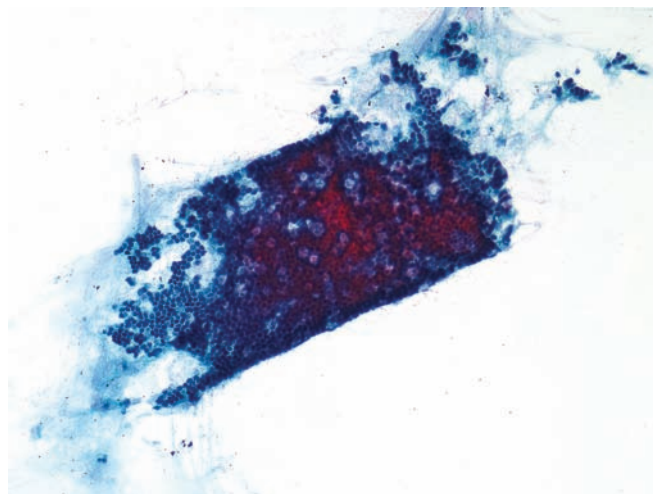
Figure 1.14 — Normal gastrointestinal tract contamination (transduodenal EUS-guided FNA). This monolayer of columnar epithelium contains goblet cells. Note the villous-like architecture on the left-hand side. The distinction of normal gastrointestinal tract contamination from pancreatic ductal epithelium can be extremely difficult and occasionally impossible in such cases. (Papanicolaou stain, low power)
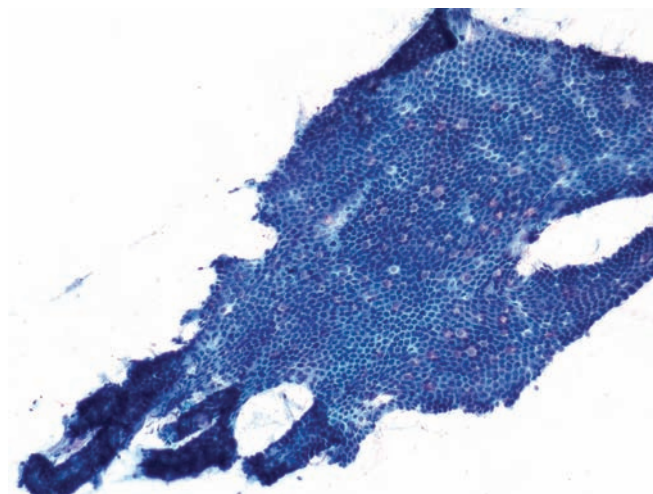
Normal Gastrointestinal Tract Contamination

Figure 1.15 — Normal gastrointestinal tract contamination (transduodenal EUS-guided FNA). This field contains a large fragment of intestinal epithelium with numerous goblet cells and a prominent villous architecture. Peripheral palisading of the nuclei is clearly evident. Such structures should not be confused with the papillary architecture of an intraductal papillary mucinous neoplasm. (Papanicolaou stain, low power)
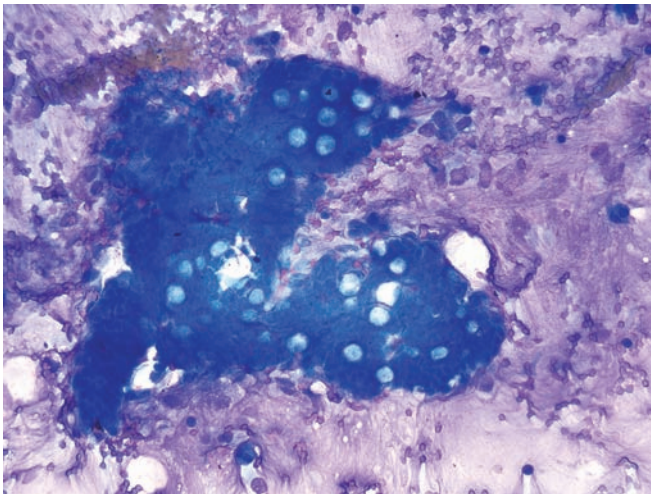
Figure 1.16 — Normal gastrointestinal tract contamination (transduodenal EUS-guided FNA). This large fragment of intestinal epithelium contains numerous goblet cells in a densely mucinous background. An accurate recognition of goblet cells (often involving changing the planes of focus) is extremely important. (Diff Quik stain, low power)
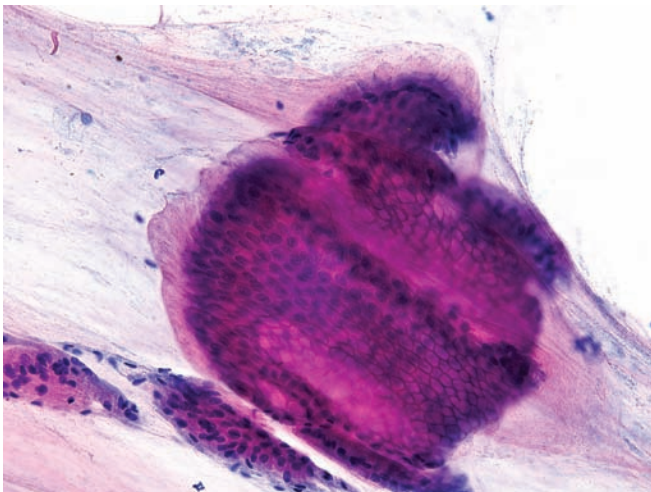
Figure 1.17 — Normal gastrointestinal tract contamination (transgastric EUS-guided FNA). This mucinous glandular epithelium has clear pale pink cytoplasm. When abundant, such tissue fragments in an aspirate may be confused with mucinous neoplasm of the pancreas, particularly when the patient has a cystic lesion. (Papanicolaou stain, low power)

Normal Gastrointestinal Tract Contamination

Figure 1.18 — Normal gastrointestinal tract contamination (transgastric EUS-guided FNA). This monolayered glandular fragment displays cells with abundant mucinous cytoplasm. The nuclei are small, uniform and mostly centrally placed. A small projection of the epithelial cells towards the top gives this fragment a "papillary-like" appearance. Gastric-type epithelium in pancreatic aspirates can be extremely difficult to differentiate from mucinous neoplasms due to significant morphologic overlap and may lead to an overinterpretation on EUS-guided FNA. (Papanicolaou stain, medium power)
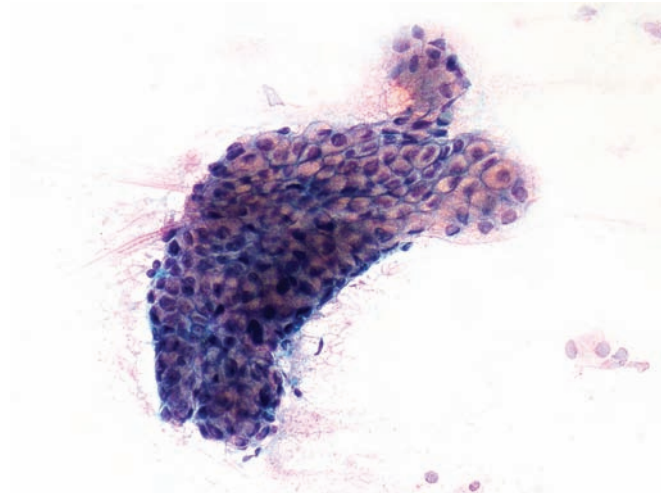
Contaminating Mesothelium
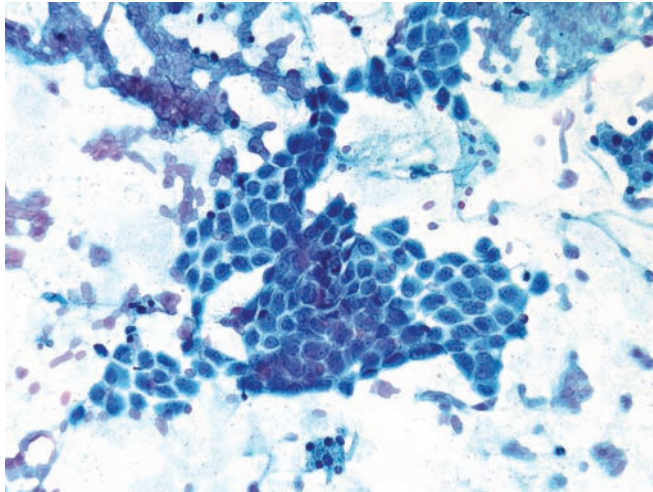
Figure 1.19 — Contaminating mesothelium (CT-guided transabdominal FNA). This monolayered tissue fragment is composed of epithelioid cells with uniform, centrally located, round-to-ovoid nuclei and moderate cytoplasm. This morphology is similar to that of sheets of mesothelial cells commonly seen in pelvic washings or in transthoracic fine needle aspirations. These cells should not be confused with glandular epithelium of the pancreas as this may lead to an erroneous "atypical" diagnosis. (Papanicolaou stain, medium power)
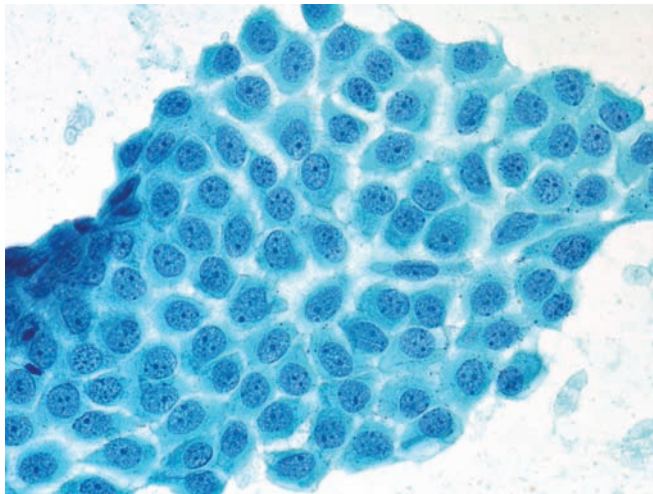
Figure 1.20 — Contaminating mesothelium (CT-guided transabdominal FNA). This sheet of cells is composed of benign mesothelial cells. Nuclei are round or ovoid with uniform "vesicular" chromatin, small chromocenters, and micronucleoli. The cells have a moderate amount of cytoplasm. Numerous desmosomal junctions can be seen in the clear spaces among the cells, so called "cell windows." An accurate distinction from ductal epithelium can be easily achieved if the possibility of mesothelial contamination is kept in mind in transabdominal FNAs. (Papanicolaou stain, high power)
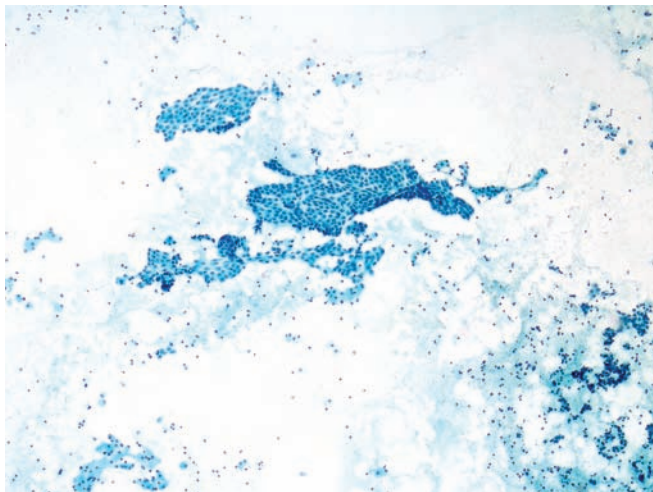
Figure 1.21 — Contaminating mesothelium (CT-guided transabdominal FNA). Numerous monolayered tissue fragments and single discohesive cells are interspersed with occasional glandular cells. A flat monolayered appearance is quite evident even at this low magnification. (Papanicolaou stain, low power)

Contaminating Mesothelium

Figure 1.22 — Contaminating mesothelium (CT-guided transabdominal FNA). This cellular aspirate contains a large folded monolayer tissue fragment imparting a crowded look which led to an "atypical" diagnosis in this case. Note a total lack of 3-dimensional glandular appearance or an acinar cell differentiation. Mesolthelial cells are often seen as large fragments or "sheets" when they contaminate a traversing needle. (Papanicolaou stain, low power)
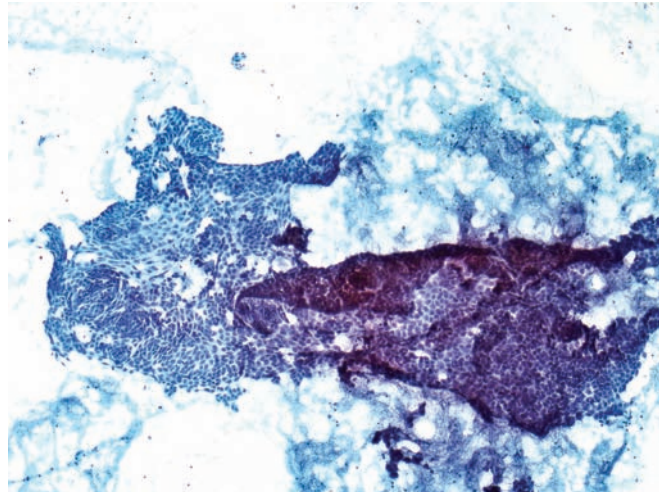
Normal Liver Contamination
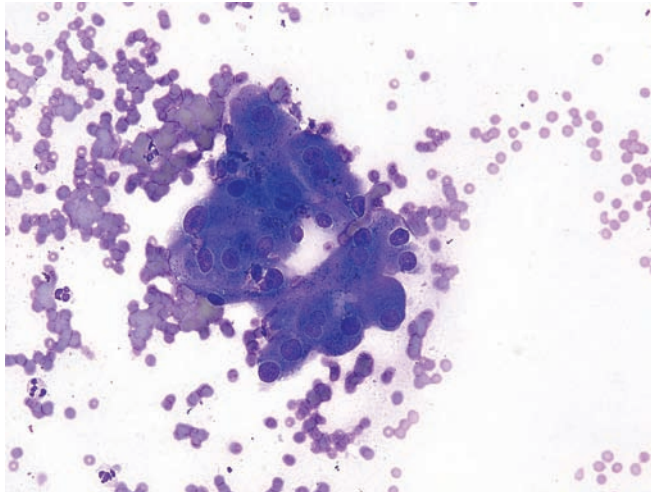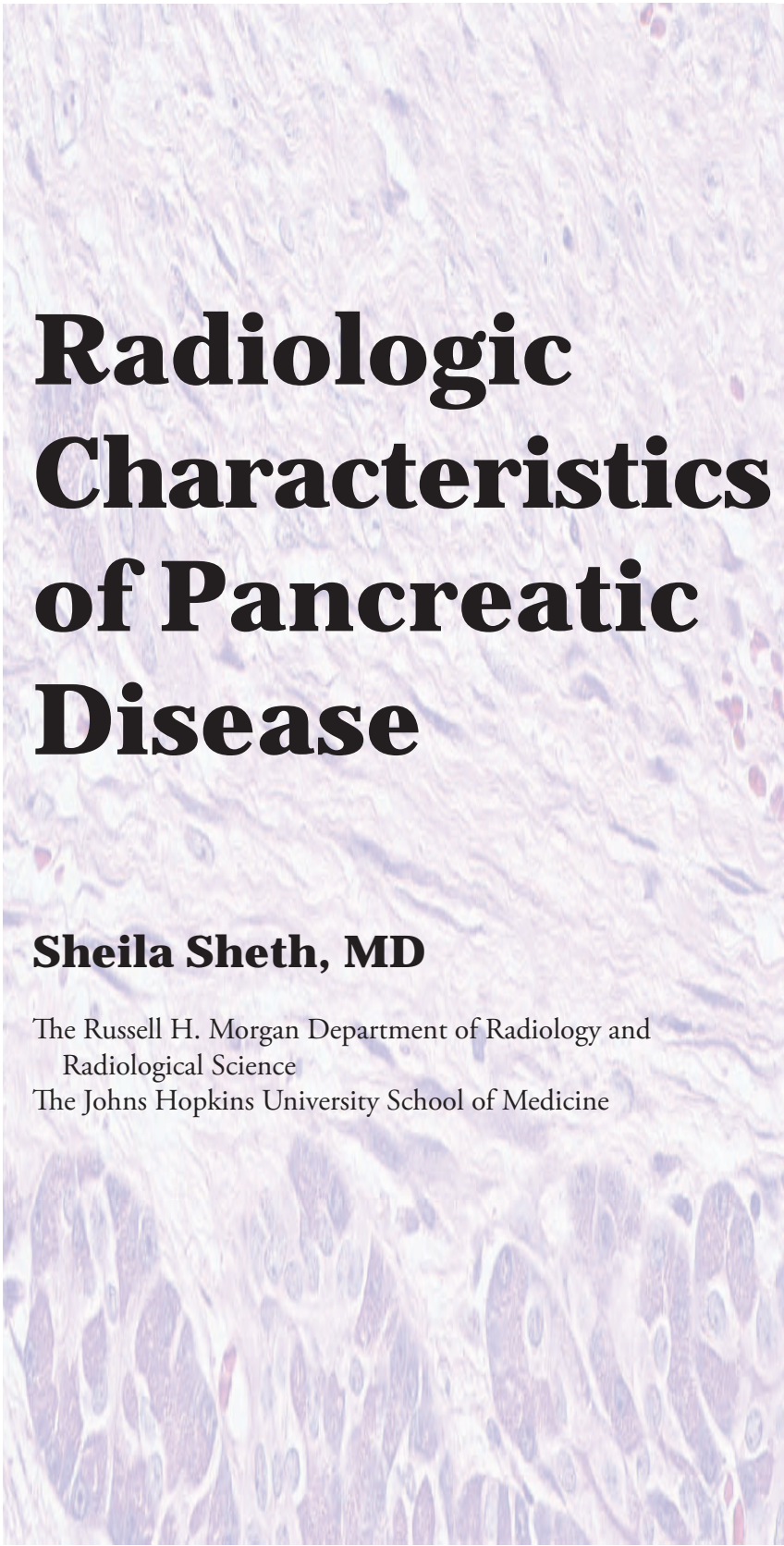
Figure 1.23 — Normal liver contamination (CT-guided transabdominal FNA). These benign hepatocytes contain round, uniform nuclei, conspicuous nucleoli, and relatively abundant granular cytoplasm. These cells contain intracytoplasmic pigment consistent with bile. Differential diagnosis would include normal and neoplastic acinar epithelium and, rarely, a metastatic hepatocellular carcinoma to the pancreas. Contamination by liver is unusual but may occur in aspirations of a pancreatic head mass. (Diff Quik stain, high power)

Radiologic Characteristics of Pancreatic Disease

2

Sheila Sheth, MD

The Russell H. Morgan Department of Radiology and
  Radiological Science
The Johns Hopkins University School of Medicine

Synopsis

Computed tomography (CT) with intravenous contrast remains the imaging modality of choice in the evaluation of patients with suspected pancreatic abnormality. At our institution, we acquire dual-phase images in the arterial and portal venous phase of enhancement and routinely perform coronal and sagittal reconstruction. This approach can be used to not only diagnose and characterize pancreatic neoplasms but also to evaluate associated findings that are critical for patient management and to determine surgical resectability. Careful evaluation for arterial or venous encasement, liver metastases, invasion of the stomach or duodenum, and findings such as ascites and omental masses suggestive of carcinomatosis is mandatory.

In patients who cannot receive iodinated contrast because of allergic reaction, magnetic resonance (MR) with gadolinium is an excellent alternative to CT. MR cholangiography also can be used to evaluate the biliary and pancreatic ducts.

If the pancreatic tumor is deemed unresectable, or if a histologic diagnosis is deemed necessary prior to surgery, percutaneous image-guided biopsy or endoscopic ultrasound-guided biopsy can be performed.

Ductal Adenocarcinoma

Adenocarcinoma is the most common malignant neoplasm of the pancreas. Contrast-enhanced CT has made a major contribution to the detection of this tumor, and current multidetector CT technology allows exquisite evaluation of the adjacent vasculature, a key determinant of tumor resectability.

Adenocarcinoma of the pancreas presents as a hypodense mass, which is less vascular and therefore enhances less than the normal pancreas. Imaging findings associated with vascular encase-

ment include loss of the fat planes surrounding the celiac axis, hepatic artery, and superior mesenteric artery with soft tissue growing along, and sometimes narrowing, these critical vessels. Adenocarcinoma may also significantly narrow or occlude the portal confluence or the superior mesenteric vein. Significant vascular encasement, nodal metastases, and liver metastases are also well depicted at CT, and these patients are usually deemed unresectable.

Intraductal Papillary Mucinous Neoplasm

Intraductal papillary mucinous neoplasms (IPMNs) are tumors that arise from the main pancreatic duct or its branches and are characterized by abundant mucin production, mucin retention in the pancreatic duct, and a papillary growth pattern. They can be associated with an invasive adenocarcinoma.

IPMNs appear as cystic masses in the pancreas. Significant dilatation of the pancreatic duct, caused by abundant mucin production, is one of the characteristic features of an IPMN. Multiplanar reconstruction may help depict communication between the lesion and the pancreatic duct. Findings suggestive of malignancy include size >3 cm, marked dilatation of the main pancreatic duct, enhancing mural nodule or mass, and metastases.

Pancreatic Endocrine Neoplasm (Islet Cell Tumor)

Functioning pancreatic endocrine neoplasms (PENs) are usually small (<2 cm) and most are curable. The diagnosis of a functioning PEN is al-

most always established on the basis of symptoms and specific biochemical tests, and the challenge on imaging is to locate the tumor to facilitate surgical resection. Nonfunctioning PENs usually present when they have reached a large size and patients present with abdominal pain, jaundice, or weight loss.

Thanks to their rich vascular supply, PENs present as hypervascular masses on contrast-enhanced CT or MR. Conspicuity of small functioning PEN may be greatest in the arterial phase, although some PENs are better seen in the venous phase. Small PENs appear as homogeneous masses hyperattenuating compared to the normal pancreas. Large PENs tend to outgrow their blood supply and have a more heterogeneous pattern of enhancement. Central areas of necrosis and calcifications are not uncommon.

Pancreatic Lymphoma

Although lymphoma—predominantly the non-Hodgkin B-cell type—can involve peripancreatic lymph nodes and secondarily spread to the pancreas, primary lymphoma of the pancreas is uncommon. At CT, pancreatic or peripancreatic lymphoma appear as solitary or multiple hypodense masses or diffuse enlargement of the gland mimicking pancreatitis. Dilatation of the pancreatic duct is uncommon—a sign helpful in differentiating lymphoma from adenocarcinoma.

Metastases to the Pancreas

With the widespread use of cross-sectional imaging techniques, metastases to the pancreas are being recognized with increasing frequency. Many are silent and discovered incidentally in patients with widespread metastatic disease. Renal cell carcinoma is among the more common primary tumors reported to metastasize to the pancreas. Some patients present more than 10–15 years after the initial diagnosis and nephrectomy, and patients may have isolated involvement of the pancreas. On CT, metastatic renal cell carcinoma to the pancreas presents as a single or multiple hypervascular masses in the pancreas, mimicking the CT appearance of PEN. Other primary tumors that can metastasize to the pancreas include lung, breast, and colon cancer and melanoma. In some cases the tumor initially metastasizes to the peripancreatic nodes and compresses the pancreatic tissue or invades the pancreas secondarily.

Selected Cases Illustrating Salient Radiologic Characteristics

Case 1 Resectable adenocarcinoma of the pancreas (72-year-old woman presenting with 10-lb weight loss and jaundice). (A) Venous phase contrast-enhanced axial CT of the upper abdomen demonstrating moderate dilatation of the pancreatic duct (arrow). A stent is present in the common bile duct (arrowhead).

(B) Venous phase contrast-enhanced axial CT of the upper abdomen revealing an ill-defined, slightly hypodense infiltrating mass in the uncinate process (arrows).
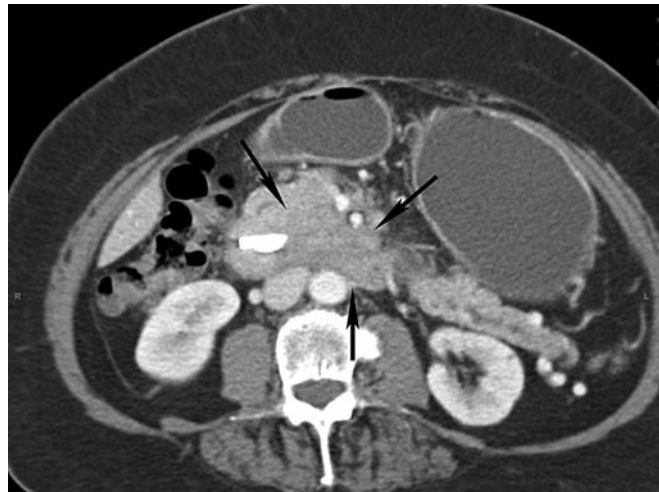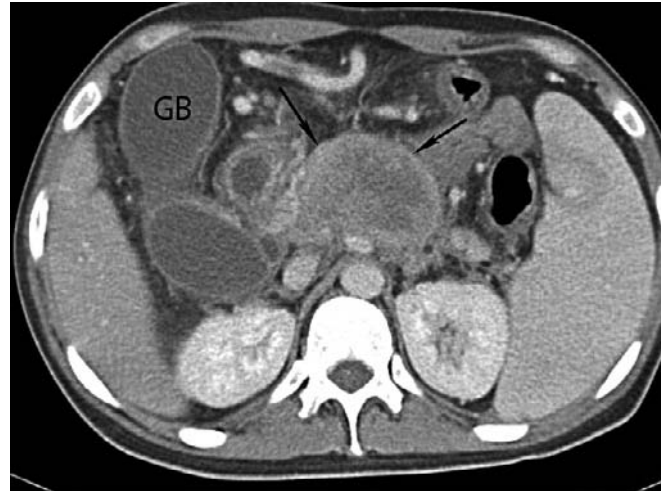

(C) Coronal reconstruction of contrast-enhanced CT confirms the presence of the mass (arrow).
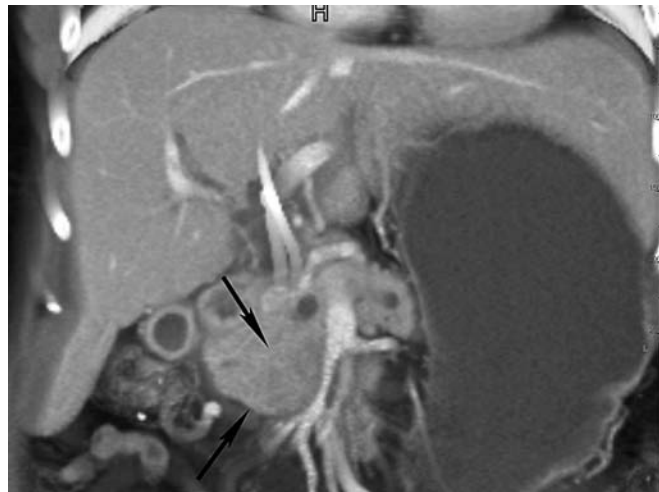
Selected Cases Illustrating Salient Radiologic Characteristics
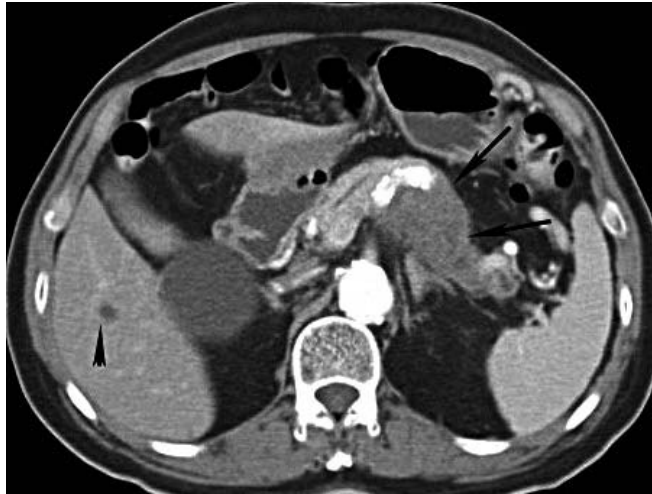
Case 2 Adenocarcinoma of the pancreas unresectable due to liver metastasis (79-year-old man with history of chest pain; asymptomatic pancreatic abnormality seen on chest CT). (A) Venous phase contrast-enhanced axial CT of the upper abdomen, shows a hypodense mass infiltrating the body and tail of the pancreas (arrows). The mass is occluding the splenic vein. Note the small hypodense liver mass compatible with metastasis (arrow head).

(B) Venous phase contrast-enhanced axial CT of the upper abdomen at a higher level shows multiple collateral veins around the stomach (arrows), confirming that the splenic vein is occluded by the tumor.

Selected Cases Illustrating Salient Radiologic Characteristics

Case 3 Adenocarcinoma of the pancreas, unresectable due to venous encasement (64-year-old woman with abdominal bloating). (A) Venous phase contrast-enhanced axial CT of the upper abdomen demonstrating a dilated pancreatic duct with atrophy of the pancreatic tail (arrowhead). There is an ill-defined hypodense mass in the neck of the pancreas (arrows). The mass is very subtle, and the main clue that a tumor is present is the dilatation of the pancreatic duct.

(B) Coronal reconstruction of contrast-enhanced CT with maximum intensity projection in the venous phase highlights focal narrowing of the portal confluence (arrow), indicating the tumor has encased the portal confluence and is not resectable.
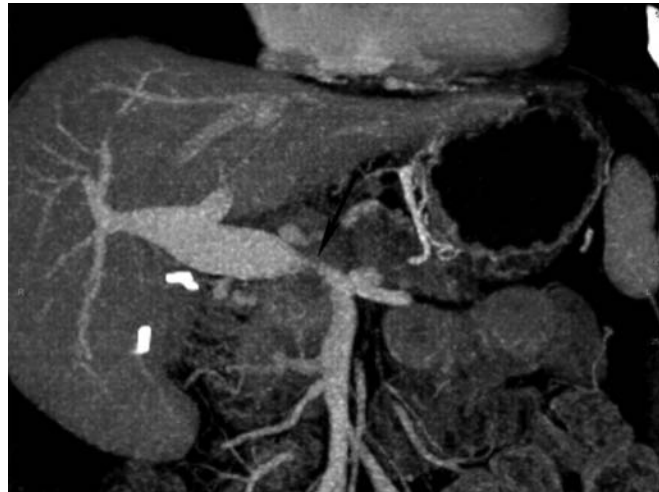
Selected Cases Illustrating Salient Radiologic Characteristics

Case 4 Adenocarcinoma of the pancreas unresectable due to arterial and venous encasement (61-year-old man with right upper quadrant and back pain). (A) Arterial phase contrast-enhanced axial CT of the upper abdomen showing a hypodense infiltrating mass arising from the uncinate process of the pancreas (arrows). Note the dilated pancreatic duct (arrowhead).

(B) Arterial phase contrast-enhanced axial CT of the upper abdomen demonstrating that the tumor is growing around the superior mesenteric artery (arrows).

(C) Arterial phase contrast-enhanced axial CT of the upper abdomen showing that the tumor has encased the celiac axis (arrows).

Selected Cases Illustrating Salient Radiologic Characteristics

Case 5 Incidental side branch intraductal papillary mucinous neoplasms (IPMNs) (incidental finding of pancreas abnormality on ultrasound triggered CT in this 70-year-old woman). (A) Venous phase contrast-enhanced axial CT of the upper abdomen demonstrating a 7-mm lesion in the head of the pancreas (arrow).

(B) Venous phase contrast-enhanced axial CT of the upper abdomen highlighting a second 8-mm hypodense lesion in the body of the pancreas (arrow).

Selected Cases Illustrating Salient Radiologic Characteristics

Case 6 Infiltrating adenocarcinoma arising in an IPMN with markedly dilated pancreatic duct (84-year-old woman with painless jaundice and pancreatic abnormality). (A) Venous phase contrast-enhanced axial CT of the upper abdomen showing a cystic mass with a small enhancing nodule lateral to the common duct in the uncinate process of the pancreas (arrows). Note the common bile duct stent (arrowhead) and the dilated pancreatic duct.
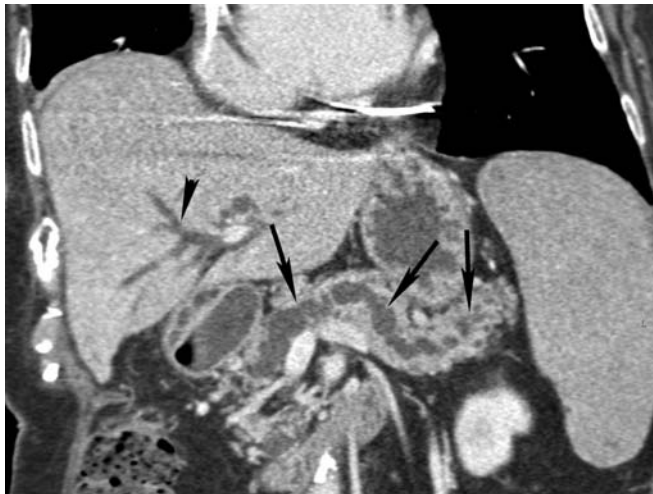
(B) Venous phase contrast-enhanced CT of the upper abdomen with multiplanar reconstruction highlighting the tortuous dilated pancreatic duct (arrows). The intrahepatic biliary tree is also dilated (arrowhead).

Selected Cases Illustrating Salient Radiologic Characteristics

Case 7 A small insulinoma in an 83-year-old man with life-threatening hypoglycemia. (A) Arterial phase contrast-enhanced axial CT of the upper abdomen shows a small homogeneous hyperattenuating mass (arrow) in the neck of the pancreas. The lesion is more conspicuous in the arterial phase.

(Reproduced with permission from AJR 2002:179; 725–730. Sheth S, Hruban RH and Fishman EK. Helical CT of islet cell tumors of the pancreas: typical and atypical manifestations.)

(B) Venous phase contrast-enhanced axial CT of the upper abdomen demonstrates the lesion, but the changes are more subtle because the difference in enhancement between the normal pancreas and the mass is less.

Selected Cases Illustrating Salient Radiologic Characteristics

Case 8 Small pancreatic endocrine neoplasm (45-year-old man with history of non insulin dependent diabetes). (A) Arterial phase contrast-enhanced axial CT of the upper abdomen shows a small slightly hypervascular mass in the neck of the pancreas (arrows). Note the thin calcified rim.
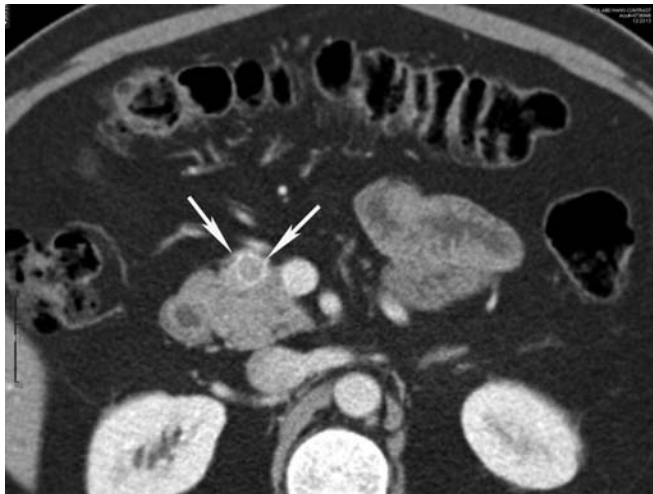
(B) Venous phase contrast-enhanced axial CT of the upper abdomen shows that the mass is still hypervascular in the venous phase.
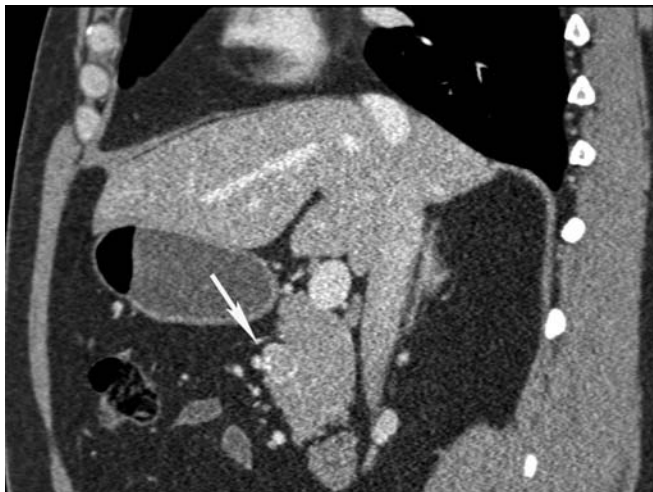
(C) Sagittal reconstruction of venous phase contrast-enhanced CT confirms the small mass in the anterior portion of the neck of the pancreas.

Selected Cases Illustrating Salient Radiologic Characteristics

Case 9 A large hypervascular pancreatic endocrine neoplasm (34-year-old man with recent onset of severe hypertension and blurred vision). (A) Arterial phase contrast-enhanced axial CT of the upper abdomen shows a large hypervascular mass in the body and tail of the pancreas (arrows). Note there is cavernous transformation of the portal vein (arrowhead) and occlusion of the splenic vein.
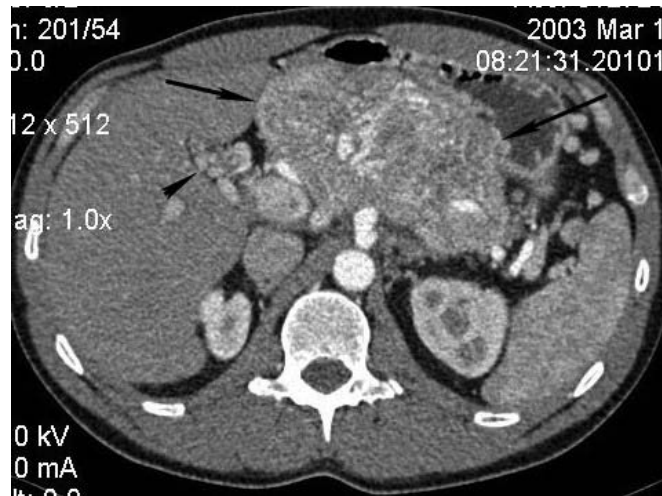
(B) Delayed phase contrast-enhanced axial CT of the upper abdomen shows the mass to enhance less intensely (arrows).
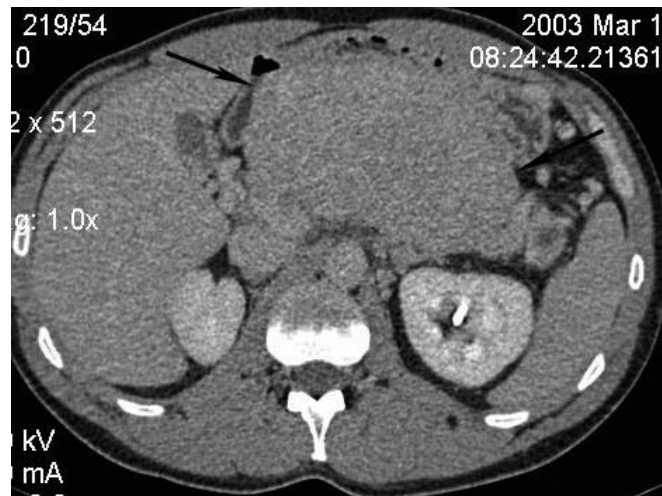
Selected Cases Illustrating Salient Radiologic Characteristics

Case 10 Large nonfunctioning pancreatic endocrine neoplasm (47-year-old woman with large pancreatic mass). (A) Arterial phase contrast-enhanced axial CT of the upper abdomen shows a very large mass in the tail of the pancreas (arrows). The tumor has an enhancing rim and a necrotic center. It invades into the splenic hilum and has occluded the splenic vein with multiple varices seen (arrowheads).

(B) Venous phase contrast-enhanced axial CT of the upper abdomen confirms the mass (arrows) and shows the collateral veins (arrowheads) to better advantage.
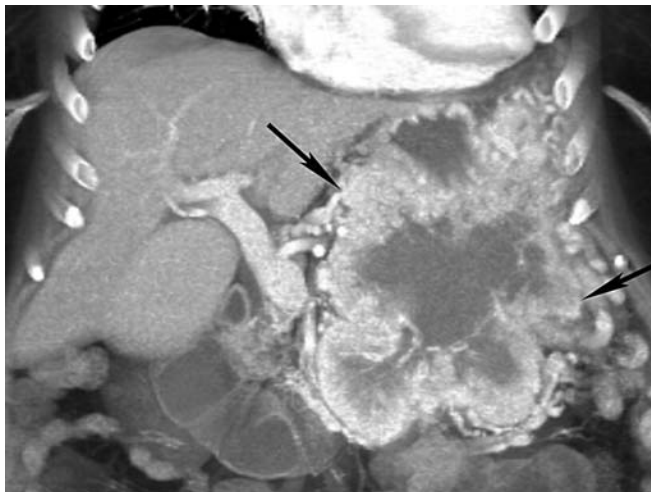
(C) Coronal reconstruction of venous phase contrast-enhanced CT confirms the extent of the tumor (arrows).

Selected Cases Illustrating Salient Radiologic Characteristics

Case 11 Pancreatic lymphoma (29-year-old man with fever, lower abdominal pain, and weight loss). (A) Venous phase contrast-enhanced axial CT of the upper abdomen shows a large heterogeneous mass in the uncinate process of the pancreas (arrows).

(B) Venous phase contrast-enhanced axial CT of the upper abdomen confirming the mass and showing it extending into the body of the pancreas (arrows).

(C) Venous phase contrast-enhanced axial CT of the upper abdomen shows multiple small nodes in the mesentery (arrows).

Selected Cases Illustrating Salient Radiologic Characteristics
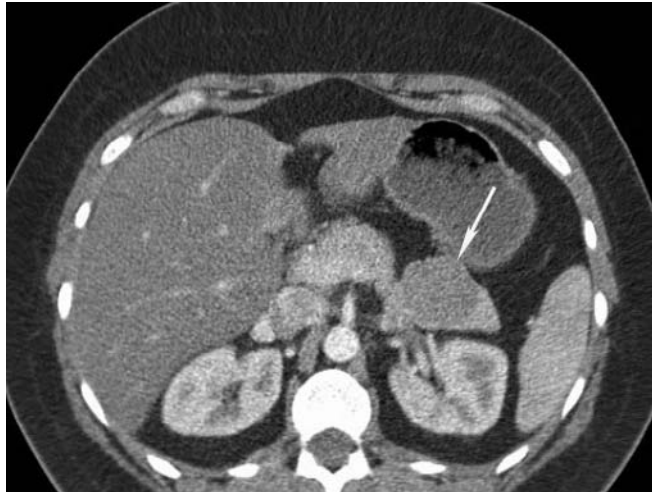
Case 12 Solid-pseudopapillary neoplasm of the pancreas (42-year-old woman, pancreatic tail mass found incidentally on CT performed for vague abdominal symptoms). (A) Contrast-enhanced axial CT of the upper abdomen shows a cystic mass in the tail of the pancreas (arrows).

(B) T2-weighted sequence abdominal MR, confirms the presence of a cystic mass in the tail of the pancreas (arrows).
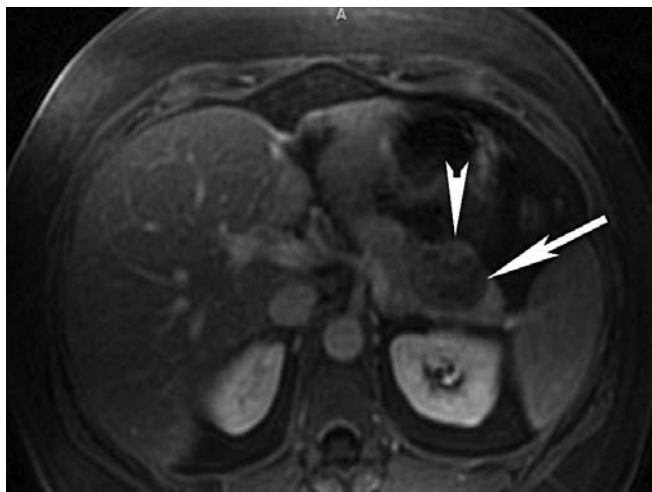
(C) Gadolinium-enhanced MR in venous phase shows subtle nodular enhancement within the mass (arrowhead).

Selected Cases Illustrating Salient Radiologic Characteristics

Case 13 Renal cell carcinoma metatstatic to the pancreas (69-year-old man with a history of nephrectomy for renal cell carcinoma 10 years before). Axial CT images of the pancreas in the arterial (A) and venous (B) phases show a hyperattenuating mass (arrows) in the body and tail of the pancreas. The enhancement within the lesion is more pronounced in the arterial phase. A small hypervascular hepatic metastasis is seen in the arterial phase (arrowhead in A) and this mass in the liver becomes isoattenuating to the liver parenchyma in the venous phase (B). There has been a left nephrectomy.

Nonneoplastic Lesions

3

Chronic Pancreatitis

Lymphoplasmacytic
  Sclerosing Pancreatitis

Hamartoma

Heterotopic Spleen

Pseudocyst

Epidermoid Cyst

Lymphoepithelial Cyst

Paraduodenal
  Wall Cyst

Chronic Pancreatitis

Figure 3.1 — Chronic pancreatitis. Cross section of a pancreas with marked chronic pancreatitis. The normal tan-yellow lobular parenchyma is replaced by firm white bands of fibrosis. A few ducts remain, and most of them, as is often seen in alcoholic chronic pancreatitis, contain large calculi. Localized chronic pancreatitis can be caused by a focal mass lesion, and when pancreatitis is localized, care should be taken to rule out an underlying neoplasm.

Chronic Pancreatitis
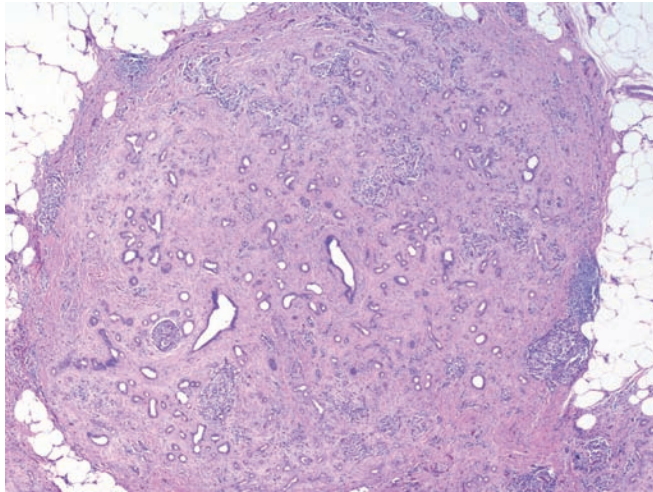
Figure 3.2 — Chronic pancreatitis. The exocrine parenchyma is lost and replaced with dense scar tissue. In contrast to infiltrating ductal adenocarcinoma, the lobular architecture is preserved. In other examples of chronic pancreatitis the exocrine parenchyma is completely replaced by fatty connective tissue. In these instances, residual islets of Langerhans may be the only clue that the tissue was once pancreas. (Hematoxylin and eosin stain, low power)
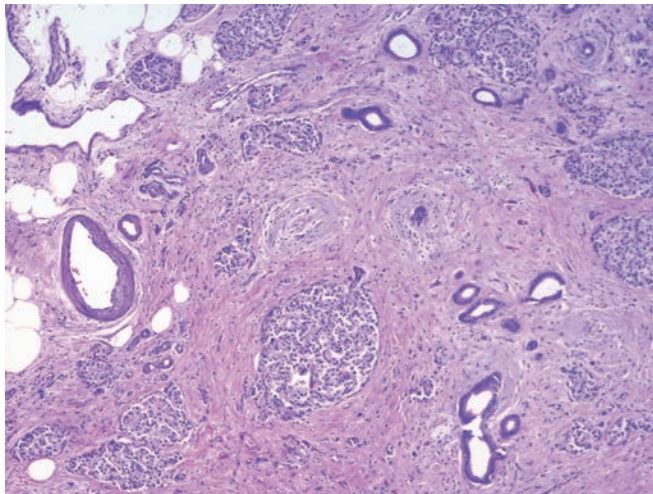
Figure 3.3 — Chronic pancreatitis. This field highlights a number of features of chronic pancreatitis including marked fibrosis, acinar loss, and aggregation of the islets of Langerhans to form large islets. Even though the arrangement of the ducts is slightly distorted by the extensive fibrosis in this case, the glands are separated from the muscular vessels. In long-standing chronic pancreatitis the aggregated islets can mimic a well-differentiated pancreatic endocrine neoplasm. The latter would be larger and usually monoclonal on immunolabeling for insulin, glucagon, and somatostatin. (Hematoxylin and eosin stain, medium power)
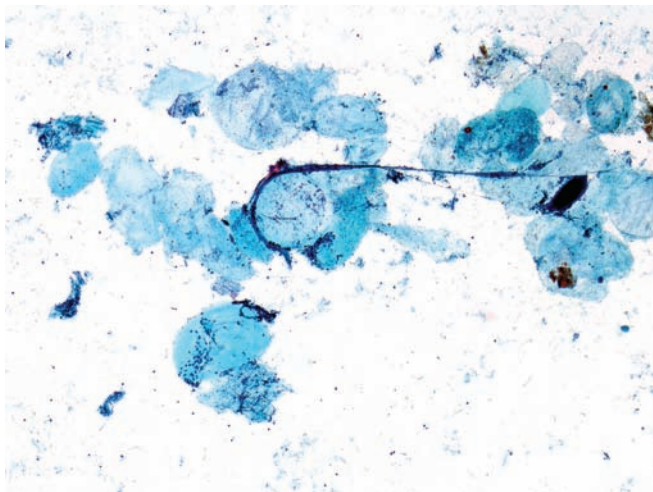
Figure 3.4 — Chronic pancreatitis. This hypocellular specimen is composed of rare small epithelial tissue fragments in a background showing degenerated adipose tissue and cellular debris. Microcalcifications are often seen in such cases in the cytologic smears. Despite the lack of cellular material, this picture strongly suggests chronic pancreatitis with associated fat necrosis. (Papanicolaou stain, low power)

Chronic Pancreatitis

Figure 3.5 — Chronic pancreatitis. Inflammatory cells with predominance of lymphocytes, display nuclear crush artifact. The cytopathologic appearance is non-specific and chronic pancreatitis is often a diagnosis of exclusion. (Papanicolaou stain, low power)
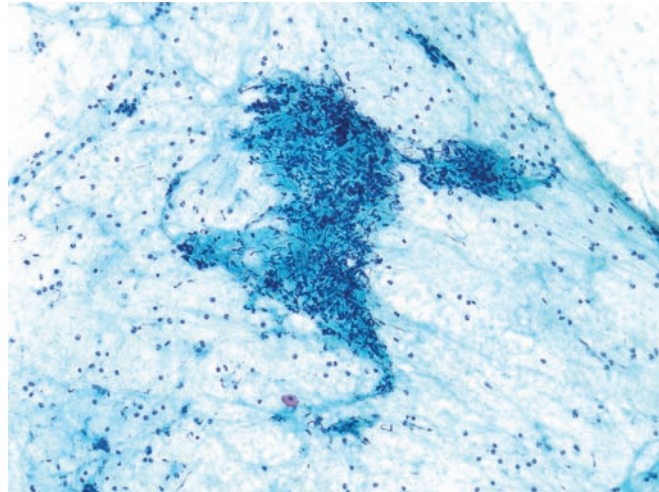
Figure 3.6 — Chronic pancreatitis. A large disorganized mesenchymal tissue fragment signifies extensive fibrosis that accompanies such cases resulting in a relatively lack (or absence) of pancreatic epithelium. (Diff Quik stain, low power)
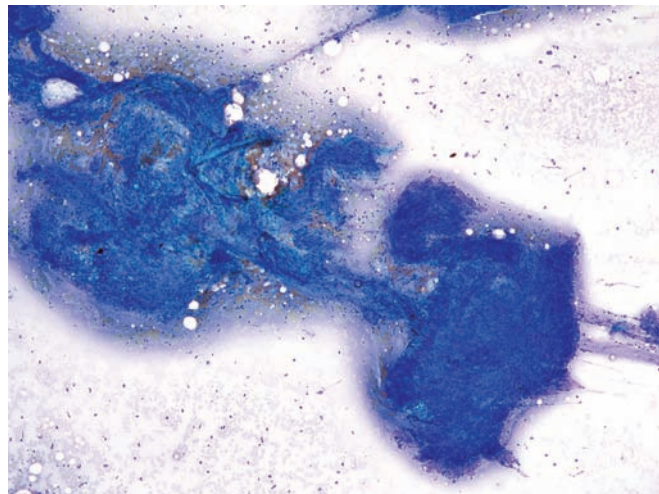
Figure 3.7 — Chronic pancreatitis. An intact fragment of islet cells (3 o'clock) is juxtaposed to a large fibrous tissue fragment. Background is clean, devoid of hemorrhage and blood. Islet cells are often seen as intact or partially intact structures in cases of chronic pancreatitis, where the atrophy of the exocrine portion is accompanied by a prominent endocrine component. The cells appear uniform with round-to-oval hyperchromatic nuclei giving the cells a high N/C ratio. Pancreatic endocrine neoplasms typically show a more dispersed single-cell pattern rather than cohesive intact cell fragments of normal/prominent islets. (Papanicolaou stain, medium power)
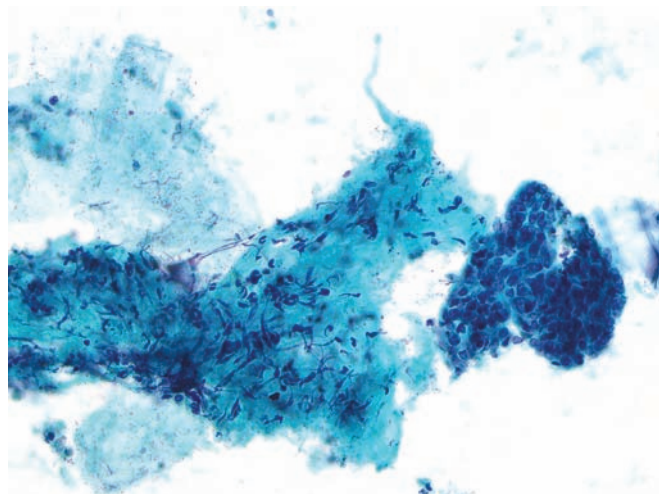
Chronic Pancreatitis
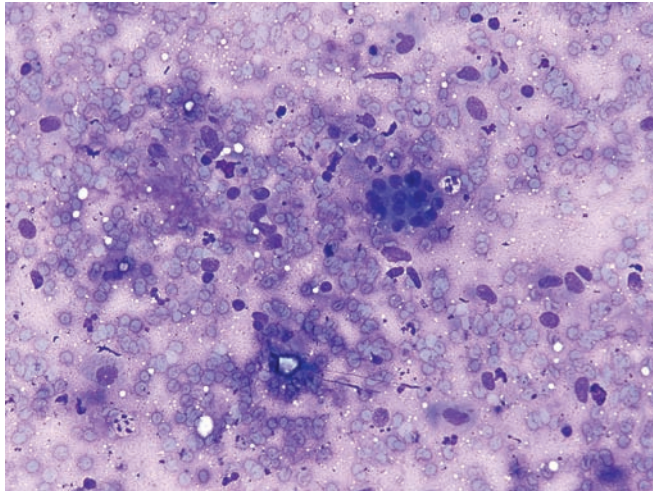
Figure 3.8 — Chronic pancreatitis. Hypocellular smear with a small partially intact islet of Langerhans in a background of numerous bland fibroblastic nuclei is noted. Aspirates from cases of chronic pancreatitis are often hypocellular and a definite diagnosis requires correlation with clinical and radiographic findings. (Diff Quik stain, medium power)
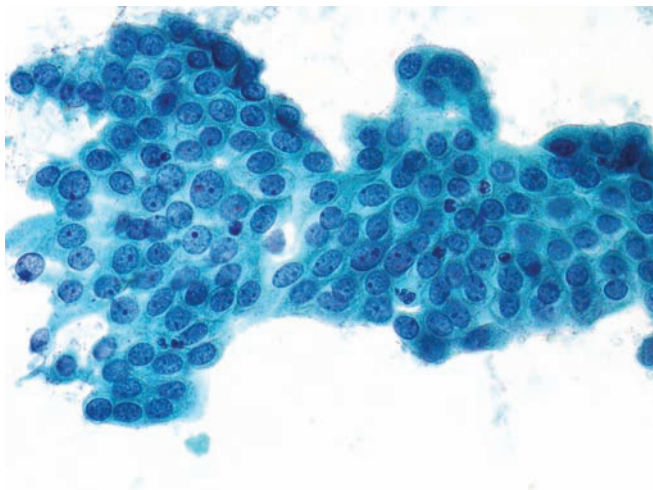
Figure 3.9 — Chronic pancreatitis. A fragment of columnar epithelium with reactive changes is observed. Enlarged nuclei with micronucleoli and scattered neutrophils are a common finding in chronic pancreatitis. The mild cytologic atypia can be ascribed to reactive cellular changes secondary to prolonged inflammation of the pancreas.

It is imperative to have a higher threshold for "atypical" or neoplastic diagnosis when dealing with cases of chronic pancreatitis. Note the clean smear background. (Papanicolaou stain, high power)
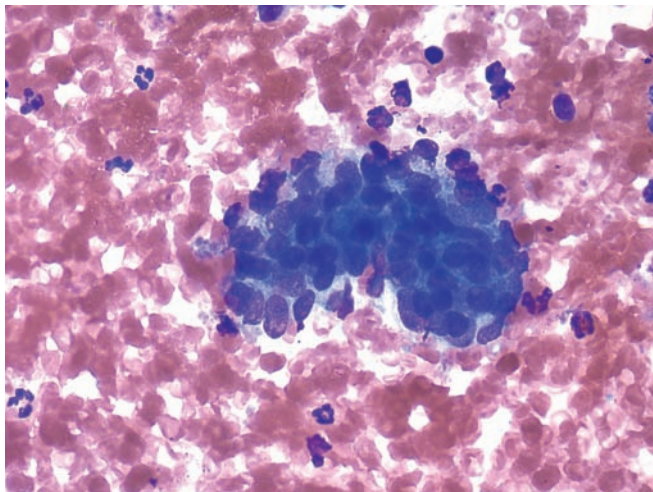
Figure 3.10 — Chronic pancreatitis. Cells with significant epithelial atypia are present. They have disorganized and enlarged nuclei, which appear hyperchromatic, forming three-dimensional structures. The changes are not enough to justify an "atypical" or "suspicious" interpretation. (Diff Quik stain, high power)

Chronic Pancreatitis

Figure 3.11 — Chronic pancreatitis. Numerous fragments of glandular epithelium, fibrous tissue, and marked background chronic inflammation give this smear a hypercellular appearance. The polymorphous cellular composition clearly favors a benign reactive process in this case. (Hematoxylin and eosin stain, low power)
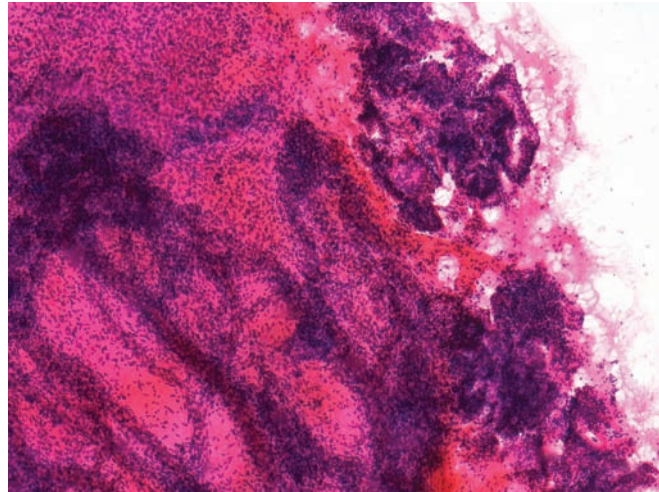
Figure 3.12 — Chronic pancreatitis. Two fragments of "atypical" columnar epithelium are present. Note nuclear enlargement and marked disorganization of the architecture with loss of nuclear polarity. Although not diagnostic, an adenocarcinoma cannot be entirely excluded in this case. Follow-up showed extensive chronic pancreatitis. Also note scattered background inflammatory cells. (Hematoxylin and eosin stain, high power)
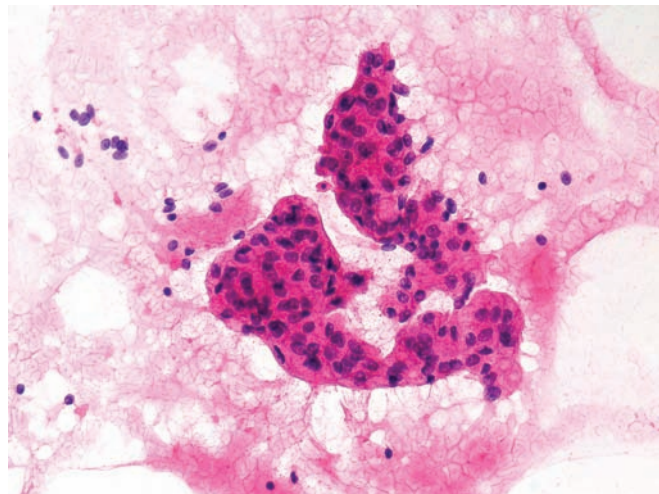
Lymphoplasmacytic Sclerosing Pancreatitis
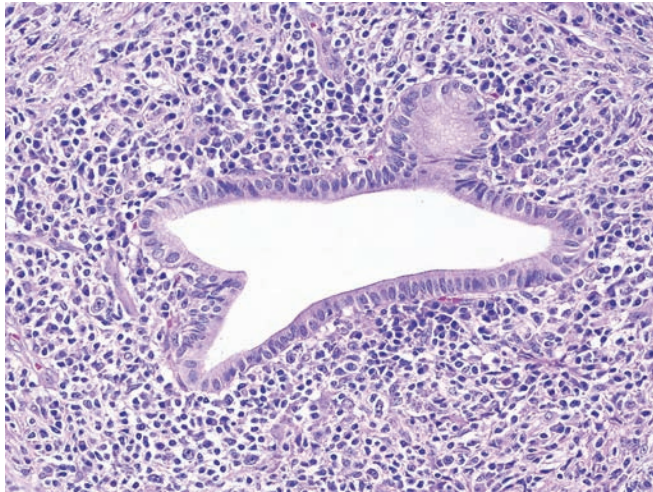
Figure 3.13 — Lymphoplasmacytic sclerosing pancreatitis (autoimmune pancreatitis). A mixed inflammatory cell infiltrate composed of lympho-cytes, plasma cells, and occasional eosinophils is centered on a pancreatic duct. The inflammatory cell infiltrate in other forms of pancreatitis is typically more diffuse. Intraluminal concretions and calculi are more typical of alcoholic pancreatitis. (Hematoxylin and eosin stain, low power)
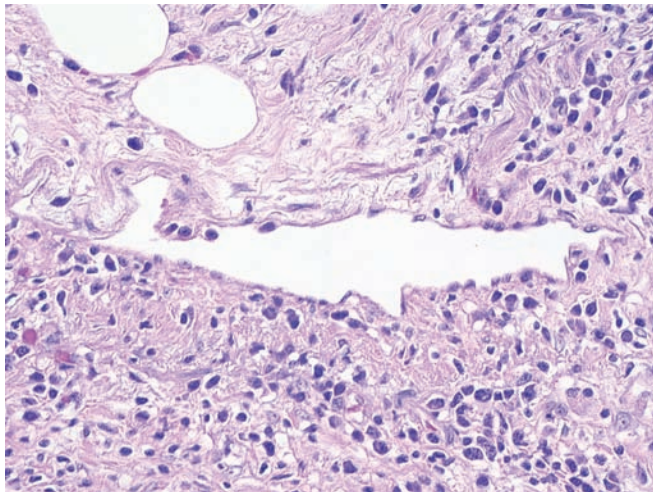
Figure 3.14 — Lymphoplasmacytic sclerosing pancreatitis (autoimmune pancreatitis). Venulitis, as shown here, is often best appreciated at the periphery of the inflammatory process. These vascular lesions should be distinguished from other forms of vasculi-tis. Polyarteritis nodosa strikes medium-sized mus-cular arteries, not the veins. (Hematoxylin and eosin stain, high power)
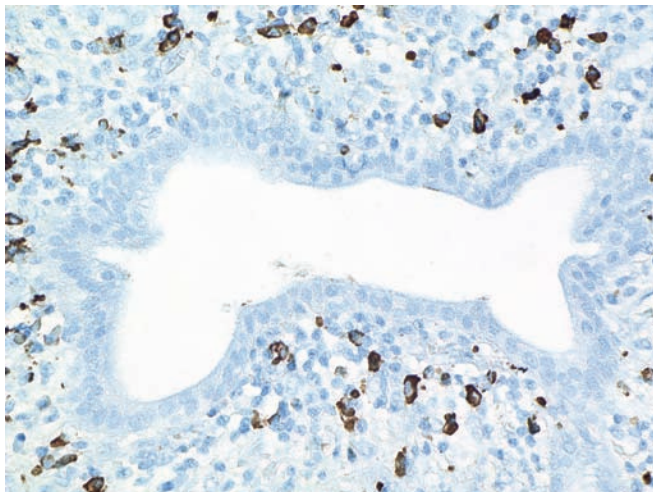
Figure 3.15 — Lymphoplasmacytic sclerosing pancreatitis (autoimmune pancreatitis). Immuno-labeling for IgG4 highlights increased numbers (greater than 10/high-power field) of IgG4-positive plasma cells, helping to confirm the diagnosis. (Immunolabeling for IgG4, high power)

Hamartoma

Figure 3.16 — Hamartoma. This mass-forming lesion is composed of disorganized mature ductal and stromal elements. Hamartomas can be cystic or solid and are distinguished from chronic pancreatitis because they are localized, form a mass, and lack islets of Langerhans. (Hematoxylin and eosin stain, low power)
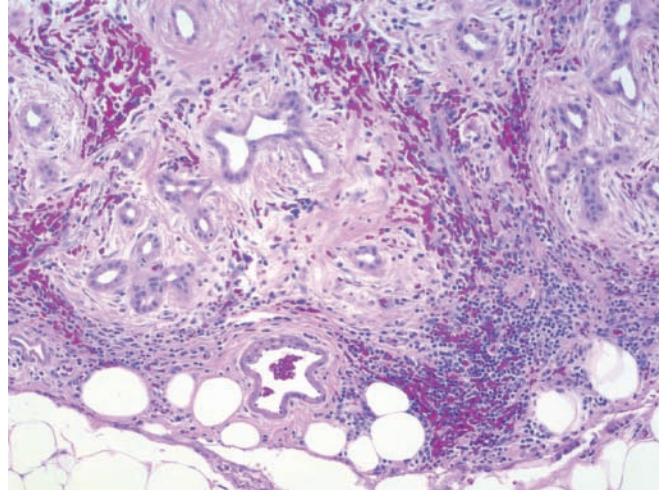
Heterotopic Spleen
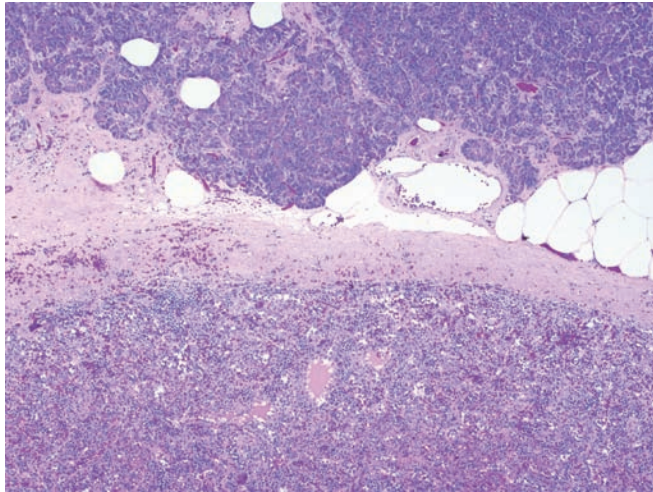
Figure 3.17 — Heterotopic spleen in the tail of the pancreas. This nodule of splenic tissue (bottom) is present in the normal pancreas (top). While these lesions can clinically mimic a well-differentiated endocrine neoplasm, the microscopic diagnosis is usually obvious. Other malformations can mimic a pancreatic neoplasm. For example, duodenal diverticuli can extend into the substance of the head of the pancreas and imitate a cystic neoplasm such as an intraductal papillary mucinous neoplasm. (Hematoxylin and eosin stain, low power)

Pseudocyst
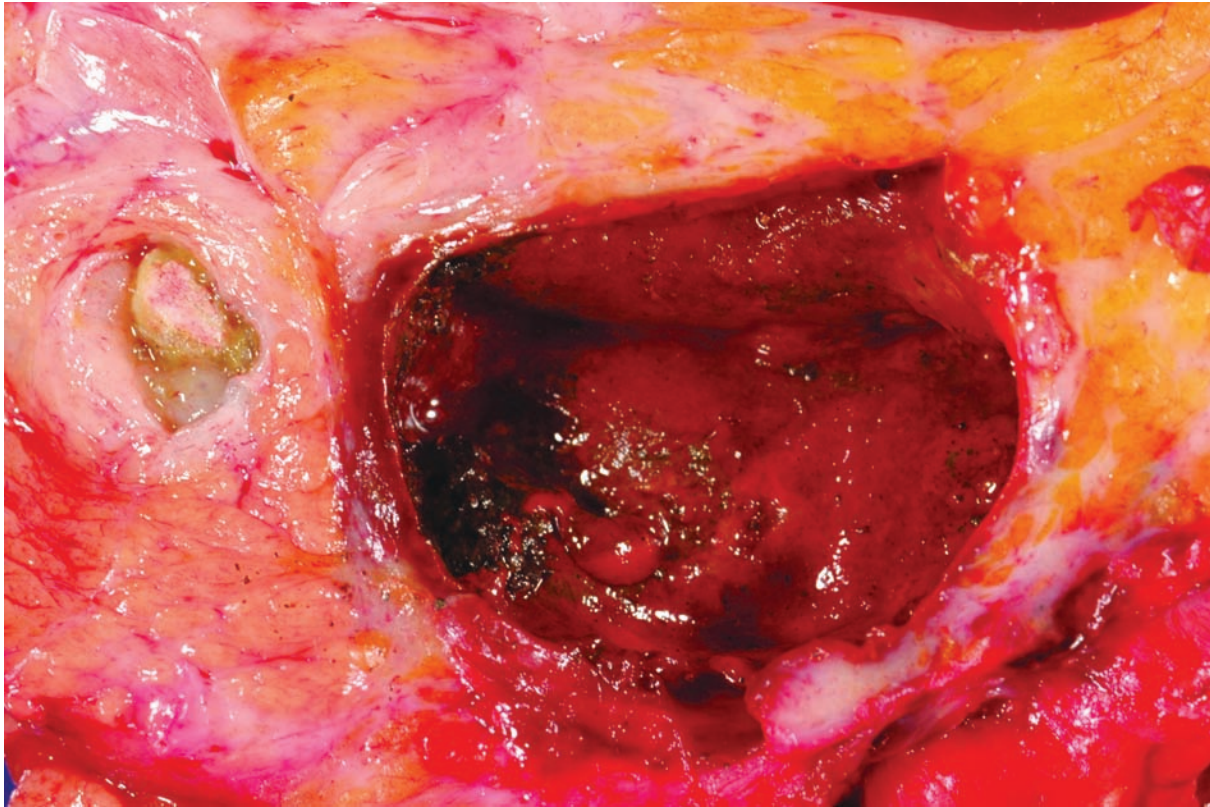
Figure 3.18 — Pseudocyst. This poorly demarcated cyst was filled with blood and necrotic debris. The calculus in the adjacent pancreatic duct (left) suggests that this pseudocyst may have arisen in a patient with chronic alcoholic pancreatitis. Solid-pseudopapillary neoplasms can have a similar gross appearance as they also contain blood and necrotic debris. In contrast to solid-pseudopapillary neoplasms, most pseudocysts are extrapancreatic.

Pseudocyst
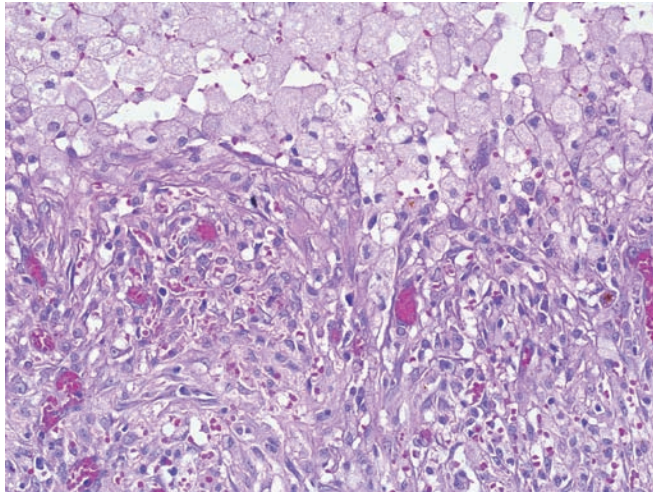
Figure 3.19 — Pseudocyst. The cyst contains necrotic debris and is lined by macrophages and granulation tissue. The epithelium lining cystic neoplasms of the pancreas, such as the mucinous cystic neoplasm, can be focally denuded, mimicking a pseudocyst. Careful attention to the nature of the stroma (ovarian-type in mucinous cystic neoplasms) and adequate sampling can avoid this diagnostic pitfall. (Hematoxylin and eosin stain, medium power).
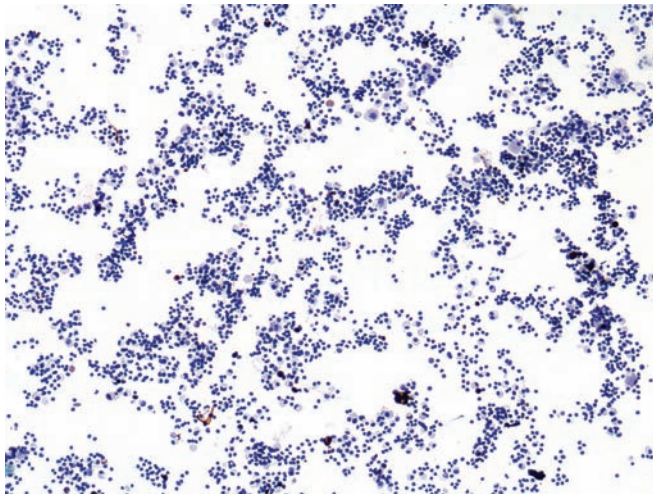
Figure 3.20 — Pseudocyst. Polymorphous cellular infiltrate with predominantly lymphocytes and histiocytes is seen. No pancreatic epithelium is noted, and no mucin is present in the smear background. The typical differential diagnosis of pseudocyst involves serous and mucinous cyst forming neoplasms of the pancreas. In occasional cases of pseudocyst, the aspirate may be contaminated by duodenal or normal pancreatic epithelium, creating diagnostic issues on cytologic interpretation. (Papanicolaou stain, low power)
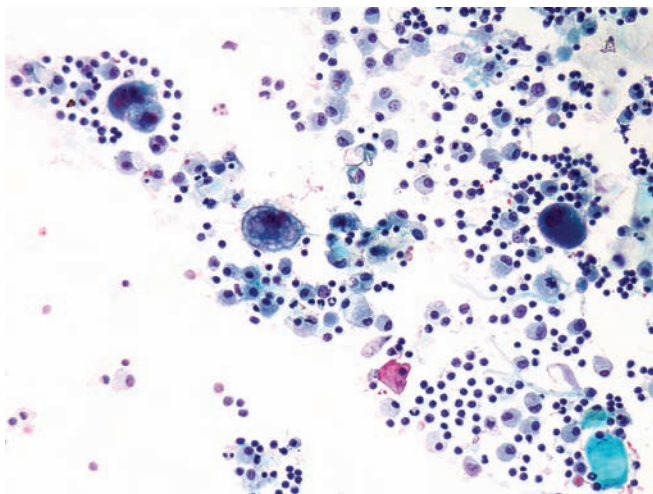
Figure 3.21 — Pseudocyst. Predominantly lymphocytes and histiocytes are present in this smear. The several large cells with atypical nuclei and vacuolated cytoplasm are consistent with histiocytes. Nuclear polymorphism with sharp irregularities of the nuclear borders and prominent nucleoli, as seen here, may be present in reactive/degenerative conditions. (Papanicolaou stain, high power)

Pseudocyst

Figure 3.22 — Pseudocyst. An unusual case composed predominantly of cellular and crystalline debris. Only rare inflammatory cells and histiocytes were noted in other areas of the smear. (Diff Quik stain, low power)
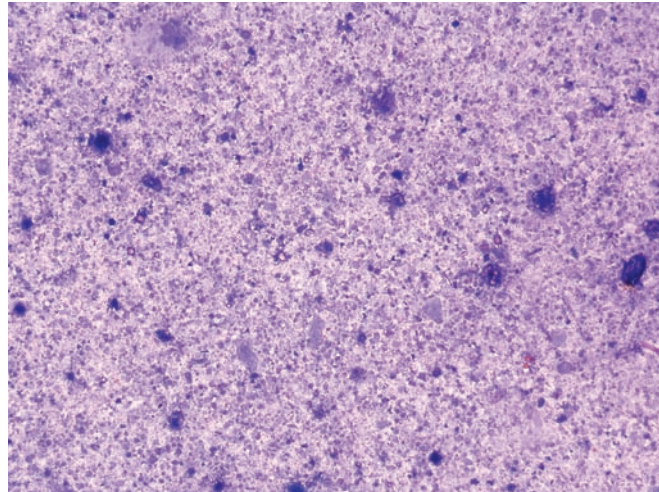
Figure 3.23 — Pseudocyst. Higher magnification of the previous case, illustrating the thick inspissated contents of a pancreatic pseudocyst and a lack of cellular component. A careful correlation with clinical and radiologic findings is advisable in such cases. (Diff Quik stain, high power)
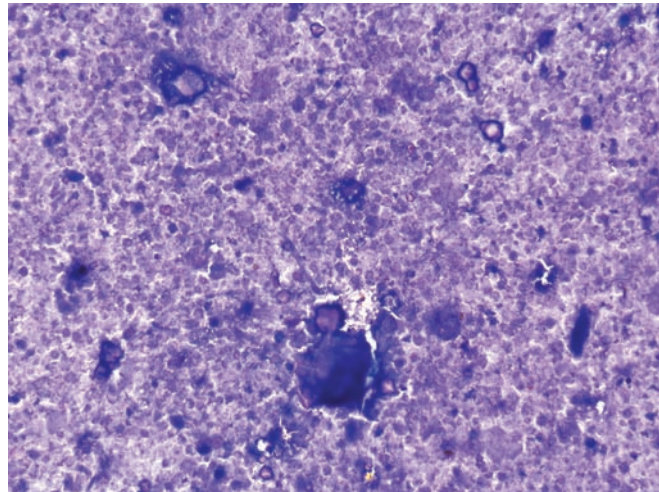
Figure 3.24 — Pseudocyst. This polymorphous infiltrate contains inflammatory cells and cyst lining cells (with more ovoid stripped nuclei), hemosiderin-laden macrophages, and background degenerated blood. (Diff Quik stain, high power)
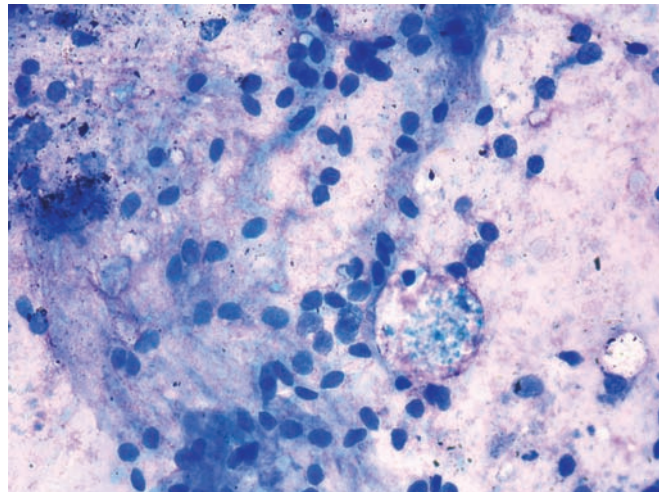
Epidermoid Cyst
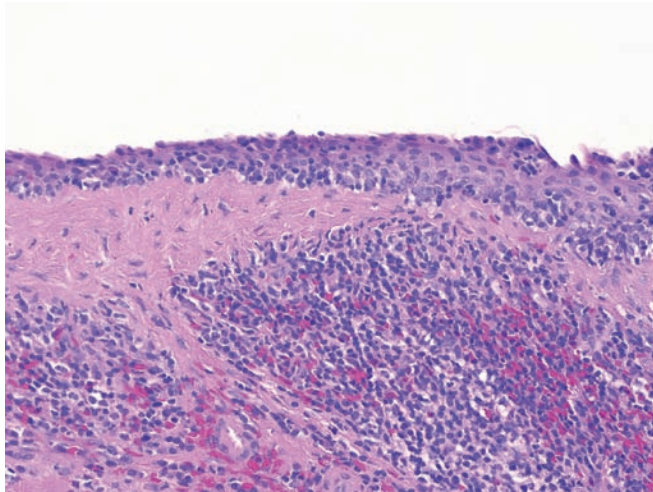
Figure 3.25 — Epidermoid cyst in intrapancreatic heterotopic spleen in the tail of the pancreas. This cyst arose in splenic parenchyma abnormally located within the parenchyma of the pancreas and is lined by mature squamous epithelium without atypia. The lymphoepithelial cyst (lymphoid, not splenic, tissue surrounding the cysts) and dermoid cyst (other germ cell components represented) top the differential diagnosis. Identification of splenic elements will usually lead to the correct diagnosis. (Hematoxylin and eosin, high power)

Lymphoepithelial Cyst

Figure 3.26 — Lymphoepithelial cyst. This dramatic example contains peculiar small (less than 1 cm) rounded proteinaceous concretions. The cyst has a thin wall. Lymphoepithelial cysts usually contain paste-like material. Oligocystic serous cystadenoma, mucinous cystic neoplasm, retention cyst, and epidermoid cyst in heterotopic spleen should all be considered in the differential diagnosis of a thin-walled unilocular cyst in the pancreas.

Lymphoepithelial Cyst
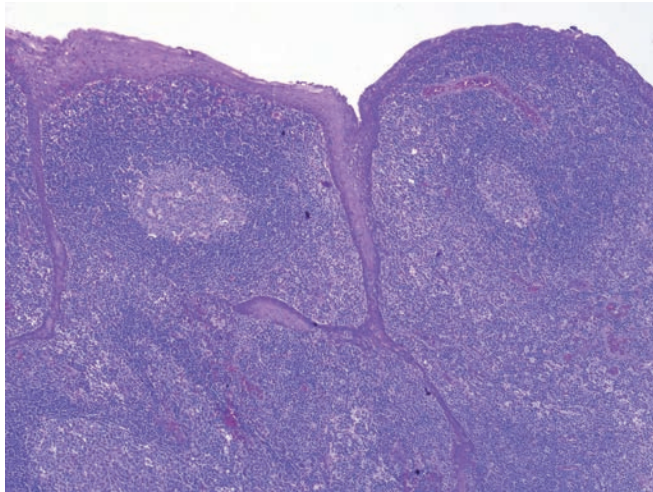
Figure 3.27 — Lymphoepithelial cyst. The cyst is lined by a mature squamous epithelium that lacks atypia. A dense lymphoid infiltrate with germinal center formation dominates the stroma. The lining will be similar in epidermoid cysts in intrapancreatic heterotopic spleen, but the stroma in epidermoid cysts in intrapancreatic heterotopic spleen will obviously be splenic. (Hematoxylin and eosin stain, low power)
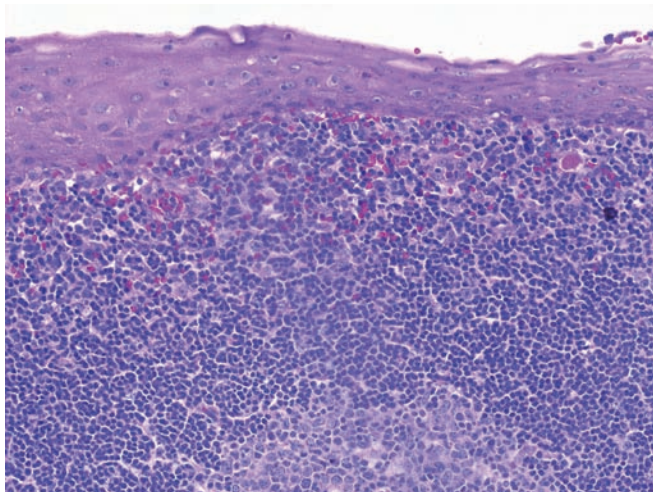
Figure 3.28 — Lymphoepithelial cyst. The squamous epithelium matures toward the surface, the nuclei are small and uniform, and the edge of an underlying germinal center is seen. Adenosquamous carcinomas are also composed of squamous cells, but the epithelium of adenosquamous carcinomas has an infiltrative pattern of growth as well as significant dysplasia. (Hematoxylin and eosin stain, high power)
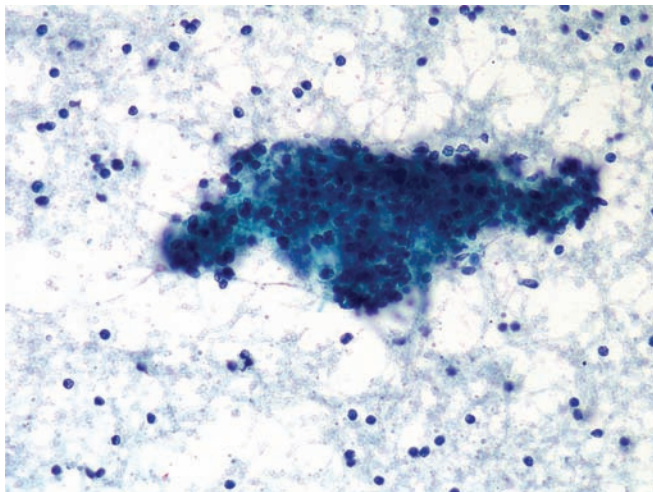
Figure 3.29 — Lymphoepithelial cyst. A loose aggregation of lympho-histiocytic cells is present. Numerous isolated background lymphocytes are present as well. This appearance is nonspecific, particularly if no other cellular component is identified. Chronic pancreatitis should be considered in the differential diagnosis, as well as sampling of a peripancreatic lymph node. Radiologic correlation would help to establish the diagnosis. (Papanicolaou stain, low power)

Lymphoepithelial Cyst

Figure 3.30 — Lymphoepithelial cyst. The characteristic admixture of benign squamous cells in a lymphocytic background is seen. The squamous cells appear mature and normal. Squamous cells in a pancreatic FNA raise a differential diagnosis of squamous cell contamination from the tubular esophagus (in EUS-guided aspirates), epidermoid cyst, dermoid cyst, primary adenosquamous and metastatic squamous cell carcinoma. Lack of any cytologic atypia and presence of a significant lymphocytic population will rule out a carcinoma. (Papanicolaou stain, medium power)
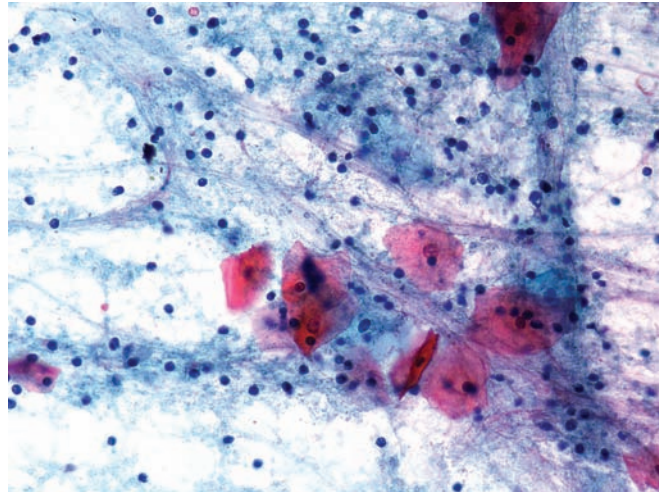
Figure 3.31 — Lymphoepithelial cyst. A thick aggregation of lymphocytes and histiocytes corresponding possibly to germinal center differentiation in a hyperplastic lymphoid follicle in the cyst wall is noted. Lack of squamous cells in such cases will make the diagnosis of a lymphoepithelial cyst extremely difficult. (Papanicolaou stain, medium power)
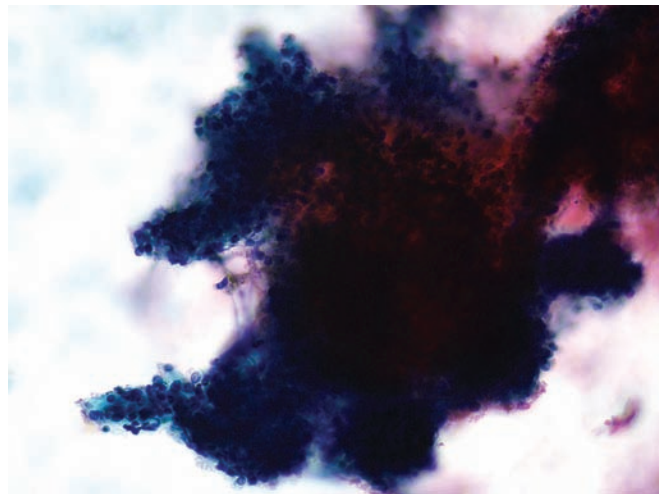
Lymphoepithelial Cyst
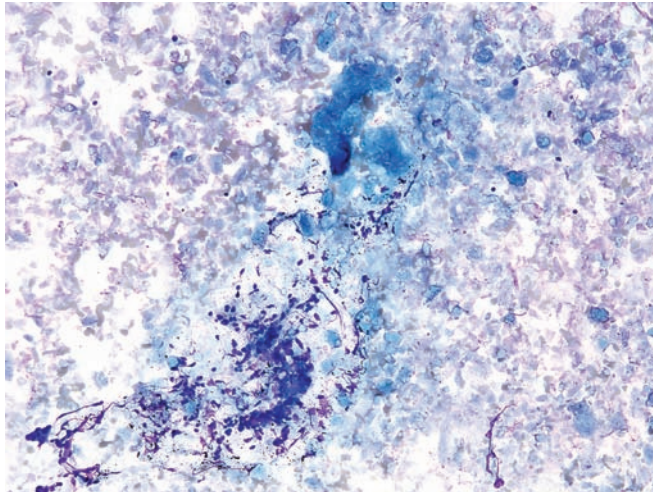
Figure 3.32 — Lymphoepithelial cyst. This thick pasty looking aspirate (grossly) contains innumerable anucleate squames and keratinaceous debris admixed with scant crushed lymphocytes. Care should be taken not to confuse the keratinaceous debris with inpissated mucin in such cases. (Diff Quik stain, low power)
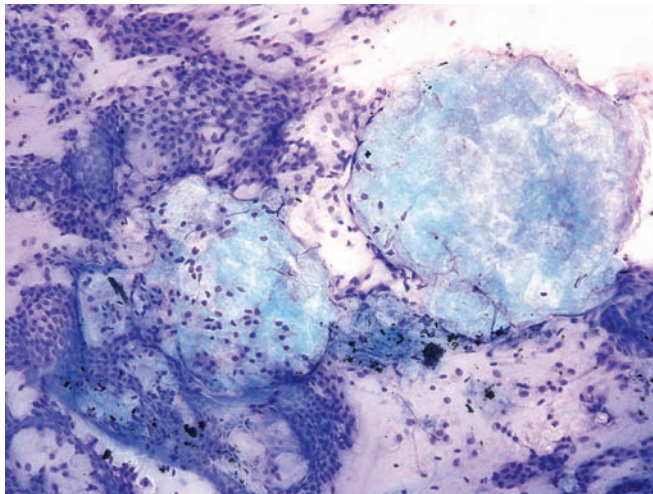
Figure 3.33 — Lymphoepithelial cyst. On a transgastric FNA in this case, round globules of amorphous-looking material are seen admixed with benign contaminating gastric epithelium. This case was suspected to be a mucinous cystic neoplasm but on follow-up the lesion turned out to be a lymphoepithelial cyst. (Diff Quik stain, medium power)
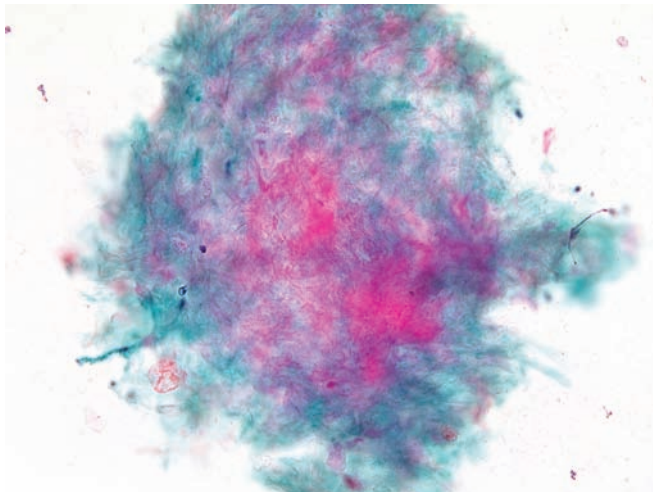
Figure 3.34 — Lymphoepithelial cyst. The same globules of amorphous material from the above case stained red on Papanicolaou stain consistent with keratinaceous debris from a lymphoepithelial cyst. This amorphous material should not be confused with thick mucin. (Papanicolaou stain, high power)

Lymphoepithelial Cyst

Figure 3.35 — Lymphoepithelial cyst. An intimate admixture of polymorphous lymphocytes and super-ficial-type squamous epithelial cells and anucleate squames is seen. A bimodal admixture of these two cell types is highly suggestive of lymphoepilthelial cyst. (Papanicolaou stain, high power)
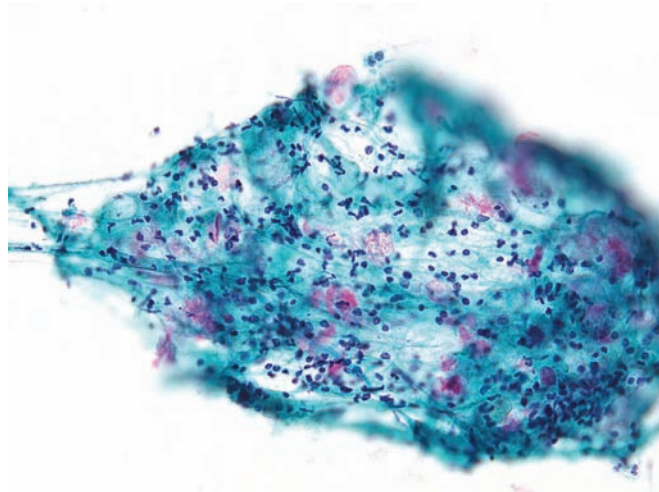
Figure 3.36 — Lymphoepithelial cyst. Cell block section displays an aggregate of lymphoid tissue and juxtaposed benign squamous epithelium, which forms the lining of the cystic structure. An additional helpful finding, beautifully illustrated here, is an admixture of abundant anucleate squames and blood in the back-ground. (Hematoxylin and eosin stain, low power)
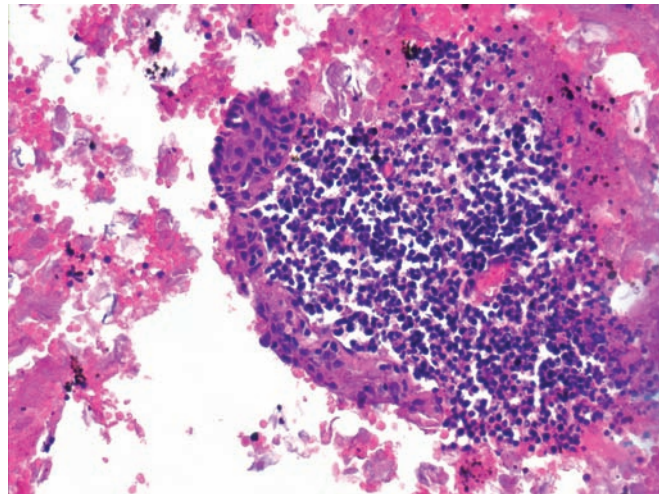
Paraduodenal Wall Cyst
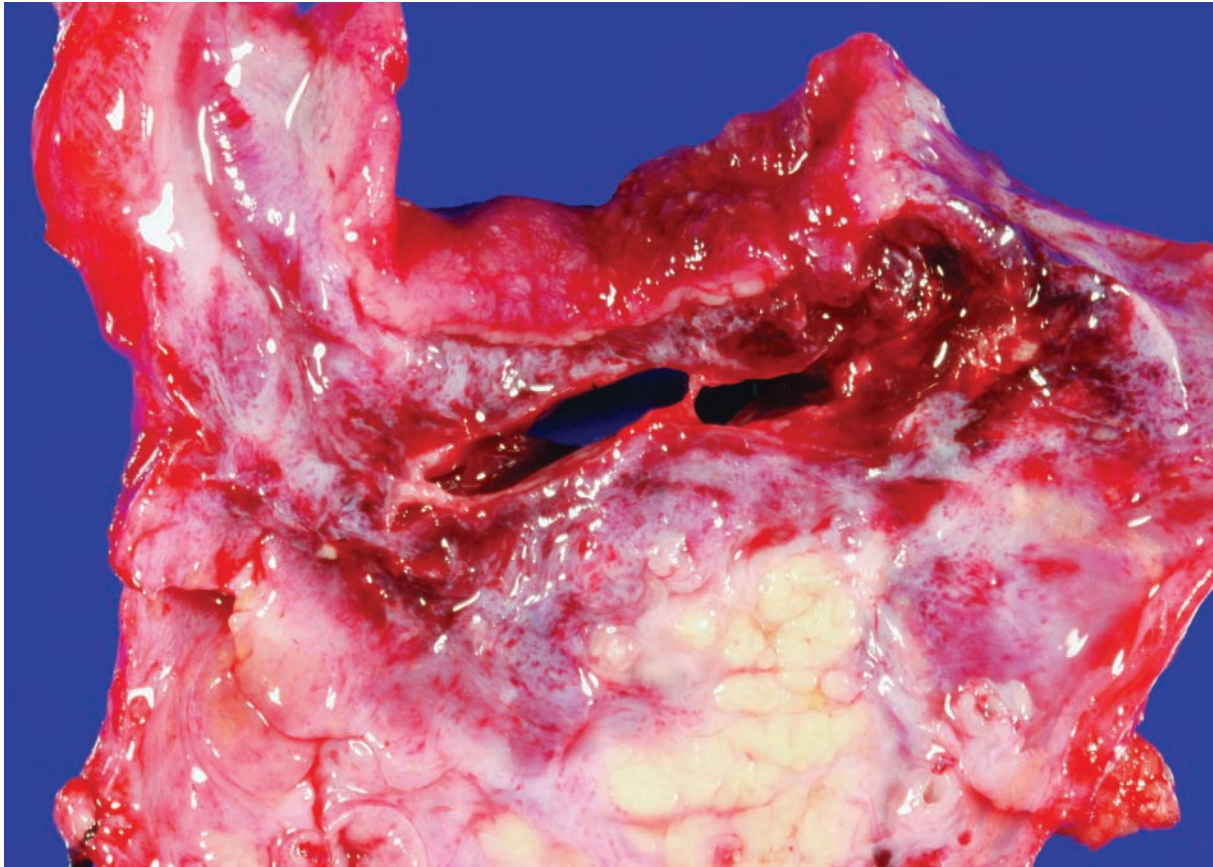
Figure 3.37 — Paraduodenal wall cyst (groove pancreatitis). Two slightly hemorrhagic cysts sit between the duodenum (top) and the pancreas (bottom). This form of pancreatitis can mimic both cystic and solid neoplasms of the pancreas. Recognition that this lesion is located in the groove region (bordered by the minor papilla, the bile duct, the head of the pancreas, and the duodenum) helps establish the correct diagnosis.

Paraduodenal Wall Cyst

Figure 3.38 — Paraduodenal wall cyst (groove pancreatitis). The cysts are believed to result from the obstruction of small ducts feeding into the minor papillae. As a result, the cysts are partially lined by reactive, presumably preexisting epithelium (top right), while other areas lack an epithelial lining (left). This lesion can imitate a pseudocyst, but the characteristic location and the presence of an epithelial lining, even if the lining is focal, help establish the correct diagnosis. (Hematoxylin and eosin stain, low power)
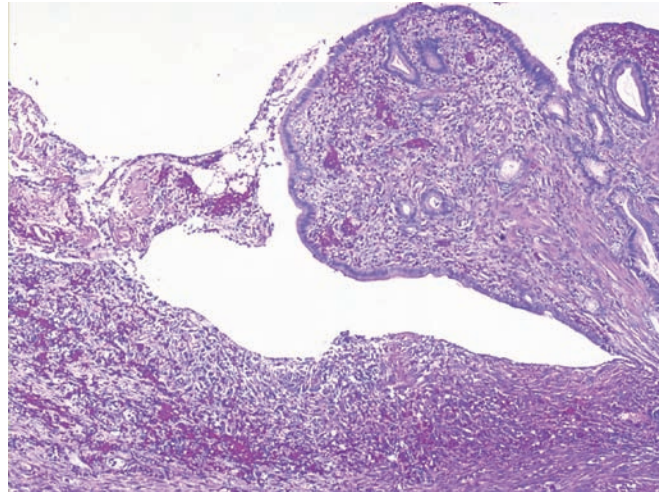
Figure 3.39 — Paraduodenal wall cyst (groove pancreatitis). An intense reactive spindle cell proliferation, composed of fibroblasts, extravasated red blood cells, and scattered inflammatory cells, is associated with a denuded cyst. This spindle cell proliferation can be so exuberant as to mimic a spindle cell neoplasm. (Hematoxylin and eosin stain, low power)
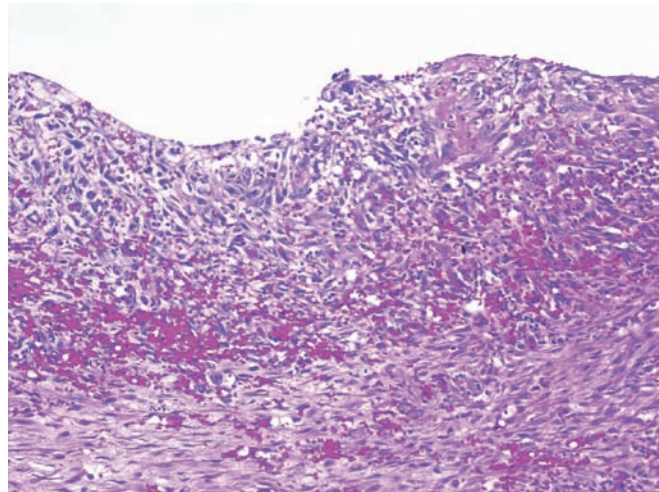
Figure 3.40 — Paraduodenal wall cyst (groove pancreatitis). A nonspecific picture with histiocytes and inflammatory cells in a mucoid background is present. No other cellular component is seen. The diagnosis can be difficult and is dependent on excluding other nonneoplastic entities (such as pseudocyst) and cystic neoplasms. (Papanicolaou stain, low power)
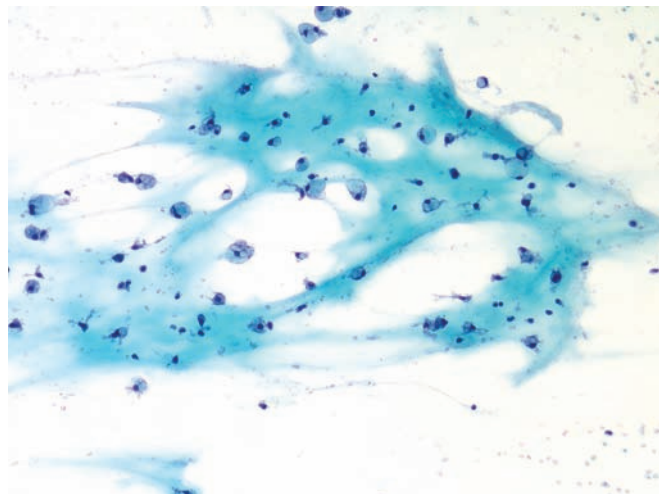
Paraduodenal Wall Cyst
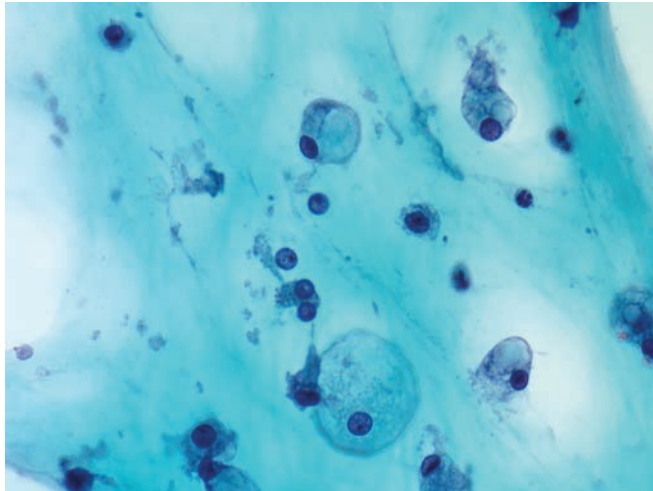
Figure 3.41 — Paraduodenal wall cyst (groove pancreatitis). Histiocytes and rare lymphocytes in a mucoid background are seen. Histiocytes with clear or vacuolated cytoplasm differ from signet ring cell carcinoma by their small round or ovoid nuclei, which lack the prominent nucleoli of a carcinoma. (Papanicolaou stain, high power)
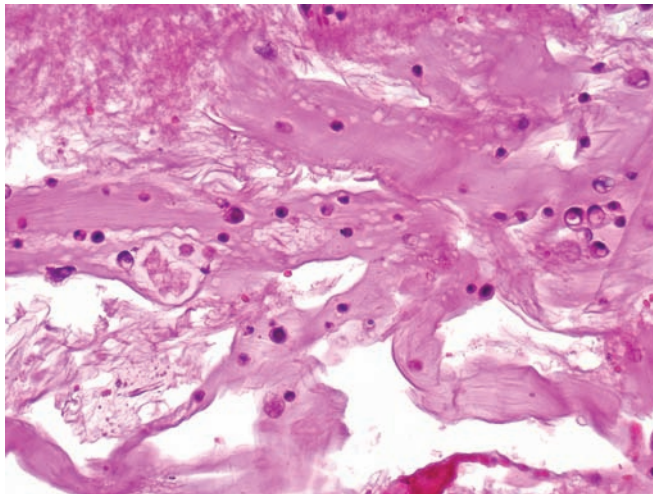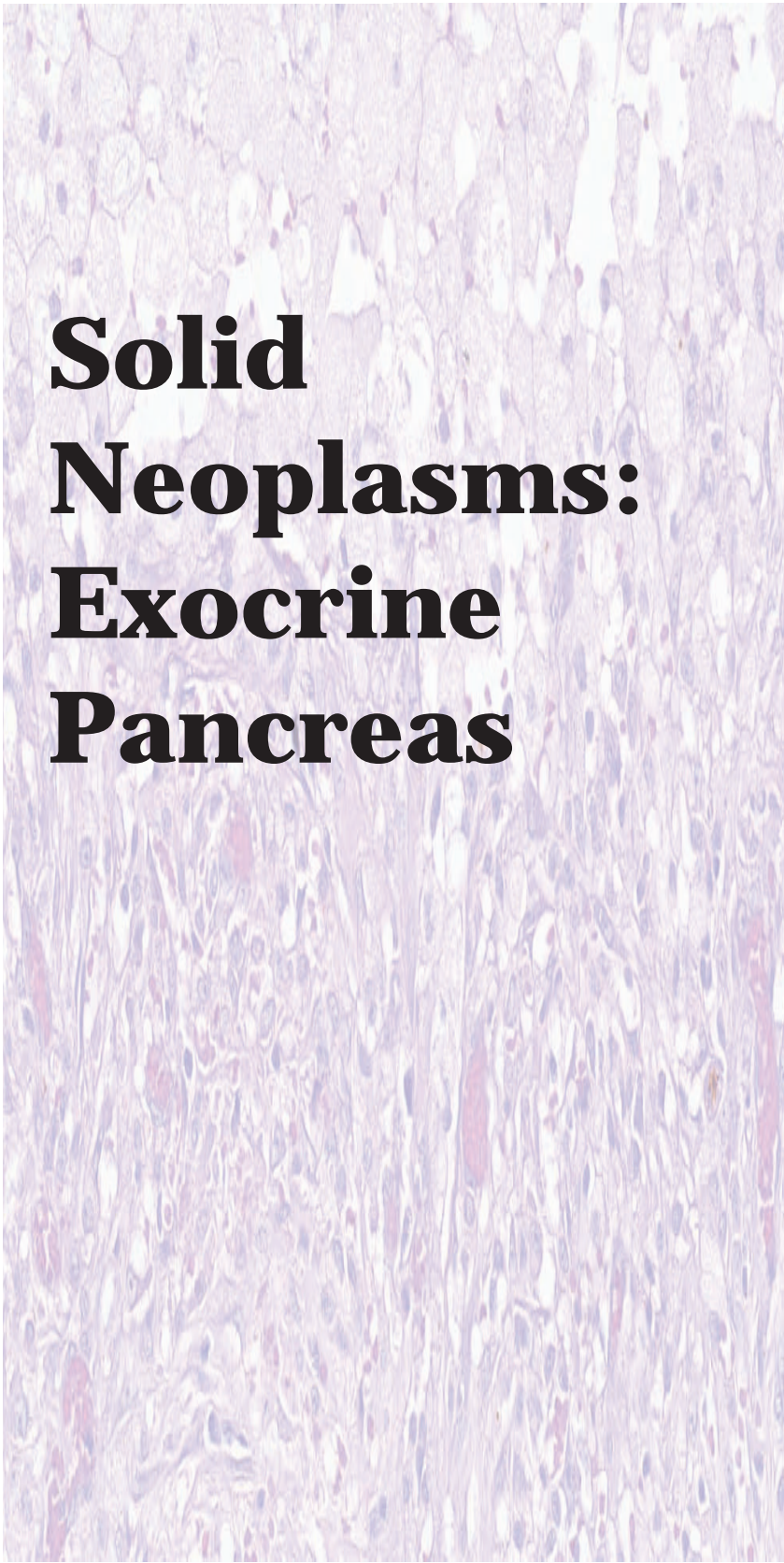
Figure 3.42 — Paraduodenal wall cyst (groove pancreatitis). Cell block section displays histiocytes and inflammatory cells in a thick mucoid background. Differential diagnosis in cases with limited radiologic information may include a pancreatic pseudocyst and less often, a cystic mucinous neoplasm. (Hematoxylin and eosin stain, low power)

Solid Neoplasms: Exocrine Pancreas

4

Ductal Adenocarcinoma
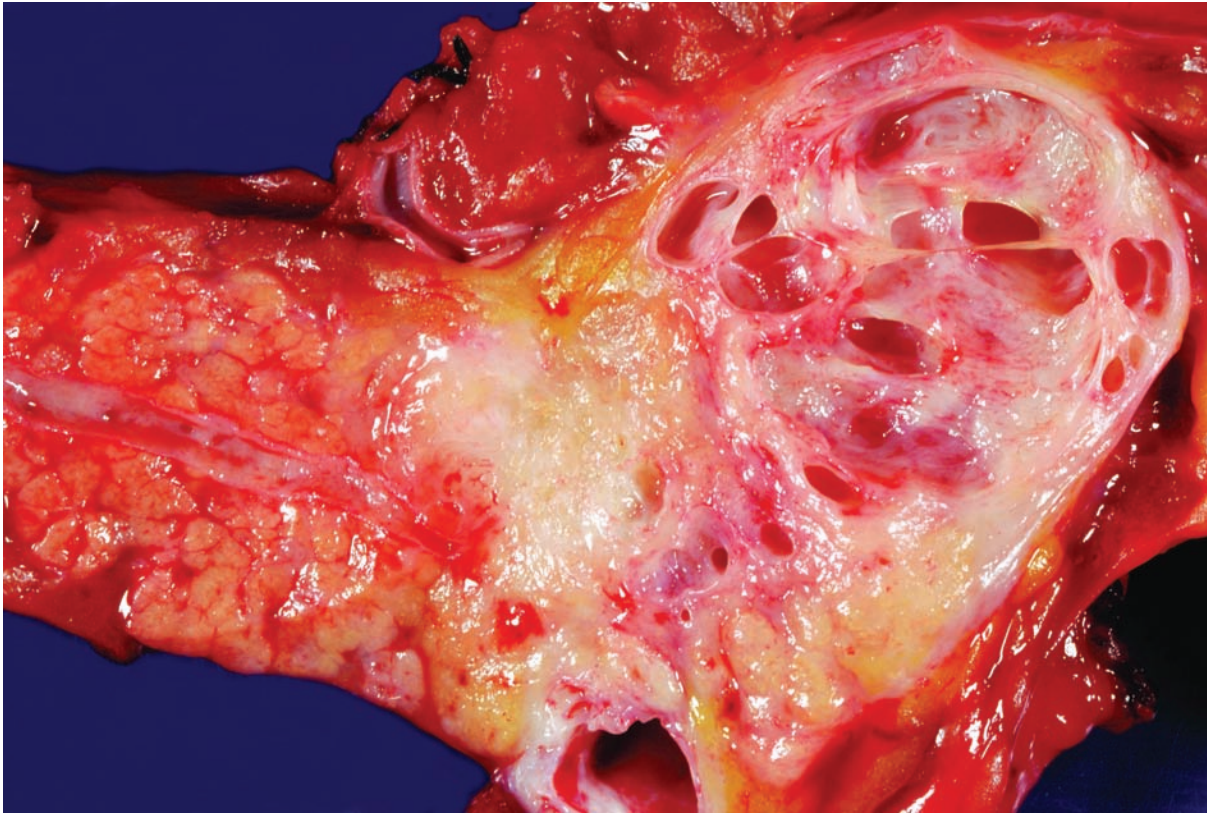
Figure 4.1 — Infiltrating ductal adenocarcinoma in the tail of the pancreas. Note the normal pancreatic parenchyma downstream from the mass (left), the relatively small sclerotic, poorly demarcated carcinoma in the center of the field, and the large retention cysts upstream from the carcinoma (right). This gross appearance is almost diagnostic of an infiltrating ductal adenocarcinoma, but focal chronic pancreatitis and other neoplasms of the pancreas, such as the well-differentiated pancreatic endocrine neoplasm, should be considered in the differential diagnosis.

Ductal Adenocarcinoma
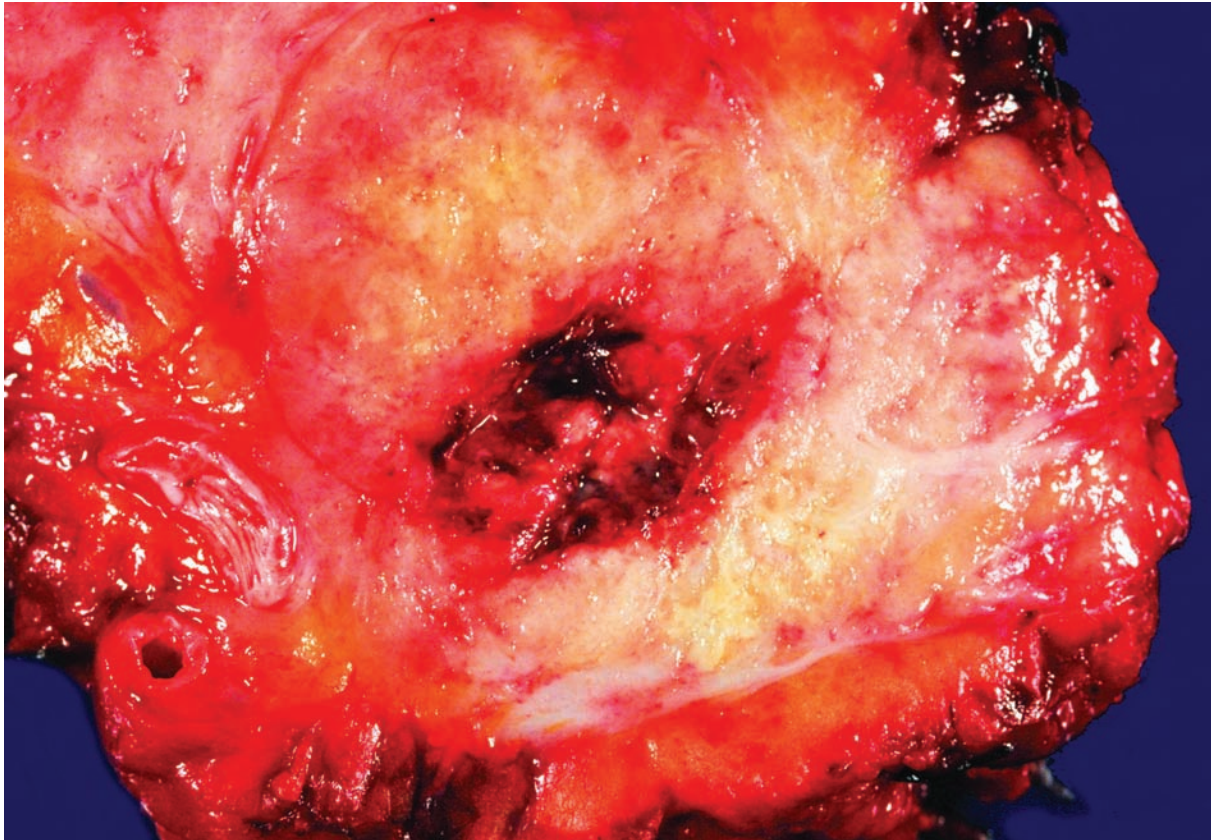
Figure 4.2 — Infiltrating ductal adenocarcinoma. As in Figure 4.1, this neoplasm forms a sclerotic, poorly defined mass. This carcinoma is large and has an area of central necrosis that forms a cyst. Cystic change in an infiltrating ductal adenocarcinoma can mimic a cystic neoplasm of the pancreas such as a mucinous cystic neoplasm (well-defined thick-walled cysts containing mucin) or an intraductal papillary mucinous neoplasm (the cysts communicate with a large pancreatic duct).

Ductal Adenocarcinoma

Figure 4.3 — Infiltrating ductal adenocarcinoma. Three features stand out at low magnification. The relatively low neoplastic cellularity and abundant desmoplastic reaction are characteristic of ductal adenocarcinoma. The third feature, the haphazard arrangement of the glands, is an extremely useful diagnostic finding. Chronic pancreatitis, which would have a lobular arrangement of the glands, tops the differential diagnosis. (Frozen section stained with hematoxylin and eosin, low power)
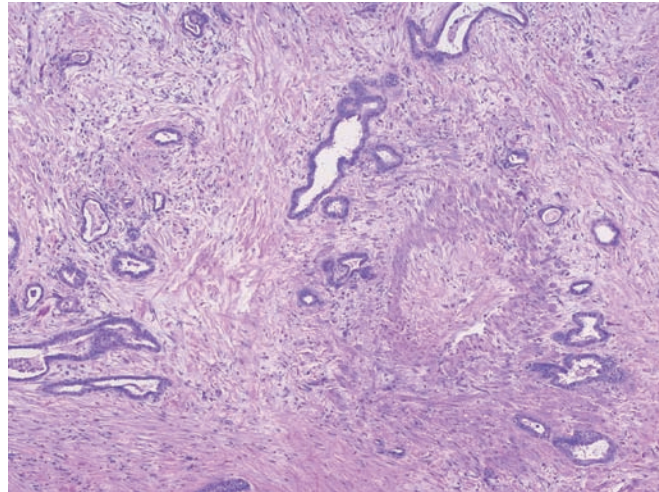
Figure 4.4 — Infiltrating ductal adenocarcinoma. A well-differentiated gland is adjacent to a vessel. Glands are normally located at the center of pancreatic lobules, while the muscular vessels are found at the periphery. The finding of a gland, even a well-differentiated gland, immediately adjacent to muscular vessel, suggests a violation of the normal lobular architecture of the pancreas and is therefore strongly suggestive of an infiltrating ductal adenocarcinoma. (Frozen section stained with hematoxylin and eosin, high power)
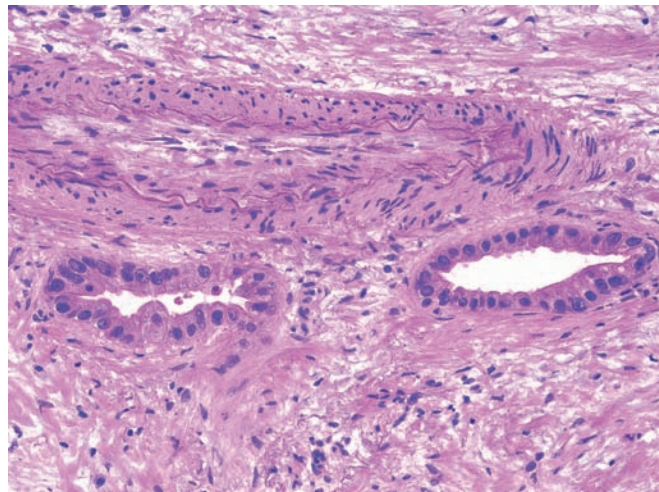
Figure 4.5 — Infiltrating ductal adenocarcinoma. Perineural invasion, as demonstrated in this case, is virtually diagnostic of an infiltrating ductal adenocarcinoma. Benign endocrine cells and, extremely rarely, benign glands can abut a nerve in cases of severe chronic pancreatitis. In these cases immunolabeling for endocrine markers and the overall pattern of growth of the glands can help establish the correct diagnosis. (Frozen section stained with hematoxylin and eosin, high power)
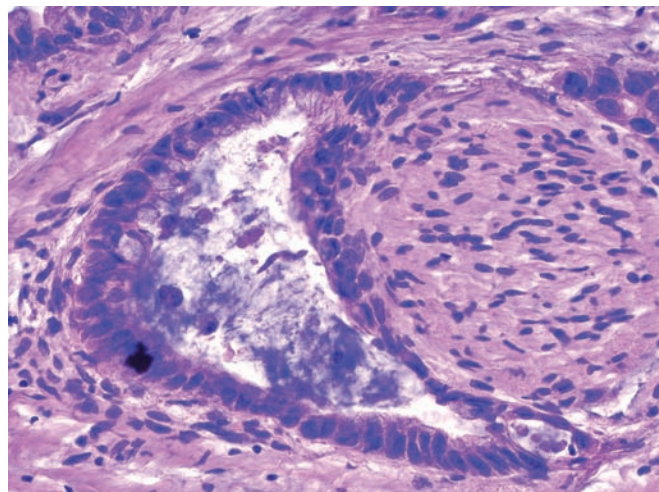
Ductal Adenocarcinoma
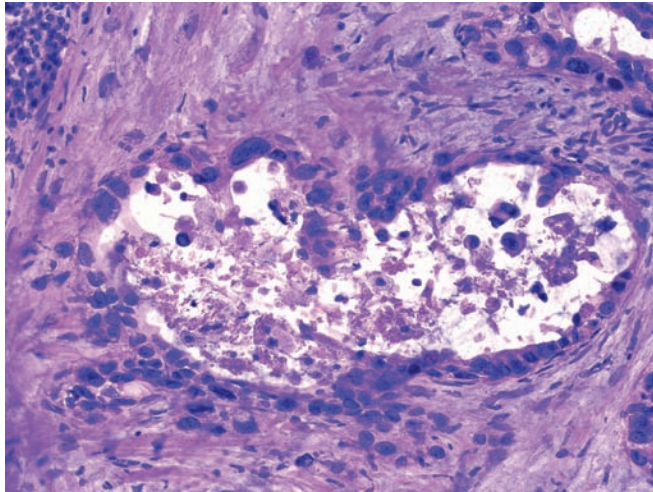
Figure 4.6 — Infiltrating ductal adenocarcinoma. This field highlights three features of infiltrating ductal adenocarcinoma: luminal necrosis, incomplete lumina (the lumen directly abuts stroma without any intervening epithelium), and the "4-to-1 rule" (variation in the nuclear area of cells lining a lumen of more than four to one). Other diagnostic features of an infiltrating carcinoma include vascular and perineural invasion, a haphazard growth pattern, and a gland immediately adjacent to a muscular vessel. (Frozen section stained with hematoxylin and eosin, high power)
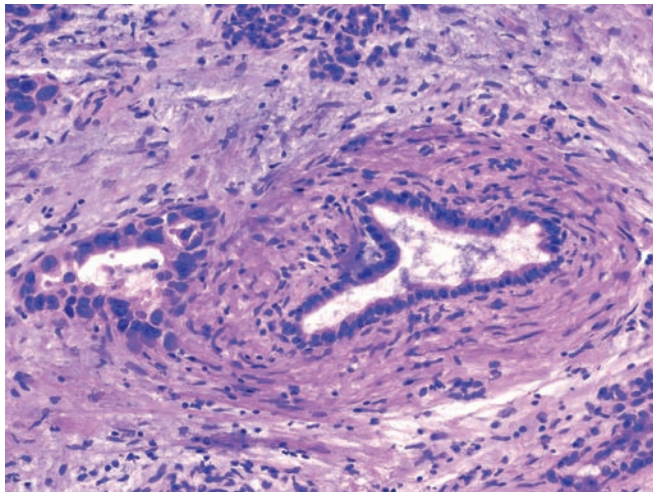
Figure 4.7 — Infiltrating ductal adenocarcinoma. Vascular invasion and a gland immediately adjacent to a muscular vessel, as shown in this field, are both features of an infiltrating ductal adenocarcinoma. Note how the neoplastic cells have replaced the endothelial cells and line the inner surface of the vessel (right), mimicking pancreatic intraepithelial neoplasia. When this happens the thick muscular wall can be used to establish that the neoplastic cells are in a vessel (see Figure 4.8). (Frozen section stained with hematoxylin and eosin, high power)
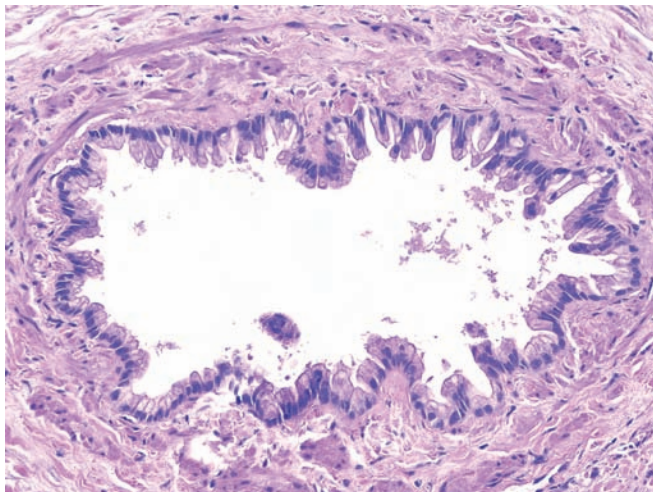
Figure 4.8 — Infiltrating ductal adenocarcinoma. In this focus of vascular invasion, the neoplastic cells have completely relined the vessel. This pattern of vascular invasion can mimic a pancreatic intra-epithelial neoplasia (PanIN) lesion. The muscular wall helps establish this as a focus of vascular invasion and not a PanIN. (Hematoxylin and eosin, medium power)

Ductal Adenocarcinoma

Figure 4.9 — Pancreatic carcinoma metastatic to the ovary. Immunolabeling for DPC4 (SMAD4) demonstrating the complete loss of DPC4 in the neoplastic cells and retention of DPC4 expression in the non-neoplastic stroma. In a patient with a history of pancreatic cancer and an ovarian mass, the loss of DPC4, bilateral involvement of the ovaries, and size of the ovarian neoplasm greater than 10 cm all support the diagnosis of a carcinoma of the pancreas metastatic to the ovary over a separate ovarian primary. (Immunolabeling for DPC4, high power)
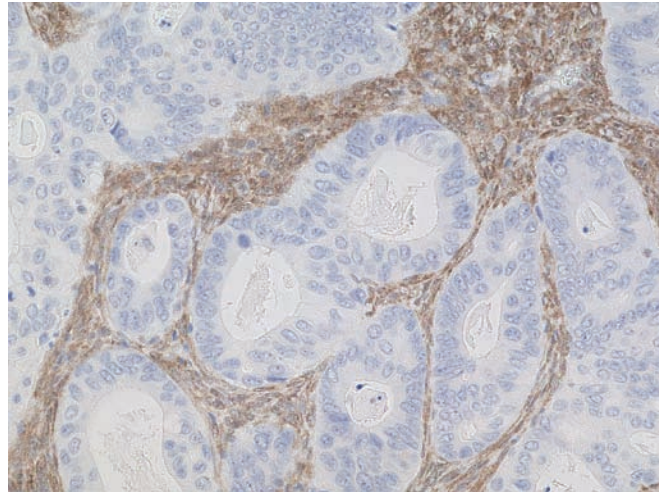
Figure 4.10 — Well-differentiated adenocarcinoma. A large tissue fragment of ductal-type epithelium, which is composed of cells with enlarged uniform ovoid nuclei, is noted. Such well-differentiated carcinomas can often be exceedingly difficult to diagnose in cases with limited cellularity. (Diff Quik stain, low power)
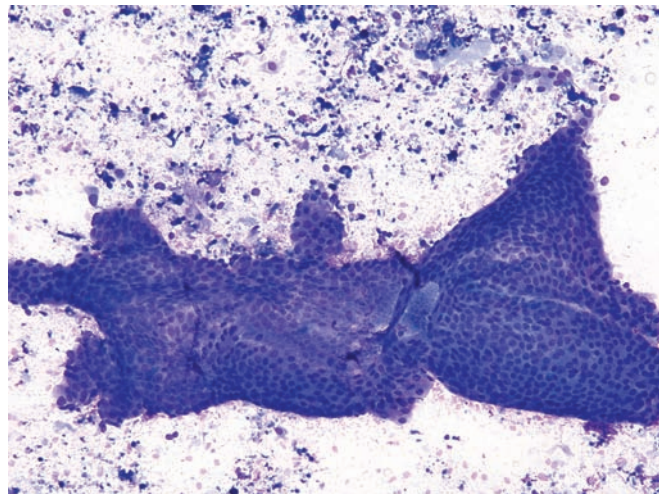
Figure 4.11 — Well-differentiated adenocarcinoma. The normal architecture (honeycomb appearance) is only slightly disturbed. The background cellular debris and scattered degenerated cells with atypical nuclei. The cells within the fragment show mild anisonucleosis but have markedly elevated N/C ratios. Reactive atypia (such as in some cases of chronic pancreatitis) should be carefully excluded in such cases. (Diff Quik stain, medium power)
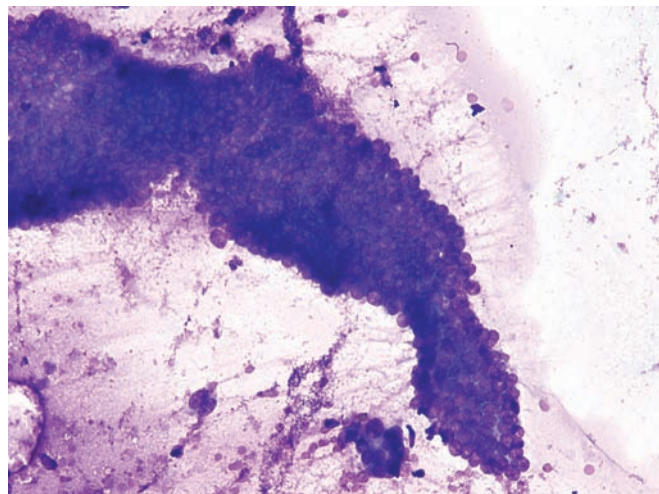
Ductal Adenocarcinoma
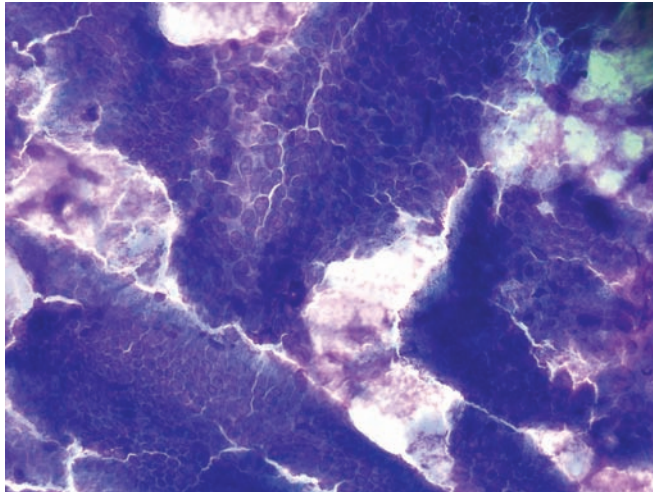
Figure 4.12 — Well-differentiated adenocarcinoma. Note the several large tissue fragments of atypical columnar epithelium. The lower fragment has features similar to reactive columnar epithelium. The architecture is fairly well preserved, with tall columnar epithelium present at the periphery. There is, however, nuclear enlargement, crowding, and overlapping. The fragment above has features consistent with a well-differentiated adenocarcinoma. Note the markedly enlarged nuclei with prominent nucleoli and irregular nuclear borders. There is also apparent loss of normal "honeycomb" architecture. (Diff Quik stain, high power)
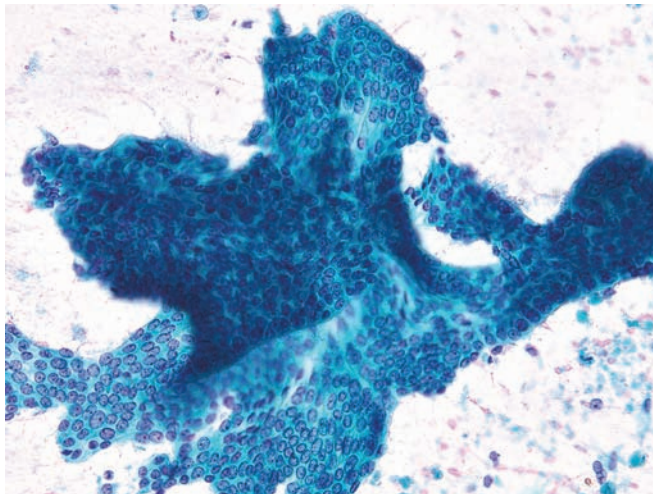
Figure 4.13 — Well-differentiated adenocarcinoma. Two monolayer tissue fragments of ductal-type epithelium, one superimposed on top of the other, are observed. The large fragment has a papillary-like configuration. The cells have ovoid nuclei with bland chromatin and small, single nucleoli. N/C ratio is increased. There are foci of cellular crowding with variations in the size of the nuclei. Differential diagnosis would include reactive epithelial atypia in chronic pancreatitis. (Papanicolaou stain, low power)
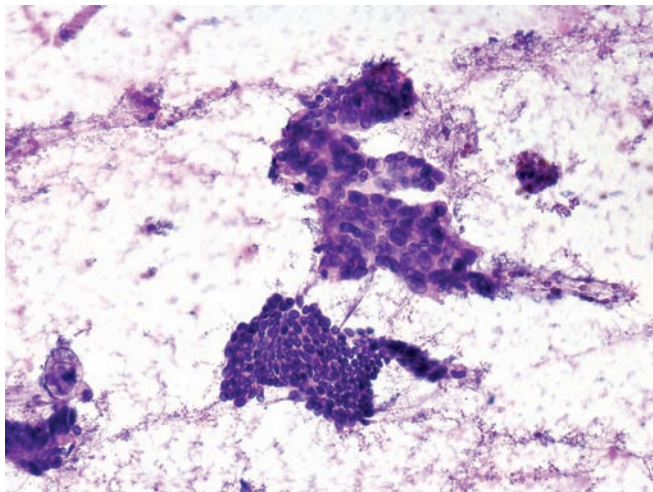
Figure 4.14 — Well-differentiated adenocarcinoma. Two tissue fragments in the center have distinctly different morphology. The lower fragment shows only minimal deviation from normal ductal epithelium with slightly increased nuclear size and N/C ratio. The upper fragment shows clear features of malignancy. The normal "honeycomb" appearance is lost, but glandular differentiation is recognized, with acinar formations and luminal borders formed by atypical columnar cells. Neoplastic cells vary in size but are generally large and contain oval or round nuclei with moderate-to-high N/C ratio. (Diff Quik stain, low power)

Ductal Adenocarcinoma

Figure 4.15 — Well-differentiated adenocarcinoma.
Two tissue fragments of ductal-type epithelium with enlarged nuclei and small nucleoli are present. Cellular atypia and architectural changes are minimal but definitely present and are beyond what typically would be seen in a reactive process (such as epithelial atypia in chronic pancreatitis). (Papanicolaou stain, medium power)
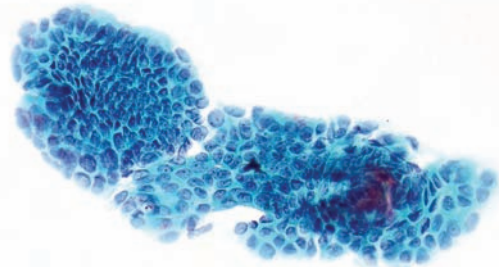
Figure 4.16 — Well-differentiated adenocarcinoma.
Atypical columnar epithelial cells, some with secretory vacuoles forming an acinus, are seen. Note the enlarged nuclei, some with irregular borders and irregular cell distribution. Cellular debris (possibly necrosis) is seen in the smear background. Such findings are highly suspicious for an adenocarinoma. A definitive diagnosis however would require evaluating more cells. (Papanicolaou stain, medium power)
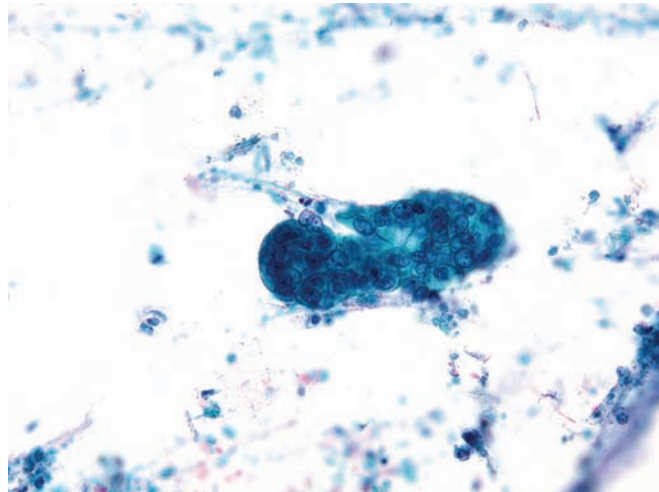
Figure 4.17 — Well-differentiated adenocarcinoma.
Monolayer fragments of columnar epithelium with minimal nuclear enlargement and overlap/crowding. There is some resemblance to intestinal epithelium. Irregular acinar formations distinguish them from the latter. Abundant degenerated blood and necrosis is present as well. Abundant gastrointestinal tract contamination, obscuring blood and thick mucin can make such diagnoses extremely difficult to render. (Papanicolaou stain, low power)
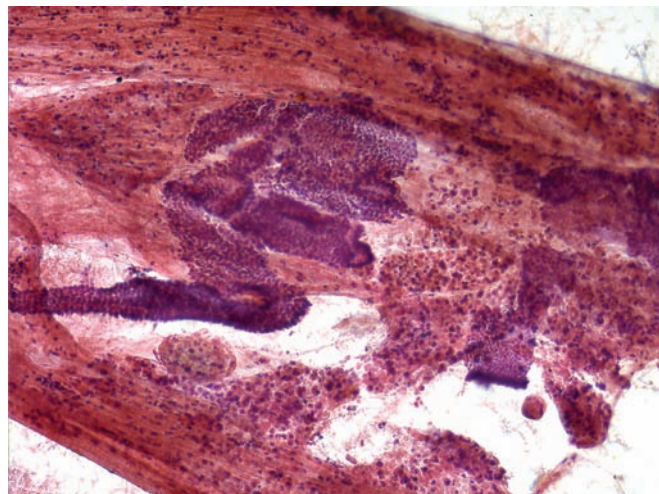
Ductal Adenocarcinoma
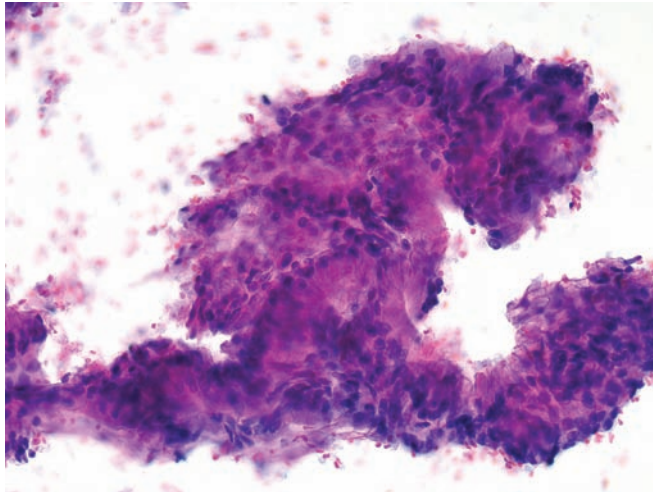
Figure 4.18 — Well-differentiated adenocarcinoma. Strips of atypical columnar epithelium with somewhat cleared cytoplasm, which contains mucin, are present. At the upper right there are back-to-back, small glandular formations. There is no significant cellular atypia. Abnormal architecture is the main evidence of cancer. (Papanicolaou stain, high power)
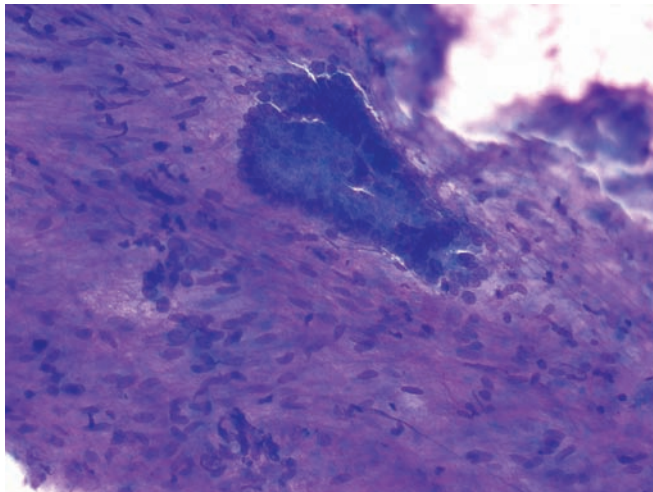
Figure 4.19 — Well-differentiated adenocarcinoma. A tissue fragment composed of several back-to-back glandular formations. This is a typical example of a well-differentiated adenocarcinoma. Tall columnar neoplastic cells contain large, oval, basally located nuclei. They have a vesicular chromatin pattern, slight nuclear border irregularities, and occasional grooves. Focal nuclear crowding and overlapping are also observed. (Diff Quik stain, low power)
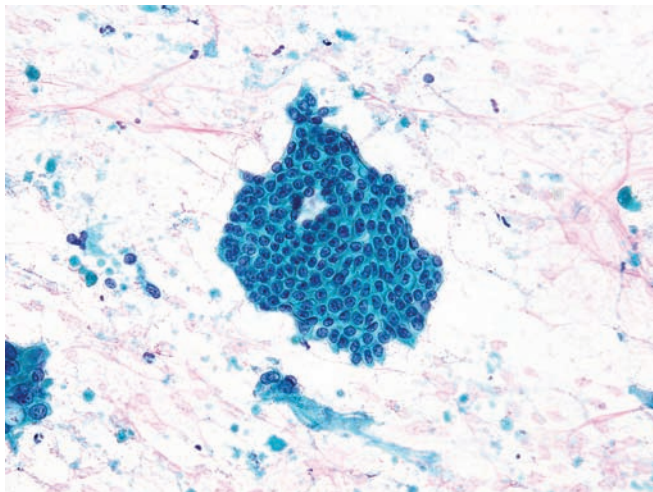
Figure 4.20 — Well-differentiated adenocarcinoma. Atypical monolayer tissue fragment showing minimal architectural and individual cellular changes. These changes include focal crowding and disorderly grouping of the cells along with variation in size of the nuclei and nuclear cytoplasmic relation (e.g., location, N/C ratio), rare grooves, and inconspicuous nucleoli. Also note degenerated neoplastic cells and some necrotic debris in the background. (Papanicolaou stain, low power)

Ductal Adenocarcinoma

Figure 4.21 — Well-differentiated adenocarcinoma.
Two atypical tissue fragments are present. Normal architecture is lost. Crowded, overlapping nuclei that vary in size and shape are seen. A small shred of fibrous tissue and abundant background mucin are noted as well. Chronic pancreatitis with associated epithelial atypia should be carefully excluded in such cases. (Papanicolaou stain, high power)
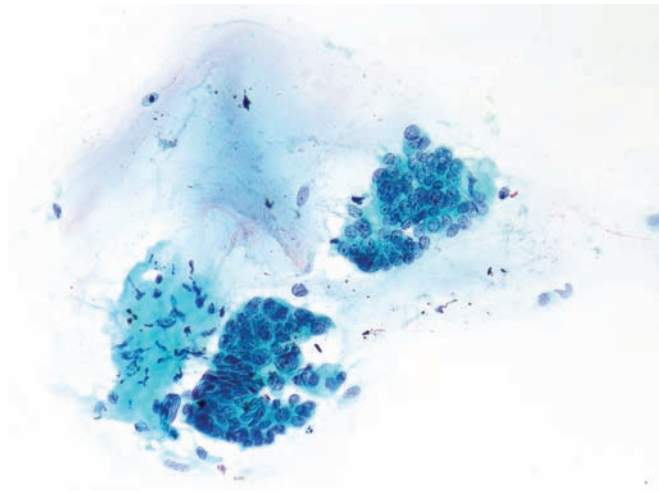
Figure 4.22 — Well-differentiated adenocarcinoma.
Marked variation in nuclear size and shape, nuclear location, and the amount of cytoplasm (N/C ratio) in a tissue fragment, as shown here, are reliable features of malignancy. They are especially helpful in the diagnosis of adenocarcinoma without apparent nuclear changes (e.g., hyperchromasia, irregular chromatin distribution, marked irregularities of nuclear border). (Papanicolaou stain, high power)
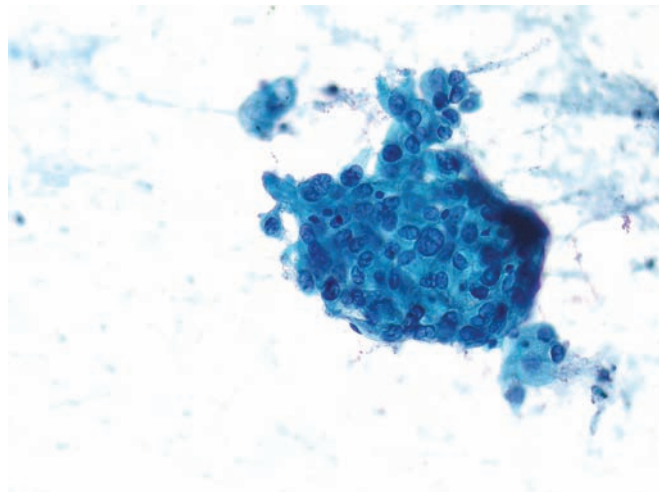
Figure 4.23 — Well-differentiated adenocarcinoma.
A large tissue fragment of atypical ductal epithelium is seen. Nuclear atypia is minimal. Neoplastic cells have enlarged round or ovoid nuclei with uniformly bland chromatin and small nucleoli. The diagnostic features here are loss of the uniform honeycomb pattern, patchy crowding, and more widely spaced areas caused by variation in N/C ratio and the location of the nuclei among the neoplastic cells. (Papanicolaou stain, medium power)
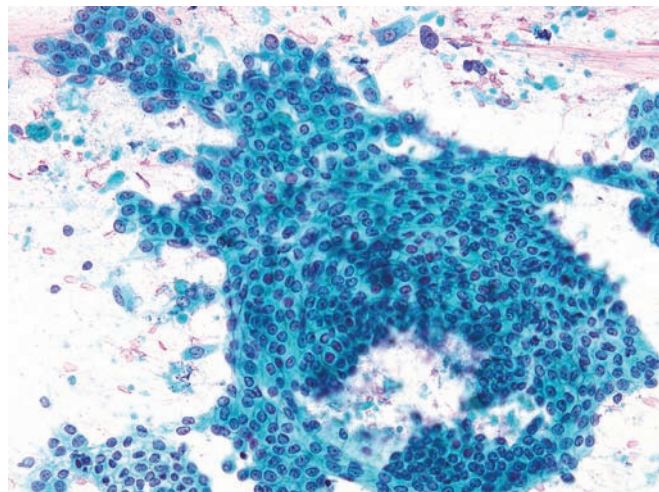
Ductal Adenocarcinoma
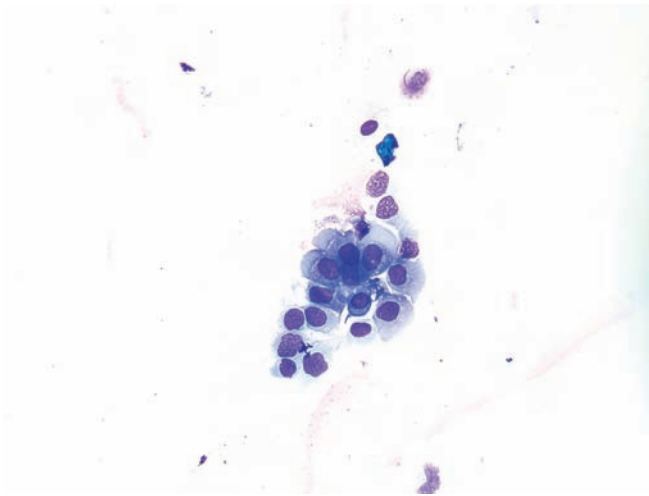
Figure 4.24 — Well-differentiated adenocarcinoma. A loose group of single neoplastic cells is noted. Most have moderate amounts of cytoplasm and round or ovoid nuclei with markedly irregular nuclear borders. Although these cells should raise a strong suspicion of a carcinoma, a definitive diagnosis of cancer should not be made without additional evidence. (Diff Quik stain, high power)
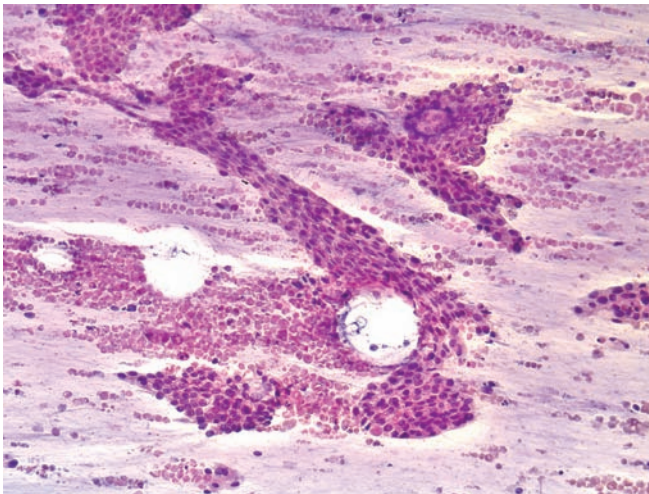
Figure 4.25 — Well- to moderately differentiated adenocarcinoma. Several atypical epithelial tissue fragments are present in a mucinous background with innumerable necrotic cells. There is a slight variation in nuclear size and chromasia and minimal disturbance of cellular architecture. A cytopathologic diagnosis of malignancy can be difficult in cases with limited cellularity. (Papanicolaou stain, low power)
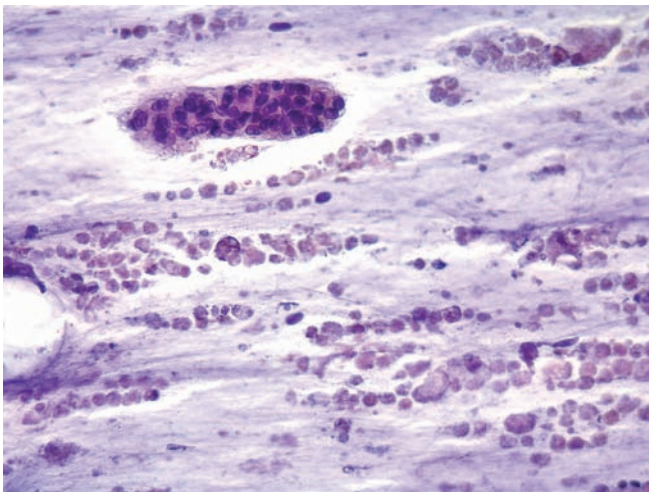
Figure 4.26 — Moderately differentiated adeno-carcinoma. An atypical tissue fragment in a mucoid background with extensive necrotic cellular debris is present. Atypical cells have large, moderately hyperchromatic nuclei with irregular borders and indistinct cytoplasmic borders. Abnormal cellular architecture with irregular distribution of cells, nuclear crowding, and overlapping, along with cellular atypia, is diagnostic for carcinoma. One area of gland-like formation and the suggestion of a luminal border (upper margin of the fragment) are consistent with an adenocarcinoma. (Papanicolaou stain, medium power)

Ductal Adenocarcinoma

Figure 4.27 — Moderately differentiated adenocarcinoma. Two small tissue fragments of neoplastic cells with glandular features are seen. Neoplastic cells with large hyperchromatic nuclei and moderate amounts of cytoplasm form back-to-back small, disorganized glands. (Hematoxylin and eosin stain, medium power)
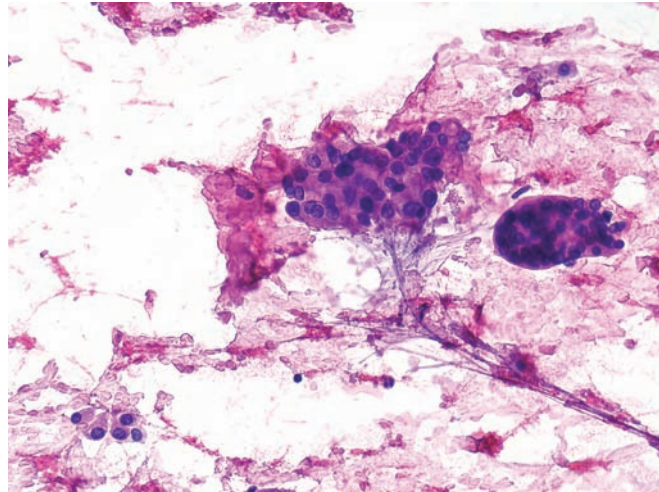
Figure 4.28 — Moderately differentiated adenocarcinoma. A large hypercellular tissue fragment of tumor with glandular differentiation is observed. Although glandular differentiation by the neoplastic cells is apparent, the overall organization of the fragment is disturbed. The nuclei are enlarged with moderately hyperchromatic nuclei and conspicuous nucleoli. (Hematoxylin and eosin stain, high power)
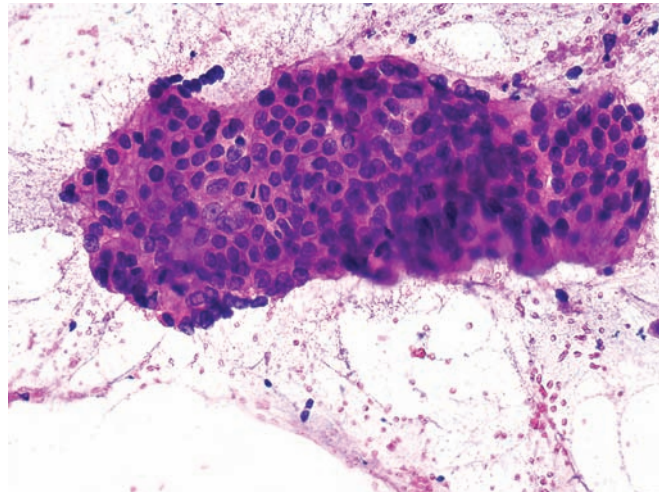
Figure 4.29 — Moderately differentiated adenocarcinoma. Loose aggregates of neoplastic cells with large nuclei, occasional nuclear grooves, and prominent nucleoli are admixed with cells with small nuclei and back-to-back acinar formations. The former cells are clearly neoplastic; the latter probably represent a better differentiated area of the tumor. (Hematoxylin and eosin stain, high power)
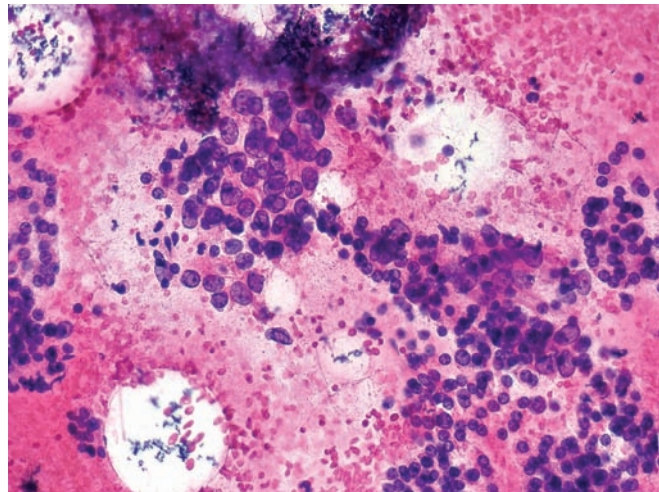
Ductal Adenocarcinoma
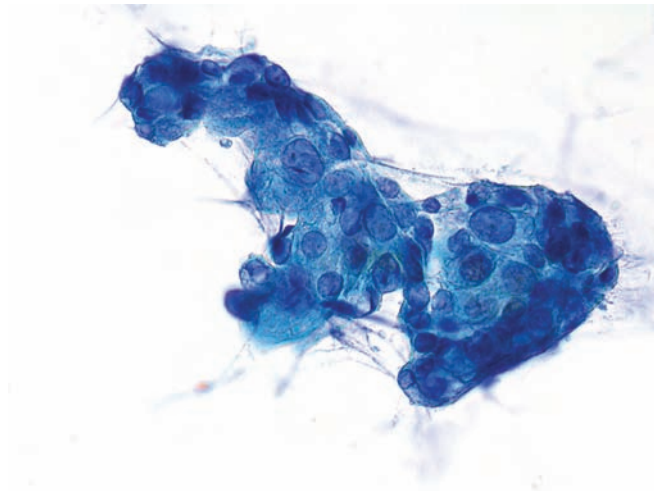
Figure 4.30 — Moderately differentiated adenocarcinoma. Neoplastic cells in this tissue fragment have markedly enlarged nuclei with significant variation in size and shape. In the upper left area of the fragment, the formation of an acinus and luminal border indicates glandular differentiation. (Papanicolaou stain, high power)
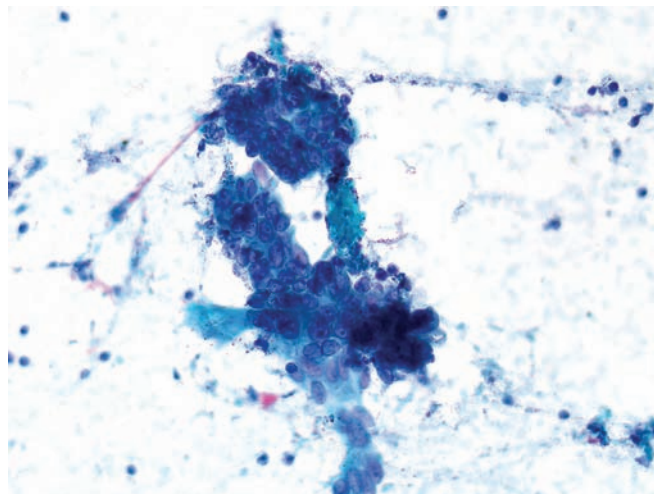
Figure 4.31 — Moderately differentiated adenocarcinoma. Two hypercellular tissue fragments are composed of neoplastic cells that have large nuclei with small to prominent nucleoli and bland chromatin. Cellular crowding with nuclear overlapping is apparent. The presence of luminal spaces in the crowded areas and atypical tall columnar epithelium indicate glandular differentiation. (Papanicolaou stain, medium power)
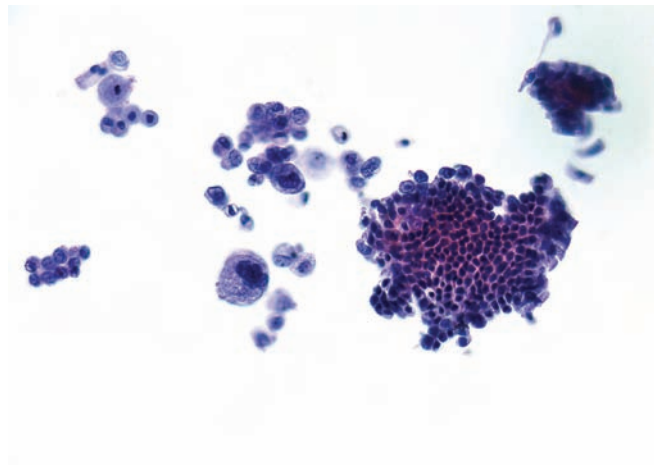
Figure 4.32 — Moderately differentiated adenocarcinoma. This predominantly cystic lesion shows two tissue fragments, several smaller groups of cells, and a single atypical epithelial cell. The cells have varying morphology, centrally or eccentrically located nuclei with scant or abundant cytoplasm. The larger tissue fragment has a benign appearance, but there are focal atypical changes in the lower border, and several markedly atypical cells are attached to the upper border. (Papanicolaou stain, low power)

Ductal Adenocarcinoma

Figure 4.33 — Moderately differentiated adenocarcinoma. Two tissue fragments and single neoplastic cells are noted. Marked pleomorphism and disorganization indicate the malignant nature of the lesion. Glandular differentiation is less apparent. A few cells at the edge of the fragments have a columnar shape, basally located nuclei, and flat "luminal" borders, indicating glandular differentiation. (Diff Quik stain, medium power)
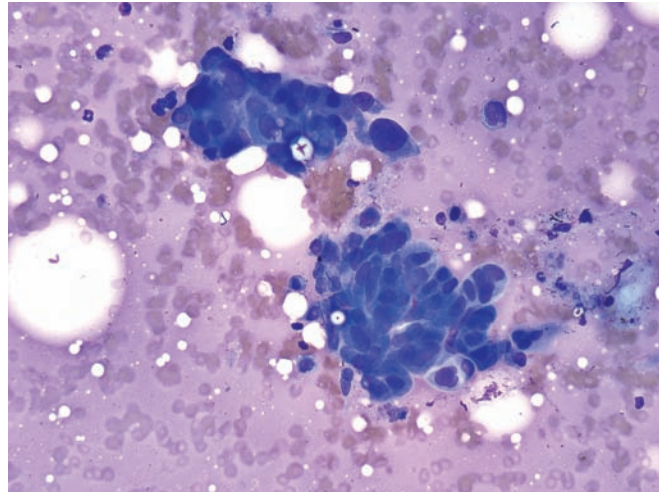
Figure 4.34 — Moderately differentiated adenocarcinoma. Several loosely attached tissue fragments and a multinucleated neoplastic cell can be seen. Neoplactic cells have enlarged nuclei with a uniform chromatin pattern. Most have single or double prominent nucleoli. Columnar differentiation is seen in the upper border of the large fragment. (Papanicolaou stain, high power)
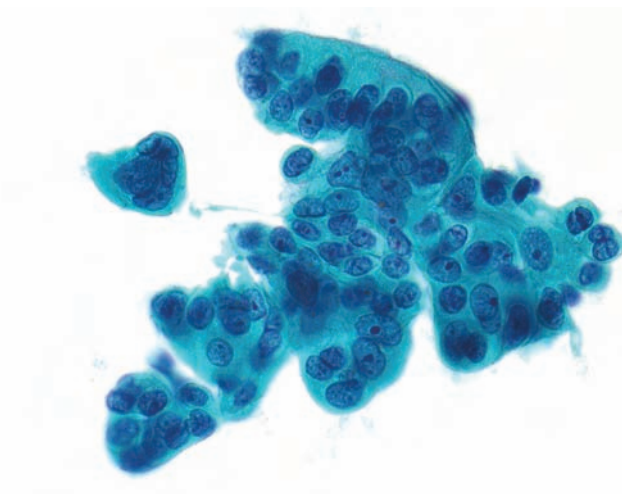
Figure 4.35 — Moderately differentiated adenocarcinoma. Malignant features here are subtle and mostly based on individual cell atypia. In the upper fragment, these features are marked variation in nuclear size, variation in N/C ratio, and irregular cellular distribution. Neoplastic cells have uniformly distributed chromatin and small nucleoli. Most nuclei have evenly thickened, smooth nuclear borders. One cell, at 3 o'clock, has a sharp indentation in the nuclear envelope. The lower fragment, which is composed of poorly preserved atypical columnar cells, also shows prominent nucleoli. (Papanicolaou stain, high power)
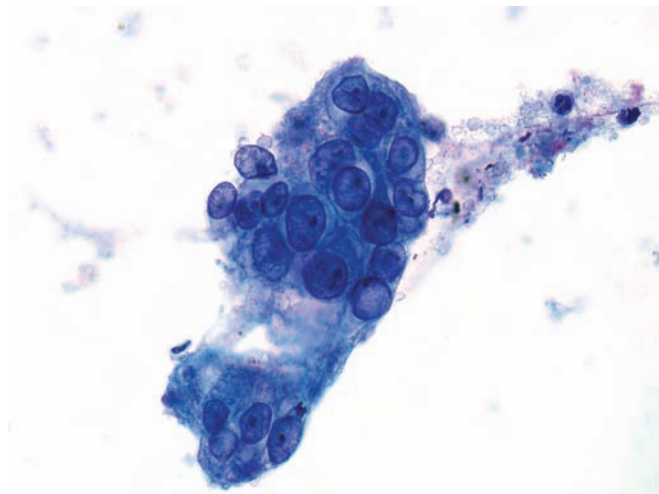
Ductal Adenocarcinoma
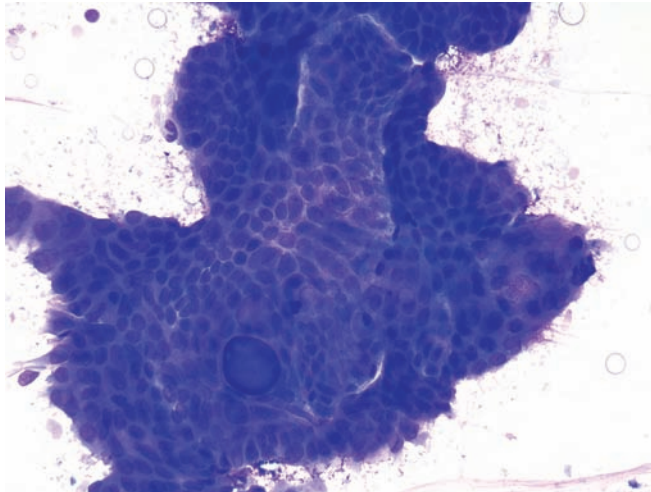
Figure 4.36 — Moderately differentiated adenocarcinoma. A large epithelial tissue fragment composed of cells with enlarged ovoid nuclei and bland chromatin pattern. The normal organization of the ductal epithelium is markedly disturbed. One acinus filled with secretion is present. Variations in the nuclear orientation and N/C ratio are more apparent at the margins of the fragment. (Diff Quik stain, medium power)
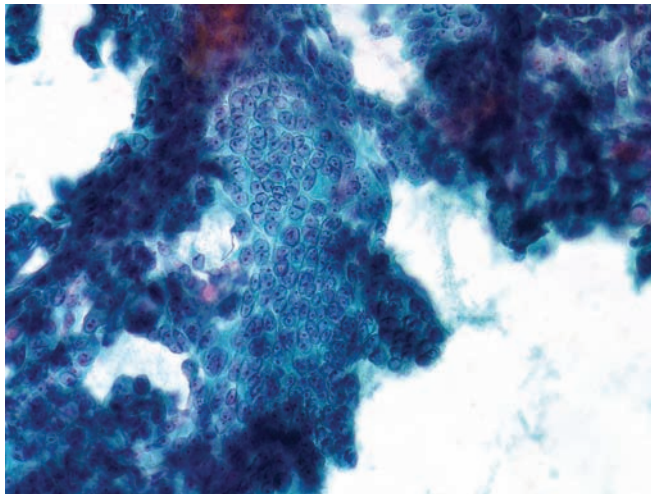
Figure 4.37 — Well-to moderately differentiated adenocarcinoma. A hypercellular tissue fragment with overcrowded nuclei is seen. Uniformly enlarged round or oval nuclei have one or two micronucleoli and a bland chromatin pattern. In the areas of tightly packed nuclei, cytoplasmic outlines are invisible imparting syncytial appearance. Columnar differentiation with luminal border is seen at the margin of the fragment (3 o'clock). Differential diagnosis includes benign proliferative changes with atypia. Large atypical tissue fragments with this morphology are unusual for benign reactive/proliferative changes. However, in limited material, such as a few small fragments, a definitive cancer diagnosis requires further morphologic evidence of malignancy. As always, clinical and radiologic correlation would help to establish the diagnosis in borderline cases. (Papanicolaou stain, high power)

Ductal Adenocarcinoma

Figure 4.38 — Moderately differentiated adenocarcinoma. A large epithelial tissue fragment in an extensively necrotic background is noted. The cells have moderately enlarged, ovoid nuclei with bland chromatin and one or two micronucleoli. Architectural changes include markedly increased cellularity and several gland-like formations in the fragment. The atypical tissue fragment, observed in a necrotic background containing markedly atypical degenerated cells, is diagnostic of a carcinoma. (Papanicolaou stain, low power)
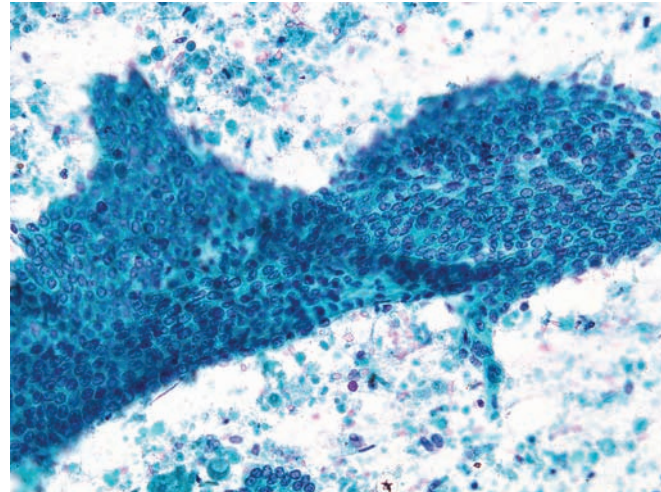
Figure 4.39 — Moderately differentiated adenocarcinoma. A large folded tissue fragment of ductal-type neoplastic epithelium is present. Hyperchromatic large nuclei with irregular borders are seen in the lower position of the fragment. The cytomorphologic features are well-developed and an interpretation of adenocarcinoma is quite straight forward in such cases. (Papanicolaou stain, medium power)
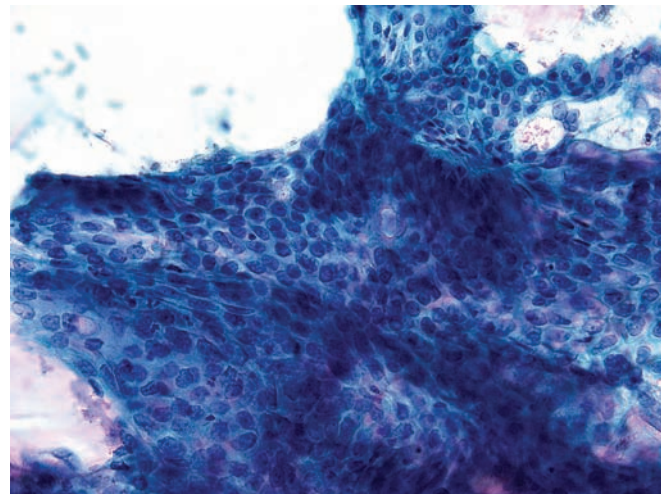
Figure 4.40 — Moderately differentiated adenocarcinoma. Note the hypercellularity with marked nuclear enlargement, focal nuclear overlapping, crowding and occasional prominent nucleoli. There is marked anisonucleosis. Several acinar formations, some containing mucin, are also present. The cytomorphalogic characteristics seen here are diagnostic of an adenocarcnoma, even in a limited sample. (Papanicolaou stain, high power)
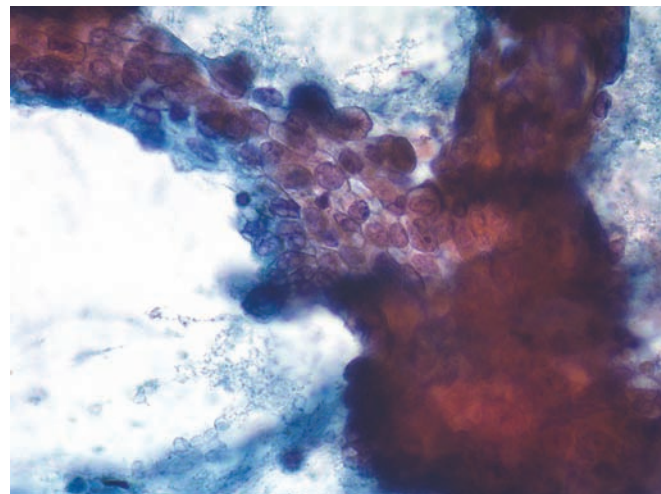
Ductal Adenocarcinoma
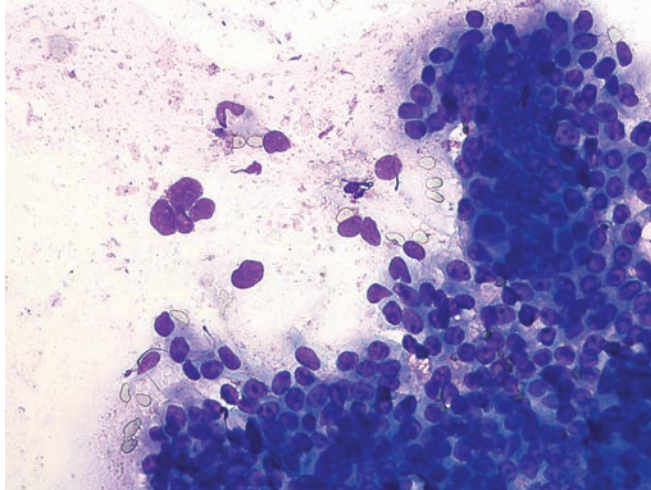
Figure 4.41 — Moderately differentiated adenocarcinoma. This smear contains tissue fragments, cellular aggregates, and single tumor cells. On the right-hand side, the majority of the neoplastic cells have large round or ovoid nuclei with prominent nucleoli. Cytoplasmic borders are indistinct. Cellular organization varies from rosette-like formations to disorganized crowding of the cells. Some neoplastic cells have columnar configurations. There is also a group of pleomorphic, naked nuclei, which appear to represent degenerated neoplastic cells and which look similar to the nuclei of the malignant cells in the crowded groups. (Diff Quik stain, high power)
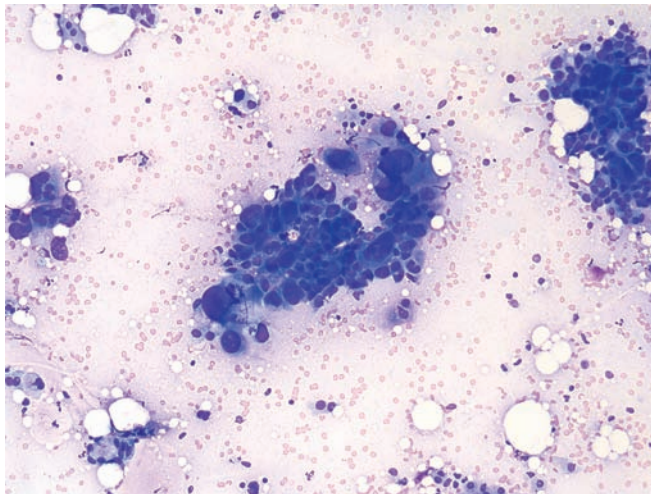
Figure 4.42 — Poorly differentiated adenocarcinoma. These neoplastic cells vary markedly in size and shape and have a significantly high N/C ratio. There is no evidence of glandular differentiation. Diagnosis in such cases is usually not difficult. However, other primary cancers (such as variants of ductal carcinoma and acinar cell carcinoma) should be considered in the differential diagnosis. (Diff Quik stain, low power)
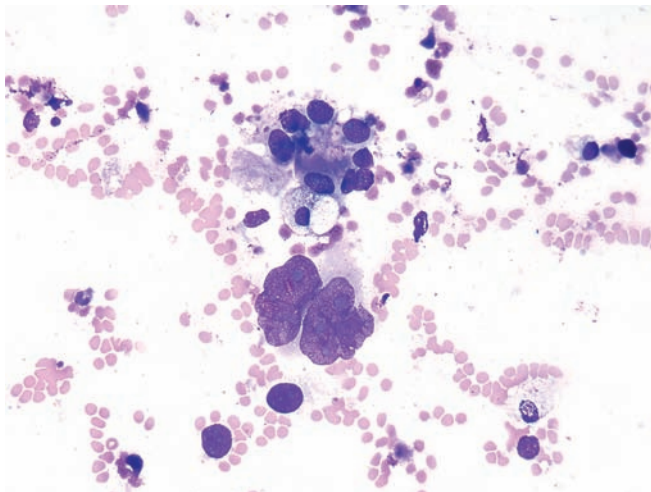
Figure 4.43 — Poorly differentiated adenocarcinoma. In addition to neoplastic cells with bizarre markedly enlarged nuclei and macronucleoli, better differentiated tumor cells form an acinus. (Diff Quik stain, high power)

Ductal Adenocarcinoma

Figure 4.44 — Poorly differentiated adenocarcinoma. The large pleomorphic glandular cells display extreme pleomorphism. Nuclei are hyperchromatic with irregular nuclear membranes ("Idaho potato-like"). Few intracytoplasmic mucin vacuoles are seen, and there is extensive background necrosis containing karyorrhectic nuclear debris. (Papanicolaou stain, high power)
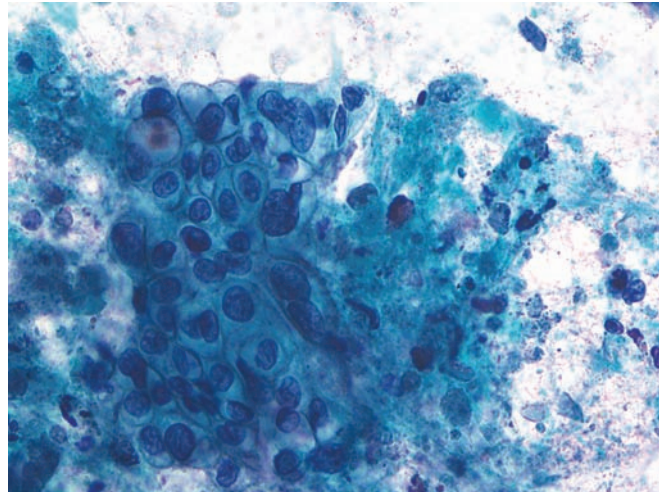
Figure 4.45 — Poorly differentiated adenocarcinoma (cell block section). A neoplastic tissue fragment is associated with large necrotic areas. Neoplastic cells have large, pleomorphic nuclei and macronucleoli. Two partial lumen formations are present in the upper portion of the fragment. (Hematoxylin and eosin stain, medium power)
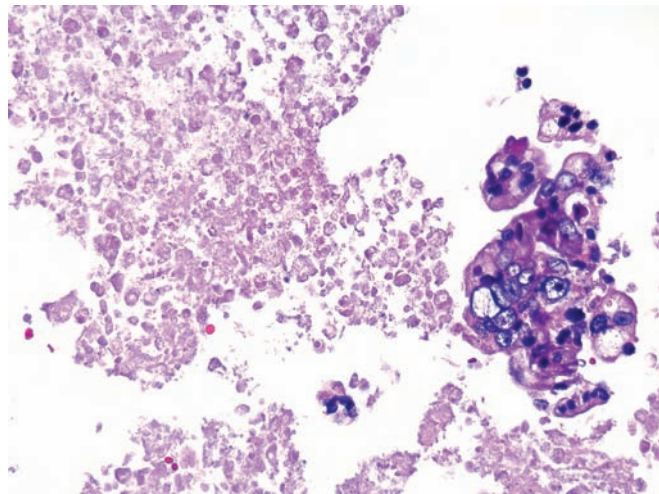
Figure 4.46 — Poorly differentiated adenocarcinoma (cell block section). Another tissue fragment from the same tumor, shown in Figure 4.45, is seen at higher magnification. Malignant cellular features as well as degenerative changes are quite apparent. Although some of the nuclear changes, such as thickened and irregular nuclear borders, irregular clumping, and clearing of chromatin and hyperchromasia, can be caused by degeneration, extreme variation in the size of the nuclei as well as nuclear cytoplasmic relation (location of nucleus, N/C ratio) and disorganized architecture of the tissue establish the definitive diagnosis of cancer. The presence of intracytoplasmic vacuoles with eccentrically located nuclei suggests glandular differentiation, but similar changes may occur in degeneration. Mucin stains are needed to confirm the secretory nature of the intracytoplasmic vacuoles. (Hematoxylin and eosin stain, high power)
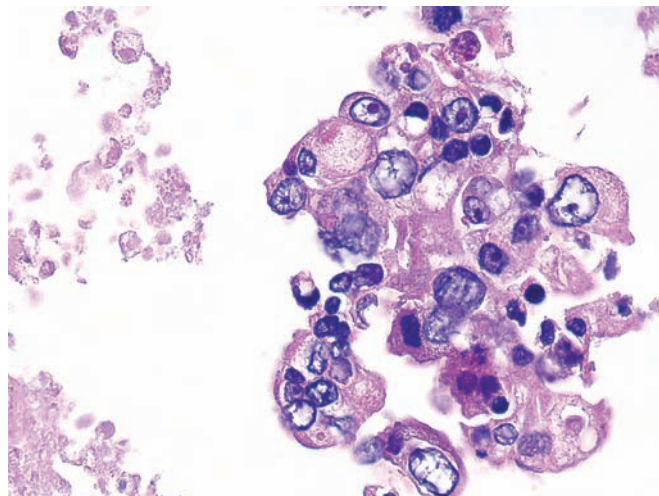
Ductal Adenocarcinoma
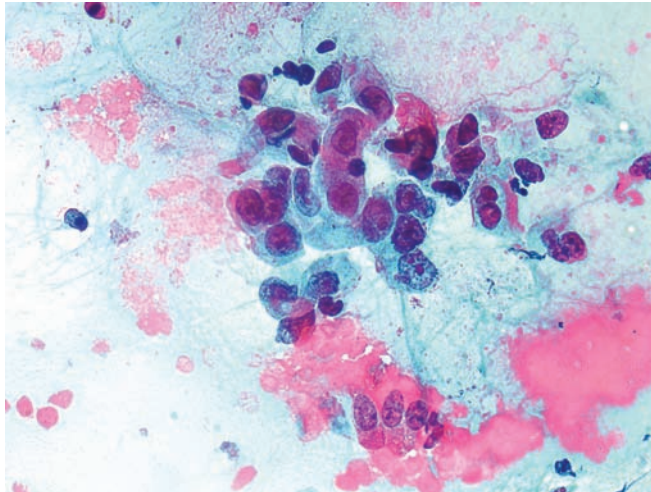
Figure 4.47 — Poorly differentiated adenocarcinoma. A group of neoplastic cells with enlarged nuclei, macronucleoli, and moderate amounts of cytoplasm is present. Several neoplastic cells have columnar-shaped cytoplasm with basally located nuclei suggestive of glandular differentiation. (Papanicolaou stain, high power)
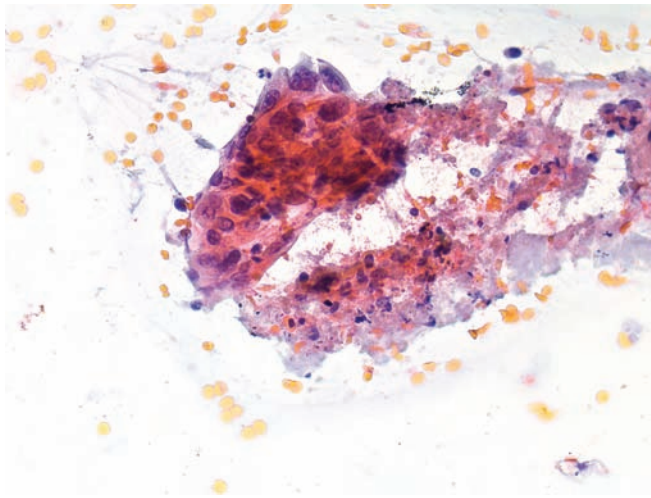
Figure 4.48 — Poorly differentiated adenocarcinoma. A tissue fragment of tumor cells is seen. Note the nuclear pleomorphism, disorganization and focal necrosis. The cytoplasmic orangeophilia is a manifestation of air-drying artifact and should not be confused with keratinization of these cells. (Papanicolaou stain, high power)
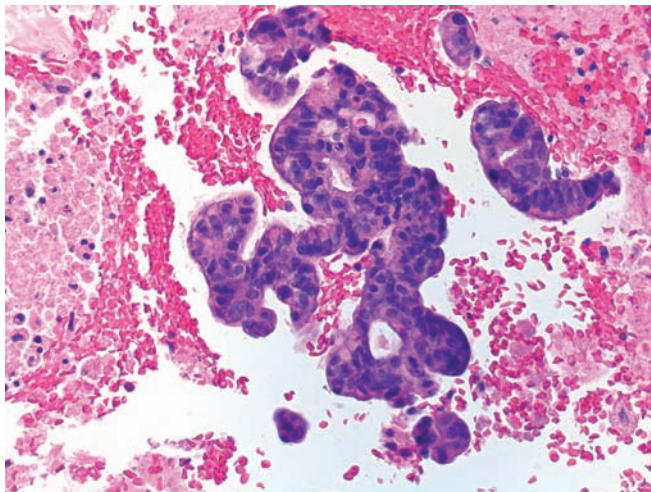
Figure 4.49 — Poorly differentiated adenocarcinoma (cell block section). Atypical, back-to-back glandular formations representing moderately diferentiated components of the tumor are seen. The nuclei are enlarged, hyperchromatic and show prominent stratification. (Hematoxylin and eosin stain, low power)

Ductal Adenocarcinoma

Figure 4.50 — Poorly differentiated adenocarcinoma.
Undifferentiated neoplastic cells form a loosely attached small tissue fragment. There is marked anisonucleosis. This size variation of the malignant cell nuclei is highly predictive of carcinoma when noted within the same tissue fragment. (Diff Quik, high power)
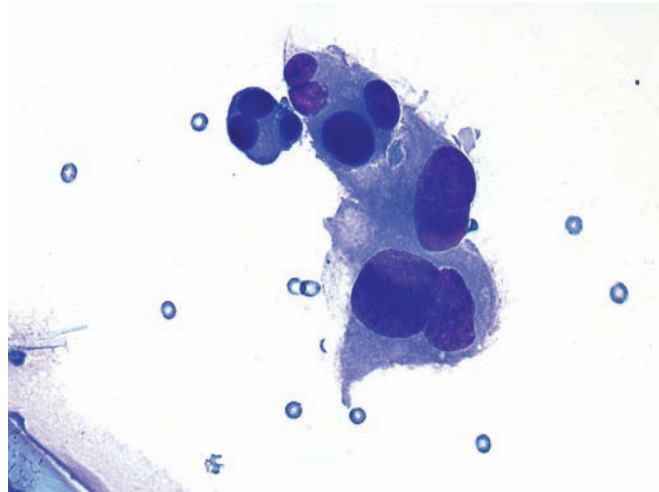
Figure 4.51 — Poorly differentiated adenocarcinoma.
Hypercellular tissue fragments of poorly differentiated columnar epithelium are composed of disorganized neoplastic cells with large, pleomorphic nuclei displaying focal palisading and stratification. Focal areas of luminal borders suggestive of glandular differentiation are present as well as focal necrosis. (Diff Quik stain, medium power)
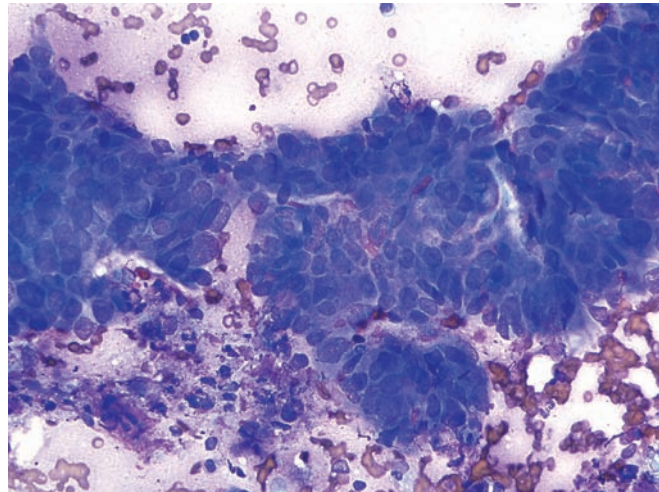
Figure 4.52 — Poorly differentiated adenocarcinoma.
A large tissue fragment of adenocarcinoma is present in the cell block. Although cellular atypia is pronounced here (macronucleoli, marked anisonucleosis), focal glandular differentiation is more readily recognized than the glandular features seen in the previous illustration. (Hematoxylin and eosin stain, medium power)
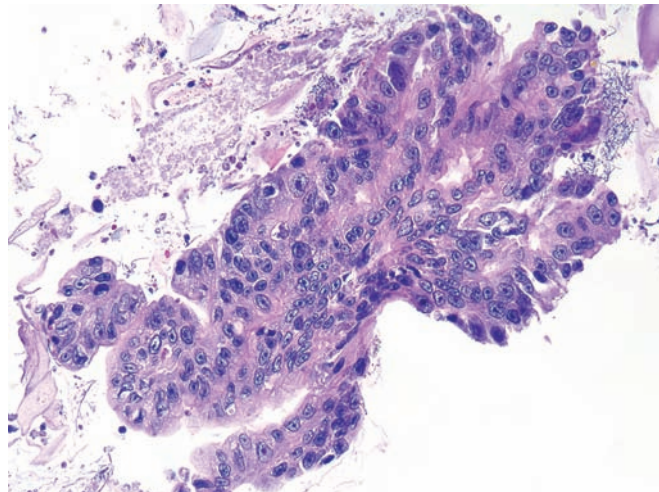
Ductal Adenocarcinoma
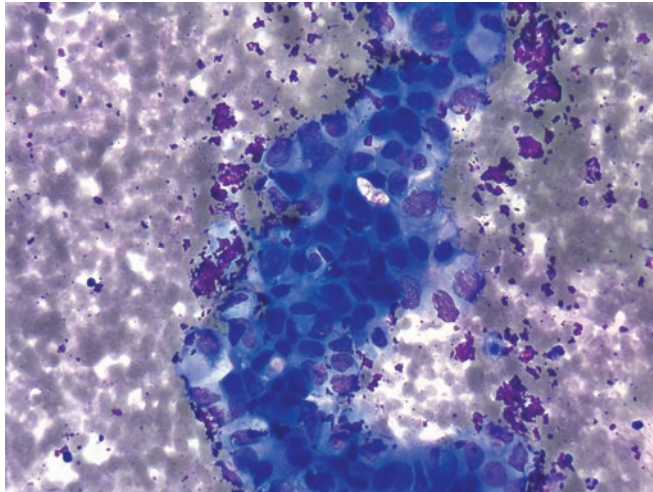
Figure 4.53 — Poorly differentiated adenocarcinoma. A cellular tissue fragment composed of undifferentiated neoplastic cells with large pleomorphic nuclei and prominent nucleoli. Although both the papillary-like configurations with distinct smooth borders and some cells with clear or delicate cytoplasm suggest an adenocarcinoma, no definitive evidence of glandular differentiation is present in this field. (Diff Quik stain, high power)
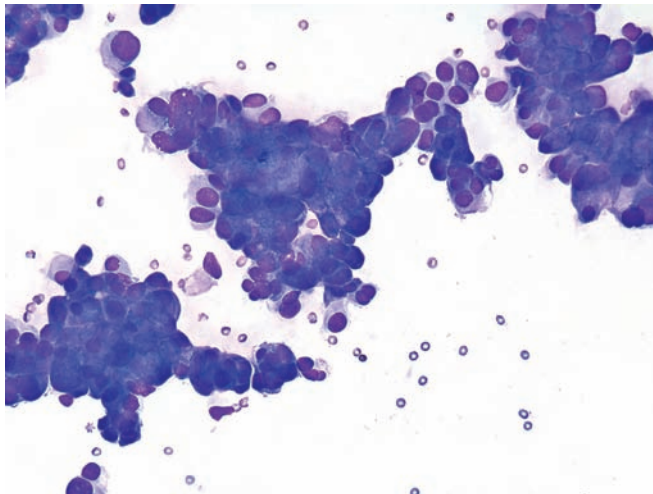
Figure 4.54 — Poorly differentiated adenocarcinoma. These hypercellular tissue fragments are composed of neoplastic cells with large round or ovoid nuclei. Focal nuclear pleomorphism is present. Some single neoplastic cells have eccentrically located nuclei suggestive of glandular differentiation. Columnar differentiation is more clearly seen in the fragment at 2 o'clock. (Diff Quik stain, low power)
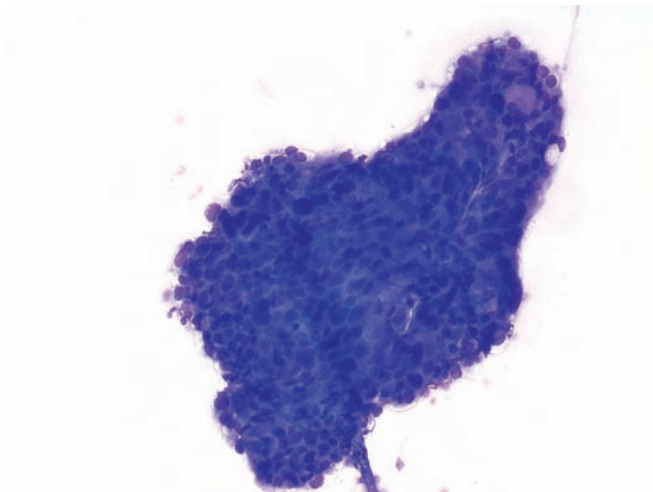
Figure 4.55 — Poorly differentiated adenocarcinoma. A hypercellular tissue fragment composed of neoplastic cells with round or ovoid nuclei, which vary markedly in size. At upper right there is a round, clear area possibly representing a lumen or large secretory vacuole, which is the only evidence of glandular differentiation. (Diff Quik stain, low power)

Ductal Adenocarcinoma

Figure 4.56 — Poorly differentiated adenocarcinoma.
A large irregular tissue fragment with prominent nuclear pleomorphism and disorganization is seen. The only signs of columnar differentiation are the "luminal borders" in the upper right and lower middle portions of the fragment. Poorly differentiated adenocarcinomas often lose the flat monolayered arrangements and appear more crowded and 3-dimensional in their architecture. (Diff Quik stain, high power)
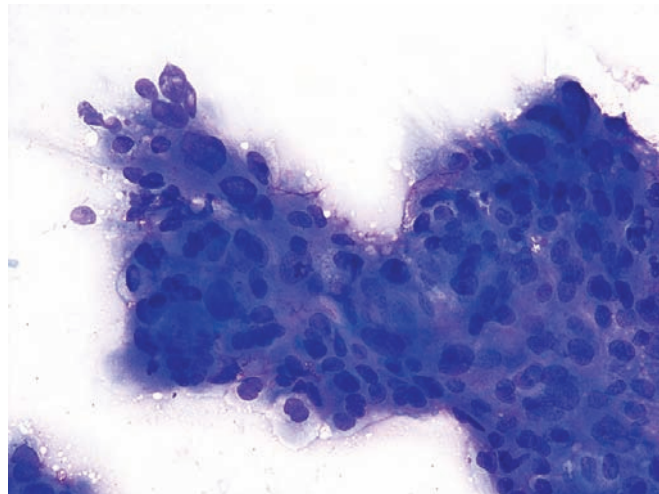
Figure 4.57 — Poorly differentiated adenocarcinoma.
Neoplastic cells forming loose groups and small tissue fragments are observed. Note the haphazard organization of the neoplastic cells, which have markedly enlarged and hyperchromatic nuclei and varying amounts of cytoplasm. A diagnosis of malignancy is rarely an issue when such features are apparent. (Papanicolaou stain, low power)
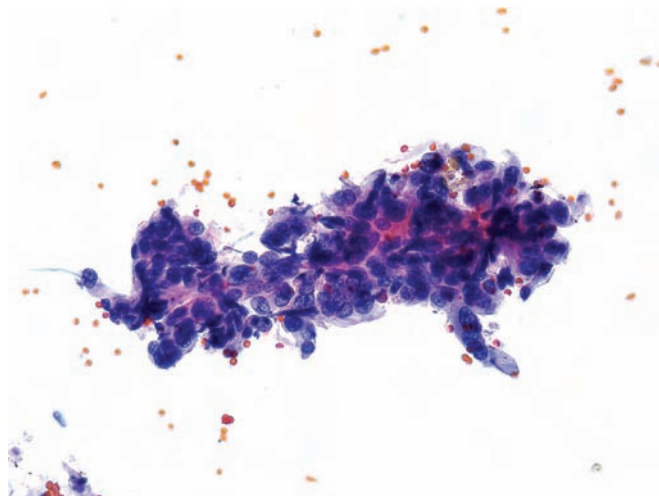
Figure 4.58 — Poorly differentiated adenocarcinoma.
Extensively necrotic tumor is present. Rare viable cells are seen with markedly enlarged pleomorphic nuclei. Extensive necrosis in an untreated pancreatic ductal adenocarcinoma is uncommon and is usually seen in poorly differentiated (high-grade) tumors. (Papanicolaou stain, medium power)
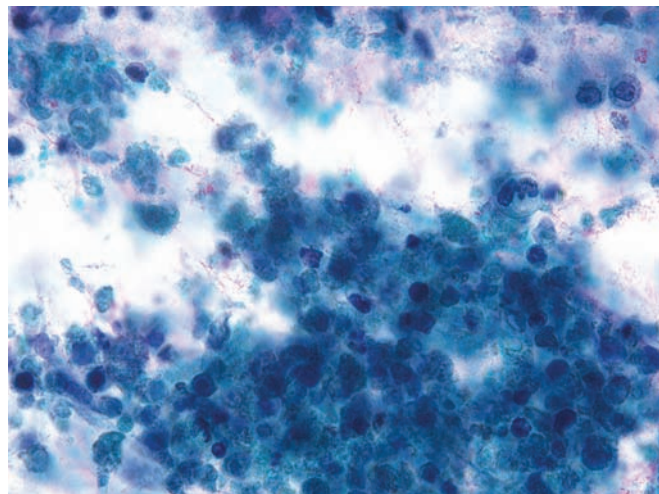
Ductal Adenocarcinoma
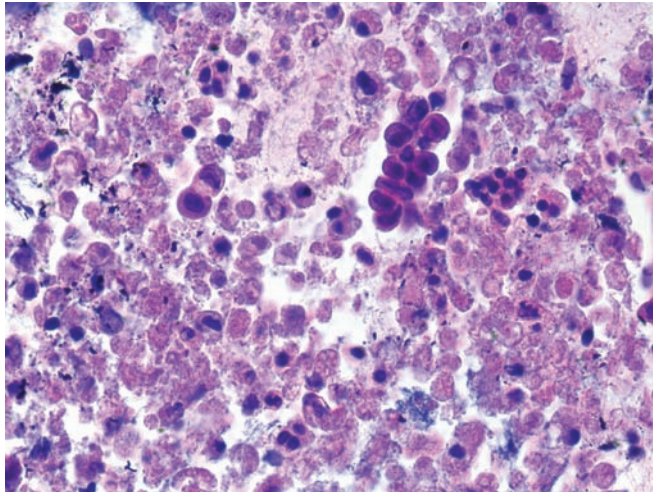
Figure 4.59 — Poorly differentiated adenocarcinoma. The same features are observed in the cell block section as in Figure 4.58. Rare viable tumor cells are noted in an extensively necrotic background. (Hematoxylin and eosin stain, medium power)
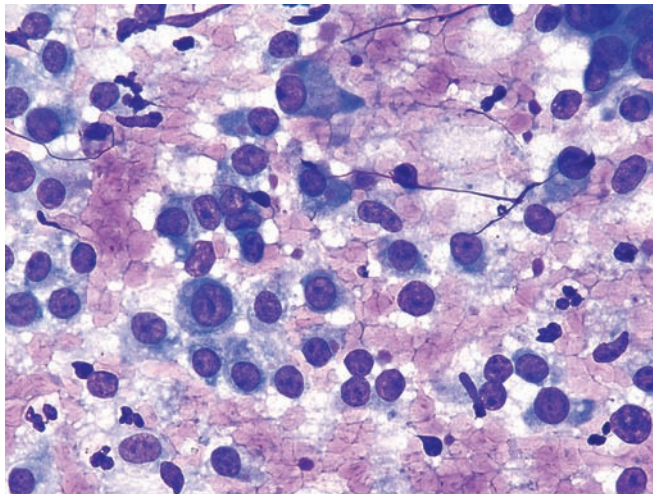
Figure 4.60 — Poorly differentiated adenocarcinoma. Predominantly large atypical single cells consistent with a high-grade malignant neoplasm are noted. Neoplastic cells have large nuclei with coarsely granular chromatin and prominent, irregularly shaped nucleoli. Differential diagnosis would include a number of primary and metastatic cancers (such as a malignant melanoma). (Diff Quik stain, high power)
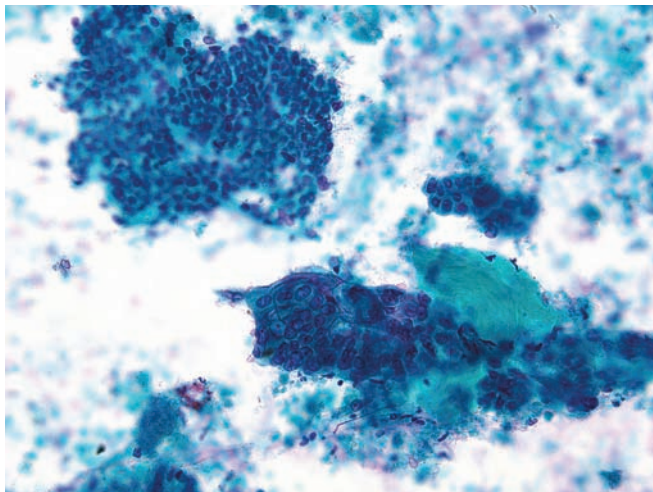
Figure 4.61 — Poorly differentiated adenocarcinoma. Several tissue fragments are present in a necrotic background. In one of the fragments (lower middle), the cells have large round or ovoid nuclei with bland chromatin and conspicuous nucleoli wrapping around a fragment of densely fibrotic tissue. The cells are disorganized, with focal crowding. Some of the cells at the periphery suggest squamous differentiation. (Papanicolaou stain, low power)

Ductal Adenocarcinoma

Figure 4.62 — Poorly differentiated adenocarcinoma.
Fragments of atypical epithelium in a background of fibrous tissue, mucin, and rare single malignant cells are observed. Most fragments have well-defined borders and are composed of disorganized epithelial cells with large nuclei and prominent single or multiple nucleoli. The chromatin pattern is bland. Focal areas of glandular differentiation (luminal border formation and columnar configuration) are present. (Papanicolaou stain, low power)
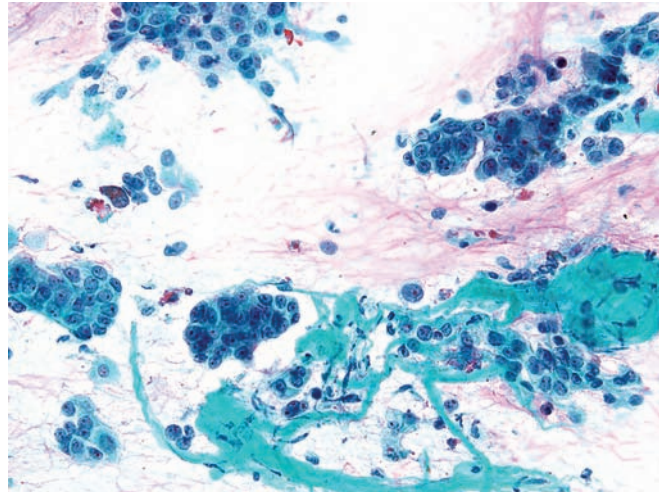
Figure 4.63 — Poorly differentiated adenocarcinoma.
A tumor tissue fragment with large atypical cells displaying large nuclei with single or multiple nucleoli, prominent chromocenters, and minimal irregularities of the nuclear envelope is seen. Cytoplasmic borders are indistinct. A mitotic figure is seen at the 3 o'clock position in the central fragment. Architectural abnormalities, i.e., focal crowding and irregular spacing of cells, are seen. No clear glandular differentiation is evident. The above changes may mimic reactive atypia in chronic pancreatitis. (Papanicolaou stain, medium power)
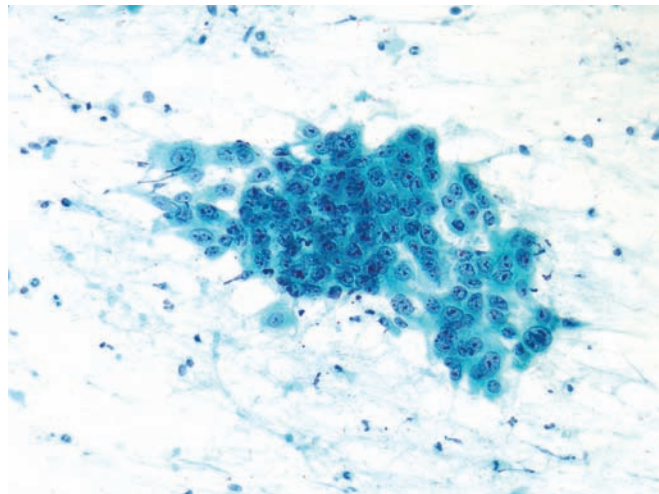
Figure 4.64 — Poorly differentiated adenocarcinoma.
Hypercellular atypical tissue fragments are noted. The cells have markedly enlarged nuclei with a bland chromatin pattern and mostly single, prominent "cherry-red" nucleoli. Three mitoses, including an atypical one, are present. There is distinctly abnormal organization with crowded groupings of cells with high N/C ratio and less crowded areas of cells with more cytoplasm. This tissue fragment is diagnostic of cancer. (Papanicolaou stain, high power)
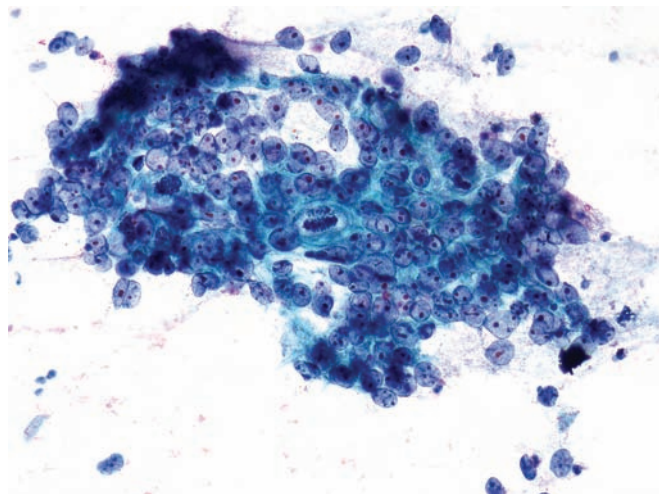
Ductal Adenocarcinoma
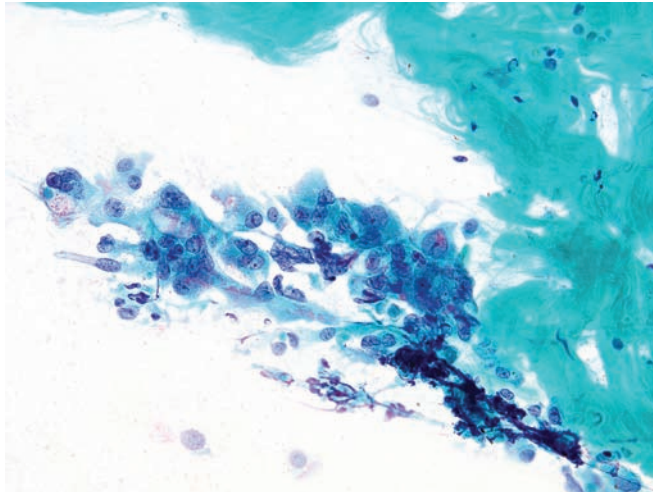
Figure 4.65 — Poorly differentiated adenocarcinoma. Markedly atypical cells are admixed with abundant fibrous tissue related to tumor desmoplasia or a prior chronic pancreatitis. Atypical cells have single or multiple nuclei with conspicuous nucleoli. Nuclei vary in size and shape, with some irregularities of the nuclear borders. Some of the cells have columnar configuration. Although these changes suggest a malignancy, there are significant degenerative changes—i.e., vacuolated cytoplasm, indistinct and frayed cytoplasmic borders—which should be interpreted with caution when making a definitive cancer diagnosis. Multinucleation and the atypical morphology described above may be seen in conditions with reparative/regenerative as well as degenerative cellular changes. (Papanicolaou stain, medium power)
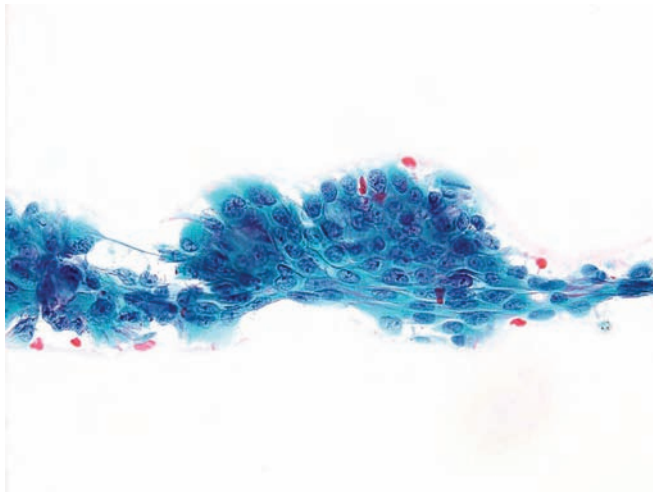
Figure 4.66 — Poorly differentiated adenocarcinoma. An atypical tissue fragment is present. The cells have round or oval nuclei, uniform chromatin pattern with micronucleoli and moderate amounts of cytoplasm. Changes suggestive of both squamous and glandular differentiation are present. At the bottom of the fragment, the cells with elongated cytoplasm appear to be squamous, and a large vacuole in the upper mid-portion of the fragment suggests glandular differentiation. (Papanicolaou stain, medium power)
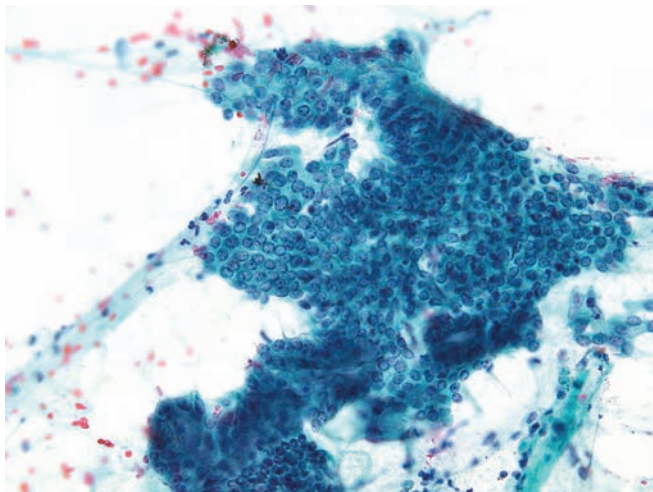
Figure 4.67 — Atypical ductal epithelium. Large fragment of atypical columnar epithelium is noted. Cellular atypia is minimal and consists of nuclear enlargement with a high N/C ratio. Architectural changes are hypercellularity (crowding of nuclei) and scattered acinar formations within the fragment. Follow-up revealed adenocarcinoma. (Papanicolaou stain, low power)

Ductal Adenocarcinoma

Figure 4.68 — Atypical ductal epithelium. Note the atypical tissue fragment composed of cells with enlarged nuclei and multiple small nucleoli. There is focal air-drying artifact, making assessment of the atypia somewhat difficult. Some of the cells have high N/C ratio, others have moderate-to-abundant cytoplasm. A mitotic figure is seen at 5 o'clock. Similar cytologic atypia can be seen in benign, reactive conditions. Follow-up revealed adenocarcinoma. (Papanicolaou stain, medium power)
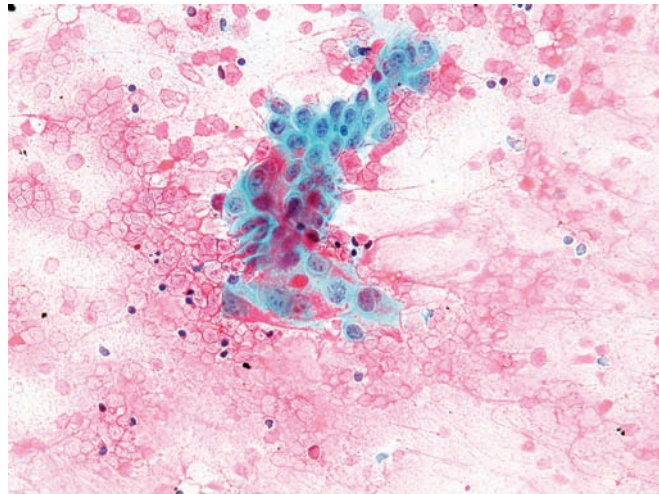
Figure 4.69 — Atypical ductal epithelium. Hypercellular areas of cell groups and loose tissue fragments are seen. The cells have enlarged, round, uniform, overlapping nuclei, most without visible cytoplasm. A branching capillary is present in the lower portion of the picture. Although these findings are consistent with an atypical proliferative process, they are not unequivocally diagnostic of malignancy. Follow-up revealed adenocarcinoma. (Diff Quik stain, low power)
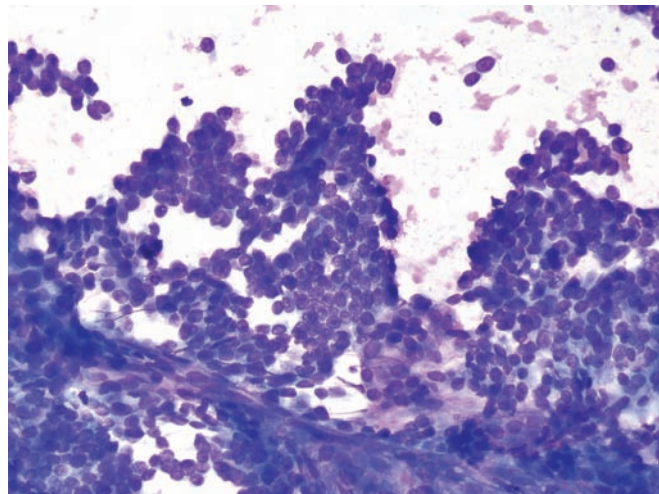
Figure 4.70 — Atypical ductal epithelium. An epithelial tissue fragment with features of squamous differentiation is noted. The cells appear polygonal in shape, have enlarged nuclei, slightly varying in size, and moderate to abundant cytoplasm. In some areas (upper margin, 12 o'clock) intercellular bridges are present. Nuclear and cytoplasmic degenerative changes (perinuclear halos due to shrinkage of the nucleus, intracytoplasmic vacuoles) are also noted. Follow-up revealed adenocarcinoma. (Diff Quik stain, high power)
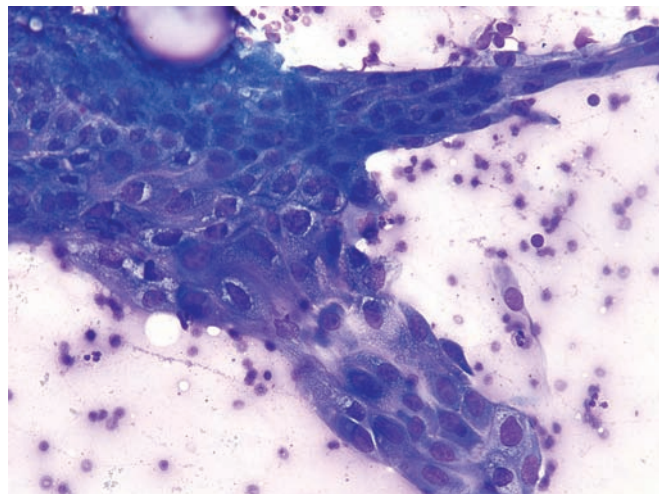
Ductal Adenocarcinoma
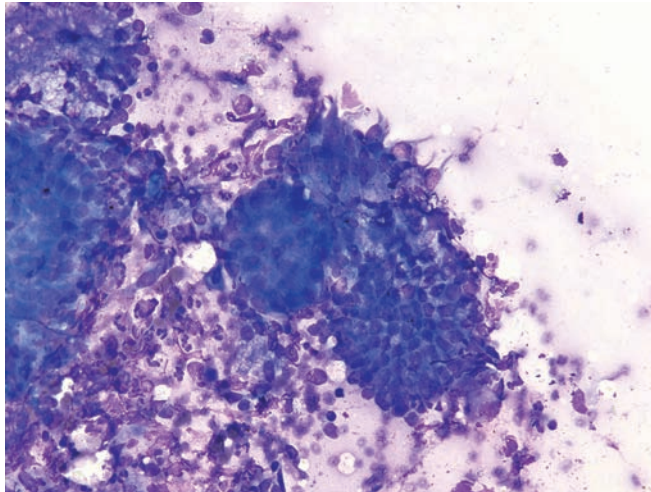
Figure 4.71 — Atypical ductal epithelium. Several epithelial tissue fragments and degenerated single atypical cells in a background of neutrophils are observed. Three fragments in the center have different cytomorphology and architecture. The upper fragment is composed of crowded cells with overlapping nuclei and several markedly atypical cells with large nuclei and cytoplasmic tailing. One fragment below is composed of smaller ductal-type cells with focal nuclear crowding. The fragment in between is composed of cells with round nuclei and moderate amounts of cytoplasm, apparently forming an acinus. These cellular findings raise the possibility of a carcinoma, but an inflammatory reactive process cannot be ruled out. Follow-up revealed adenocarcinoma. (Diff Quik stain, medium power)
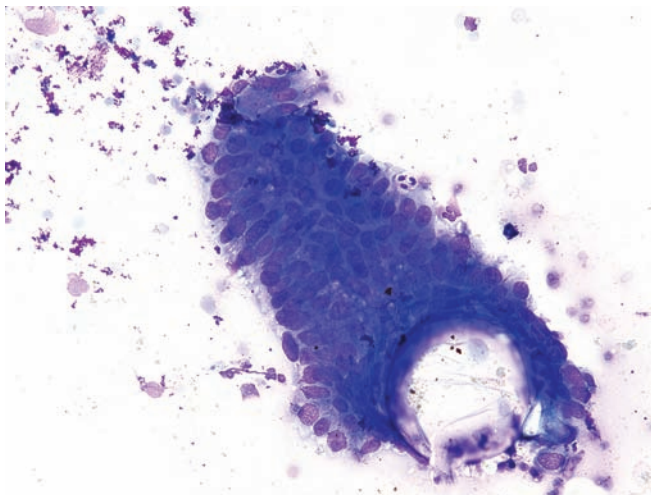
Figure 4.72 — Atypical ductal epithelium. This hypercellular tissue fragment is composed of atypical columnar epithelium with enlarged oval, moderately hyperchromatic nuclei. There is some nuclear disorientation. This may represent an intraepithelial pancreatic neoplasm, but definitive diagnosis cannot be made in this single fragment. Follow-up revealed adenocarcinoma. (Diff Quik stain, medium power)

Variants of Ductal Adenocarcinoma

Figure 4.73 — Adenosquamous carcinoma. This large adenosquamous carcinoma has two grossly distinct components. The bulk of the neoplasm is gritty tan-yellow and focally hemorrhagic. Smaller foci are softer and whiter. In some adenosquamous carcinomas the two components are intimately admixed, while in others the components are separable.
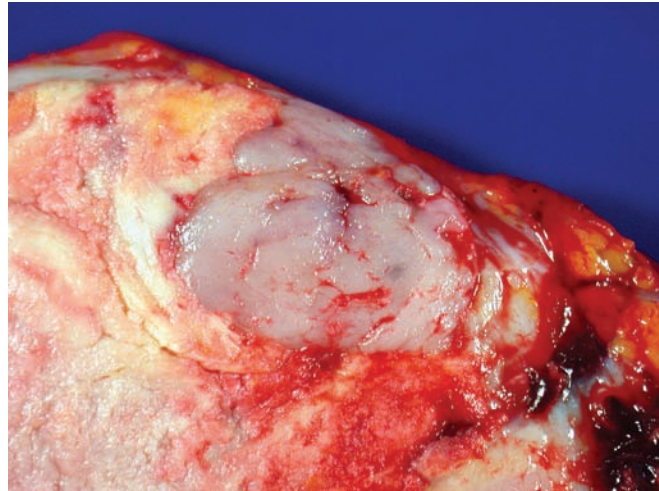
Figure 4.74 — Adenosquamous carcinoma. A large tumor in the pancreatic head with densely sclerotic, grey-white infiltrative appearance is present. Primary squamous cell carcinoma of the pancreas is rare, and the possibility of a metastatic lesion from another primary (lung, esophagus, etc.) should always be excluded.
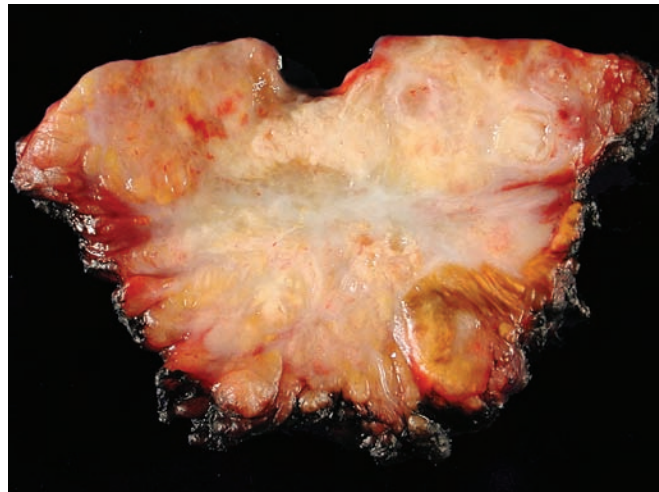
Figure 4.75 — Adenosquamous carcinoma. Histologically, in this area of squamous differentiation the neoplastic cells have hard glassy eosinophilic cytoplasm and prominent cell–cell junctions. Other areas of the neoplasm had glandular differentiation. The differential diagnosis would include an adenocarcinoma with focal squamous differentiation (by definition, the squamous component comprises ≥30% of the neoplasm in adenosquamous carcinomas) and a squamous cell carcinoma metastatic to the pancreas (a distinction made primarily based on clinical history). (Hematoxylin and eosin stain, high power)
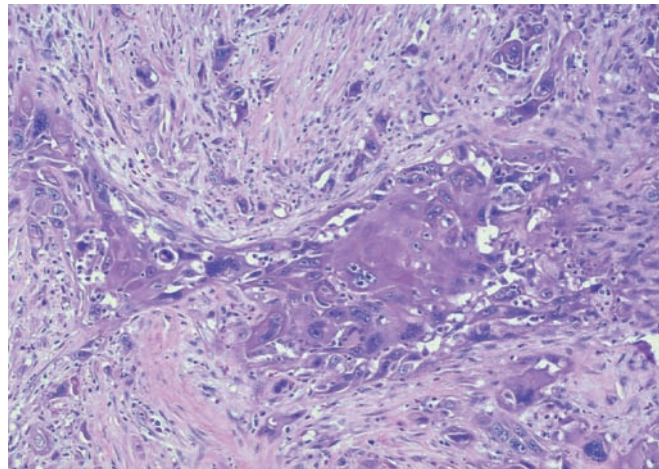
Adenosquamous Carcinoma
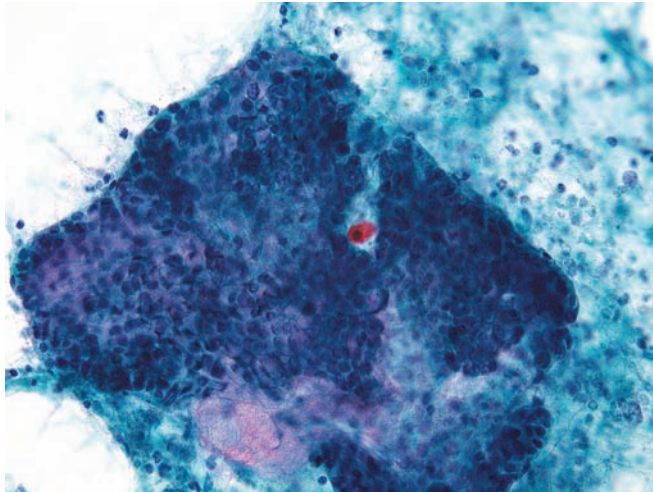
Figure 4.76 — Adenosquamous carcinoma. A large ductal-type tissue fragment and a superimposed atypical keratinized cell with hyperchromatic nucleus and cytoplasmic orangeophilia are present. The background appears to be necrotic. It is not uncommon to see occasional mature squamous cells in endoscopic ultrasound-guided aspirations as a result of esophageal contamination. However, the keratinized squamous cell in this case appears atypical. (Papanicolaou stain, low power)
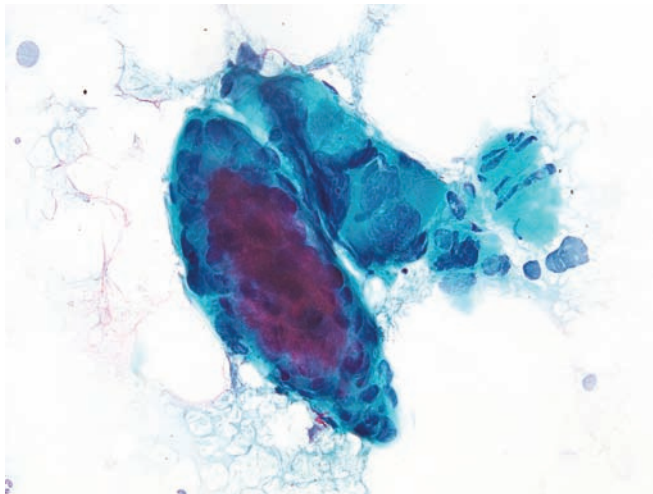
Figure 4.77 — Adenosquamous carcinoma. Two atypical tissue fragments are seen. The lower one is composed of neoplastic cells with syncytial architecture and hyperchromatic nuclei, some of which have sharply pointed poles. Dense cytoplasm and stratification suggest squamous differentiation. The upper fragment has atypical columnar cells with luminal borders. The nuclei are large, but poorly preserved and difficult to interpret. (Papanicolaou stain, high power)
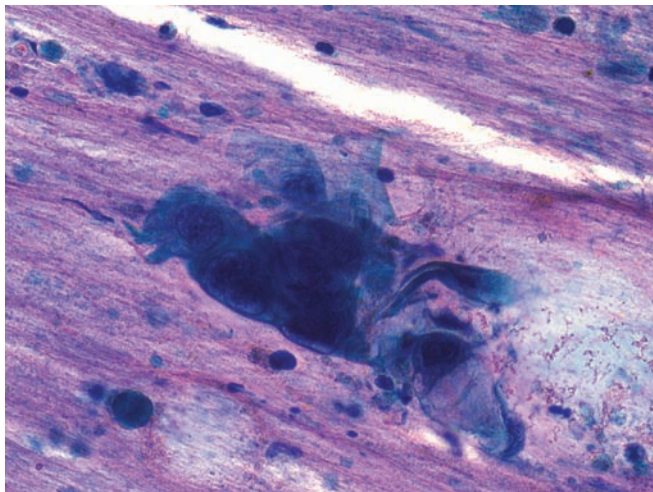
Figure 4.78 — Adenosquamous carcinoma. The large polygonal carcinoma cells with cytoplasmic opacity are consistent with squamous differentiation. Background shows abundant mucin. Such cells should not be confused with mature squamous cells from the esophagus in EUS-guided aspirations. (Papanicolaou stain, high power)

Variants of Ductal Adenocarcinoma

Figure 4.79 — Adenosquamous carcinoma. A tissue fragment of carcinoma with features suggestive of squamous and glandular differentiation is seen. Malignant features include marked variation in nuclear size and shape, number and shape of nucleoli, and the high N/C ratio. The dense, glassy appearance of the cytoplasm of some cells suggests squamous differentiation. In focal areas (12 and 8 o'clock) at the margin of the fragment, there seem to be luminal borders suggestive of glandular differentiation. (Papanicolaou stain, high power)
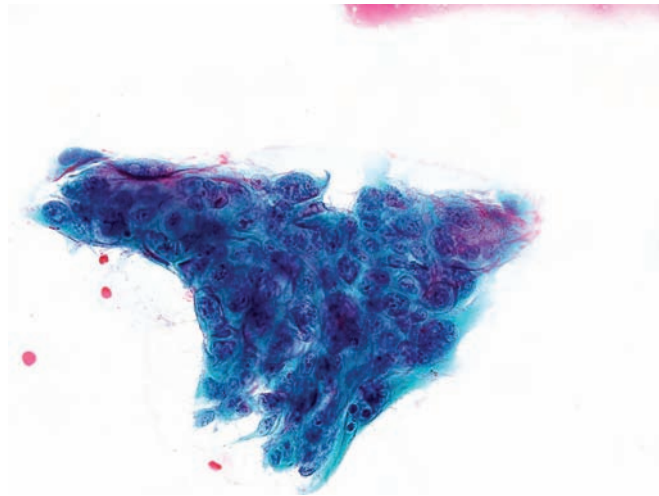
Figure 4.80 — Adenosquamous carcinoma. A group of neoplastic cells is seen with eccentrically located, irregular nuclei in a background containing cellular debris. Cytoplasmic opacity suggests squamous differentiation. The glandular or "adeno" component was not apparent in this case on FNA. A metastatic squamous cell carcinoma (such as from the lung) should always be excluded. (Diff Quik stain, high power)
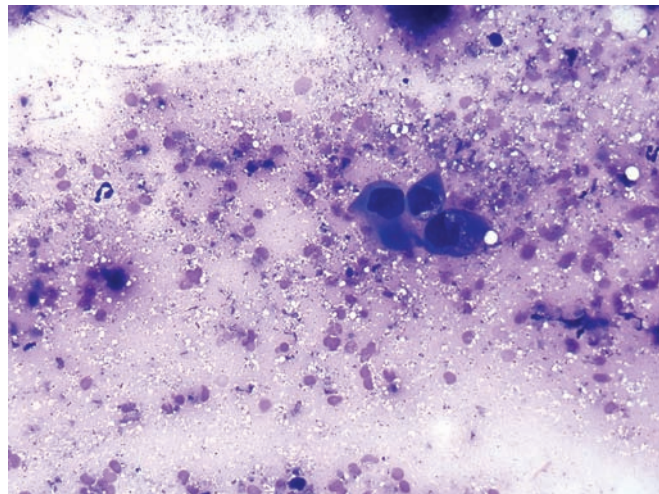
Figure 4.81 — Adenosquamous carcinoma. A single carcinoma cell with squamous differentiation is noted. The neoplastic cell has two hyperchromatic nuclei with irregular borders and keratinized cytoplasm. The background displays extensive necrosis. (Papanicolaou stain, high power)
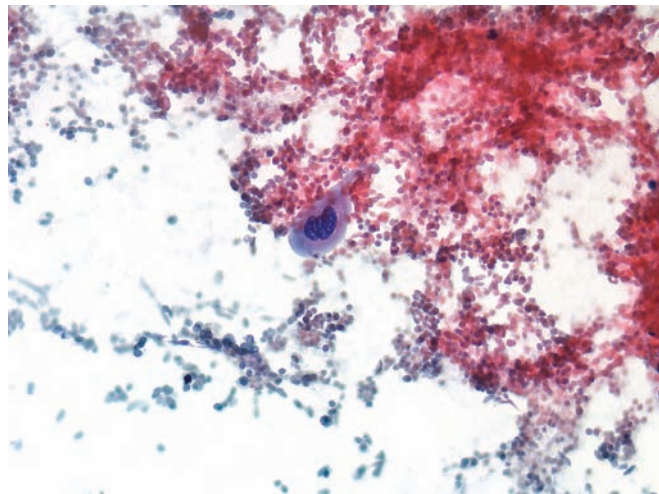
Adenosquamous Carcinoma
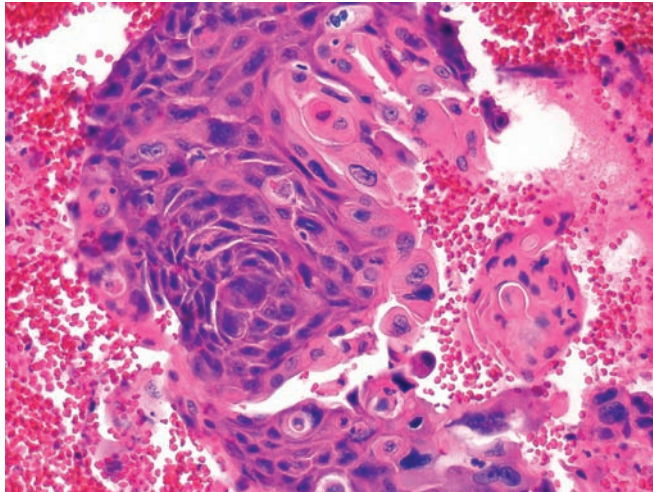
Figure 4.82 — Adenosquamous carcinoma (cell block section). Tissue fragments of squamous cell carcinoma with pleomorphic nuclei, macronucleoli, and densely eosinophilic glassy cytoplasm. Gland differentiation was apparent in the smear. Rare vacuoles containing eosinophilic, granular material may represent keratin. Pure squamous carcinoma of pancreas is rare. Mucin stains are needed in equivocal cases. (Hematoxylin and eosin stain, high power)
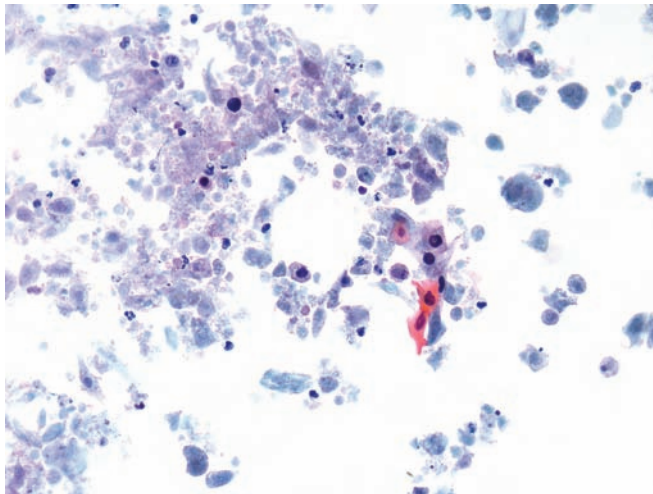
Figure 4.83 — Adenosquamous carcinoma. Atypical keratinized squamous cells are present in an extensively necrotic background. Note the large hyperchromatic nuclei with irregular borders. Well-differentiated adenosquamous carcinomas can be cystically necrotic, similar to their head and neck and pulmonary counterparts. (Papanicolaou stain, low power)
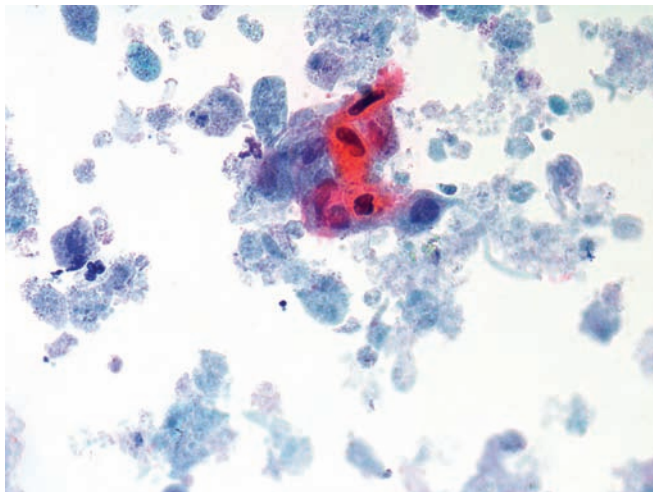
Figure 4.84 — Adenosquamous carcinoma. A group of atypical, poorly preserved squamous cells is seen. Markedly hyperchromatic nuclei and some nuclear pleomorphism (one elongated nucleus) in a necrotic background strongly suggest adenosquamous carcinoma. In the presence of only a few atypical squamous cells, a diagnosis of cancer should be made with great caution. Benign squamous cell–containing lesions (such as a lymphoepithelial cyst) can be excluded due to overt malignant features observed here as well as the extensive tumor necrosis. (Papanicolaou stain, high power)

Variants of Ductal Adenocarcinoma

Figure 4.85 — Adenosquamous carcinoma. Scattered degenerated cells with atypical nuclei are noted. Part of a poorly differentiated tumor is seen in the lower portion of the image with syncytial arrangement of the neoplastic cells. No glandular differentiation was apparent in this case on the initial FNA. However, the resection specimen had foci of ductal adenocarcinoma interspersed in a poorly differentiated squamous cell component. (Papanicolaou stain, low power)
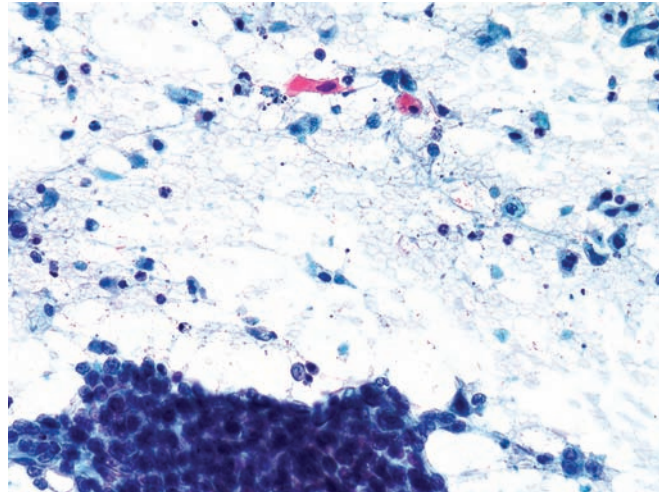
Figure 4.86 — Adenosquamous carcinoma. The malignant epithelial tissue fragment represents a poorly differentiated portion of the adenosquamous carcinoma. Diagnostic features of malignancy; i.e., disorganized, large cells with pleomorphic nuclei and prominent nucleoli, are clearly seen. (Papanicolaou stain, high power)
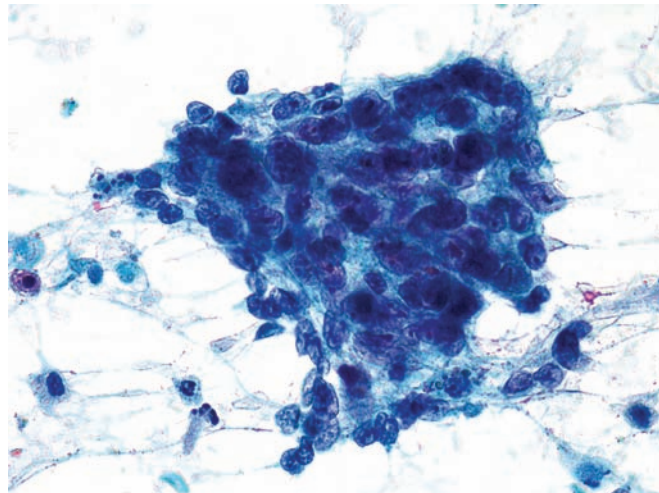
Colloid (Mucinous Noncystic) Carcinoma
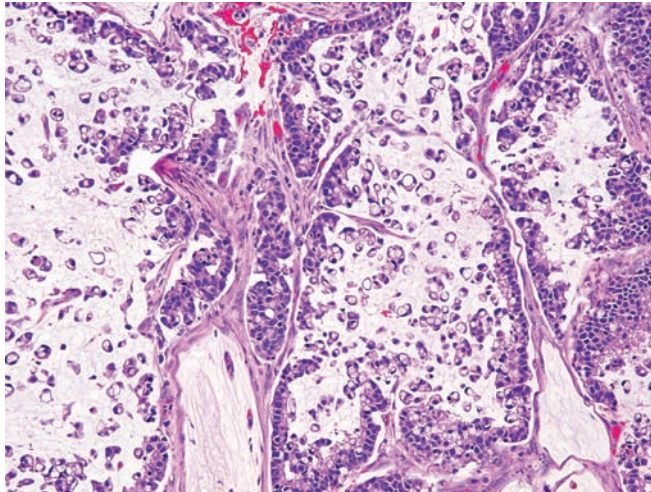
Figure 4.87 — Colloid carcinoma. Mucin-producing neoplastic epithelial cells are suspended in pools of stromal mucin in this variant of ductal adeno-carcinoma. While another component of ductal adenocarcinoma may also be present, at least 80% of the neoplasm has to have colloid differentiation to classify it as a colloid carcinoma. The differential diagnosis includes mucin extravasation from a nonin-vasive intraductal papillary mucinous neoplasm. The pools of mucin in mucin extravasation are acellular. (Hematoxylin and eosin stain, low power).
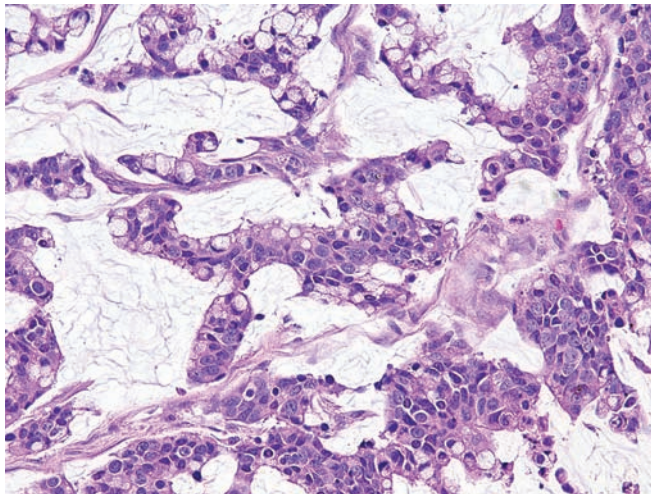
Figure 4.88 — Colloid carcinoma. Cords and trabecula of mucin-producing adenocarcinoma cells are noted floating in abundant extracellular mucin. (Hematoxylin and eosin stain, medium power)
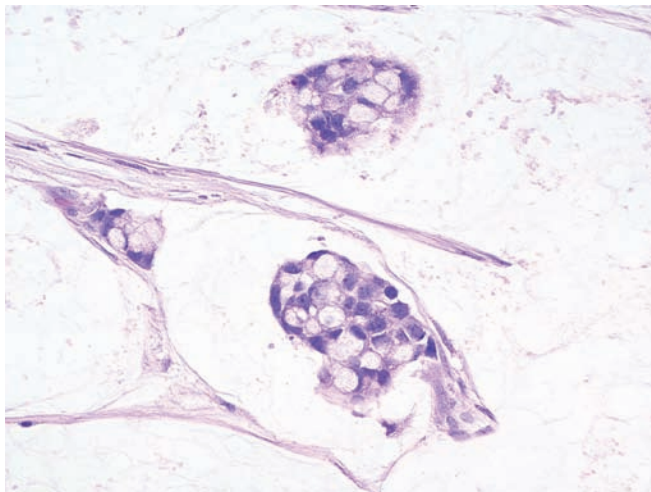
Figure 4.89 — Colloid carcinoma. Abundant pale and clear mucin is present. Malignant cells form ir-regular shaped glands containing large intracytoplas-mic mucin vacuoles. (Hematoxylin and eosin stain, high power)

Variants of Ductal Adenocarcinoma

Figure 4.90 — Colloid carcinoma. A tissue fragment of atypical columnar epithelium suspended in a thick mucoid background is noted. The cells have enlarged and hyperchromatic basally placed nuclei with focal nuclear crowding and clear mucinous cytoplasm. Small luminal formation within the tissue fragment is also present. Correlation with radiographic findings (i.e., lack of cystic mass or a dilated main duct) is often needed to rule out intraductal papillary mucinous neoplasm. (Papanicolaou stain, low power)
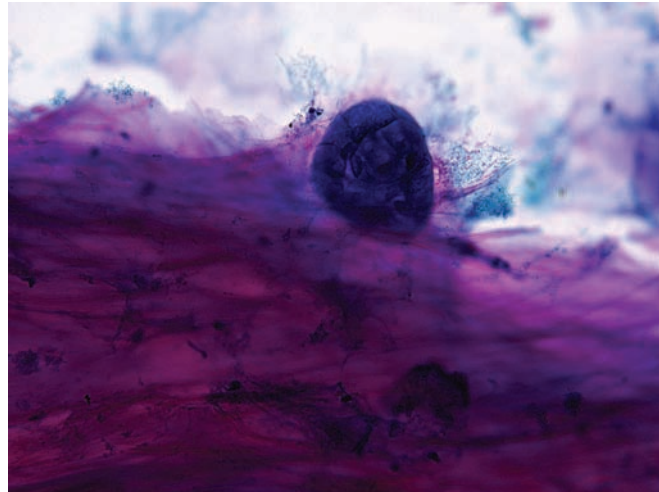
Figure 4.91 — Colloid carcinoma. Higher magnification of an adenocarcinoma tissue fragment with large pleomorphic nuclei associated with a background of dense mucoid and some necrotic material. A diagnosis of carcinoma is readily made because of overt cytomorphalogic malignant features. (Papanicolaou stain, high power)
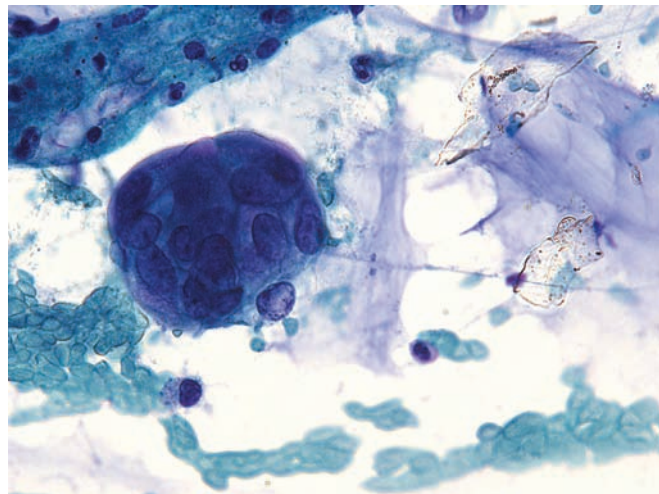
Figure 4.92 — Colloid carcinoma. An island of adenocarcinoma that appears well-differentiated suspended in pools of mucin. Nuclei are hyperchromatic with small inconspicuous nucleoli. A distinction from benign mucocele can be extremely difficult. (Papanicolaou stain, high power)

Colloid (Mucinous Noncystic) Carcinoma
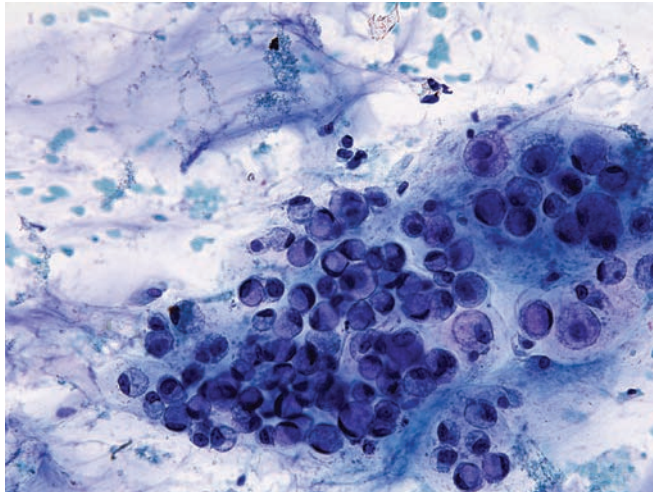
Figure 4.93 — Colloid carcinoma. Dispersed neoplastic cells with hyperchromatic, eccentrically located nuclei and large intracytoplasmic vacuoles (signet ring cells) in a mucoid background are seen. Malignant signet ring epithelial cells can be often observed in colloid carcinoma of the pancreas and should not be confused with muciphages. (Papanicolaou stain, high power)

Variants of Ductal Adenocarcinoma

Hepatoid Adenocarcinoma
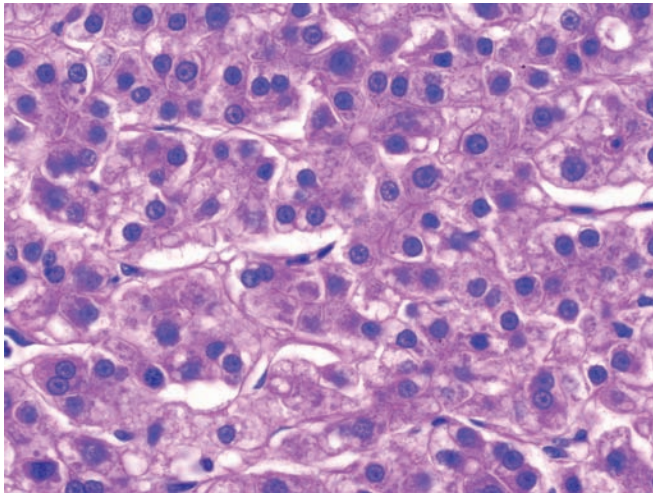
Figure 4.94 — Hepatoid variant of ductal adeno-carcinoma. This neoplasm is primary to the pancreas and is composed of large eosinophilic cells that form trabeculae and nests. The nuclei are centrally placed, and sinus spaces are evident. Differential diagnoses include metastatic melanoma, which would contain melanin pigment and express S-100 protein, and hepatocellular carcinoma metastatic to the pancreas from a liver primary. Distinguishing metastatic hepatocellular carcinoma from a lesion arising in the pancreas requires imaging of the liver. (Hematoxylin and eosin stain, high power)

Medullary Carcinoma
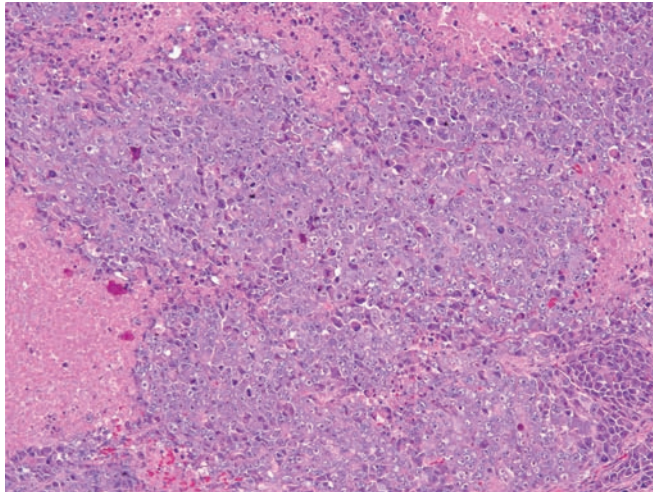
Figure 4.95 — Medullary carcinoma. This poorly differentiated carcinoma is composed of amphophilic cells with a syncytial growth pattern. Numerous intratumoral lymphocytes are noted. The carcinoma has a "pushing," not infiltrative growing edge. This medullary morphology has been associated with microsatellite instability. Acinar cell carcinoma (single prominent nucleoli, expression of exocrine pancreatic enzymes) should be included in the differential diagnosis. (Hematoxylin and eosin, low power)
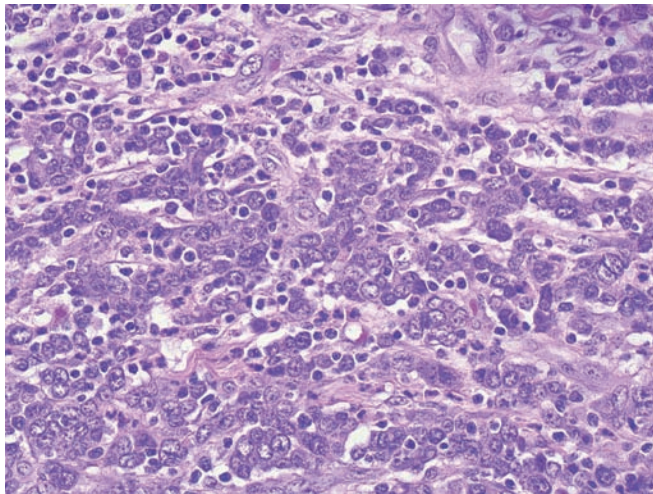
Figure 4.96 — Medullary carcinoma. High-grade carcinoma cells in syncytial arrangements and numerous interspersed lymphocytes are seen. (Hematoxylin and eosin stain, medium power)
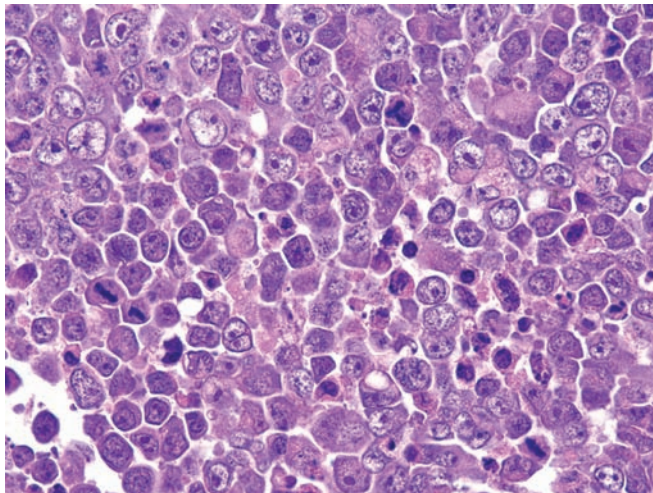
Figure 4.97 — Medullary carcinoma. Note numerous mitoses and abundant karyorrhexis. Malignant cells have extremely high N/C ratios and often prominent nucleoli. (Hematoxylin and eosin stain, high power)

Variants of Ductal Adenocarcinoma

Figure 4.98 Undifferentiated carcinoma with osteoclast-like giant cells. Pleomorphic neoplastic cells surround a large multinucleated cell with uniform nuclei. The neoplastice cells have large nuclei and prominent nucleoli. The direction of differentiation is not at all clear from the histologic appearance of the cells. The differential diagnosis is very broad and includes melanoma metastatic to the pancreas. Immunolabeling for S-100 protein, HMB-45, and Melan-A can help establish the diagnosis of a melanoma, while undifferentiated carcinomas sometimes have a lower-grade component that can be a clue to their epithelial origin, and some express cytokeratin. (Hematoxylin and eosin stain, high power)
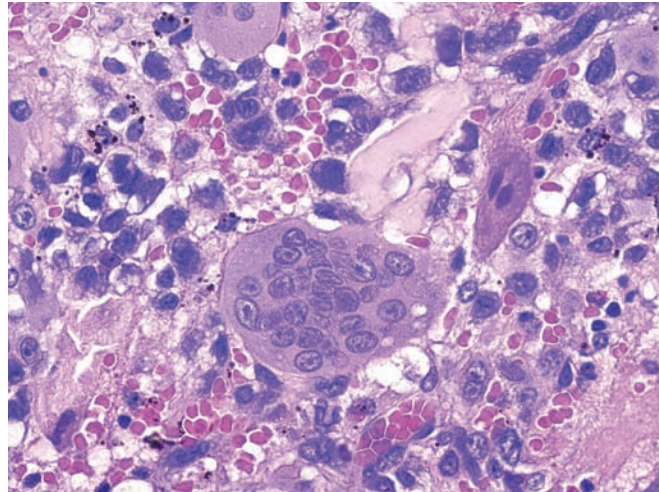
Figure 4.99 — Undifferentiated carcinoma with osteoclast-like giant cells. Strong immunolabeling of the giant cells with KP-1. The mononuclear carcinoma cells are totally negative (cell block section, Immunoperoxidase stain KP-1, medium power)
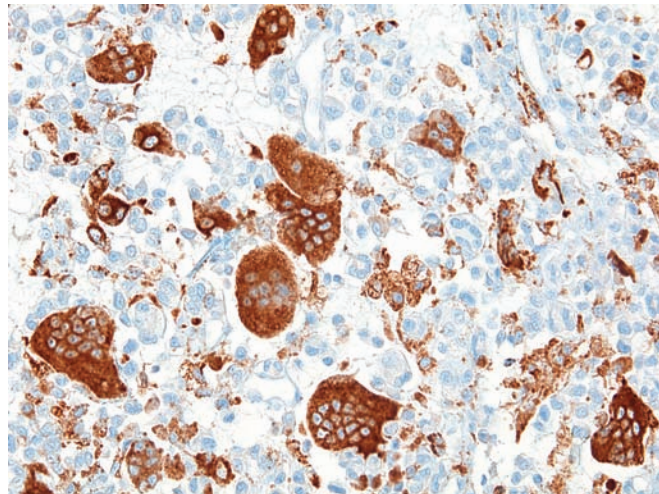
Figure 4.100 Undifferentiated carcinoma with osteoclast-like giant cells. Immunolabeling for cytokeratin AE1/AE3 helps establish the epithelial nature of the pleomorphic neoplastic cells. The expression of keratin can be focal and, in some cases, difficult to demonstrate. (Immunolabeling using cytokeratin AE1/AE3, high power)
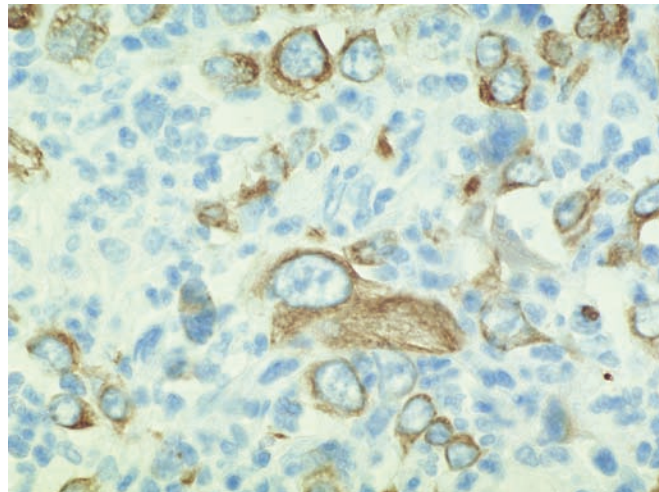
Undifferentiated Carcinoma with Osteoclast-like Giant Cells
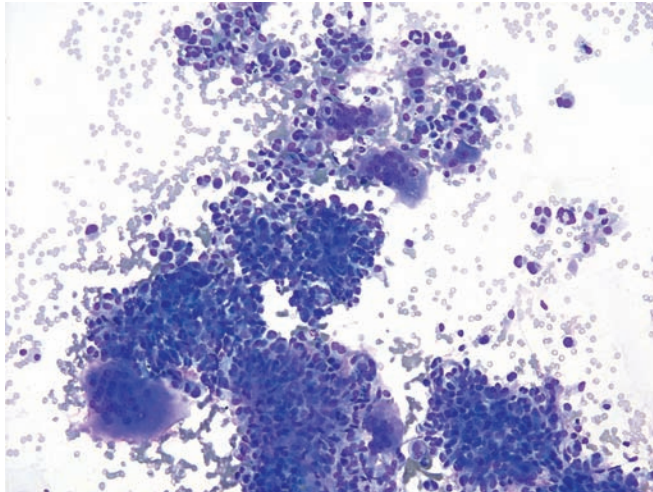
Figure 4.101 Undifferentiated carcinoma with osteoclast-like giant cells. Many large multinucleated cells with abundant cytoplasm and numerous uniform nuclei are interspersed with smaller pleomorphic cells. Although the osteoclast-like giant cells catch the eye, they are nonneoplastic. The smaller pleomorphic cells, as demonstrated by their high mitotic rate, are the neoplastic cells. (Diff Quik, low power)
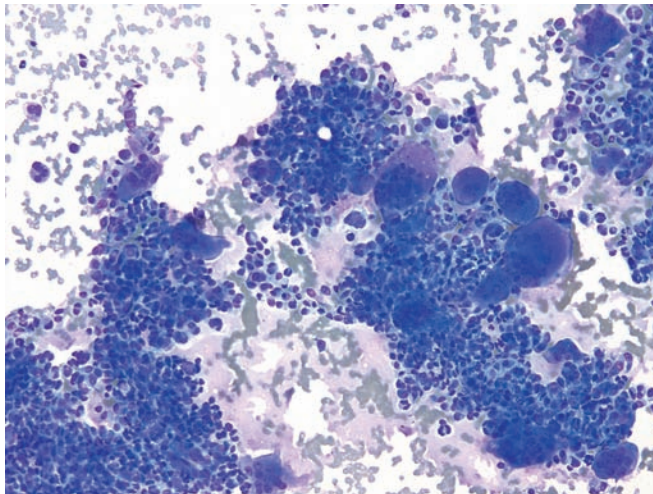
Figure 4.102 Undifferentiated carcinoma with osteoclast-like giant cells. The uniformity of the nuclei in the osteoclast-like giant cells contrasts with the nuclear pleomorphism present in the neoplastic mononuclear cells. Nonneoplastic conditions associated with multinucleated giant cells, such as tuberculosis and foreign body-type giant cell reaction, should be included in the differential diagnosis. The diagnosis is usually easy once the pleomorphic neoplastic cells are recognized. (Diff Quik stain, low power)
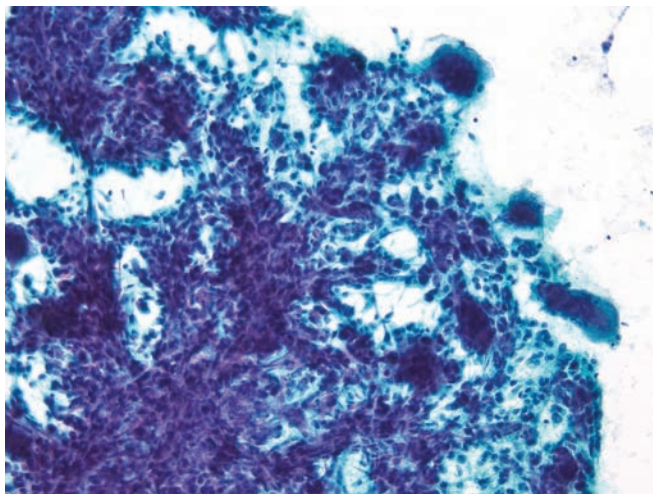
Figure 4.103 Undifferentiated carcinoma with osteoclast-like giant cells. Crowded cellular tissue fragments comprised of mononuclear spindled carcinoma cells and scattered multinucleated giant histiocytes are evident. The histiocytes have an "osteoclastic" look and may contain as many as 20–30 nuclei. (Papanicolaou stain, low power)

Variants of Ductal Adenocarcinoma

Figure 4.104 Undifferentiated carcinoma with osteoclast-like giant cells. Tissue fragments, single tumor cells, and few multinucleated giant cells are present. The majority of malignant cells have one or two nuclei and a scant to moderate amount of cytoplasm. The presence of large multinucleated giant cells (reactive histiocytes) is quite eye-catching and gives this tumor its unique name. (Diff Quik stain, medium power)
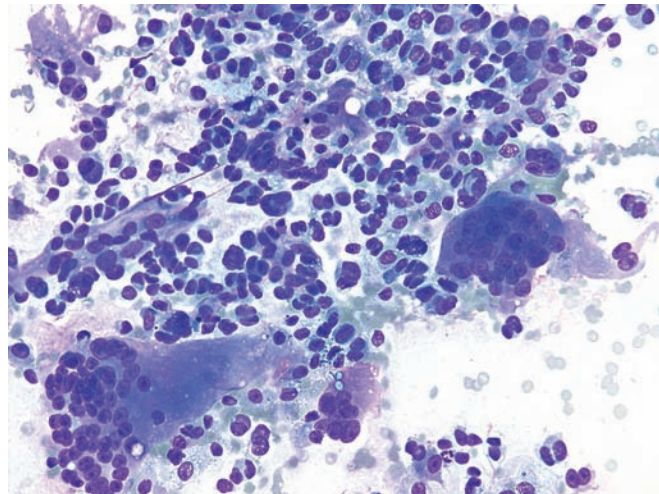
Figure 4.105 — Undifferentiated carcinoma with osteoclast-like giant cells. Discohesive groups of tumor cells and a large multinucleated cell dominate this smear. Neoplastic cells have round, oval, or irregularly shaped nuclei. Rare binucleated or multinucleated forms are present. The latter differ from osteoclast-like giant cells, which have round-to-oval uniform nuclei with small nucleoli. (Diff Quik stain, high power)
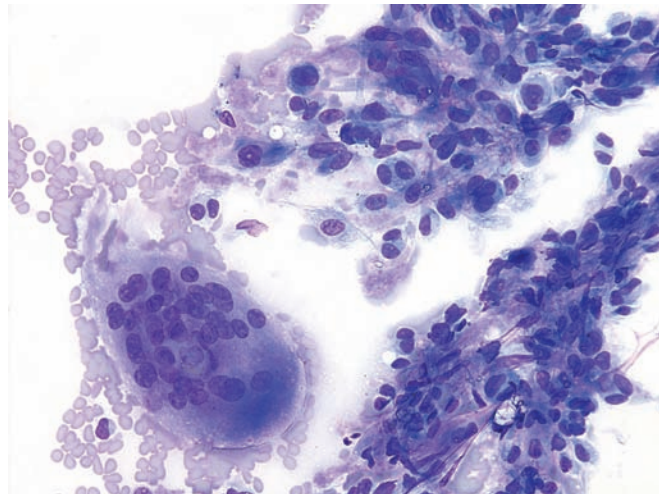
Figure 4.106 — Undifferentiated carcinoma with osteoclast-like giant cells. A large fragment of pleomorphic tumor cells with numerous interspersed multinucleated giant cells are present. This cytomorphologic appearance is characteristic and should not be confused with any other neoplastic process. (Papanicolaou stain, medium power)
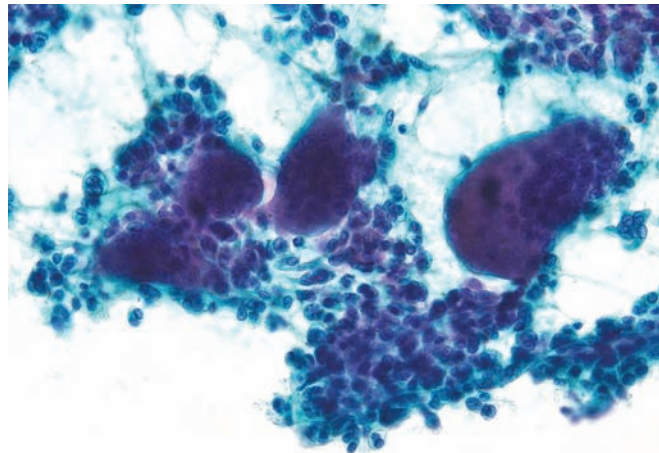
Undifferentiated Carcinoma with Osteoclast-like Giant Cells
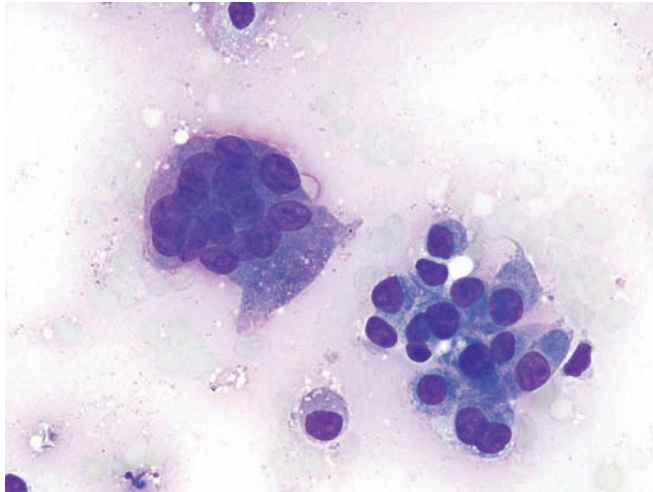
Figure 4.107 — Undifferentiated carcinoma with osteoclast-like giant cells. Another area of tumor under higher power is seen here. The bi-modal appearance (mononuclear undifferentiated carcinoma cells and large multinucleated giant histiocytes) is diagnostic of this tumor. (Diff Quik stain, high power)
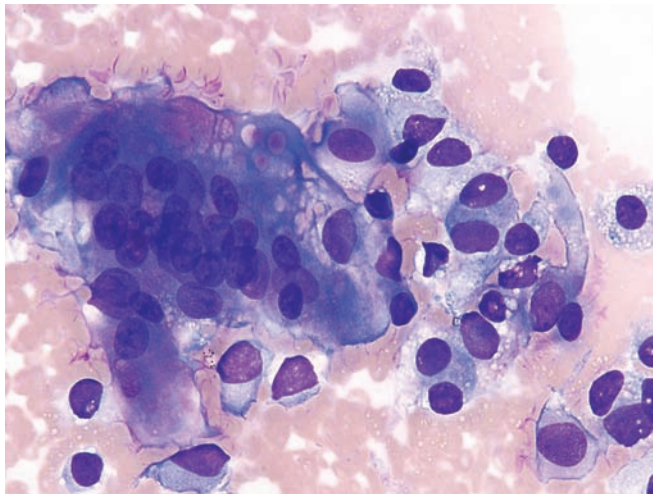
Figure 4.108 — Undifferentiated carcinoma with osteoclast-like giant cells. Tumor cells with large eccentrically-placed "plasmacytoid" nuclei are seen. Note the variation in nuclear size and shape, pointed nuclear edges and rare binucleation. (Diff Quik, high power)
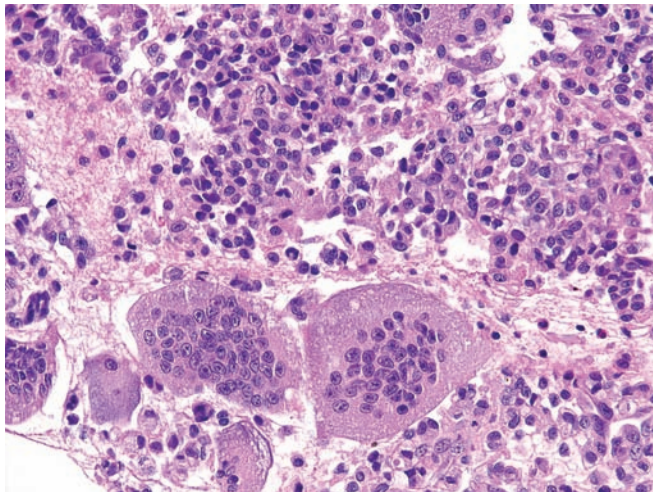
Figure 4.109 — Undifferentiated carcinoma with osteoclast-like giant cells (cell block section). Osteoclast-like giant cells are seen in sharp contrast to the background mononuclear carcinoma cells. (Hematoxylin and eosin stain, high power)

Variants of Ductal Adenocarcinoma

Figure 4.110 — Undifferentiated carcinoma with osteoclast-like giant cells. A cell block section displays pleomorphic carcinoma cells with prominent nucleoli alongside a large multinucleated giant cell. (Hematoxylin and eosin stain, high power)
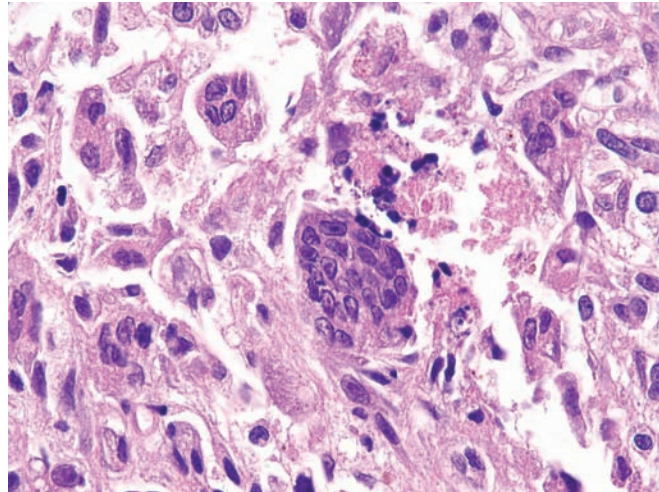
Figure 4.111 — Undifferentiated carcinoma with osteoclast-like giant cells (cell block section). Focal, weakly positive immunolabeling of the mononuclear carcinoma cells with CK20. The reactive multinucleated giant cells are negative. (Immunoperoxidase stain, CK 20, low power)
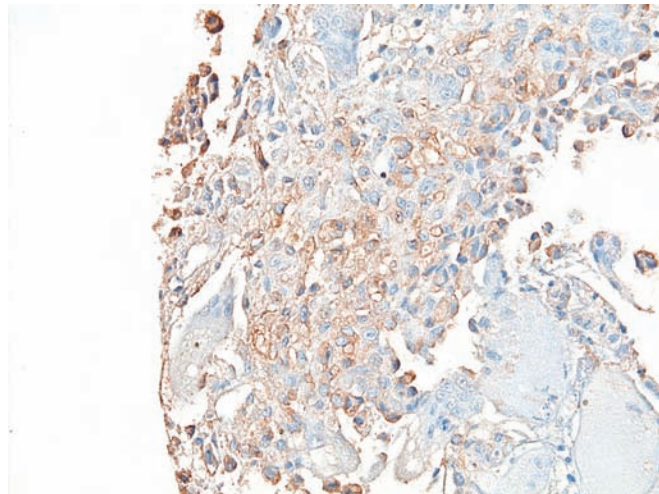
Anaplastic Carcinoma
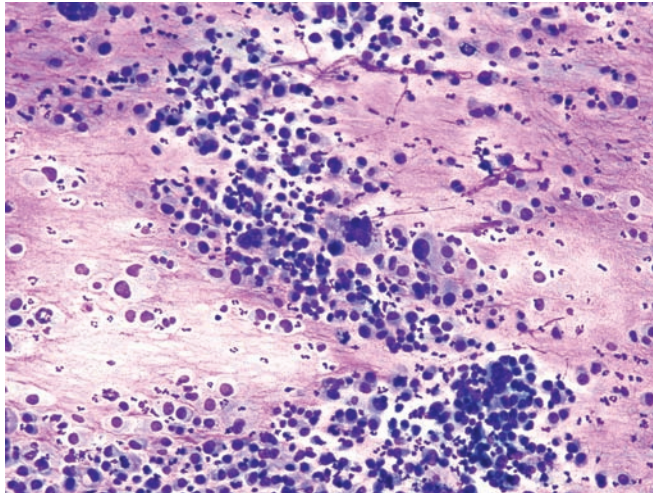
Figure 4.112 — Anaplastic carcinoma. Cellular specimen with virtually all single undifferentiated malignant cells is seen. Neoplastic cells have markedly pleomorphic, eccentrically located, large nuclei. There are also few multinucleated tumor giant cells. Mixture of acute inflammatory cells reflects tumor necrosis. The differential diagnosis would include a number of primary and metastatic neoplasms. (Diff Quik stain, low power)
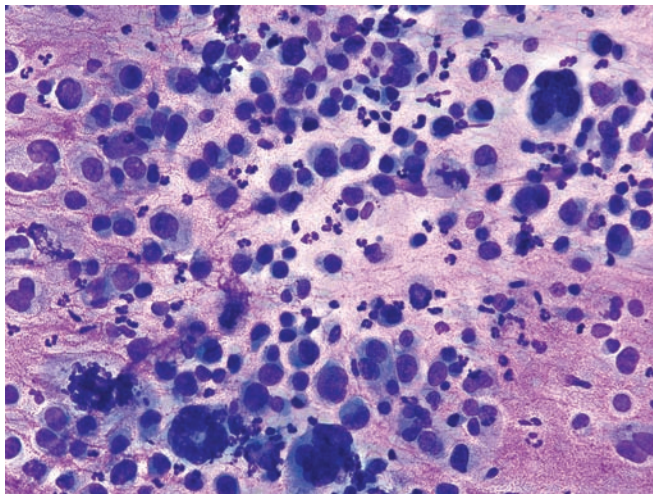
Figure 4.113 — Anaplastic carcinoma. Note the extreme variation in nuclear size/shape, multinucleated tumor giant cells, and atypical mitoses. Metastatic cancers to the pancreas (such as malignant melanoma and undifferentiated sarcoma) should be ruled out by demonstrating at least focal immunoreaction to epithelial markers. (Diff Quik stain, high power)
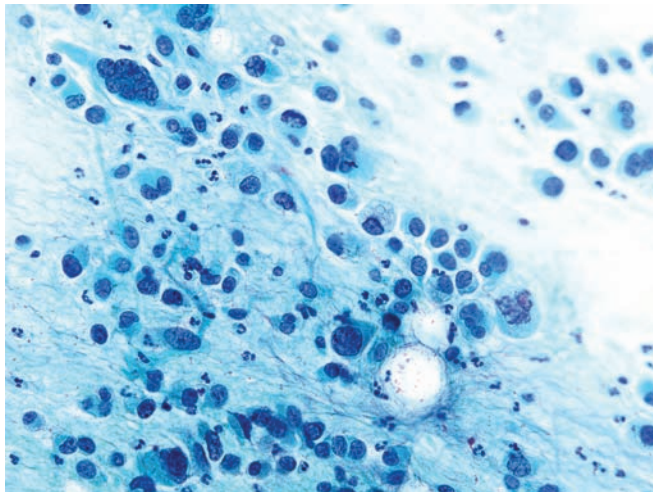
Figure 4.114 — Anaplastic carcinoma. Several neoplastic cells, including one with bizarre multinucleation, are noted. However, the appearance differs from an undifferentiated carcinoma with osteoclast-like giant cells. Anaplastic carcinoma is one of the most aggressive primary pancreatic cancers. (Papanicolaou stain, high power)

Variants of Ductal Adenocarcinoma

Figure 4.115 — Anaplastic carcinoma. One large and several smaller tissue fragments of neoplastic cells. Although the architecture of the tissue fragments is consistent with epithelial differentiation, it is disorganized and shows no evidence of specific type. Variation in the size and shape of the nuclei and N/C ratio in tissue fragments is one of the most reliable features of malignancy. (Papanicolaou stain, high power)
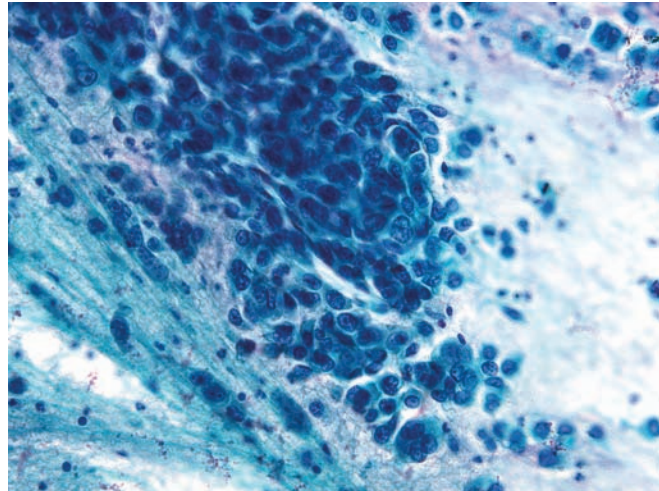
Figure 4.116 — Anaplastic carcinoma. Atypical mitotic figures, as seen here, are usually present in high-grade undifferentiated carcinomas. Background granularity and polymorphonuclear leukocytes reflect tumor necrosis. (Diff Quik stain, high power)
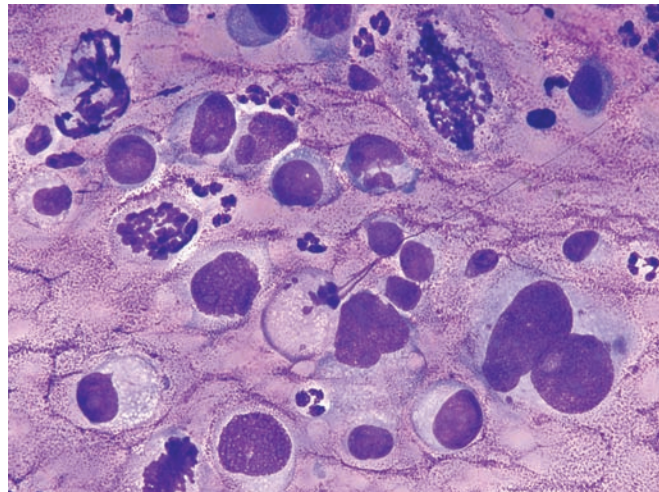
Figure 4.117 — Anaplastic carcinoma. Multinucleated tumor giant cells are readily seen in this case. Note the extreme variation and the large size of the nuclei. Anaplastic carcinoma needs to be differentiated from an undifferentiated carcinoma with osteoclast-like giant cells because of prognostic differences. Anaplastic carcinoma typically carries the worst prognosis of any primary pancreatic cancer and is often deemed unresectable at the time of initial diagnosis. (Diff Quik stain, high power)
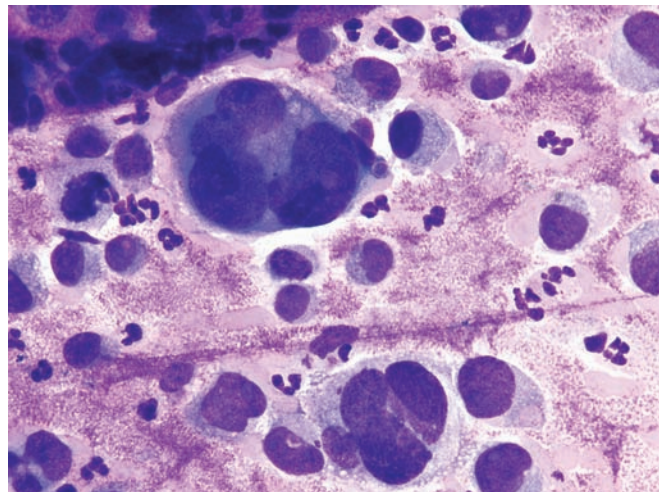
Anaplastic Carcinoma
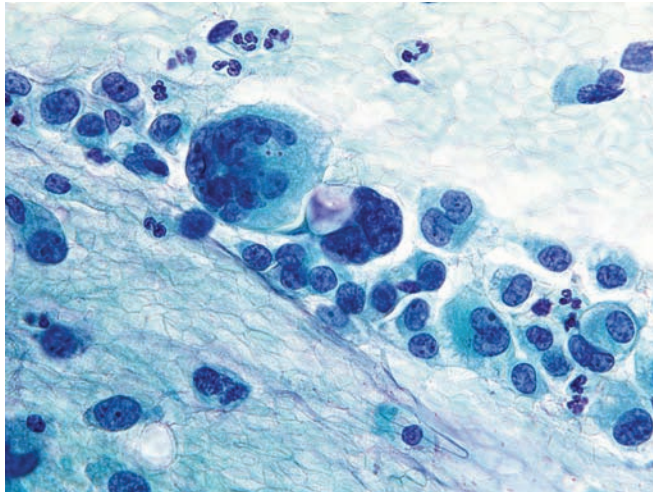
Figure 4.118 — Anaplastic carcinoma. Discohesive malignant epithelial cells and multinucleated tumor giant cells dominate this smear. Note the irregularities in the nuclear borders and variations in the shape of the nuclei. Both, the mononuclear carcinoma cells, as well as the multi-nucleated giant cells are epiltheli-al-derived cells. (Papanicolaou stain, high power)
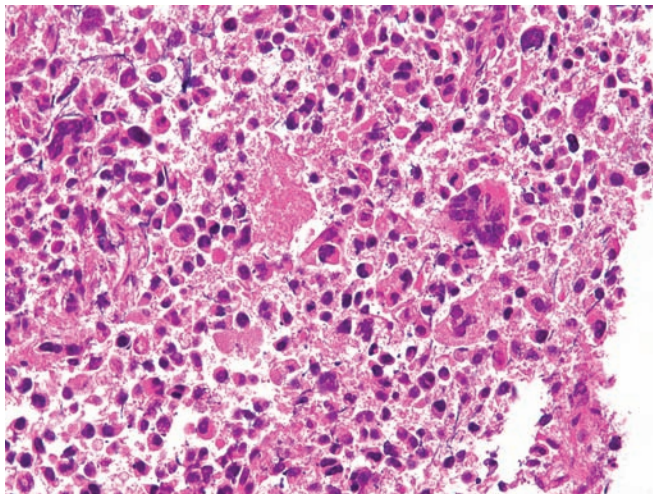
Figure 4.119 — Anaplastic carcinoma (cell block section). Cellular features similar to those in the cytologic preparations are seen. Discohesive, pleomorphic neoplastic cells with many multinucleated giant cells appear in a necrotic background. (Hematoxylin and eosin stain, low power)

Variants of Ductal Adenocarcinoma

Figure 4.120 — Signet ring cell carcinoma. As suggested by its name, this neoplasm is composed of cells with abundant intracellular mucin, which flattens and indents their nuclei. The cells are noncohesive and round. Although signet ring cell carcinomas can be primary to the pancreas, a metastasis from an extrapancreatic primary, particularly signet ring cell carcinoma of the stomach and lobular carcinoma of the breast needs to be excluded before establishing the diagnosis. This example shows numerous malignant signet ring cells from a widely invasive tumor. Note the pleomorphic eccentrically placed and indented nuclei and large intracytoplasmic mucin vacuoles embedded in a sclerotic stroma. (Hematoxylin and eosin stain, low power)
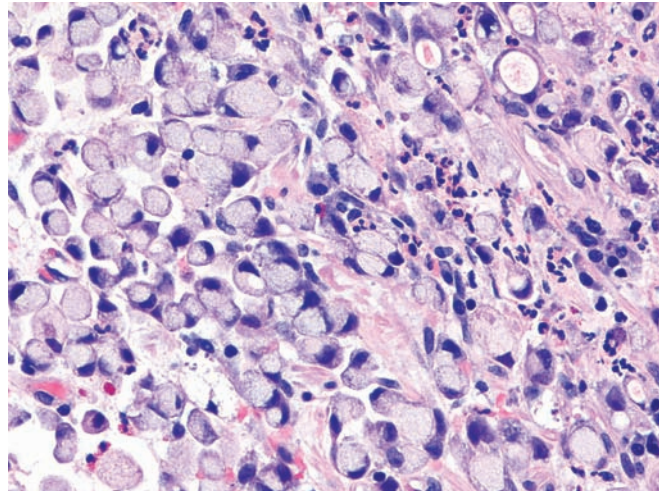
Figure 4.121 — Signet ring cell carcinoma. A large malignant epilthelial cell is seen embedded in a collagenized stroma. The cell displays the classic morphology of a "signet ring" carcinoma with a large solitary intracytoplasmic mucin vacuole pushing the indented nucleus. (Hematoxylin and eosin stain, high power)
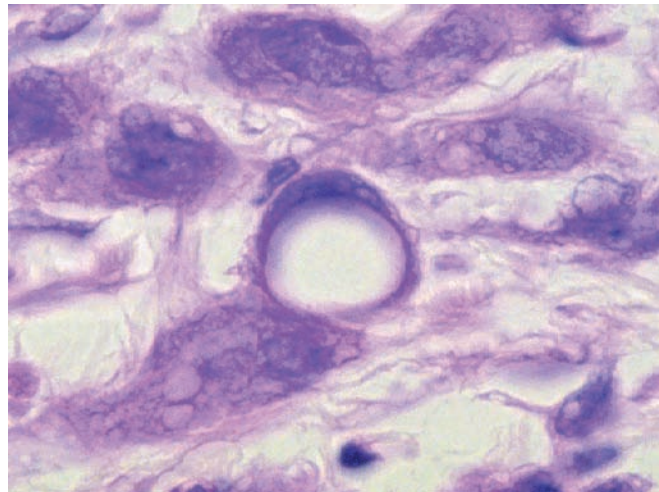
Figure 4.122 — Signet ring cell carcinoma. Abundant mucin containing few degenerated neoplastic cells with prominent signet ring morphology. The diagnostic cells are often rare in such cases and should not be confused with benign muciphages and require a careful evaluation of the entire smear. (Papanicolaou stain, low power)
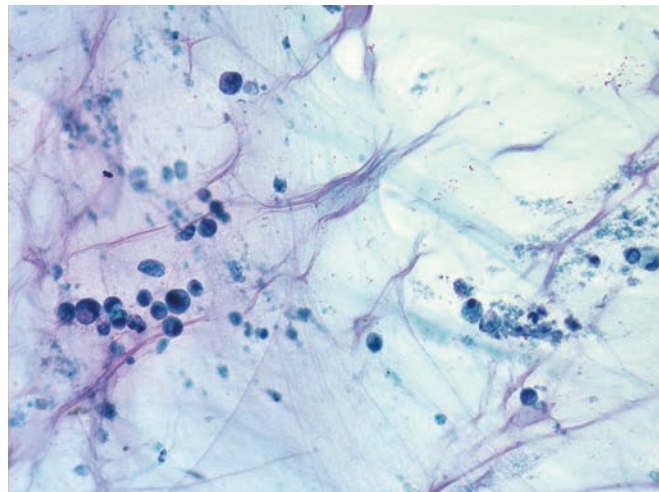
Signet Ring Cell Carcinoma
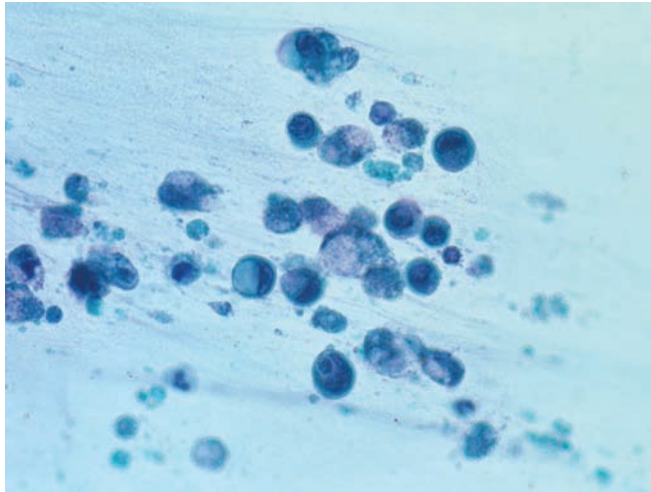
Figure 4.123 — Signet ring cell carcinoma. Higher magnification of the previous case shows the classic signet ring cell morphology with pleomorphic nuclei indented by large intracytoplasmic mucin vacuoles. Numerous degenerated cells and karyorrhectic nuclei are also seen. (Papanicolaou stain, high power)
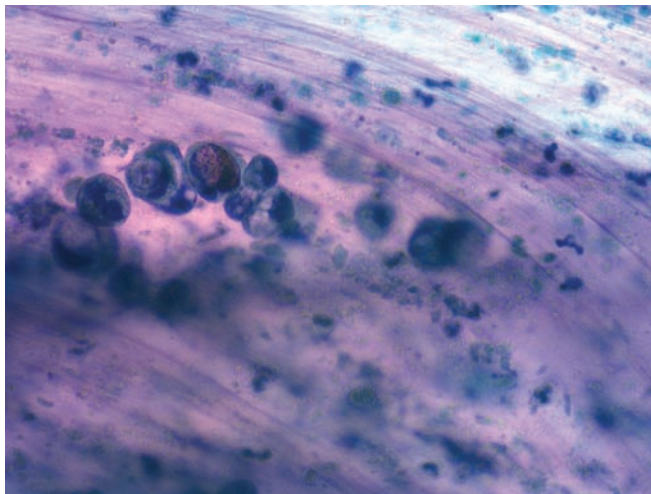
Figure 4.124 — Signet ring cell carcinoma. Another case illustrating loosely associated malignant cells. Pleomorphic nuclei and intracytoplasmic mucin vacuoles are evident. Background contains abundant mucin as well. Such cells should not be confused with histiocytes or muciphages. (Papanicolaou stain, high power)
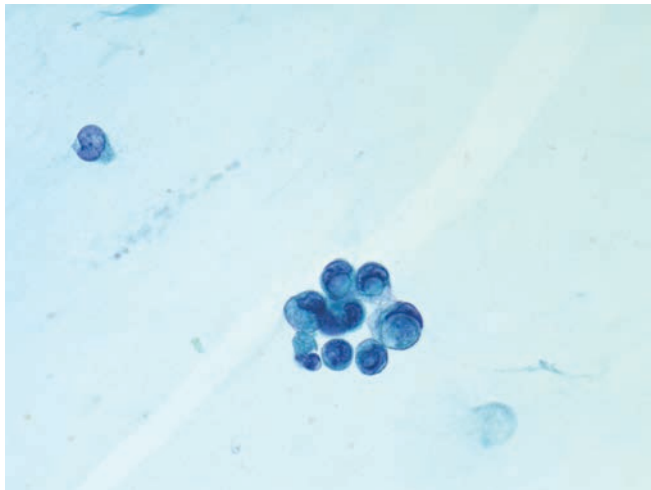
Figure 4.125 — Signet ring cell carcinoma. Findings are similar to the previous cases. Cells are small and are relatively well preserved. Intracytoplasmic mucin vacuoles are clearly apparent. Signet ring cell carcinoma often yields rare malignant cells on FNA, necessitating a careful evaluation of the smears to avoid a false-negative diagnosis. (Papanicolaou stain, high power)

Variants of Ductal Adenocarcinoma

Figure 4.126 — Signet ring cell carcinoma. This was a difficult case as the cells did not have well-formed intracytoplasmic mucin vacuoles. High N/C ratios and a "lymphocyte-like" appearance are evident in these cells. (Diff Quik stain, high power)
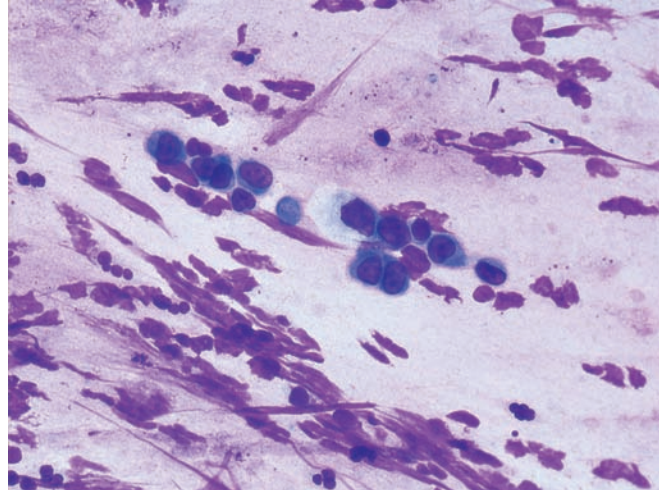
Acinar Cell Carcinoma
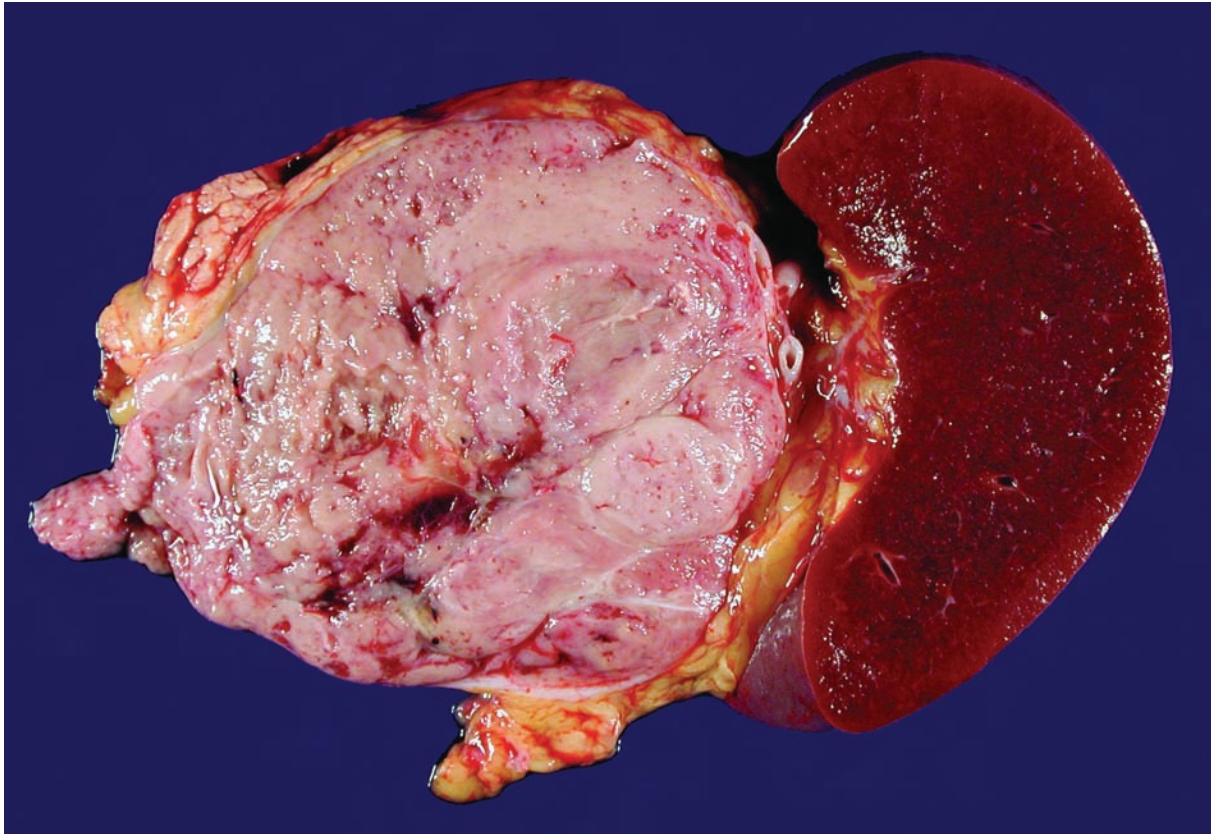
Figure 4.127 — Acinar cell carcinoma in the tail of the pancreas. As in this example, acinar cell carcinomas are typically large (10 cm), well circumscribed, soft, and fleshy. Less commonly, acinar carcinomas can be fibrotic, or they may form cystic masses. Other neoplasms that form fleshy masses in the pancreas include well-differentiated pancreatic endocrine neoplasm, pancreatoblastoma, solid-pseudopapillary neoplasm, and lymphoma. Light microscopic examination, and in some cases immunolabeling, is needed to distinguish among these entities.

Acinar Cell Carcinoma

Figure 4.128 — Acinar cell carcinoma. This cellular neoplasm with little stroma is composed of large pyramidal cells that aggregate around poorly formed small lumina. The cells have a granular eosinophilic cytoplasm and somewhat basally oriented nuclei with single prominent nucleoli. The differential diagnosis includes well-differentiated pancreatic endocrine neoplasm (trabecular, nested, or gyriform growth patterns), pancreatoblastoma (squamoid nests), and the solid-pseudo papillary neoplasm (poorly cohesive cells, nuclear grooves, delicate vessels, hyaline globules). (Hematoxylin and eosin stain, high power)
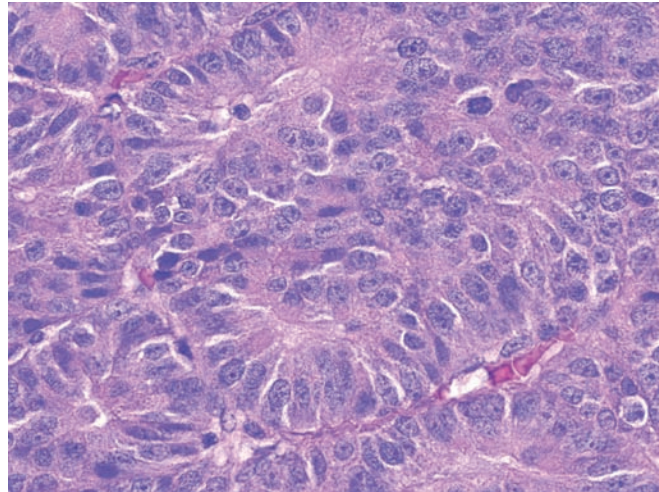
Figure 4.129 — Acinar cell carcinoma. This carcinoma is composed of sheets of large cells with granular eosinophilic cytoplasm and pleomorphic nuclei with single prominent nucleoli. As in this case, many acinar cell carcinomas do not form well-defined acinar structures. In these instances, the presence of single large nucleoli can be a clue to the diagnosis. The differential diagnosis includes other solid cellular neoplasms with minimal stroma such as the well-differentiated pancreatic endocrine neoplasm (salt and pepper chromatin) and the pancreatoblastoma (squamoid nests). Metastases to the pancreas from an extrapancreatic primary should also be considered. (Hematoxylin and eosin stain, high power)
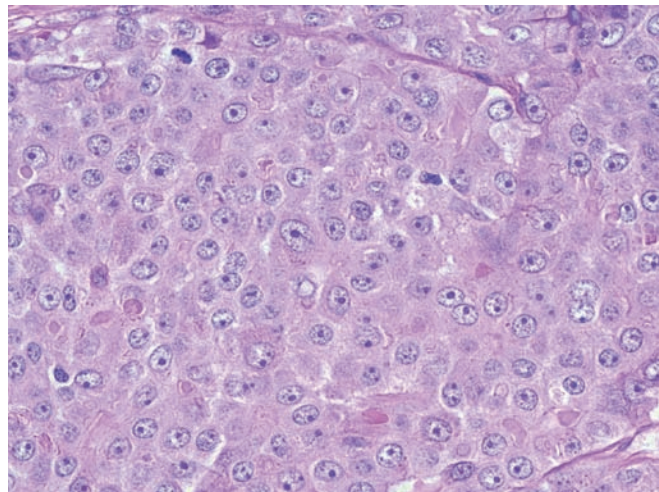
Figure 4.130 — Acinar cell carcinoma. Immunolabeling for chymotrypsin demonstrates the production of exocrine pancreatic enzymes by the neoplasm. Immunolabeling for trypsin and lipase will also be positive in most cases, and a minority of acinar cell carcinomas will focally label with antibodies to endocrine markers such as chromogranin and synaptophysin. Mixed acinar-endocrine carcinoma (≥25% endocrine differentiation) and pancreatoblastomas (squamoid nests) also express exocrine pancreatic enzymes. (Immunolabeling with antibodies to chymotrypsin, high power)
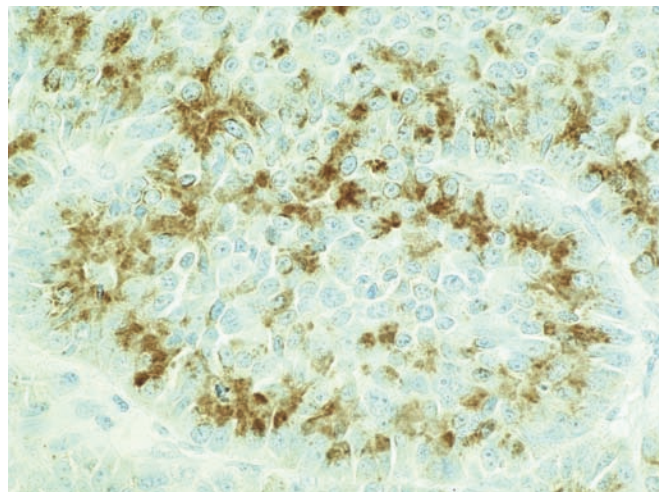
Acinar Cell Carcinoma
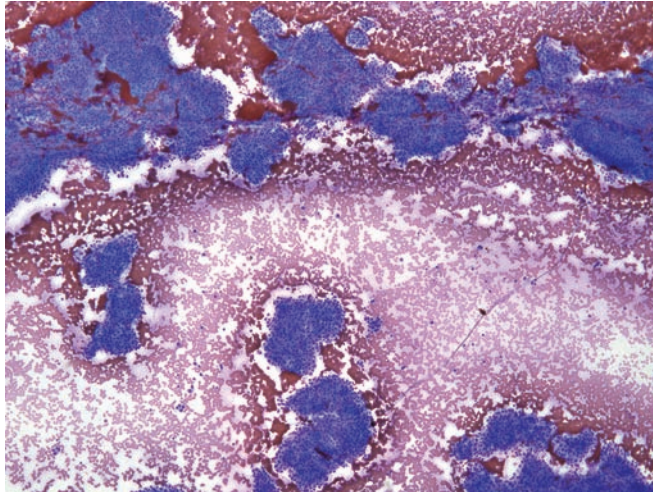
Figure 4.131 — Acinar cell carcinoma. This cellular specimen with multiple tissue fragments is composed of uniform cells with moderate amounts of cytoplasm. Neoplastic cells are arranged in monolayered sheets and also display traversing capillaries. Glandular differentiation is not evident. Differential diagnosis would include a well-differentiated endocrine neoplasm (islet cell tumor). (Diff Quik stain, low power)
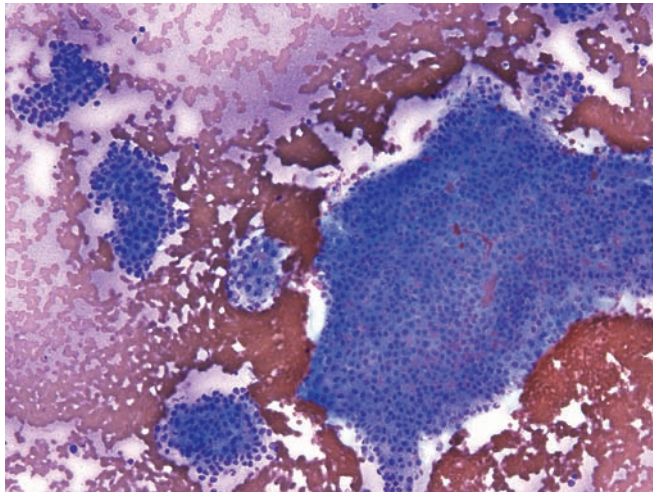
Figure 4.132 — Acinar cell carcinoma. Individual cells have uniform round nuclei and moderate amounts of densely granular, basophilic cytoplasm. Cells display nests and small acinar formations. Single cells are not evident in this case. Lack of lobular architecture with a more solid "sheet-like" architecture helps distinguish this lesion from benign acinar epilthelium. (Diff Quik stain, low power)
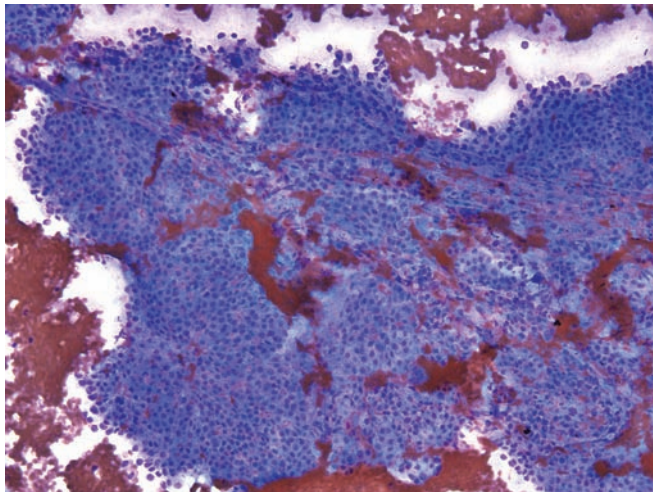
Figure 4.133 — Acinar cell carcinoma. Cytomorphology in this case is similar to the one in the previous case. There are two capillaries crossing the tissue fragments. Acinar cell differentiation is evident in the form of dense cytoplasmic basophilic granularity. (Diff Quik stain, low power)

Acinar Cell Carcinoma

Figure 4.134 — Acinar cell carcinoma. This partially intact tissue fragment with neoplastic cells has moderately hyperchromatic, uniform nuclei with occasional nucleoli and delicate basophilic granular cytoplasm. Occasional nuclei with intranuclear inclusions are also seen (7 o'clock). Lack of single dispersed cells may help to differentiate this from a pancreatic endocrine neoplasm. (Diff Quik stain, medium power)
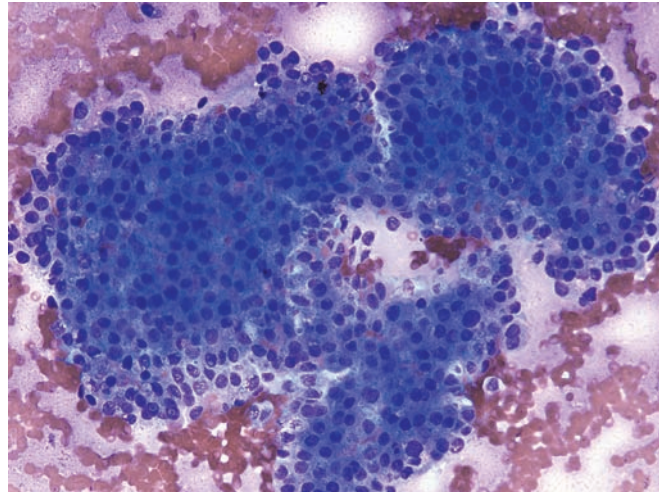
Figure 4.135 — Acinar cell carcinoma. The nuclei are mostly round or oval with mild anisonucleosis, irregular borders, and prominent nucleoli. The cells have the typical granular cytoplasm of acinic cell differentiation and do not display glandular (lumen forming) differentiation. (Diff Quik stain, high power)
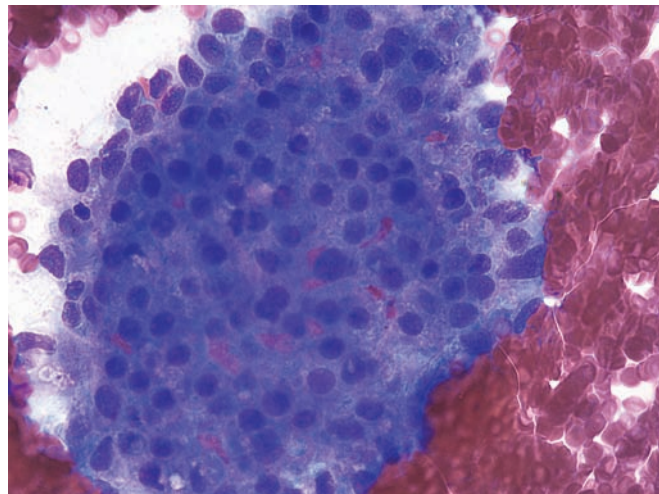
Figure 4.136 — Acinar cell carcinoma. Neoplastic cells form a syncytium. Occasional binucleated cells are present. Some nuclei have prominent nucleoli. Cytoplasm has dense basophilic granularity. (Diff Quik stain, high power)
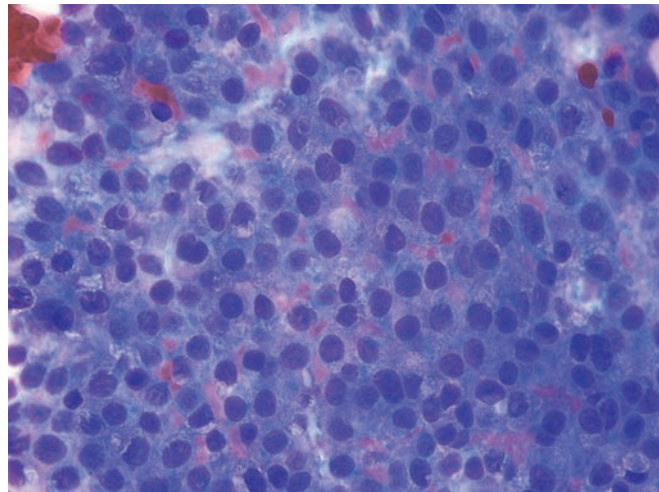
Acinar Cell Carcinoma
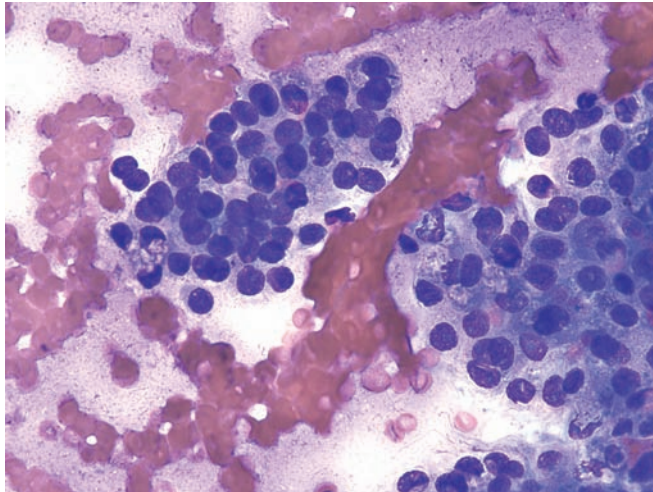
Figure 4.137 — Acinar cell carcinoma. Irregular cellular organization with slight three-dimensionality is observed. Note the neoplastic cells with overlapping nuclei next to an acinus-like formation (fragment on the left). Nuclei display prominent nucleoli. (Diff Quik stain, high power)
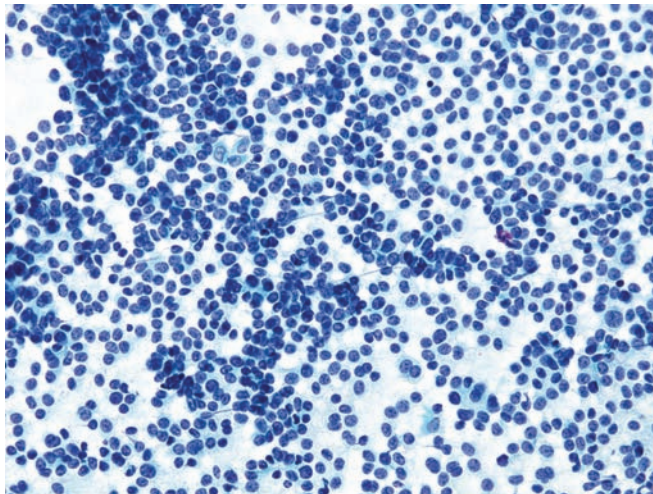
Figure 4.138 — Acinar cell carcinoma. This cellular specimen is composed predominantly of single cells with small tissue fragments and aggregates of neoplastic cells. This represents another cellular pattern of acinar cell carcinoma on FNA. Neoplastic cells have predominantly round, rarely ovoid, nuclei and delicate cytoplasm with indistinct cellular borders. In this case the nuclear monotony and single cell dispersion make the exclusion of a pancreatic endocrine neoplasm nearly impossible without immunohistochemical labeling. (Papanicolaou stain, low power)
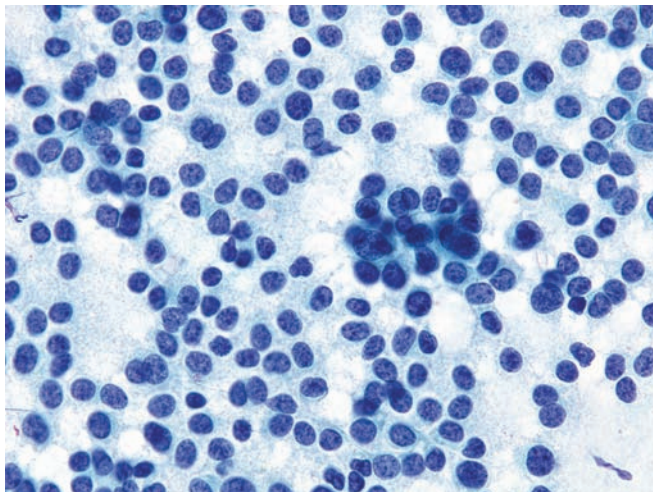
Figure 4.139 — Acinar cell carcinoma (higher magnification of Figure 4.138). Nuclei are round to oval and have a granular chromatin pattern with chromocenters and rare micronucleoli. The cytoplasm of most of the neoplastic cells is delicate, granular, and finely vacuolated, with ill-defined cytoplasmic borders. There is one atypical acinar (rosette-like) formation (right of center). The granularity in the smear background is the result of cytoplasmic disintegration on smearing. Immunostaining is mandatory in such cases to confirm acinar differentiation and exclude other tumors (such as pancreatic endocrine neoplasm and solid-pseudopapillary neoplasm). (Papanicolaou stain, medium power)

Acinar Cell Carcinoma

Figure 4.140 — Acinar cell carcinoma. Single cells with round or ovoid, centrally or eccentrically located nuclei are seen here. Some of the neoplastic cells contain intracytoplasmic vacuoles and entangled cord-like clear areas of unknown significance. A well-differentiated endocrine neoplasm is often a difficult diagnosis to exclude and all such cases should be immunolabeled before a definitive call is made. (Diff Quik stain, high power)
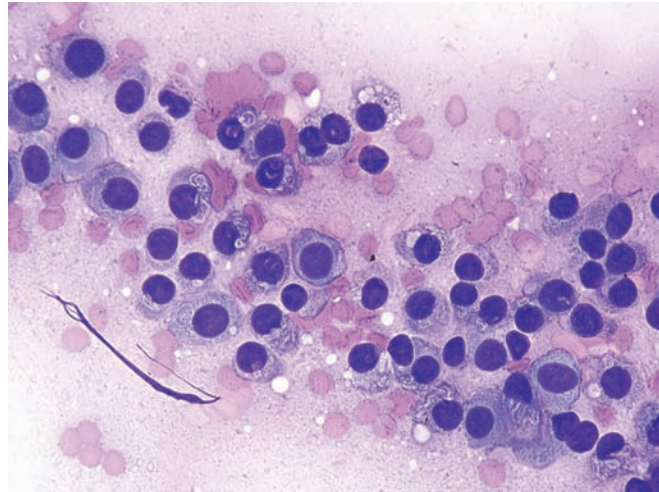
Figure 4.141 — Acinar cell carcinoma. Neoplastic cells displaying lack of discernible cytoplasm with naked nuclei and granular cytoplasm. There are scattered rosette-like or acinus-like formations. There is significant morphologic overlap with a well-differentiated pancreatic endocrine neoplasm. (Papanicolaou stain, low power)
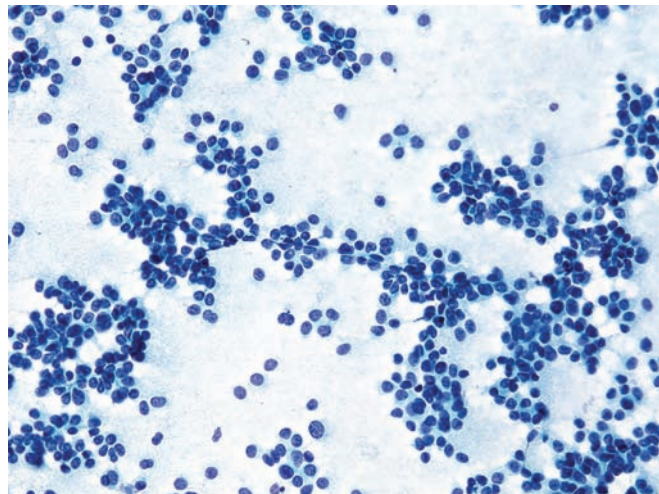
Figure 4.142 — Acinar cell carcinoma. An aggregate of loosely placed neoplastic cells with mostly single, centrally located nuclei and finely vacuolated cytoplasm. Nuclei vary slightly in size, and rare cells are binucleated. Occasional mitoses are also noted. Similar cytomorphology may also be seen in well-differentiated pancreatic endocrine neoplasm. Due to a lack of well-visualized cytoplasm, occasional cases may create diagnostic confusion with malignant lymphoma. However, occasional acinar formations and densely granular smear background is quite helpful to exclude the latter from the list of differential diagnosis. (Diff Quik stain, low power)
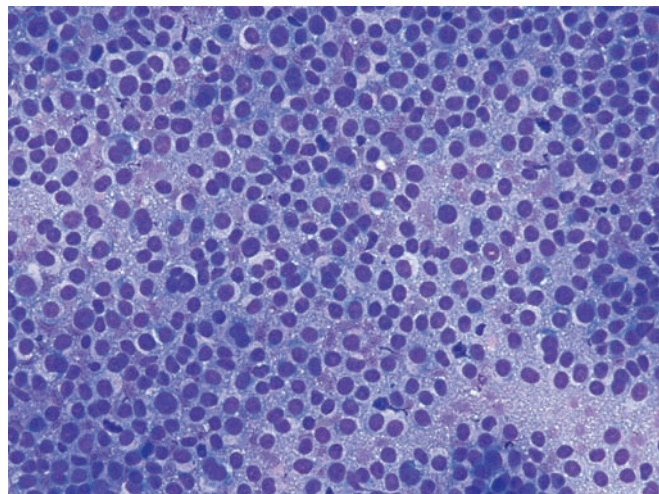
Acinar Cell Carcinoma
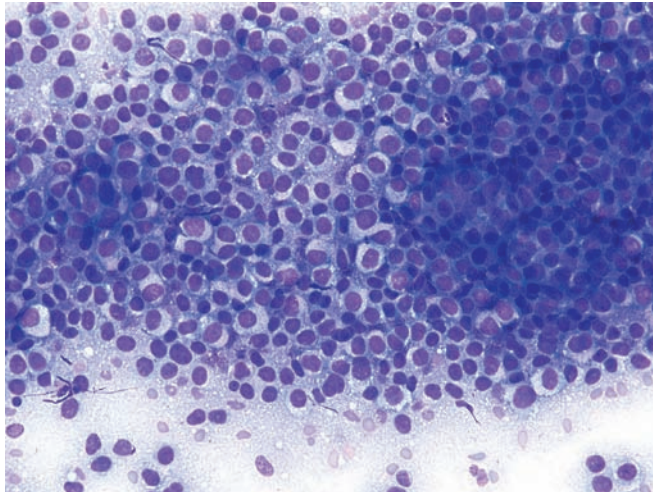
Figure 4.143 — Acinar cell carcinoma. Singly dispersed malignant cells with large nuclei, occasional prominent nucleoli and moderate amount of finely vacuolated, clear or granular cytoplasm. (Diff Quik stain, low power)
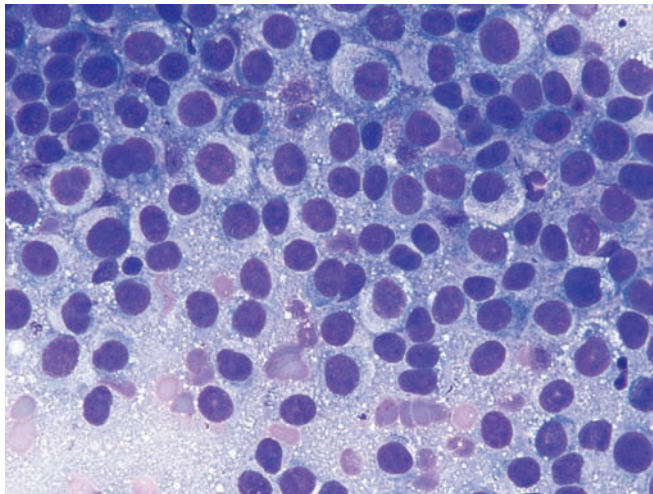
Figure 4.144 — Acinar cell carcinoma. Fine vacuolization and basophilic granularity of the cytoplasm are quite pronounced. Additionally, there is mild amisonucleosis and occasional prominent nucleoli are present. (Diff Quik stain, high power)
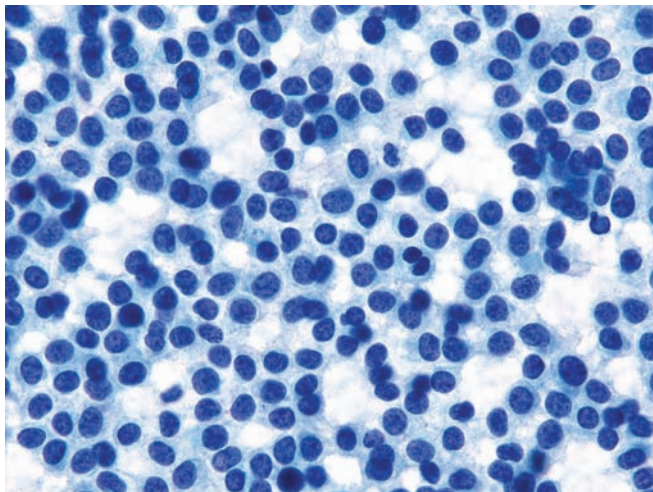
Figure 4.145 — Acinar cell carcinoma. Neoplastic cells arranged singly or in small groups. There are round or ovoid nuclei with uniform chromatin pattern and delicate, fragile cytoplasm. As shown in the previous figures, these features are typical of an acinar cell carcinoma but may also be seen in some well differentiated endocrine (islet cell) neoplasms. (Papanicolaou stain, medium power)

Acinar Cell Carcinoma

Figure 4.146 — Acinar cell carcinoma. This is an example of a poorly differentiated acinar cell carcinoma. Pleomorphic cells with hyperchromatic nuclei, markedly varying in size and shape, are seen. The cells show degenerative changes, and focal areas of necrotic debris are present in the background. Although these findings are diagnostic for cancer, the specific type of tumor cannot be determined without immunolabeling. (Papanicolaou stain, low power)
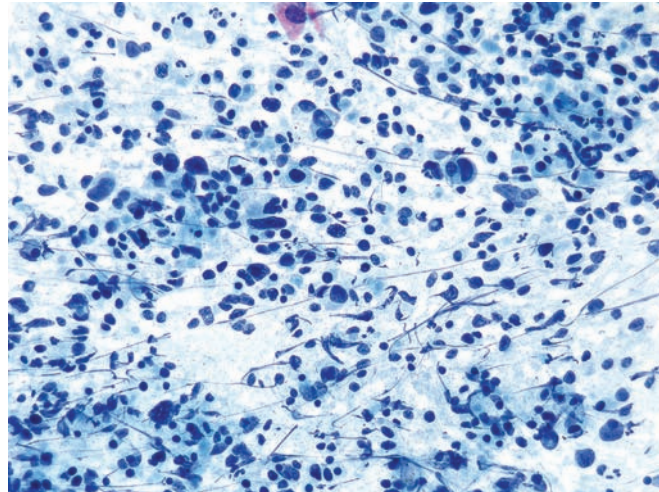
Figure 4.147 — Acinar cell carcinoma. Poorly differentiated cells with large, hyperchromatic, bizarre and pleomorphic nuclei are present. Occasional lymphocytes are present in the background, providing a size reference. An acinus-type structure is seen in the center of the image. (Papanicolaou stain, high power)
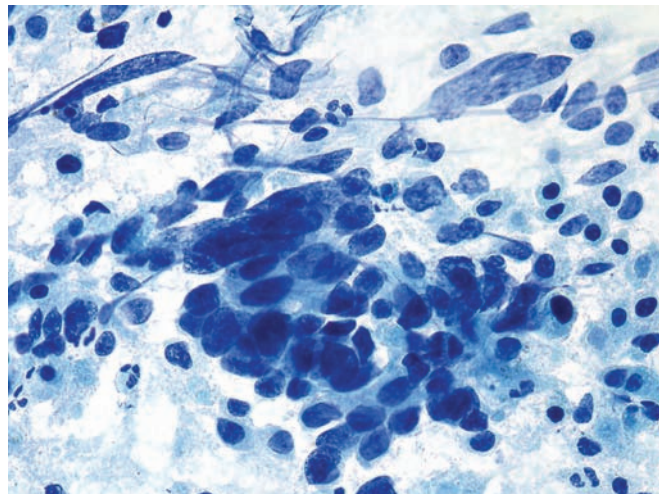
Figure 4.148 — Acinar cell carcinoma. Pleomorphic neoplastic cells with oval, round, or irregularly shaped nuclei. In the center there is an atypical acinus-like formation with slightly elongated nuclei. Nuclear crush artifact is the result of many background lymphocytes. (Diff Quik stain, high power)
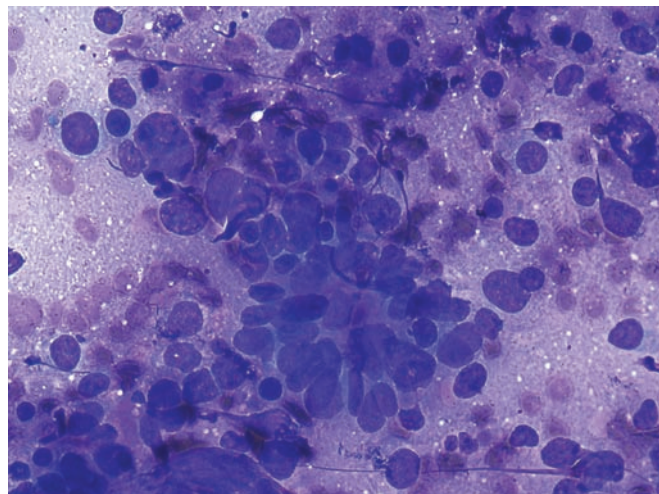
Acinar Cell Carcinoma
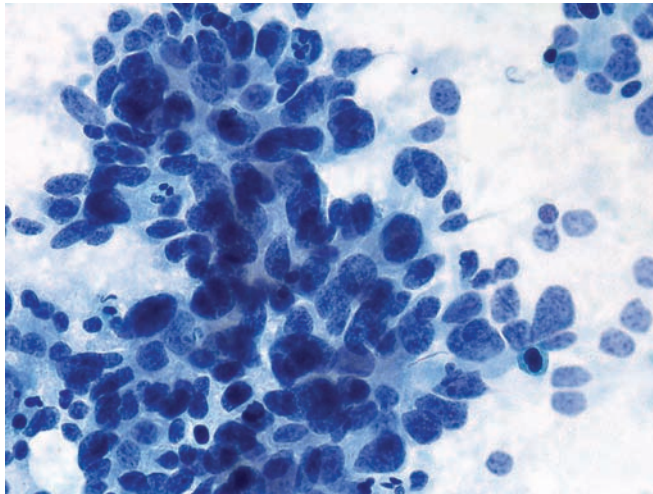
Figure 4.149 — Acinar cell carcinoma. Another example of poorly differentiated acinar cell carcinoma. Neoplastic cells are disorganized, but several atypical acinar formations are present. The acinar formations can be easily confused with "rosettes" of an endocrine neoplasm. (Papanicolaou stain, high power)
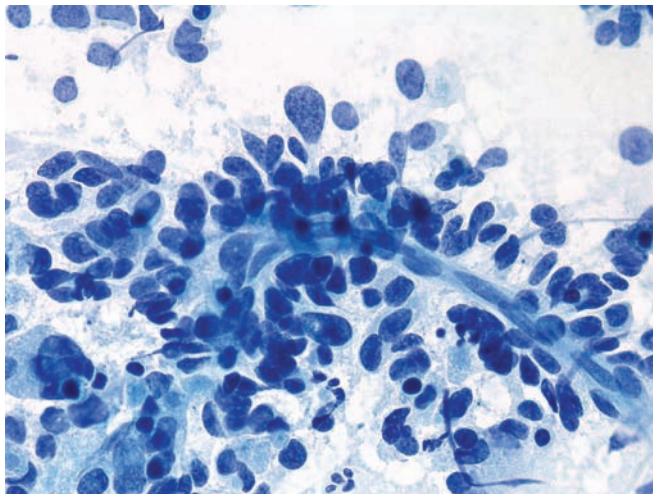
Figure 4.150 — Acinar cell carcinoma. Poorly differentiated neoplastic cells surrounding a capillary vessel are noted. Neoplastic cells are poorly preserved. Most cells have lost all or part of their cytoplasm. The fine and evenly dense nuclear chromatin raises the differential diagnosis of endocrine differentiation in such cases. (Papanicolaou stain, high power)
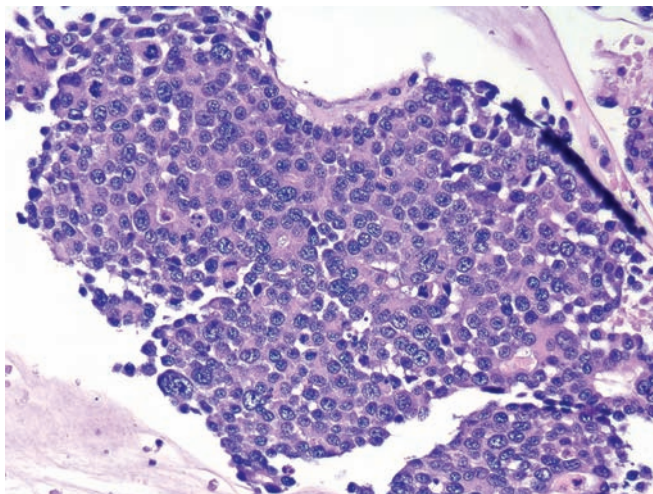
Figure 4.151 — Acinar cell carcinoma (cell block section). Poorly differentiated neoplastic cells with large nuclei exhibiting irregular chromatin clumping, variation in size. and varying N/C ratios are seen. Many mitotic figures are present, consistent with aggressive tumor growth. Focal acinar formations and delicate basophilic cytoplasm with small vacuoles are consistent with acinar cell carcinoma. (Hematoxylin and eosin stain, low power)

Acinar Cell Carcinoma

Figure 4.152 — Acinar cell carcinoma (imprint from the resected neoplasm). Poorly differentiated neoplastic cells with bizarre, pleomorphic nuclei, macronucleoli, and eosinophilic cytoplasm are observed. Several well-formed intranuclear pseudoinclusions are present. Smear background is characteristically granular. The patient also had liver metastases at the time of diagnosis. (Hematoxylin and eosin stain, medium power)
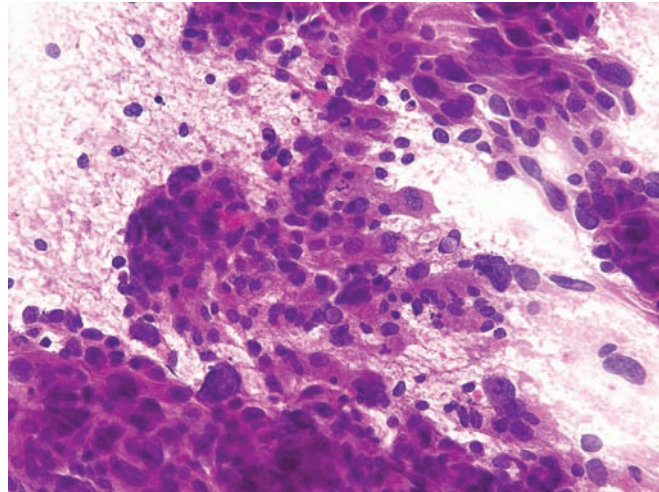
Figure 4.153 — Acinar cell carcinoma (imprint from the resected neoplasm). Poorly preserved cells with ill-defined partially intact granular cytoplasm and large pleomorphic nuclei are seen. This neoplasm was metastatic to the liver at the time of the initial diagnosis of the pancreatic mass. (Hematoxylin and eosin stain, high power)
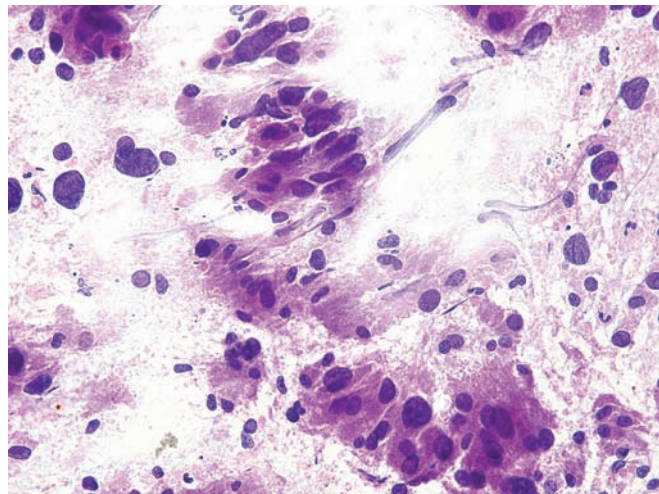
Figure 4.154 — Acinar cell carcinoma (imprint from the resected neoplasm). Neoplastic cells with intranuclear pseudoinclusions can be appreciated. Cytoplasmic features are typical for acinar cell carcinoma. Well-formed intranuclear pseudoinclusions are occasionally observed in these tumors. (Hematoxylin and eosin stain, high power)
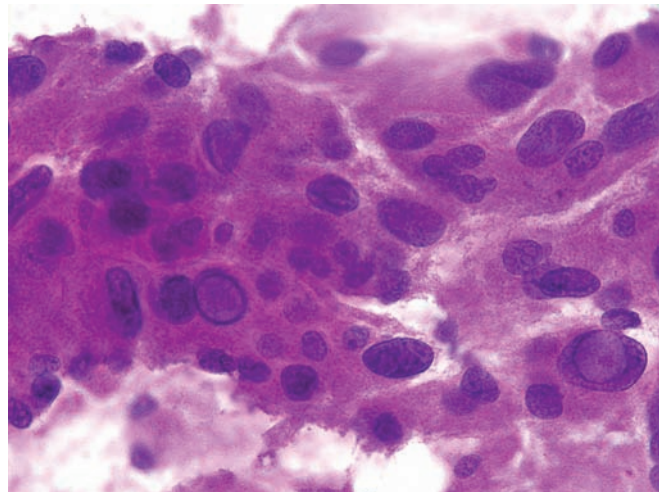
Acinar Cell Carcinoma
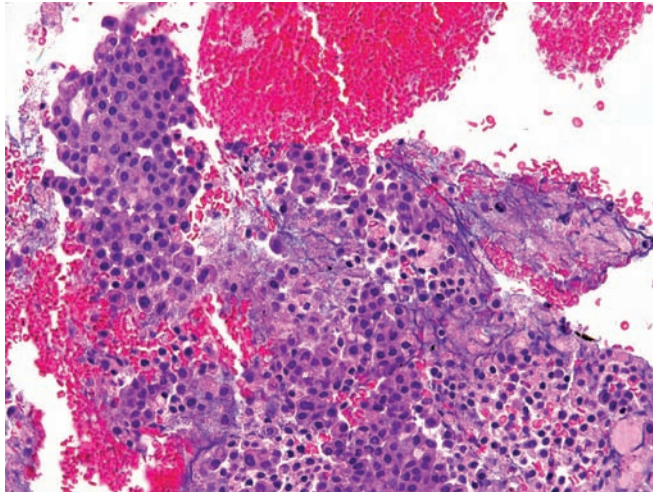
Figure 4.155 — Acinar cell carcinoma (cell block section). Note the uniform appearance of the neoplastic cells with large hyperchromatic nuclei and amphophilic cytoplasm. Acinar formations are seen in the upper left and lower middle portions of the picture. (Hematoxylin and eosin stain, low power)

Pancreatoblastoma

Figure 4.156 — Pancreatoblastoma. This solid cellular neoplasm is composed of uniform cells with centrally placed nuclei. A hint of a squamoid nest can be appreciated in the lower right corner of the field. The differential diagnosis includes other solid cellular neoplasms of the pancreas such as the well-differentiated pancreatic endocrine neoplasm (uniform "salt and pepper" nuclei, strong diffuse labeling for chromogranin and synaptophysin), a solid example of a solid-pseudopapillary neoplasm (strong expression of CD10 and nuclear labeling with antibodies to β-catenin), and acinar cell carcinoma (no squamoid nests). (Hematoxylin and eosin, high power)
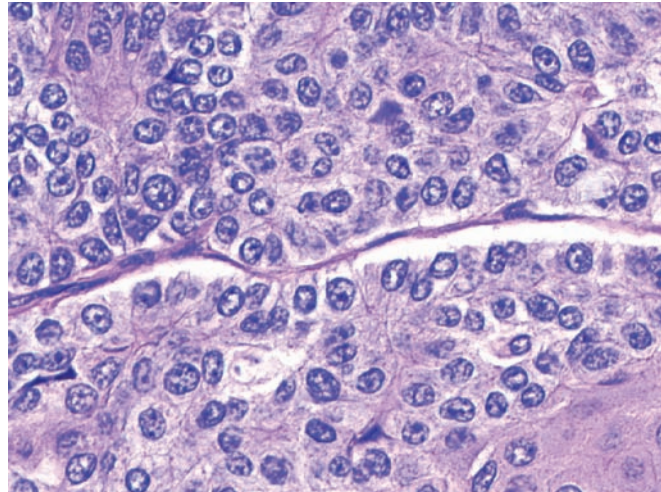
Figure 4.157 — Pancreatoblastoma. A well-defined squamoid nest emerges from a sea of cells with acinar differentiation. The cells with acinar differentiation are recognizable because of their single prominent nucleoli and can be highlighted with immunolabeling for trypsin, chymotrypsin, or lipase. Acinar cell carcinomas top the differential diagnosis. Acinar cell carcinomas would not have squamoid nests. (Hematoxylin and eosin, high power)
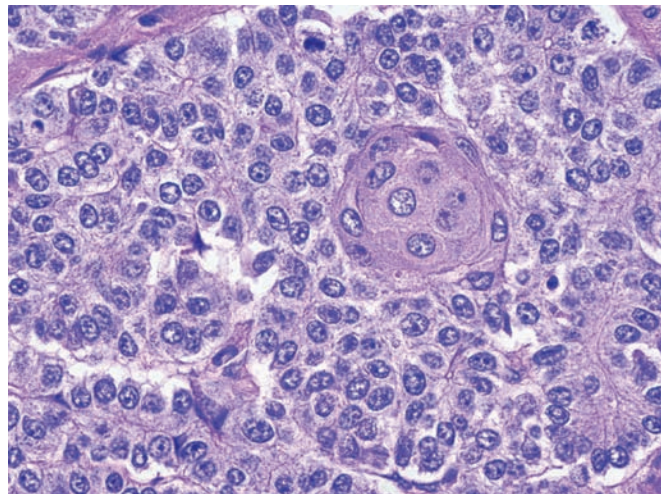
Figure 4.158 — Pancreatoblastoma. Hypercellular specimen composed of uniform, cuboidal-to-round cells with eccentrically located nuclei. The cytoplasm has a fine wispy quality, with occasional bare nuclei seen as well. These findings are similar to those seen in acinar cell carcinoma. (Papanicolaou stain, low power)
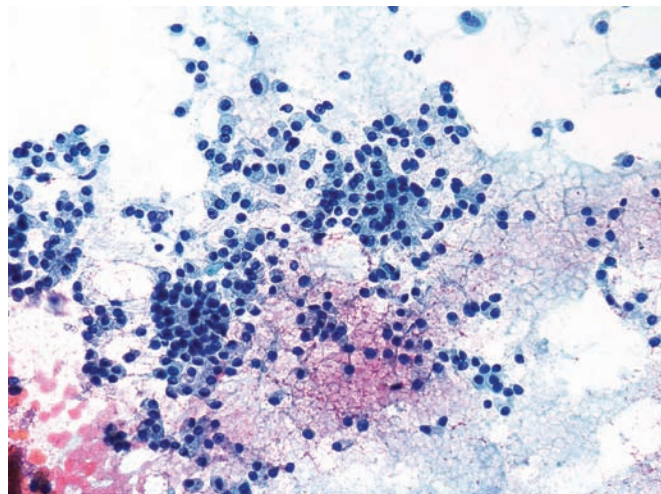
Pancreatoblastoma
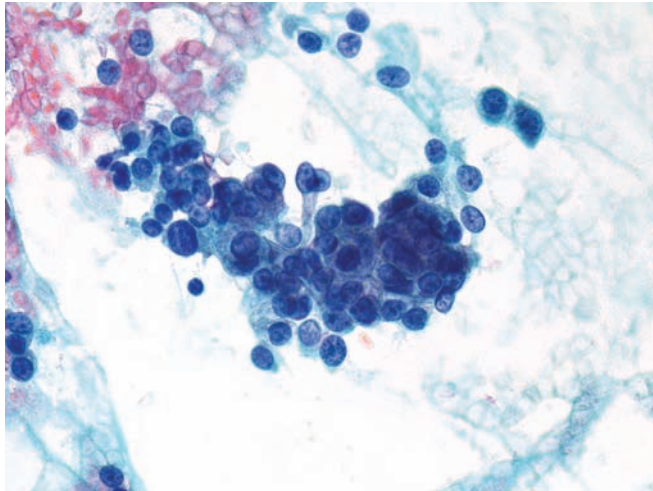
Figure 4.159 — Pancreatoblastoma. There is some variation in nuclear size with occasional nucleoli. Low columnar configuration and luminal borders indicate glandular/acinar differentiation. Pancreatoblastoma is an exceedingly difficult diagnosis on FNA due to its rarity and lack of distinct cytomorphologic characteristics. Clinical history of a mass lesion in a young patient is extremely helpful. (Papanicolaou stain, medium power)
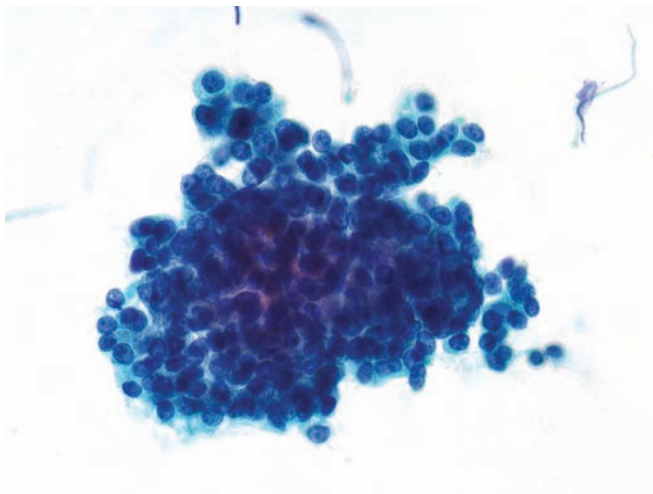
Figure 4.160 — Pancreatoblastoma. Uniform, tightly packed neoplastic cells with monotonous round-to-oval nuclei, scant cytoplasm, and indistinct cell borders. Similar morphology can be seen in acinar cell carcinoma or a well-differentiated pancreatic endocrine neoplasm. (Papanicolaou stain, medium power)
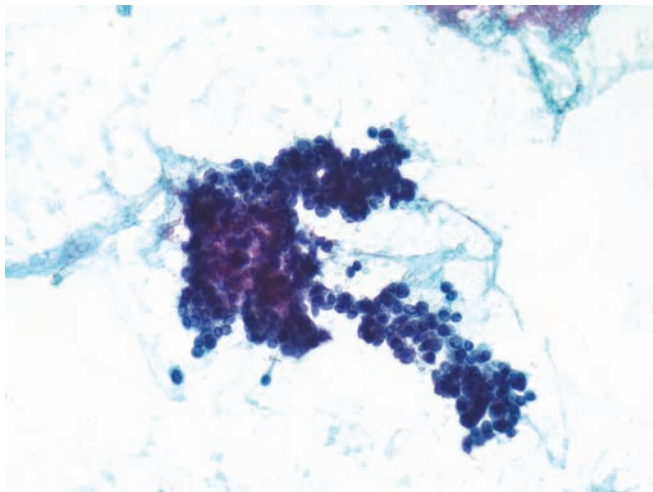
Figure 4.161 — Pancreatoblastoma. Undifferentiated round monotonous neoplastic cells with hyperchromatic nuclei and scant-to-absent cytoplasm resembling pancreatic endocrine neoplasm. Other primitive tumors with small round blue cell morphology are also included in the differential diagnosis. (Papanicolaou stain, low power)

Pancreatoblastoma

Figure 4.162 — Pancreatoblastoma. Monotonous round-to-oval nuclei some with prominent nucleoli containing acinus-like formations are present. A well-differentiated pancreatic endocrine neoplasm will be difficult to exclude without immunolabeling with appropriate markers. (Diff Quik stain, medium power)
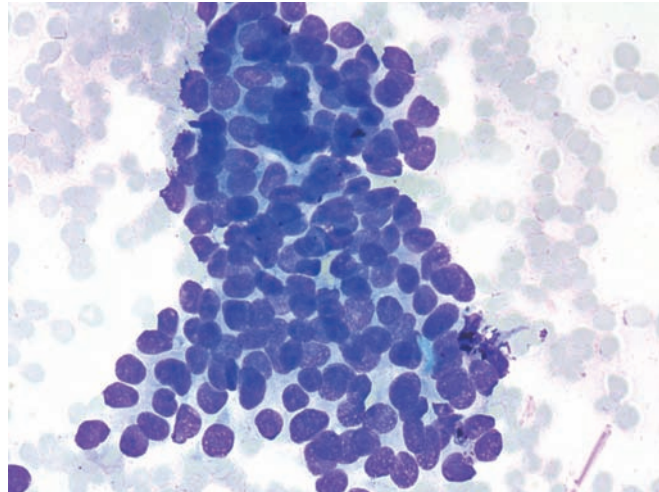
Figure 4.163 — Pancreatoblastoma. Seen here is a tightly packed cellular fragment forming a syncytium. The cells at the edge of the fragment appear as bare nuclei. No distinct cellular differentiation is apparent in this case. (Diff-Quik stain, low power)
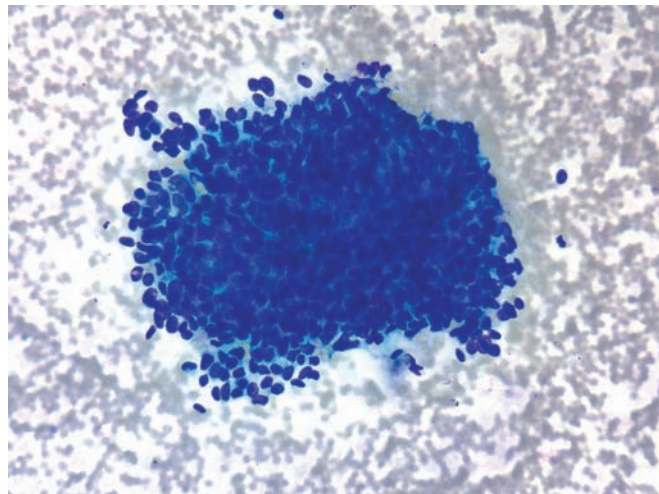
Figure 4.164 — Pancreatoblastoma. This shows a solid cellular tissue fragment with a center containing polygonal cells with pale staining cytoplasm and small nuclei reminiscent of the "squamoid nest" seen in histologic sections of this tumor. (Diff Quik stain, low power)
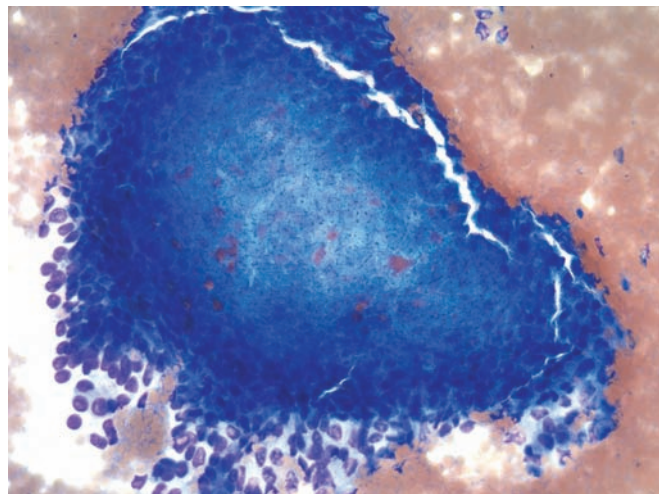
Pancreatoblastoma
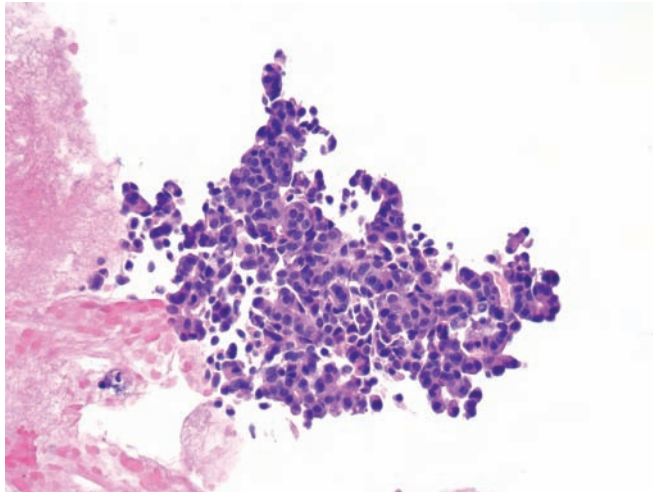
Figure 4.165 — Pancreatoblastoma (cell block section). Round to cuboidal cells with amphophilic cytoplasm displaying prominent acinar differentiation are noted. These cells expressed pancreatic enzymes on immunolabeling in this case. (Hematoxylin and eosin stain, low power)
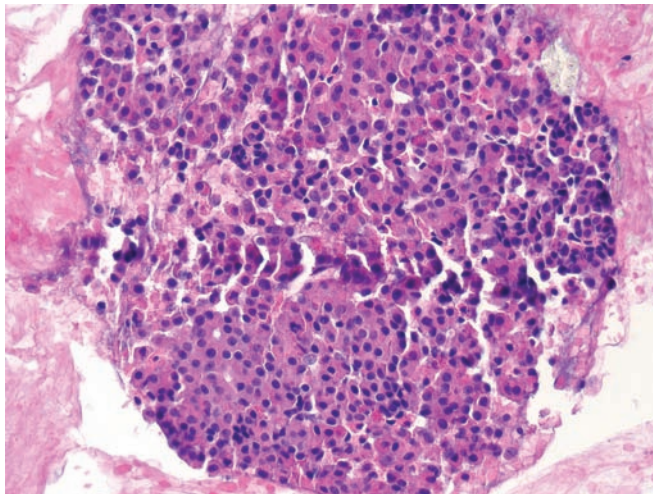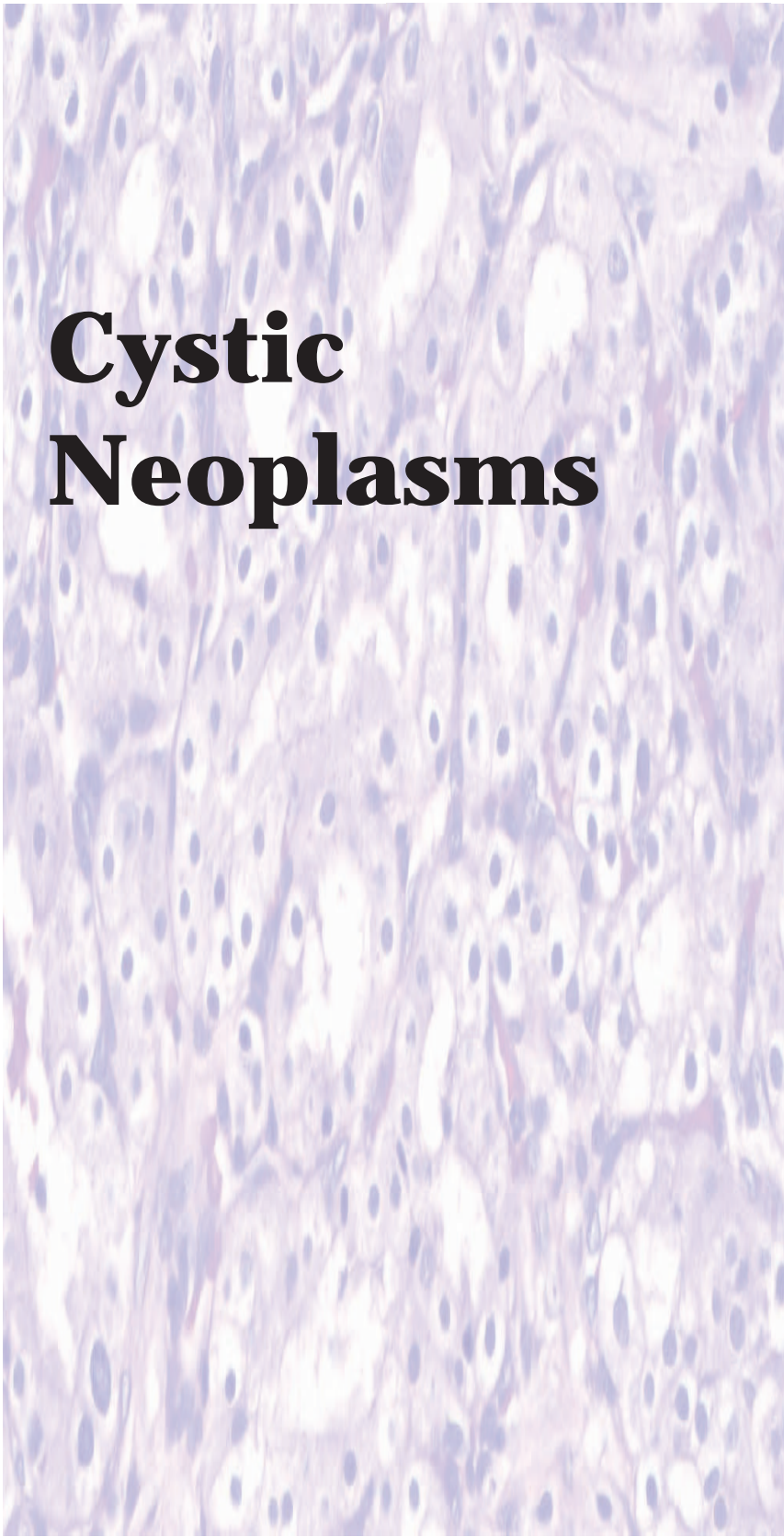
Figure 4.166 — Pancreatoblastoma (cell block section). Neoplastic cells with irregular nests, abortive and well-formed acini resembling acinar cell carcinoma. Squamoid nests are often not appreciated in fine needle aspirates. (Hematoxylin and eosin stain, medium power)

Cystic Neoplasms

5

Serous Cystic Neoplasm
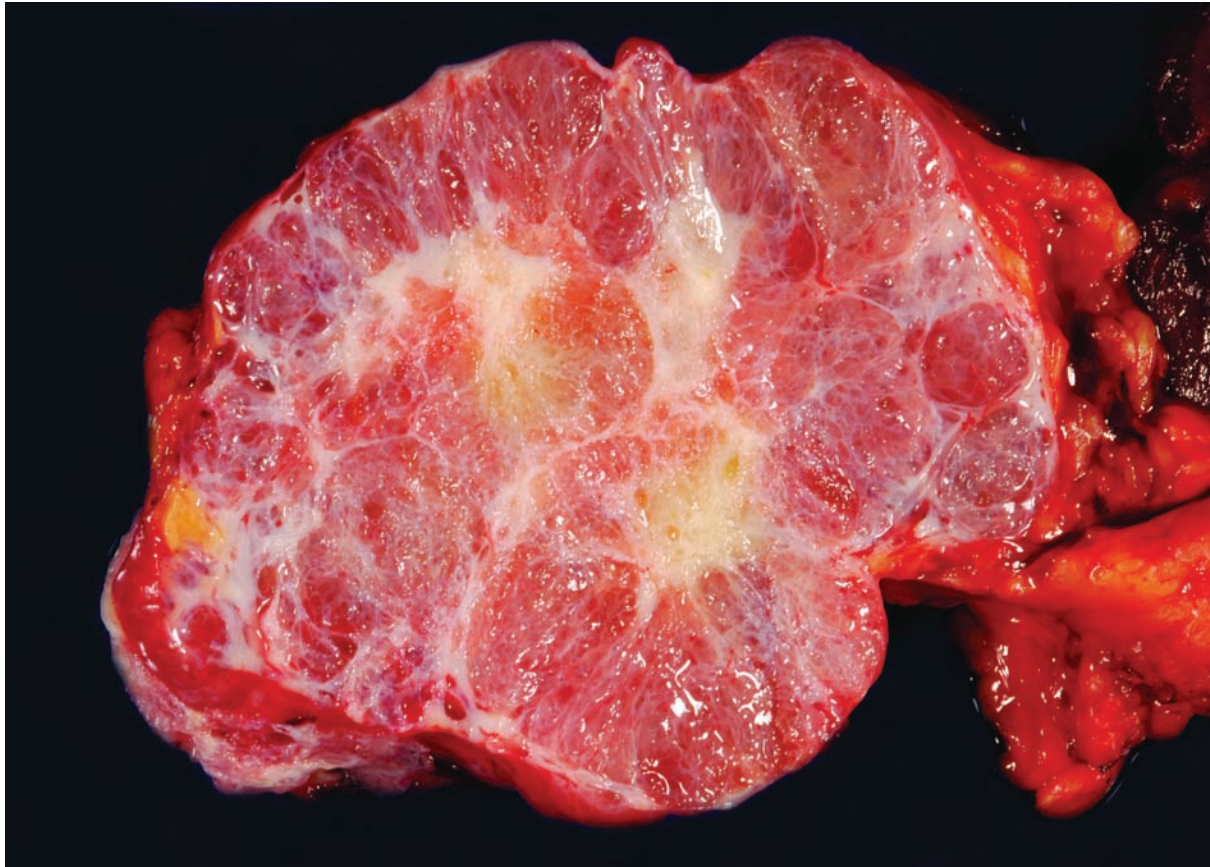
Figure 5.1 — Serous cystadenoma. This well-demarcated neoplasm has a large central scar and is composed of innumerable small thin-walled cysts filled with clear straw-colored fluid. The gross appearance is virtually diagnostic.

Serous Cystic Neoplasm
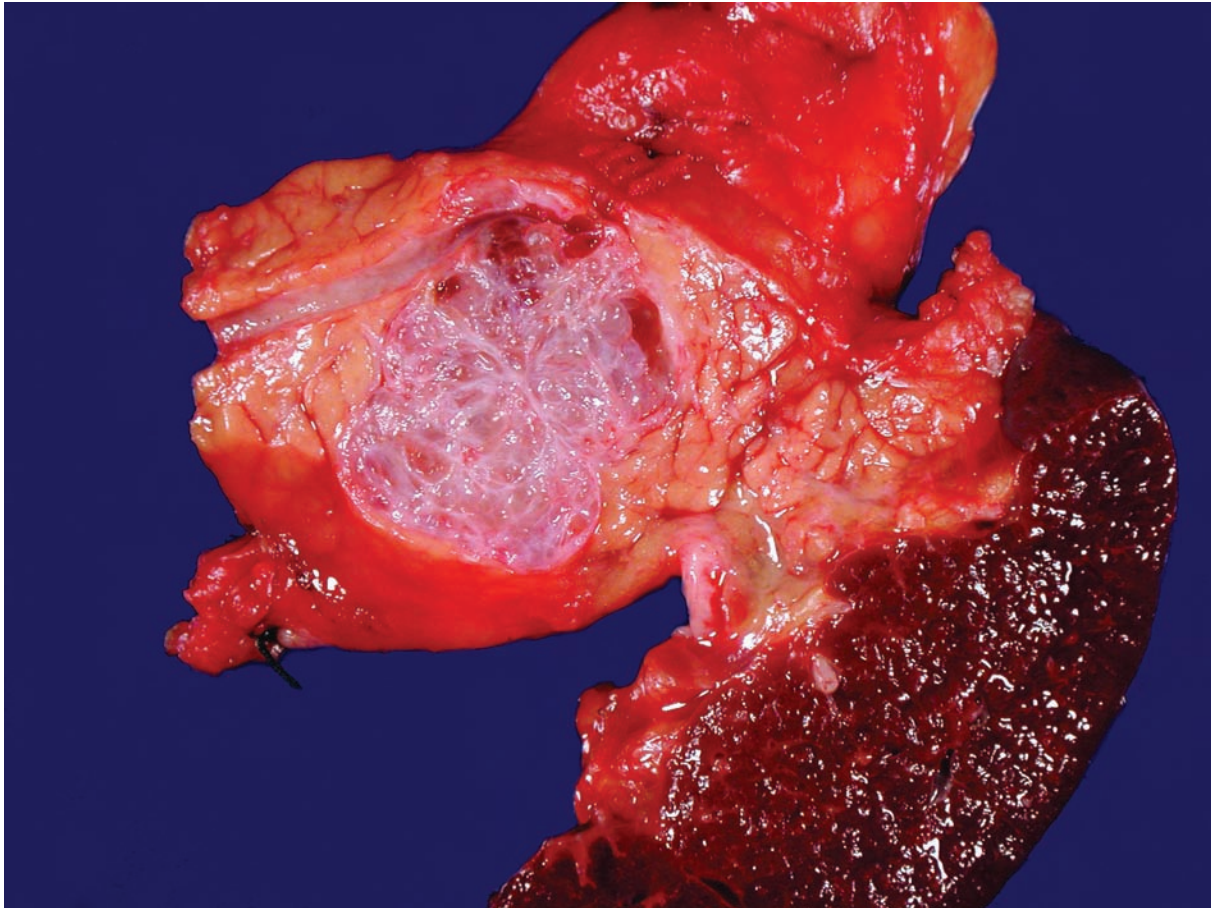
Figure 5.2 — Serous cystadenoma in the tail of the pancreas. Note how this golf ball–sized neoplasm pushes the pancreatic duct superiorly. Smaller serous cystic neoplasms may not have the central stellate scar seen in larger examples.

Serous Cystic Neoplasm

Figure 5.3 — Serous cystadenoma. This cyst is lined by cuboidal cells with uniform round nuclei. The cytoplasmic clearing is caused by the accumulation of glycogen in the neoplastic cells. By contrast, the epithelium lining mucinous cystic neoplasms can be flattened, but adequate sampling of a mucinous cystic neoplasm will reveal at least focal collections of columnar cells with abundant supranuclear mucin. (Hematoxylin and eosin stain, high power)
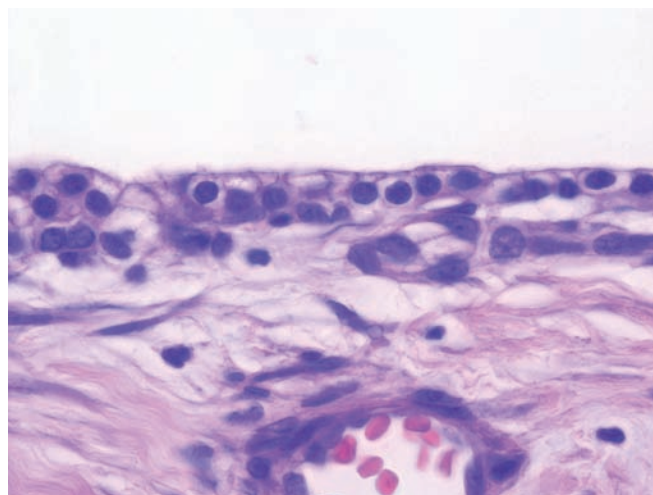
Figure 5.4 — Serous cystadenoma. Although the epithelial cells usually form a flat monolayer, focal papillary formations can be seen. These do not appear to have any prognostic significance. The vast majority of intraductal papillary mucinous neoplasms also have a papillary architecture, but in sharp contrast to the lesion shown, the papillae of intraductal papillary mucinous neoplasms will be lined by tall columnar cells with abundant mucin production. (Hematoxylin and eosin stain, medium power)
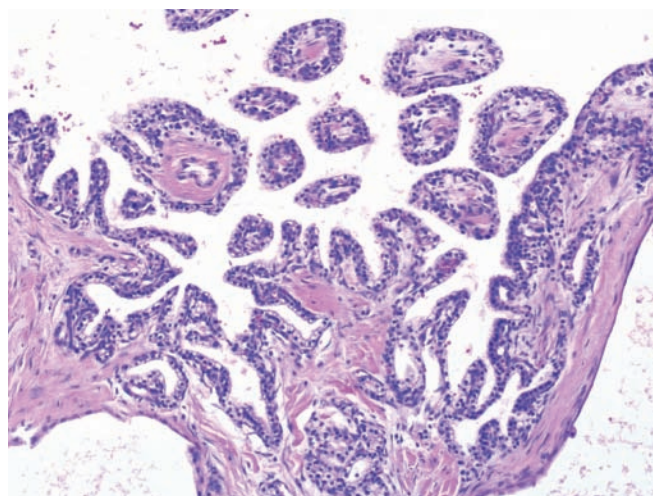
Figure 5.5 — Serous cystadenoma. This serous cystadenoma (left) is adjacent to a large pancreatic intraepithelial neoplasia (PanIN) lesion (right). This can pose a significant problem on fine needle aspiration if the PanIN lesion is sampled instead of the serous cystadenoma. Multiple passes and correlation with imaging can help avoid this diagnostic pitfall. (Hematoxylin and eosin stain, low power)
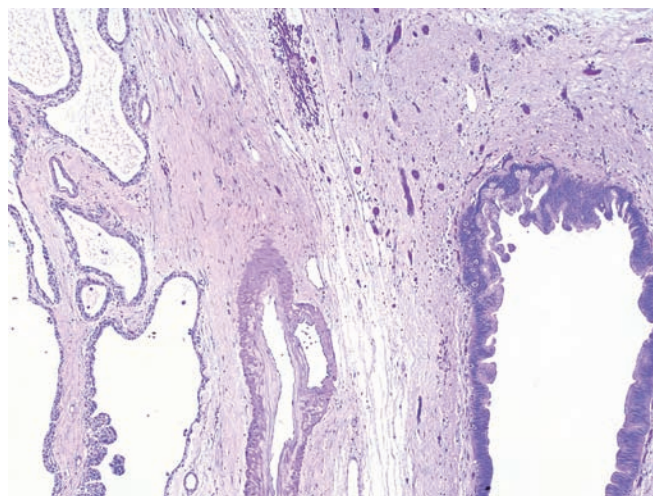
Serous Cystic Neoplasm
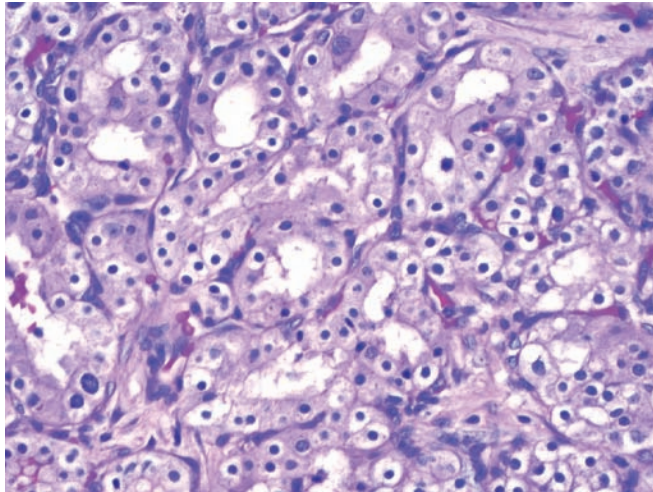
Figure 5.6 — Solid serous adenoma. While most serous neoplasms are cystic, rare grossly solid examples have been reported. These neoplasms mimic well-differentiated endocrine neoplasms, which would strongly and diffusely express synaptophysin and chromogranin, and renal cell carcinoma metastatic to the pancreas, which would express CD10 and renal cell carcinoma marker (RCCma). (Hematoxylin and eosin stain, high power)
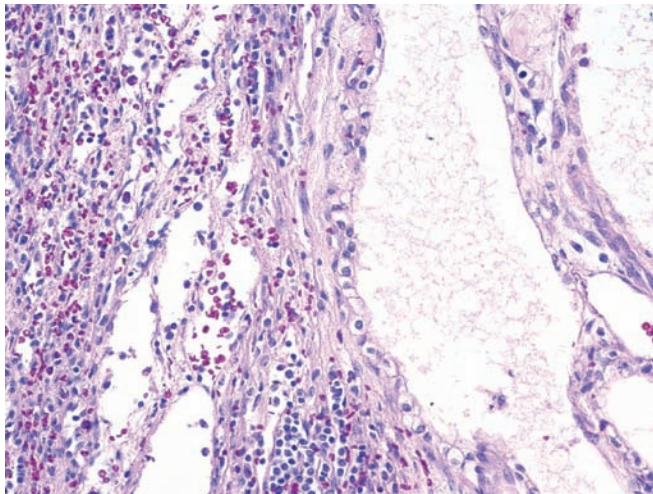
Figure 5.7 — Serous cystadenocarcinoma in the tail of the pancreas. This neoplasm (right) has invaded into the spleen (left). Although extremely rare, serous cystic neoplasms that have metastasized to distant organs have been reported. A remarkable feature of these neoplasms is that even though they are clinically aggressive, the neoplastic cells still lack significant pleomorphism. (Hematoxylin and eosin stain, low power)
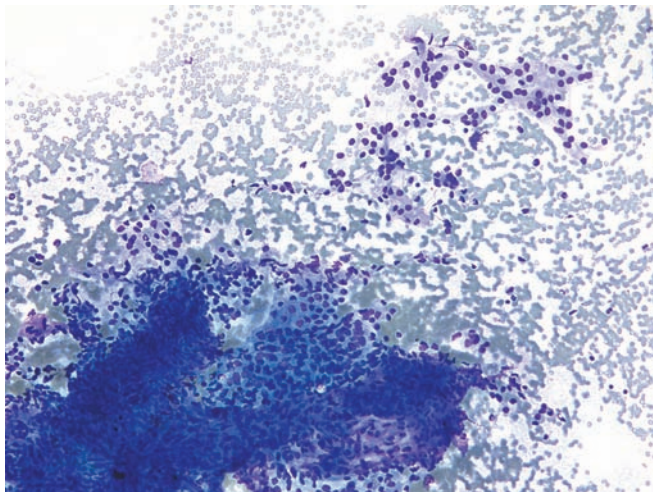
Figure 5.8 — Serous cystadenoma. Loosely cohesive small uniform cells held together by fragile wispy cytoplasm. Smears in cases of serous cystadenoma are hypocellular and may or may not contain any epithelial cells. Diagnosis is typically retrospectively established, as neoplastic cells (even when present), often do not have a distinct phenotypic appearance (such as seen here). (Diff Quik stain, low power)

Serous Cystic Neoplasm

Figure 5.9 — Serous cystadenoma. Noted here is a small tumor fragment with cells displaying uniform, round-to-oval nuclei and delicate cytoplasm. Aspirates often contain abundant clear "serous" fluid and very few cells, and are often not adequate for a cytopathologic diagnosis. (Diff Quik stain, medium power)
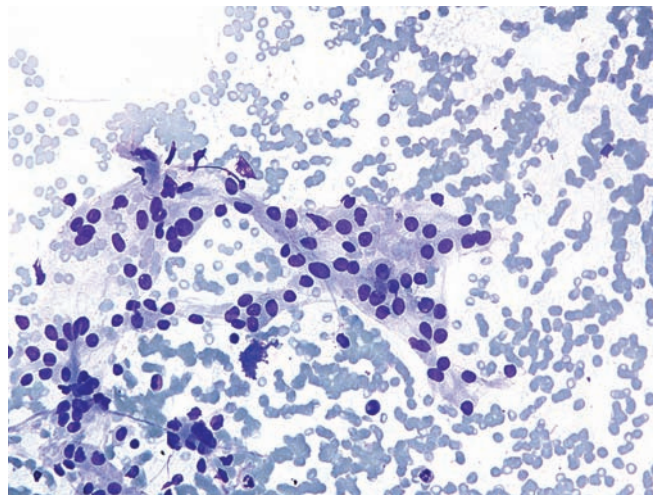
Mucinous Cystic Neoplasm
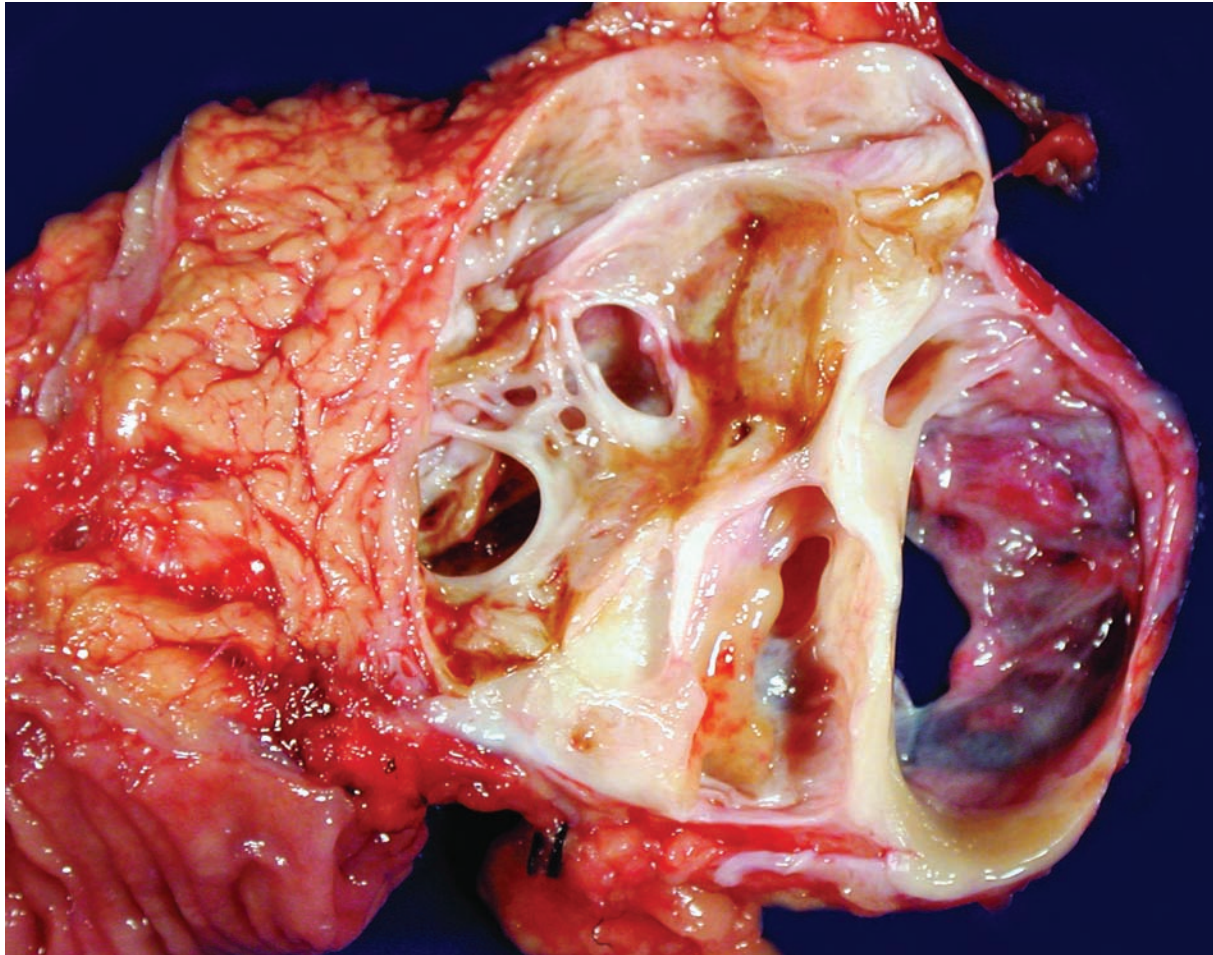
Figure 5.10 — Mucinous cystic neoplasm. This large well-demarcated mass is composed of multiple thick-walled cysts. Before they were transected, the cysts had been filled with thick sticky mucinous fluid. This case is unusual because it arose in the head of the pancreas. Although macrocystic serous cystadenomas can form large cysts, the cyst walls are usually much thinner than those of mucinous cystic neoplasms, and the cysts contain watery straw-colored fluid, not the thick mucinous fluid that was present in this case.

Mucinous Cystic Neoplasm
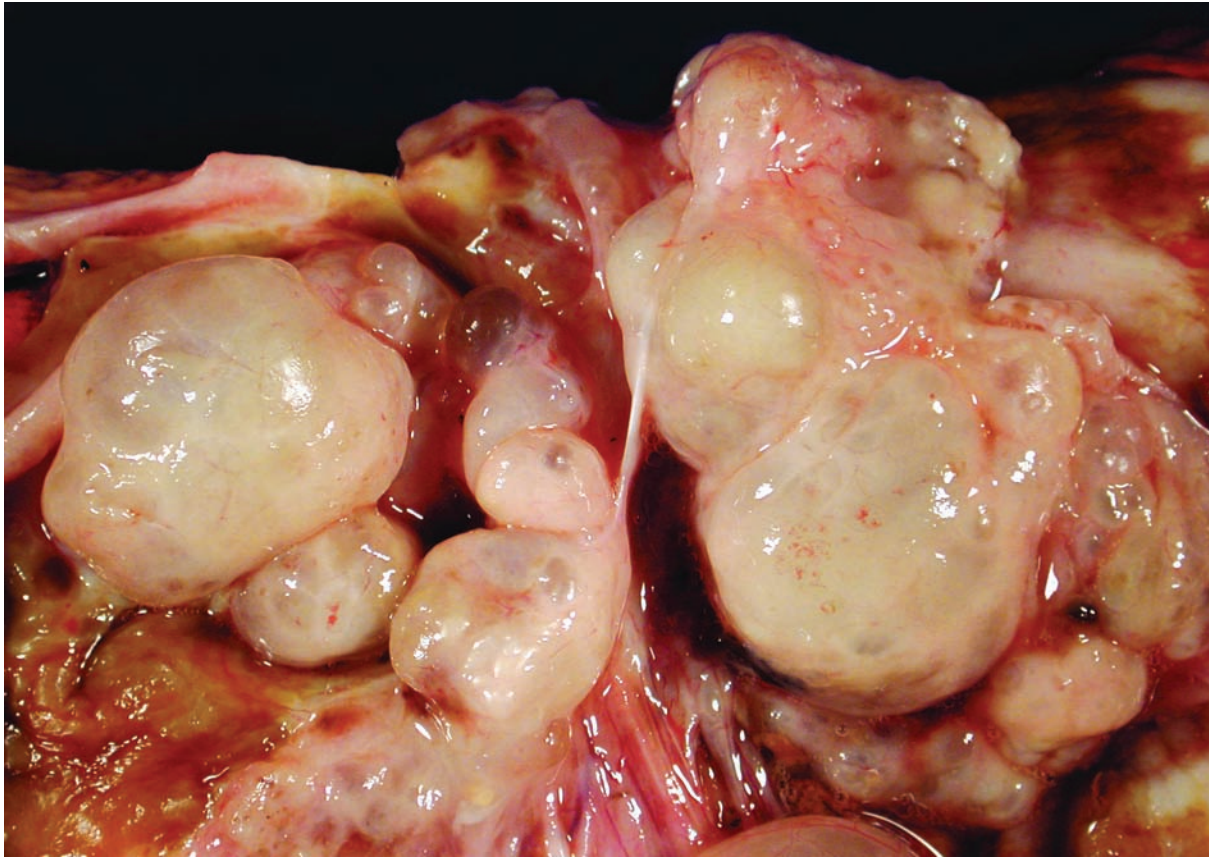
Figure 5.11 — Mucinous cystic neoplasm in the tail of the pancreas. As was true in this case, the vast majority of mucinous cystic neoplasms occur in women (female-to-male ratio 20:1). The cysts shown here are distended with mucin, and the cyst walls are so thick that they are opaque. A branch duct-type of intraductal papillary mucinous neoplasm can have a similar gross appearance. The presence or absence of ovarian-type stroma is used to distinguish between the two entities.

Mucinous Cystic Neoplasm
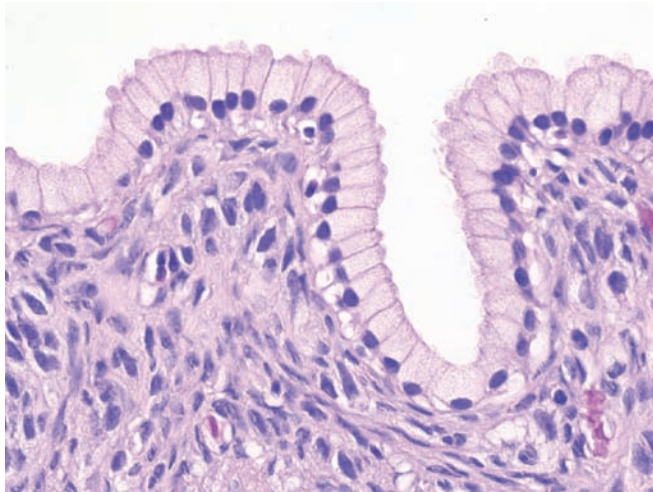
Figure 5.12 — Mucinous cystic neoplasm with low-grade dysplasia. The cyst is lined by a flat columnar mucin-producing epithelium. The nuclei are uniform and basally located. The dense ovarian-type stroma and the absence of a significant intraductal growth help distinguish these neoplasms from intraductal papillary mucinous neoplasms. (Hematoxylin and eosin stain, high power)
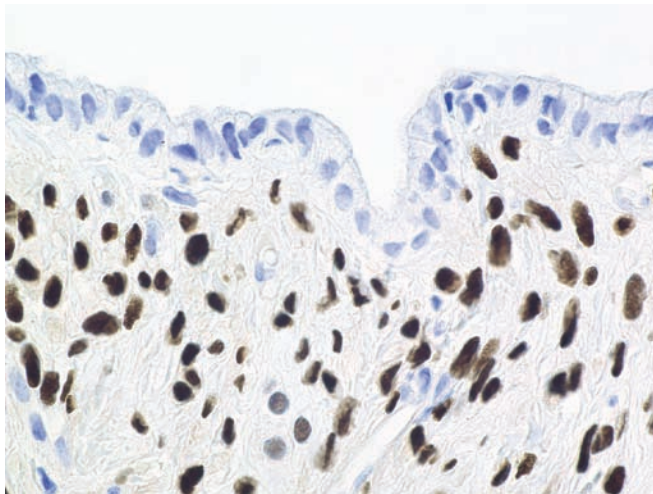
Figure 5.13 — Mucinous cystic neoplasm with low-grade dysplasia. As demonstrated here, immuno-labeling for progesterone receptors can highlight the ovarian-type stroma. The stroma usually also expresses estrogen receptors and inhibin. (Immunolabeling for progesterone receptor, high power)
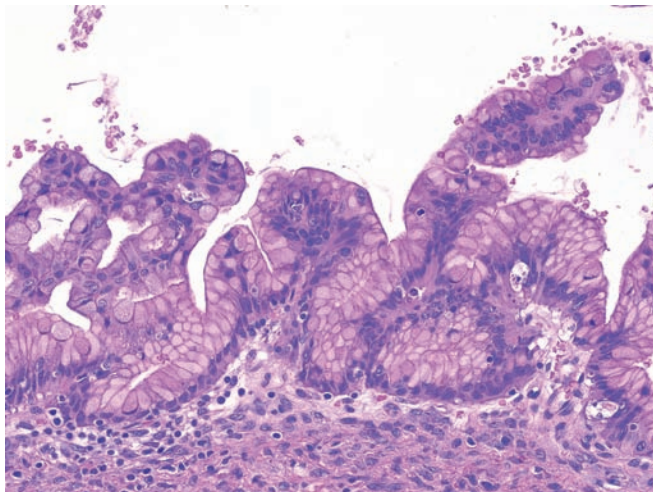
Figure 5.14 — Mucinous cystic neoplasm with moderate to high-grade dysplasia. The epithelial architecture is slightly more complex than in the case with low-grade dysplasia (Figure 5.12). Dystrophic goblet cells, scattered mitoses, and a moderate degree of nuclear pleomorphism can be appreciated. Note the ovarian-type stroma. (Hematoxylin and eosin stain, high power)

Mucinous Cystic Neoplasm

Figure 5.15 — Mucinous cystic neoplasm. Moderate dysplasia (left) and high-grade dysplasia (right) are seen. This section highlights the focal nature of dysplasia in mucinous cystic neoplasms. The degree of dysplasia can be significantly underestimated, and an associated invasive carcinoma can be missed, either on biopsy or with incomplete sampling of a resected neoplasm. (Hematoxylin and eosin stain, low power)
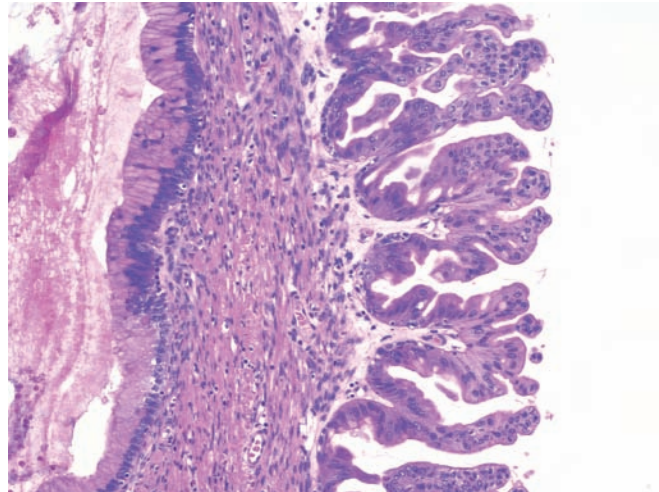
Figure 5.16 — Infiltrating adenocarcinoma arising in association with a mucinous cystic neoplasm. Individual neoplastic cells and neoplastic cells forming small lumina invade into the underlying ovarian-type stroma. These neoplastic glands can be distinguished from atrophic trapped nonneoplastic glands by the paucity of atypia, the presence of scattered acinar cells, and the lobular growth pattern of the latter. (Hematoxylin and eosin stain, high power)
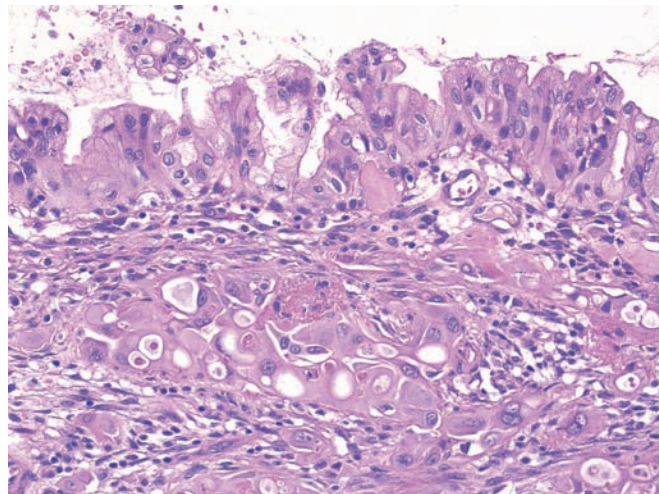
Figure 5.17 — Mucinous cystic neoplasm. Several epithelial tissue fragments and degenerated cellular debris are present in a thick mucoid background. Note that the smaller fragment on the right is disorganized. Surgical follow-up was mucinous cystic neoplasm with low-grade dysplasia (mucinous cystadenoma). (Papanicolaou stain, low power)
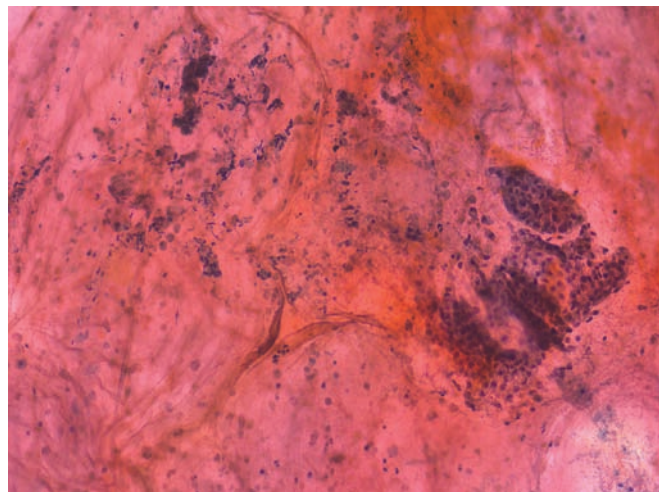
Mucinous Cystic Neoplasm
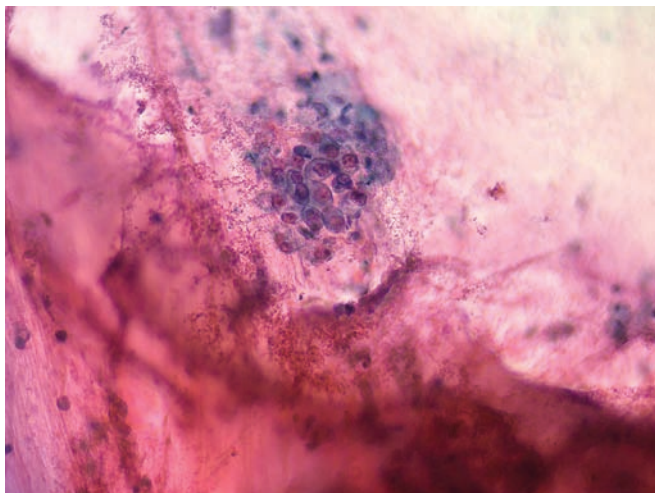
Figure 5.18 — Mucinous cystic neoplasm. A loose aggregate of atypical cells, which have eccentrically located nuclei with irregular borders and conspicuous nucleoli, is noted. Thick clear mucin coats the smear background. Surgical follow-up was mucinous cystic neoplasm with low-grade dysplasia (mucinous cystadenoma). (Papanicolaou stain, medium power)
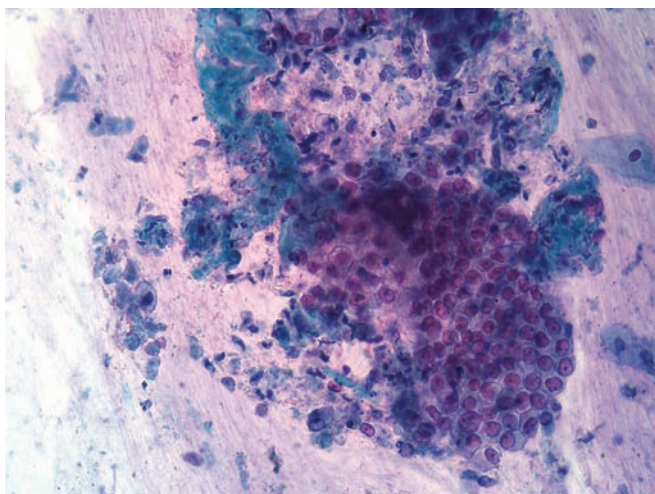
Figure 5.19 — Mucinous cystic neoplasm. Seen here is an atypical tissue fragment of columnar epithelium in a mucinous background with necrotic debris. Although the "honeycomb" pattern is preserved, the cells are crowded and have large nuclei with conspicuous nucleoli. Surgical follow-up was invasive carcinoma arising in association with a mucinous cystic neoplasm. (Papanicolaou stain, medium power)
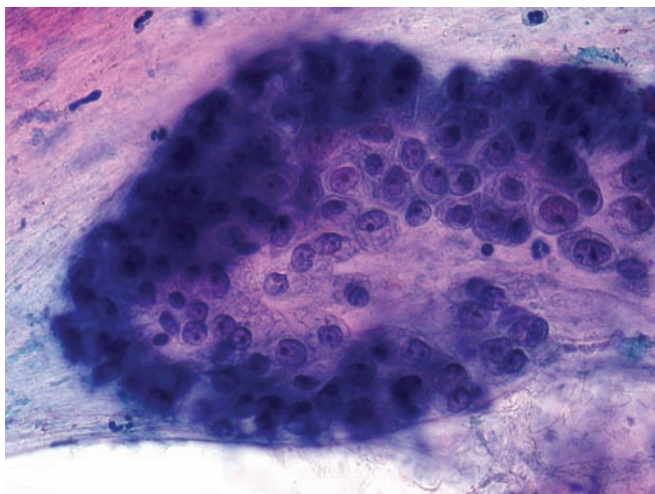
Figure 5.20 — Mucinous cystic neoplasm. A tissue fragment of atypical columnar epithelium is noted. Note large nuclei with macronucleoli and delicate vacuolated cytoplasm suggestive of a well-differentiated adenocarcinoma. Surgical follow-up was invasive carcinoma arising in association with a mucinous cystic neoplasm. (Papanicolaou stain, high power)

Mucinous Cystic Neoplasm

Figure 5.21 — Mucinous cystic neoplasm. Another fragment of atypical columnar epithelium showing changes typical of this neoplasm is present. The normal "honeycomb" appearance is disturbed. There is marked variation in nuclear size and variation in N/C ratio among the cells. Some nuclei show sharp irregularities in the borders. Surgical follow-up was invasive carcinoma arising in association with a mucinous cystic neoplasm. (Papanicolaou stain, high power)
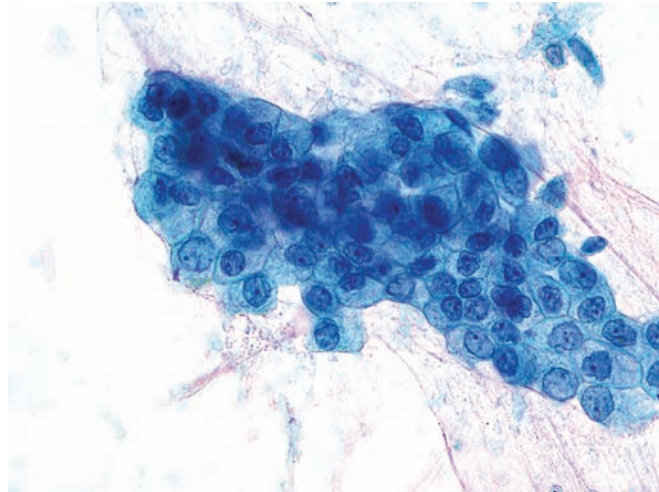
Intraductal Papillary Mucinous Neoplasm
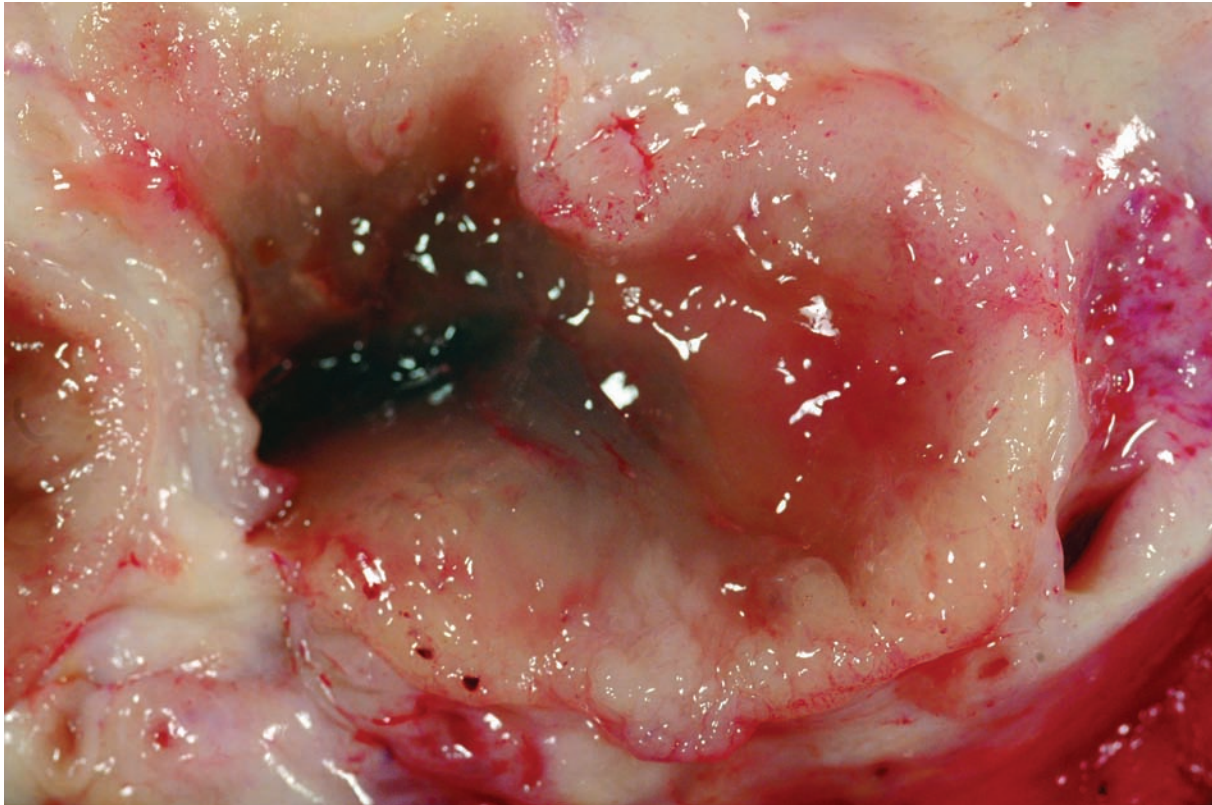
Figure 5.22 — Intraductal papillary mucinous neoplasm in the head of the pancreas. In this close-up gross photograph, the neoplastic papillary epithelium imparts a thick "shaggy rug" appearance to the normally flat pancreatic duct. Note the glistening luminal mucin.

Intraductal Papillary Mucinous Neoplasm
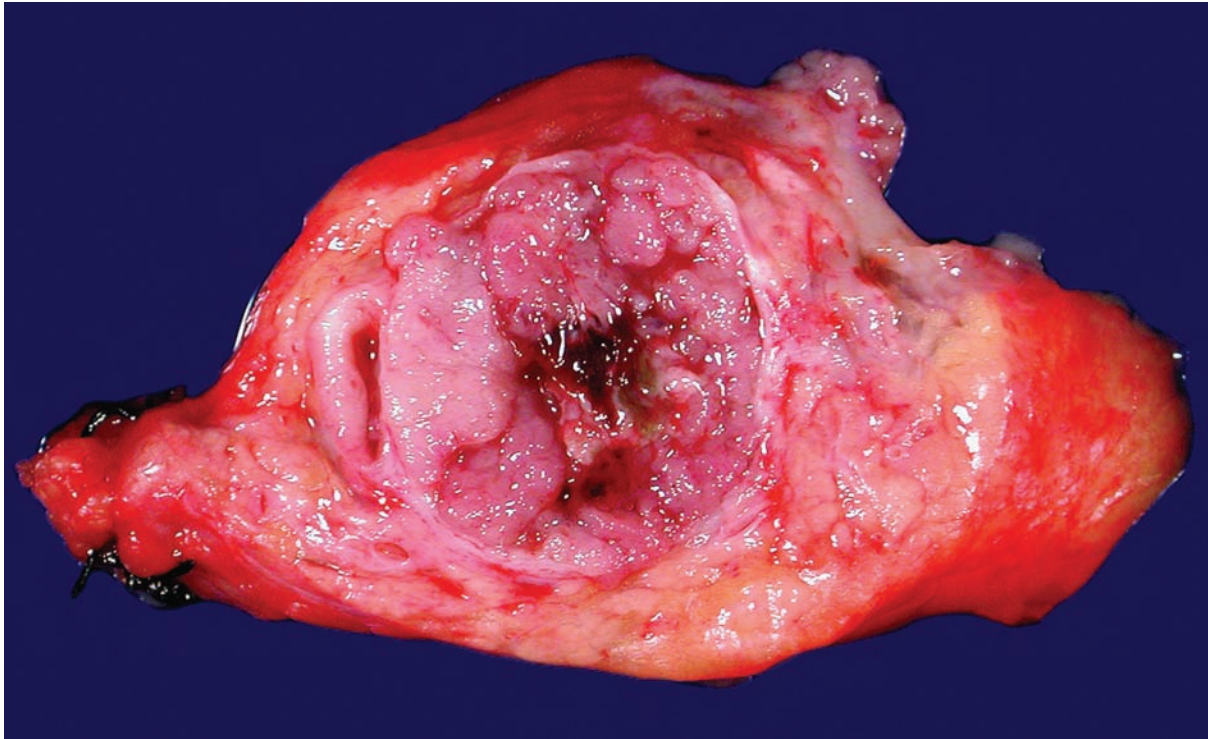
Figure 5.23 — Intraductal papillary mucinous neoplasm. The main pancreatic duct is dramatically distended by neoplastic papillae. By contrast, mucinous cystic neoplasms will only rarely contain such prominent papillary structures.

Intraductal Papillary Mucinous Neoplasm
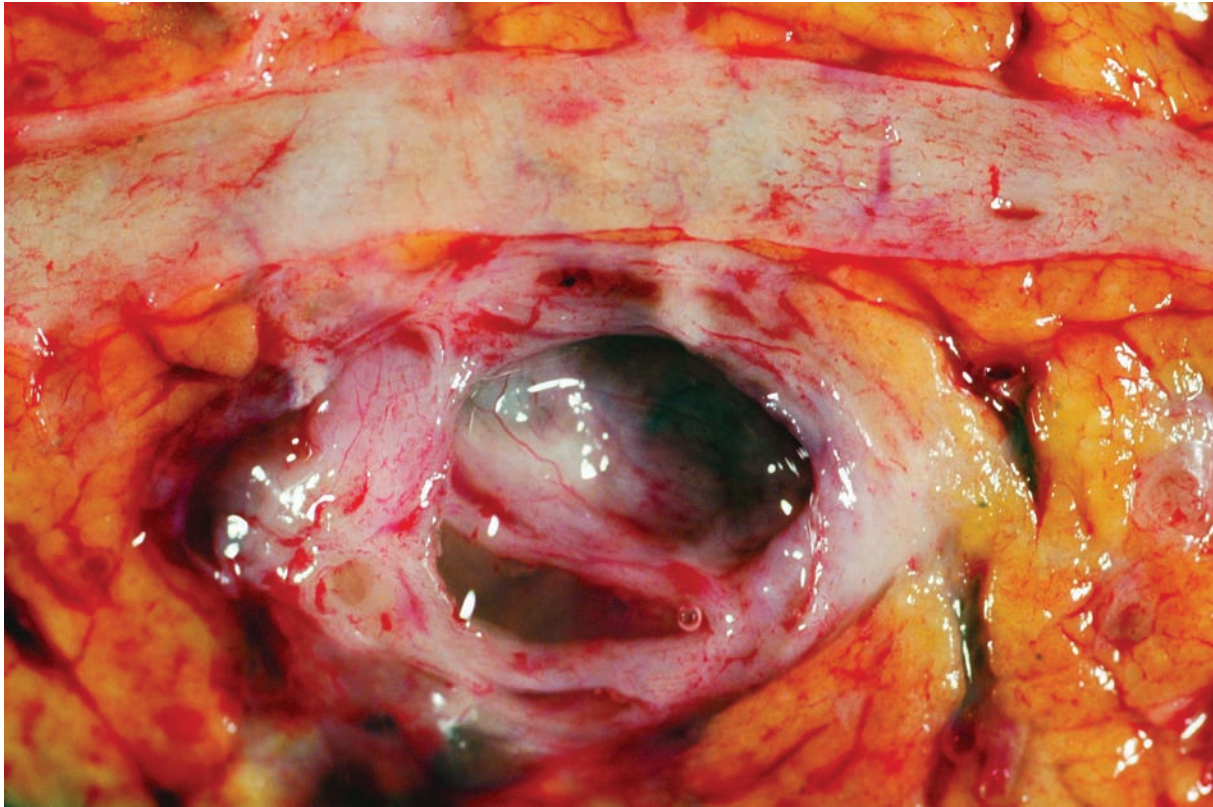
Figure 5.24 — Branch duct-type intraductal papillary mucinous neoplasm. The main pancreatic duct (top) is not involved, while a branch duct is dilated and contains copious quantities of mucin. Mucinous cystic neoplasms have a similar gross appearance and are distinguished from branch duct-type intraductal papillary mucinous neoplasms by the presence of ovarian-type stroma in the former.

Intraductal Papillary Mucinous Neoplasm

Figure 5.25 — Intraductal papillary mucinous neoplasm with low-grade dysplasia (gastric foveolar-type). Large papillae project into a distended pancreatic duct. The fibrovascular cores in this example are very edematous. On higher magnification, the papillae are lined by gastric foveolar-type of epithelium with minimal architectural and cytologic atypia. The absence of ovarian-type stroma and the intraductal growth distinguish this neoplasm from the mucinous cystic neoplasm. (Hematoxylin and eosin stain, low power)
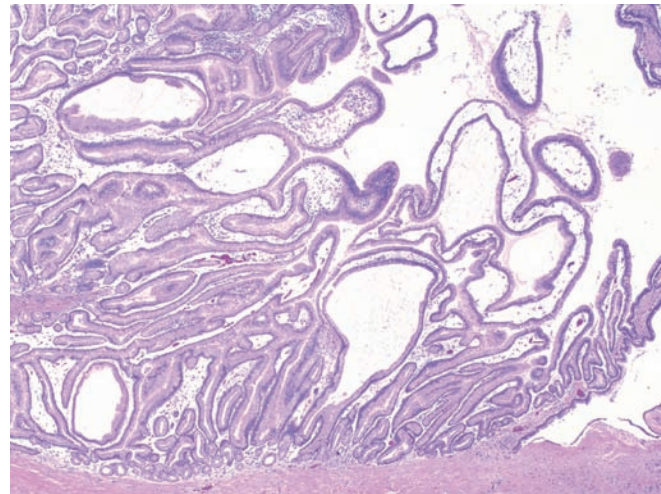
Figure 5.26 — Intraductal papillary mucinous neoplasm with low-grade dysplasia (gastric foveolar-type). Edematous fibrovascular stalks are lined by columnar epithelium with slightly eosinophilic cytoplasm and uniform basally oriented nuclei. Gastric foveolar-type intraductal papillary mucinous neoplasms often arise in branches off the main pancreatic duct ("branch duct-type"). (Hematoxylin and eosin stain, high power)

Figure 5.27 — Intraductal papillary mucinous neoplasm with moderate dysplasia (intestinal-type). This classic "intestinal-type" intraductal papillary mucinous neoplasm resembles a villous adenoma of the colon. The long papillae are lined by columnar mucin-producing epithelium with moderate dysplasia. Focal luminal mucin is seen. The large size of this lesion and long papillae distinguish it from pancreatic intraepithelial neoplasia (PanIN). (Hematoxylin and eosin stain, low power)
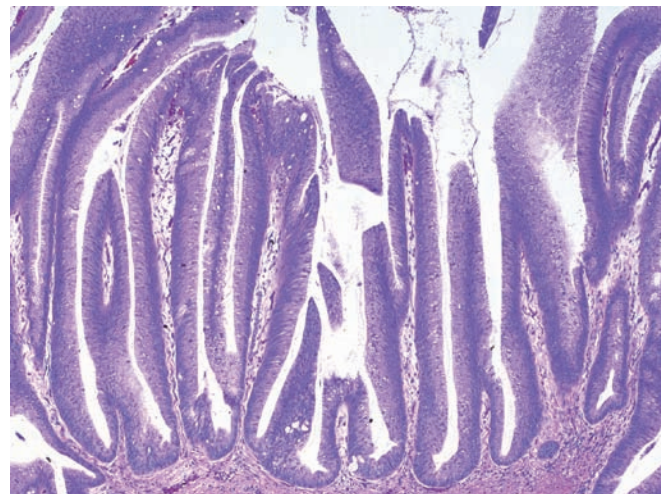
Intraductal Papillary Mucinous Neoplasm
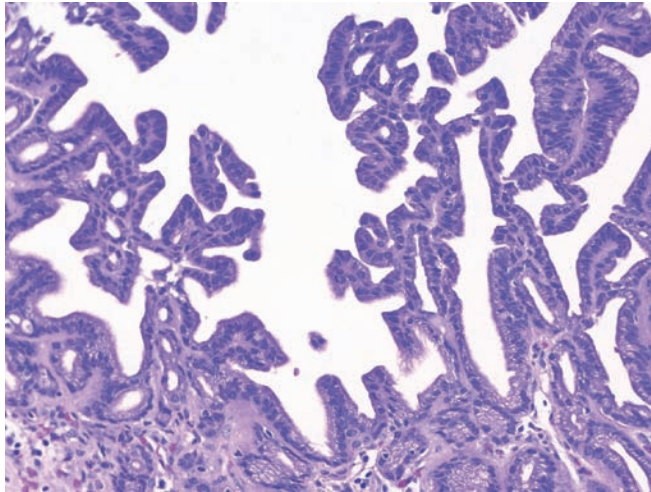
Figure 5.28 — Intraductal papillary mucinous neoplasm with high-grade dysplasia (pancreatobiliary-type). The papillae have a complex branching pattern of growth. The neoplastic epithelial cells are mostly cuboidal, and they form bridges and cribriforming structures. The nuclear features are better appreciated on higher magnification. (Hematoxylin and eosin stain, low power)
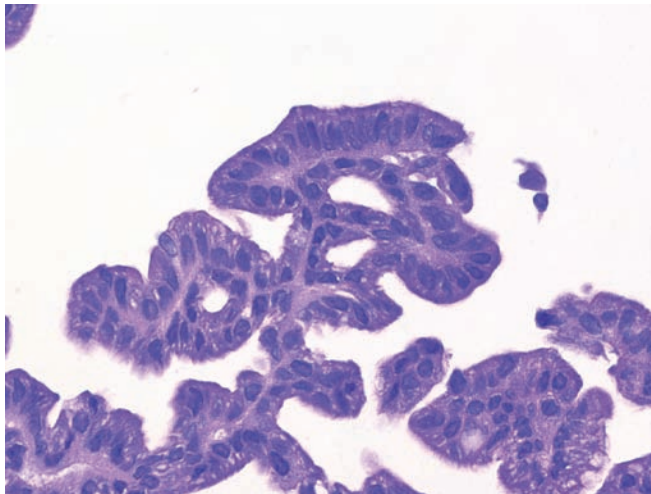
Figure 5.29 — Intraductal papillary mucinous neoplasm with high-grade dysplasia (pancreatobiliary-type). Cuboidal cells with minimal intracellular mucin form bridges between papillae and from one part of a papillary frond to another. Foci with necrosis and complex cribriform structures without fibrovascular cores were present elsewhere in the neoplasm. The presence or absence of an associated invasive carcinoma is the most important prognosticator for these lesions. (Hematoxylin and eosin stain, high power)
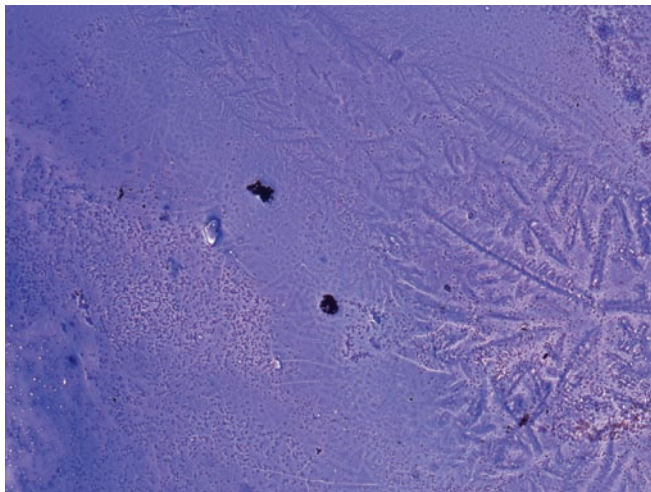
Figure 5.30 — Intraductal papillary mucinous neoplasm (IPMN). As is typical for this neoplasm, this smear is almost acellular and has a background of thick (colloid-like) mucin. The presence of abundant clean mucin along with the radiologic appearance of a dilated pancreatic duct with mucin is strong evidence supporting the diagnosis of IPMN. Differential diagnosis includes gastrointestinal tract contamination (usually "dirty" mucin), a mucocele, and a mucinous cystic neoplasm. (Diff Quik stain, low power)

Intraductal Papillary Mucinous Neoplasm

Figure 5.31 — Intraductal papillary mucinous neoplasm. Gross appearance of a smear made from a fine needle aspirate and stained with Diff Quik stain. Thick abundant mucin is strong evidence favoring an IPMN.
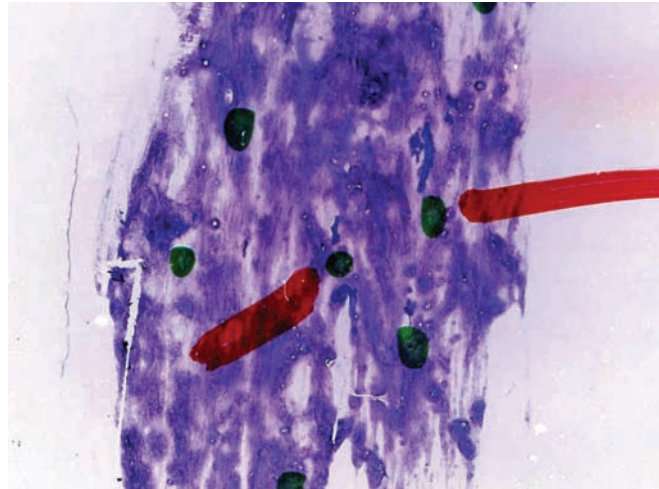
Figure 5.32 — Intraductal papillary mucinous neoplasm. A large tissue fragment of ductal-type epithelium is observed. The cells are disorganized. Focal crowding and nuclear disorientation are seen. The nuclei are generally enlarged and ovoid in shape, with focal variation in size and shape. Smear background in other areas contained abundant mucin. (Diff Quik stain, medium power)
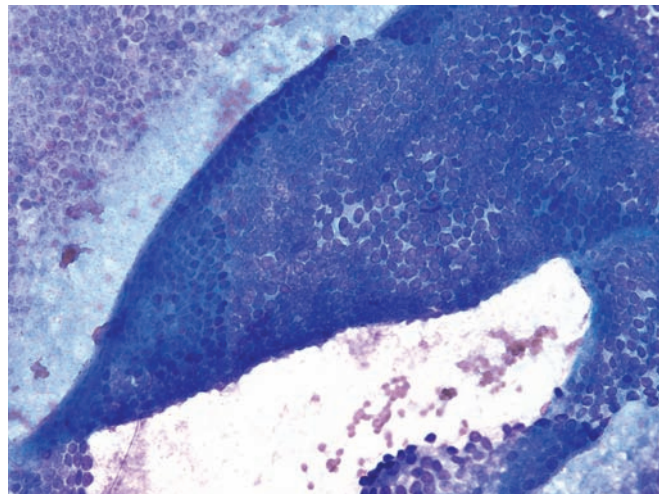
Figure 5.33 — Intraductal papillary mucinous neoplasm. A large fragment of glandular epithelium and background mucin is observed. There is only minimal deviation from the normal honeycomb architecture and no significant individual cellular atypia. Numerous cells contain intracytoplasmic mucin. Diagnosis of IPMN can only be made with additional cytopathological evidence and correlation with radiologic findings. (Papanicolaou stain, medium power)
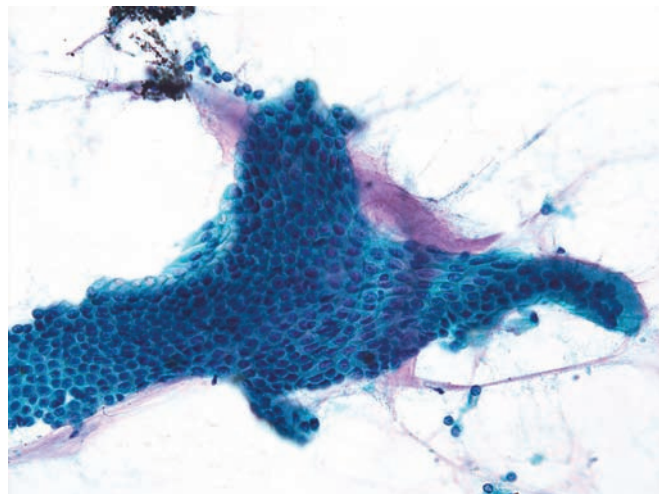
Intraductal Papillary Mucinous Neoplasm
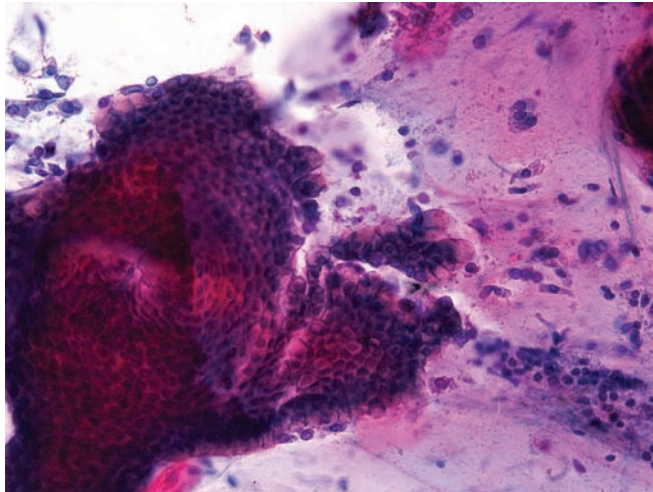
Figure 5.34 — Intraductal papillary mucinous neoplasm. A large folded fragment of mucinous epithelium is present in a dense mucinous background. Although this suggests a mucinous neoplasm, diagnosis of IPMN cannot be made without radiologic correlation. (Papanicolaou stain, medium power)
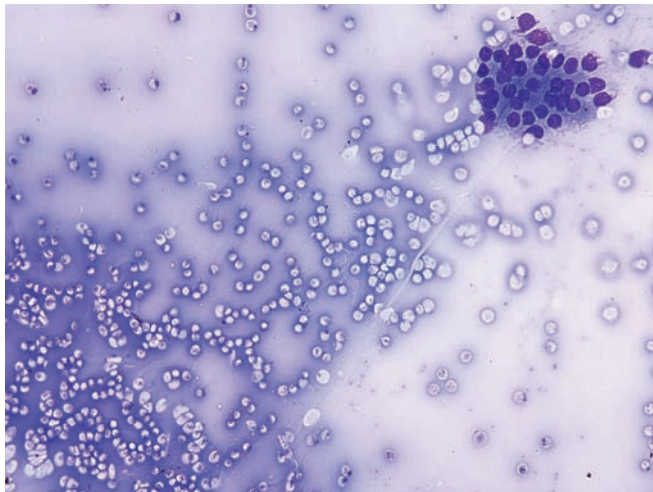
Figure 5.35 — Intraductal papillary mucinous neoplasm. A small fragment of columnar epithelium in a dense, thick mucoid background is noted. Although there is no significant epithelial atypia, the thick yet clean mucoid background strongly favors a mucinous neoplasm. (Diff Quik stain, low power)
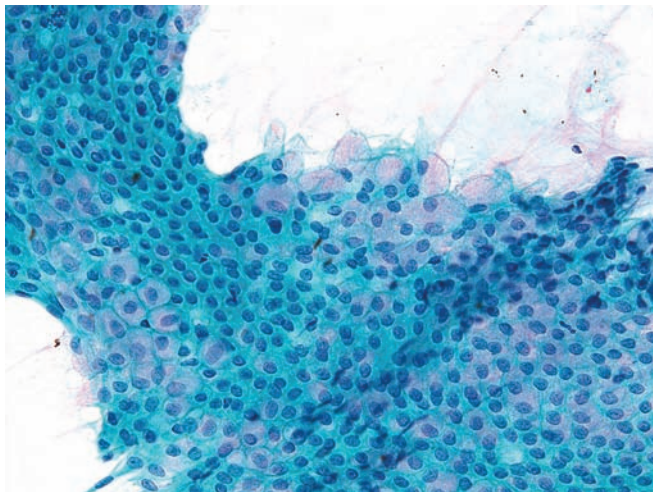
Figure 5.36 — Intraductal papillary mucinous neoplasm. Present here is a large tissue fragment of mucinous epithelium. Cellular disorganization and disorientation in this tissue fragment are consistent with a well-differentiated mucin-producing neoplasm. There is no significant nuclear atypia. Note the focal back-to-back nuclei and disorientation of the goblet cells at the upper margin. (Papanicolaou stain, medium power)

Intraductal Papillary Mucinous Neoplasm

Figure 5.37 — Intraductal papillary mucinous neoplasm. This shows a large, hypercellular tissue fragment with a vague "papillary-like" branching architecture and loss of normal nuclear polarity in the epithelial cells. Small acinus-like formations lined by uniform cuboidal cells are seen within and at the edges of the fragment. Other areas in the smear showed abundant mucin. (Diff Quik stain, low power)
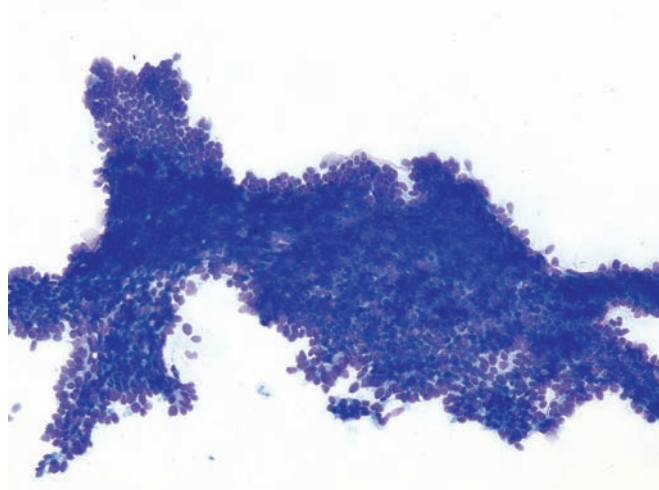
Figure 5.38 — Intraductal papillary mucinous neoplasm. An atypical tissue fragment similar to the previous case is noted. Note the marked hypercellularity, high N/C ratios, and disorganization of the architecture suggesting possible "dysplasia." (Diff Quik stain, low power)
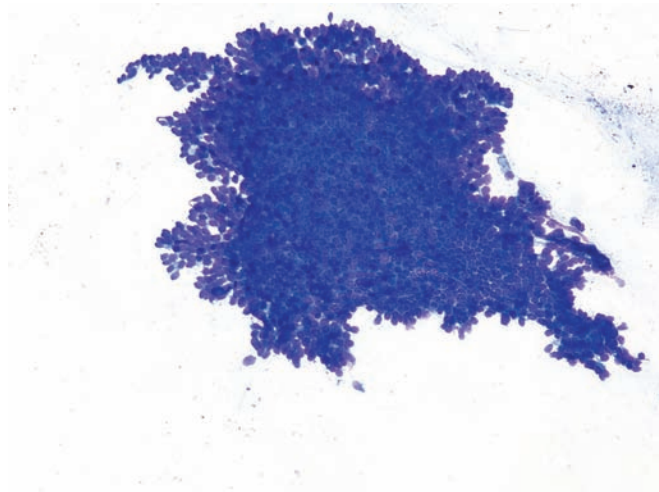
Figure 5.39 — Intraductal papillary mucinous neoplasm. An atypical tissue fragment of ductal-type epithelium in a mucinous background is seen. Nuclear pleomorphism, hyperchromasia (upper margin of the fragment), high N/C ratio, and disorganization of the cells (center) are present. These findings are consistent with at least a high-grade dysplasia. (Diff Quik stain, low power)
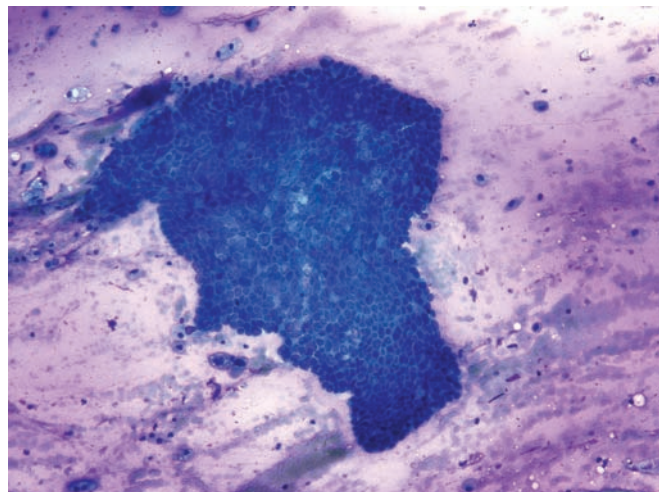
Intraductal Papillary Mucinous Neoplasm
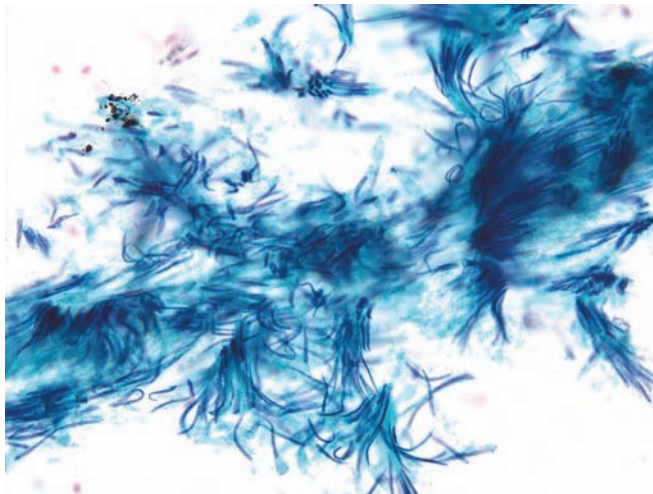
Figure 5.40 — Intraductal papillary mucinous neoplasm. A group of markedly elongated columnar epithelial cells with spindled "cigar-shaped" nuclei showing focal stratification. These features may be observed in IPMN with significant dysplasia. (Papanicolaou stain, medium power)
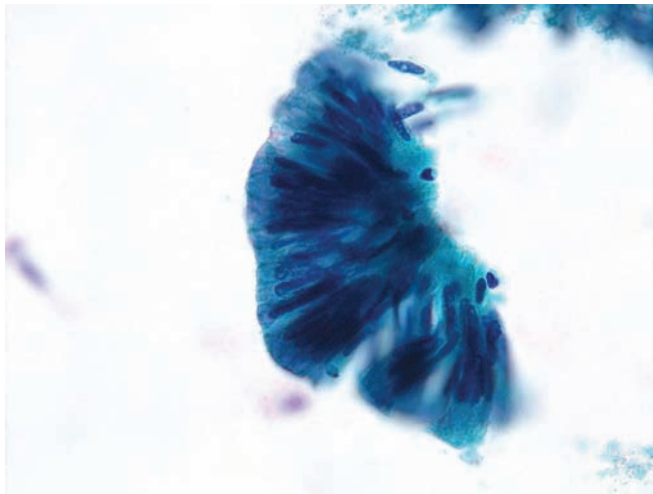
Figure 5.41 — Intraductal papillary mucinous neoplasm. The smear shows a fragment of atypical, tall columnar epithelium with elongated, crowded, and palisaded nuclei. These features are typical of an IPMN with dysplasia. (Papanicolaou stain, high power)
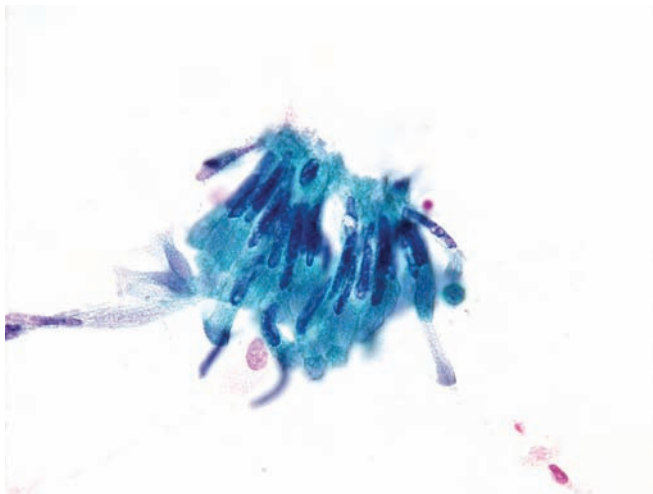
Figure 5.42 — Intraductal papillary mucinous neoplasm. Two loosely attached tissue fragments are present. They are composed of tall columnar cells with elongated, hyperchromatic nuclei, similar to those in the previous example. Differential diagnosis of such a finding also includes ampullary lesions. (Papanicolaou stain, high power)

Intraductal Papillary Mucinous Neoplasm

Figure 5.43 — Intraductal papillary mucinous neoplasm. Several tissue fragments of tall columnar epithelium and single columnar cells are present. Compared to the previous two examples, the nuclei in this case are more pleomorphic and hyperchromatic, strongly suggesting high-grade dysplasia. (Papanicolaou stain, medium power)
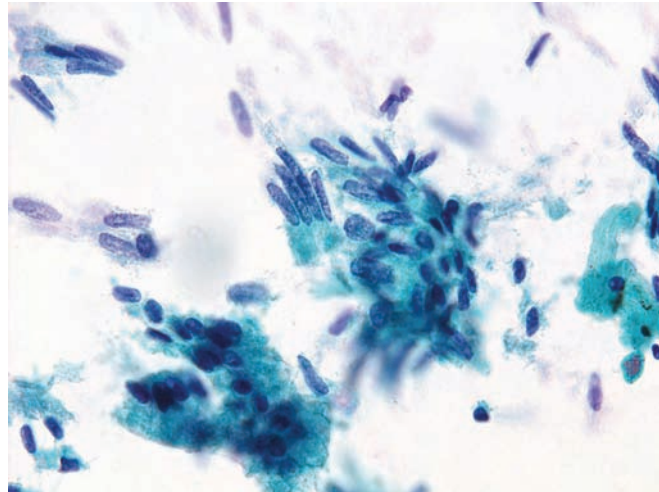
Figure 5.44 — Intraductal papillary mucinous neoplasm. Multiple tissue fragments with varying morphology are present. The upper right fragment shows preservation of the honeycomb architecture but has enlarged nuclei with high N/C ratios. The upper middle fragment has features similar to those in the previous examples (i.e., elongated and stratified nuclei). The lower fragment displays cells with abundant intracytoplasmic mucin. (Papanicolaou stain, medium power)
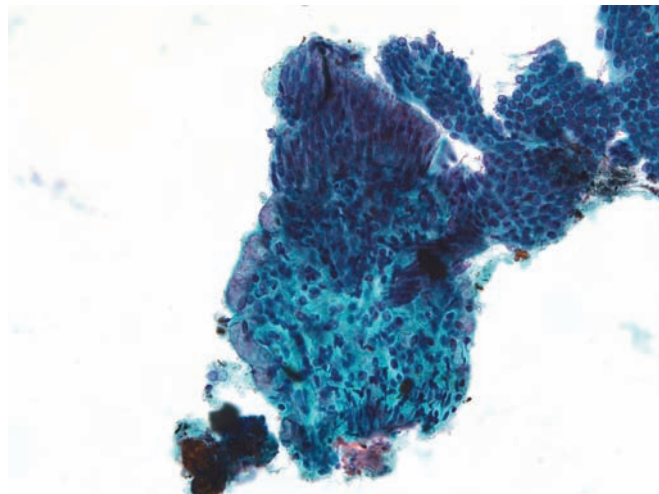
Figure 5.45 — Intraductal papillary mucinous neoplasm with dysplasia. An atypical epithelial tissue fragment in a mucoid background is observed. The cells are disorganized and have enlarged round or ovoid nuclei with slightly irregular nuclear borders. (Diff Quik stain, low power)
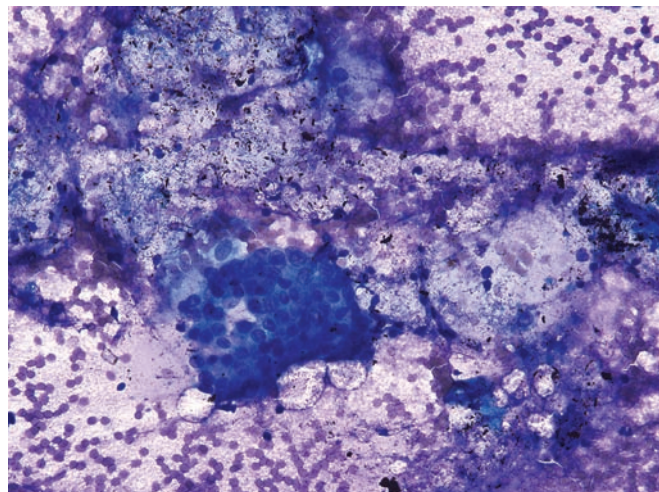
Intraductal Papillary Mucinous Neoplasm
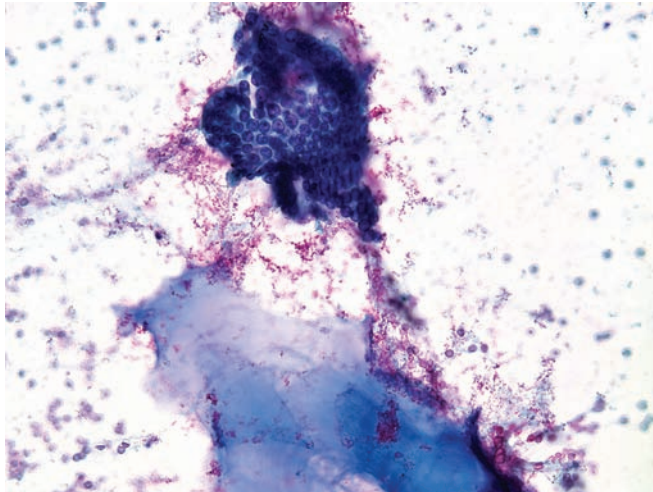
Figure 5.46 — Intraductal papillary mucinous neoplasm with dysplasia. A monolayer tissue fragment of atypical columnar epithelium associated with dense mucin is seen. Although the "honeycomb" architecture is preserved, there is cellular crowding caused by the cells with large nuclei, hyperchromasia, and high N/C ratios. (Diff Quik stain, low power)
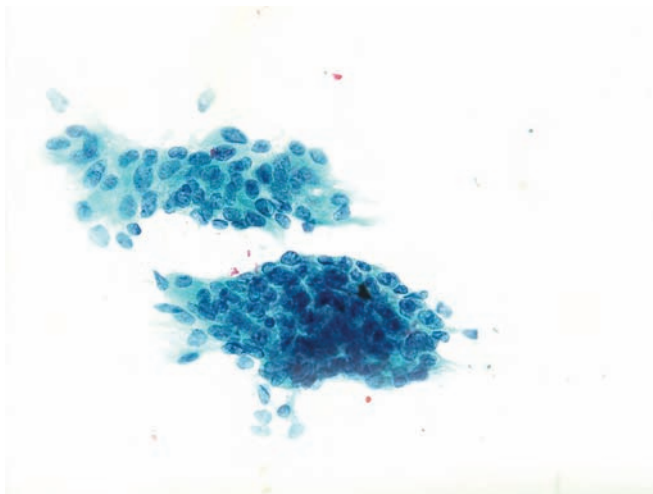
Figure 5.47 — Intraductal papillary mucinous neoplasm with dysplasia. The lesion shows markedly atypical epithelial tissue fragments composed of disorganized cells with enlarged hyperchromatic nuclei, which vary in size and have irregular borders. (Papanicolaou stain, medium power)
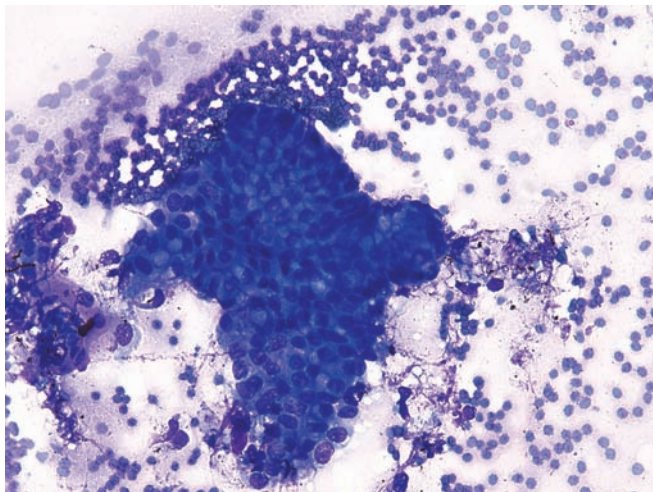
Figure 5.48 — Intraductal papillary mucinous neoplasm with dysplasia. A tissue fragment of atypical columnar epithelium is noted. Atypical cells have large round or ovoid nuclei, some with irregular borders, which vary in size and shape, and display single cytoplasmic vacuoles. The normal architecture is replaced with a disorganized, haphazard distribution of cells. (Diff Quik stain, medium power)

Intraductal Papillary Mucinous Neoplasm

Figure 5.49 — Intraductal papillary mucinous neoplasm with dysplasia. The image depicts an atypical glandular tissue fragment and single degenerated cells in a mucoid background. Note the luminal border facing the center of the fragment formed by atypical, tall columnar epithelium with large oval nuclei. In a portion of the epithelium, nuclear pleomorphism and disorganization are apparent. (Papanicolaou stain, medium power)
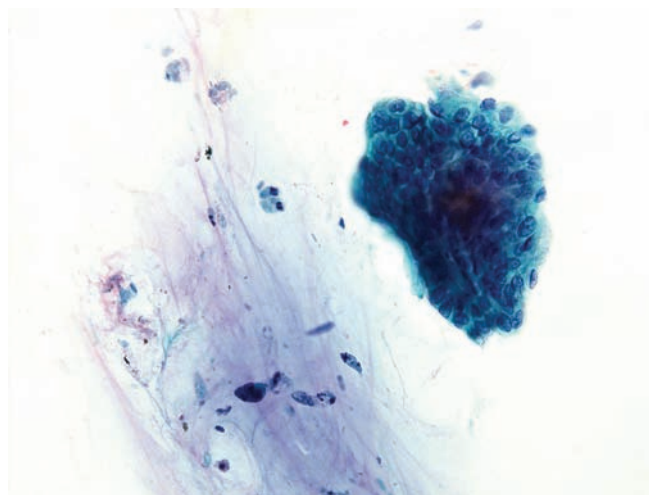
Figure 5.50 — Intraductal papillary mucinous neoplasm with dysplasia. Atypical columnar epithelium and mucin are present. The nuclei are crowded and disorganized. The neoplastic cells have tall columnar configurations with hyperchromatic, round-to-oval or elongated nuclei. (Papanicolaou stain, medium power)
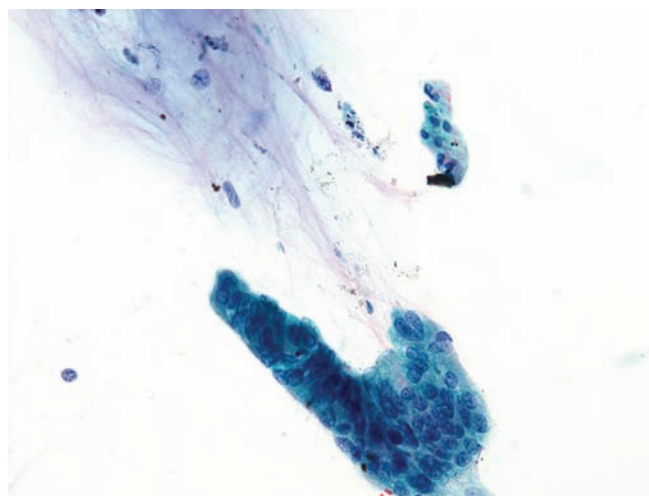
Figure 5.51 — Intraductal papillary mucinous neoplasm with dysplasia. Fragments of atypical columnar epithelium dominate this field. The neoplastic cells have enlarged, elongated, hyperchromatic nuclei occupying large portions of the cytoplasm. Focal pleomorphism with very scant cytoplasm is present. Differential diagnosis includes well-differentiated adenocarcinoma. (Papanicolaou stain, medium power)
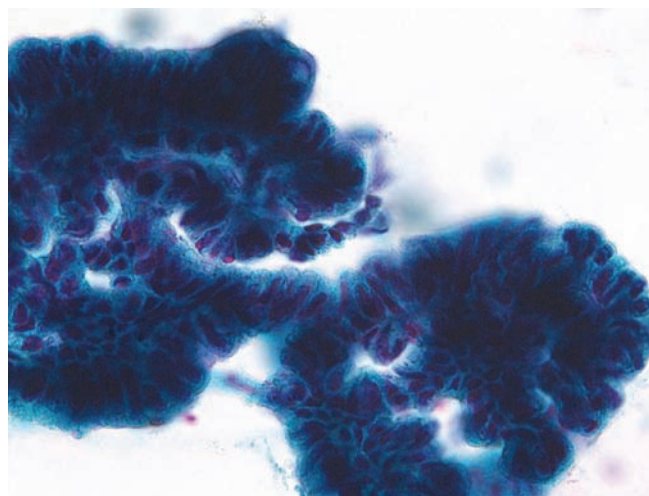
Intraductal Papillary Mucinous Neoplasm
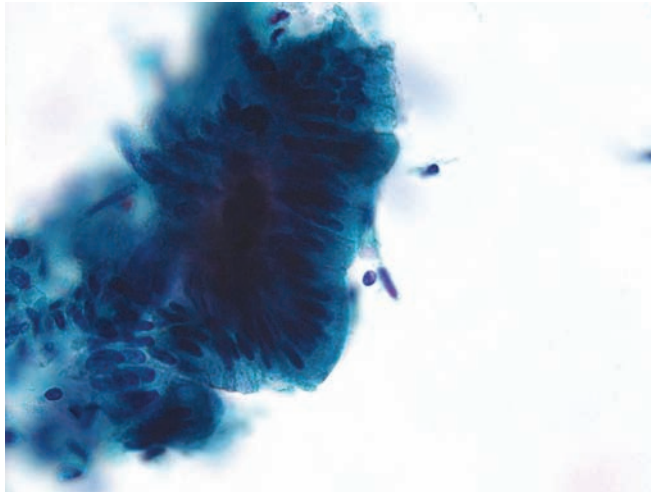
Figure 5.52 — Intraductal papillary mucinous neoplasm with dysplasia. Tissue fragments of tall columnar epithelium with atypia are present. Note that although the nuclear orientation is preserved, the nuclei are enlarged, elongated, and markedly hyperchromatic. Such cytomorphologic characteristics are also shared by ampullary neoplasms, a close differential diagnosis in this case. (Papanicolaou stain, high power)
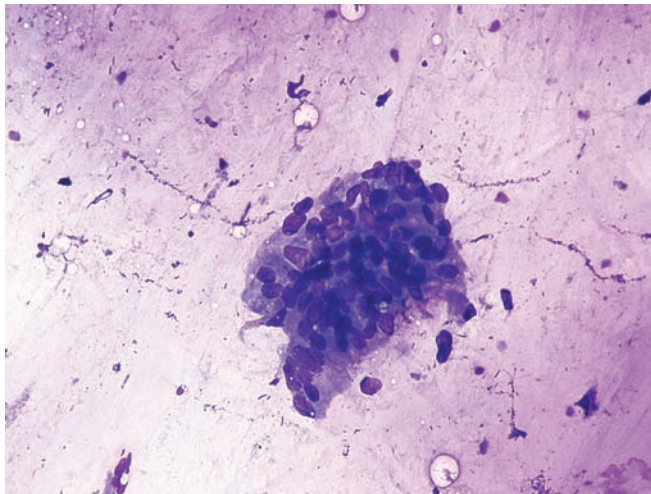
Figure 5.53 — Intraductal papillary mucinous neoplasm with high-grade dysplasia. This shows a tissue fragment of columnar epithelium in a mucinous background. Although a portion of the lower margin of the fragment has columnar differentiation (luminal border), the remaining part is composed of disorganized cells with pleomorphic nuclei. (Diff Quik stain, medium power)
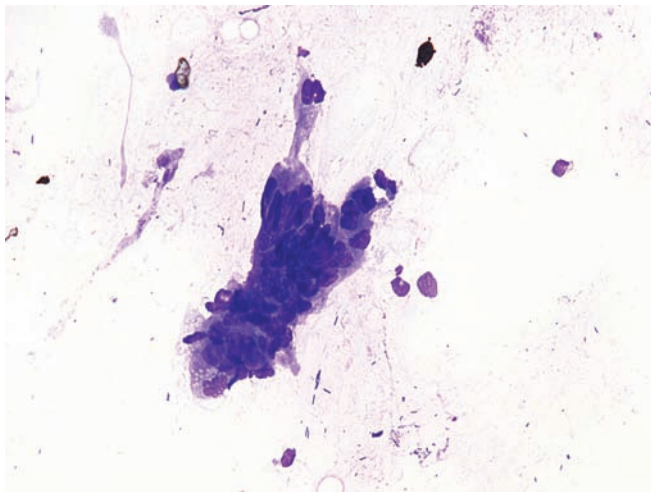
Figure 5.54 — Intraductal papillary mucinous neoplasm with high-grade dysplasia. Note the cellular epithelial tissue fragment with architectural disorganization and nuclear pleomorphism. Columnar epithelial features are seen in the upper margin of the fragment with marked nuclear crowding and palisading. (Diff Quik stain, medium power)

Intraductal Papillary Mucinous Neoplasm

Figure 5.55 — Intraductal papillary mucinous neoplasm with high-grade dysplasia. An intact tissue fragment of dysplastic epilthelium with pleomorphic, high N/C ratio cells and an architecture suggesting the tip of a papillary structure is present. The atypia observed here is significant and the possibility of duodenal contamination can be easily excluded in this case. (Papanicolaou stain, high power)
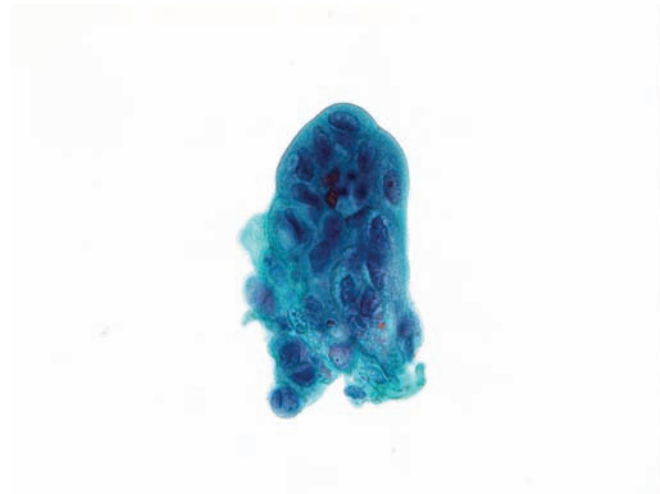
Figure 5.56 — Intraductal papillary mucinous neoplasm with high-grade dysplasia. The image depicts three tissue fragments in a mucinous background. Two small fragments show marked cellular disorganization and pleomorphism. The presence of single cells or small loosely cohesive epithelial fragments raises the possibility of an underlying invasive carcinoma. (Diff Quik stain, medium power)
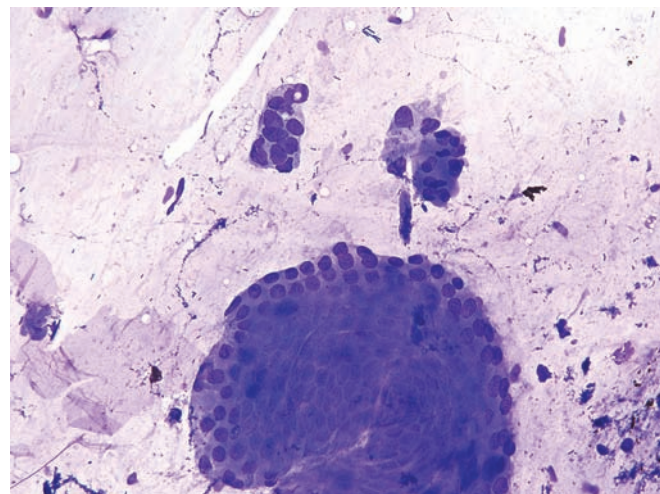
Figure 5.57 — Intraductal papillary mucinous neoplasm with dysplasia. Although subtle, there is focal disorganization in the epithelium. Several nuclei have irregular shapes with sharply pointed borders. The smaller fragment is hypercellular with overlapping nuclei which vary greatly in size. Follow-up resection displayed high-grade dysplasia. (Diff Quik stain, medium power)
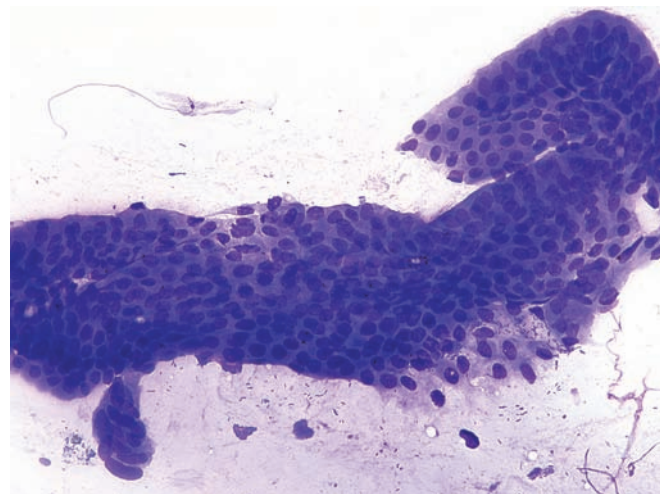
Intraductal Papillary Mucinous Neoplasm
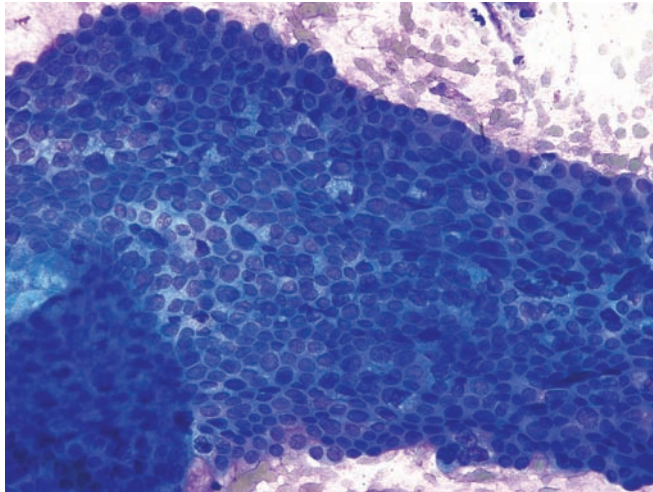
Figure 5.58 — Intraductal papillary mucinous neoplasm with high-grade dysplasia. This case shows a large epithelial tissue fragment composed of disorganized, atypical cells with nuclei which vary markedly in size and N/C ratios. The cytomorphologic features seen here begin to overlap with a well-differentiated ductal adenocarcinoma. (Diff Quik stain, medium power)
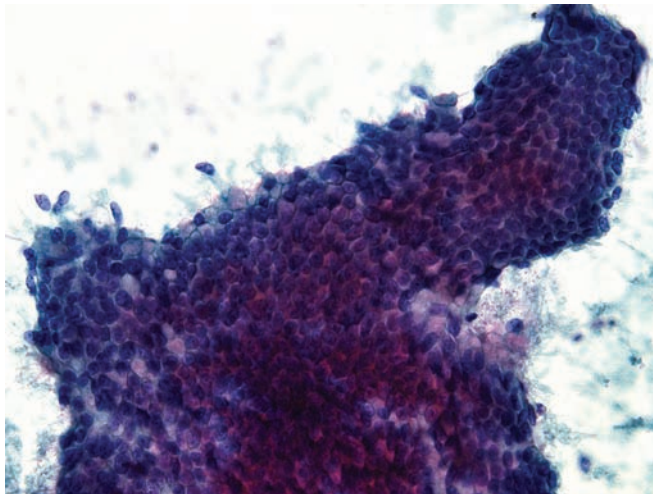
Figure 5.59 — Intraductal papillary mucinous neoplasm with high-grade dysplasia. An epithelial tissue fragment composed of atypical cells with large round nuclei and cytoplasmic mucin. Normal architecture is altered with crowded nuclear areas and gland-like spaces. The possibility of an invasive well-differentiated adenocarcinoma is hard to exclude in this case. Note the absence of single cells and a clean background. (Papanicolaou stain, medium power)
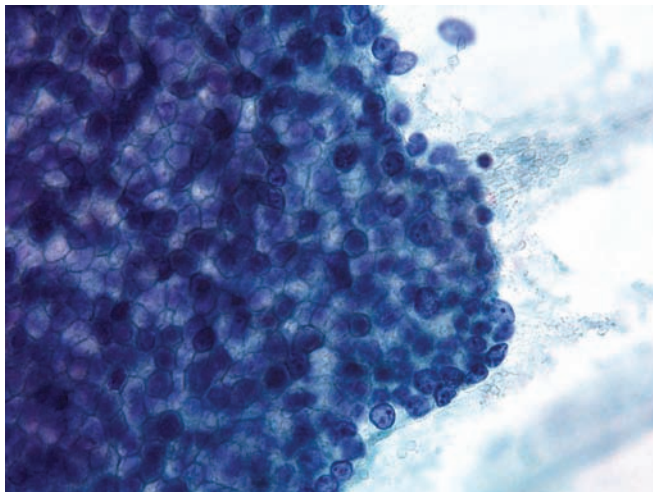
Figure 5.60 — Intraductal papillary mucinous neoplasm with high-grade dysplasia. A crowded 3-dimensional tissue fragment with enlarged hyperchromatic nuclei and prominent nucleoli. Many cells have well-defined cytoplasmic mucin vacuoles. It is not uncommon to find invasive adenocarcinoma in association with an intraductal papillary mucinous neoplasm. However, a follow-up resection in this case only revealed high-grade dysplasia. (Papanicolaou stain, high power)

Intraductal Papillary Mucinous Neoplasm

Figure 5.61 — Intraductal papillary mucinous neoplasm with invasive carcinoma. Atypical columnar epithelial cells with large pleomorphic nuclei in a necrotic background are seen. Other areas in the smear were consistent with an IPMN. Single atypical cells and small tissue fragments are typically associated with invasion in such neoplasms. (Papanicolaou stain, high power)
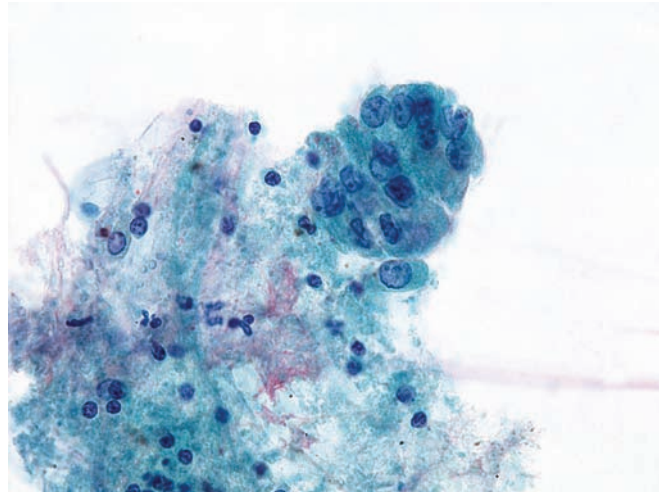
Figure 5.62 — Intraductal papillary mucinous neoplasm with invasive carcinoma. This shows an atypical epithelial tissue fragment. Note the markedly enlarged nuclei and irregular arrangement of the cells. A cytomorphologic distinction with high-grade dysplasia would be difficult in this case. (Diff Quik stain, high power)
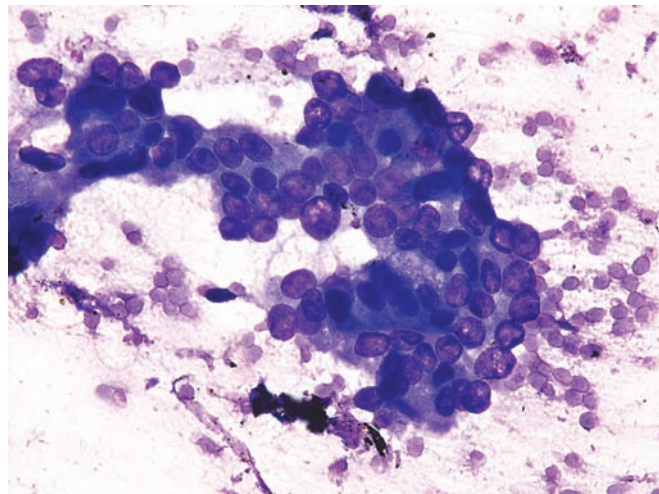
Intraductal Oncocytic Papillary Neoplasm
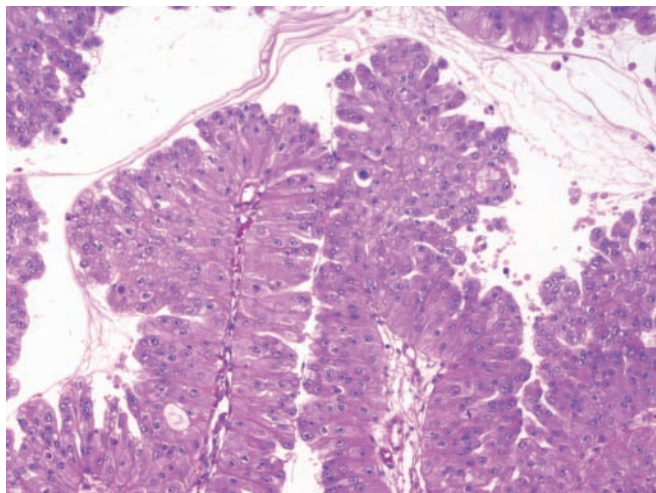
Figure 5.63 — Intraductal oncocytic papillary neoplasm. This intraductal neoplasm forms complex papillae lined by large cells with abundant granular eosinophilic cytoplasm. Note the luminal mucin associated with this neoplasm. These neoplasms are distinguished from intraductal papillary mucinous neoplasms by their abundant eosinophilic cytoplasm. Serous cystic neoplasms can rarely have oncocytic cytoplasm, but the cysts of serous neoplasms are smaller, and serous neoplasms do not arise within the duct system of the pancreas. (Hematoxylin and eosin stain, low power)
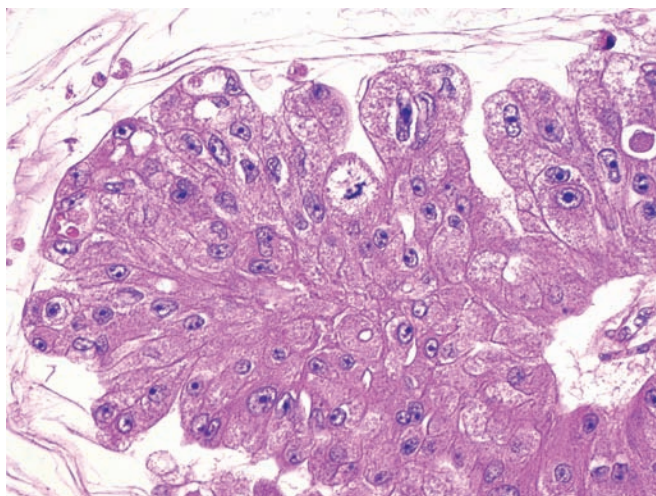
Figure 5.64 — Intraductal oncocytic papillary neoplasm. The neoplastic epithelial cells lining the papillae have abundant granular eosinophilic cytoplasm and are several cells thick. When this feature is exaggerated the lesion can mimic a solid neoplasm of the pancreas such as an acinar cell carcinoma. Intraductal papillary oncocytic neoplasms can be distinguished from solid cellular neoplasms of the pancreas by their prominent intraductal growth. (Hematoxylin and eosin stain, high power)
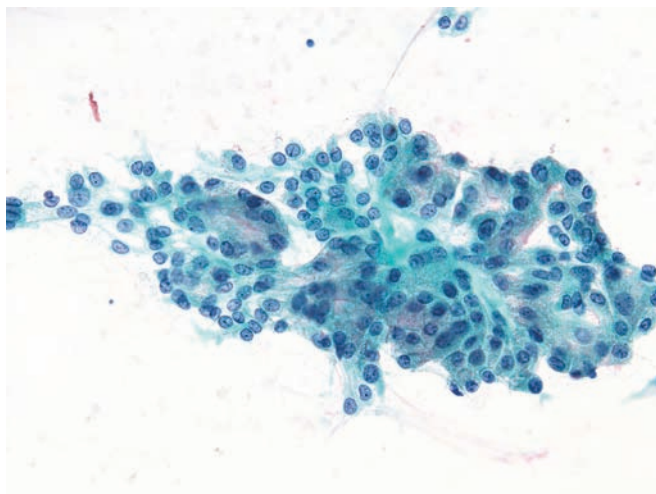
Figure 5.65 — Intraductal oncocytic papillary neoplasm. A papillary tissue fragment with atypia is present. Cells have round or ovoid nuclei and evenly distributed chromatin with occasional chromocenters and micronucleoli. Most cells have moderate to large amounts of granular or finely vacuolated cytoplasm, some containing fine red granules. (Papanicolaou stain, medium power)

Intraductal Oncocytic Papillary Neoplasm

Figure 5.66 — Intraductal oncocytic papillary neoplasm. This example shows a large tissue fragment composed of cells similar to those shown in the previous figure. Note the abnormal cellular organization (i.e., areas of crowded nuclei), as well as the varying nuclear-cytoplasmic ratios among the cells. (Papanicolaou stain, medium power)
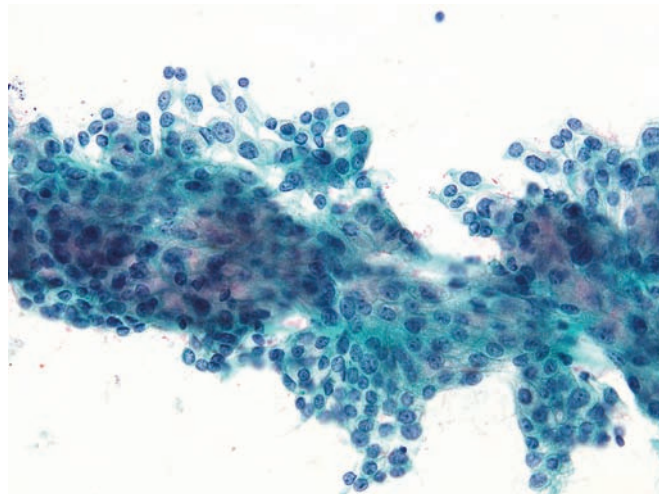
Figure 5.67 — Intraductal oncocytic papillary neoplasm. The image shows a monolayered epithelial tissue fragment. The "honeycomb" appearance is fairly well preserved, but the cells have larger nuclei with higher N/C ratios. The presence of finely or densely granular cytoplasm (rather than mucinous) distinguishes this lesion from an intraductal papillary mucinous neoplasm. (Diff Quik stain, medium power)
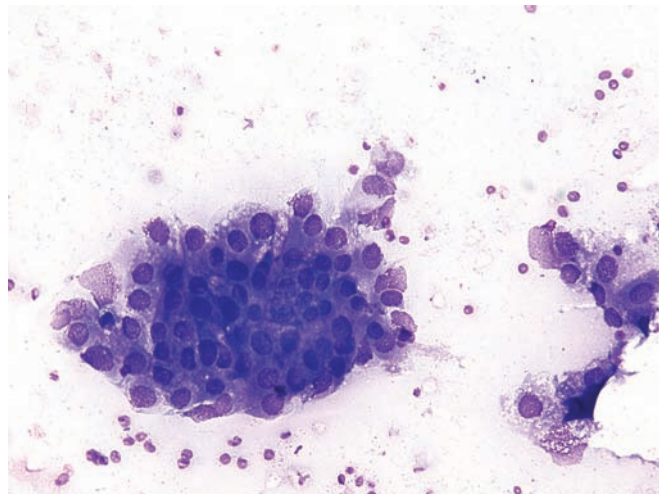
Figure 5.68 — Intraductal oncocytic papillary neoplasm (cell block section). A tissue fragment composed of oncocytic cells with atypia forming solid papillary and acinar structures is observed. The cells have eosinophilic, granular, and finely vacuolated cytoplasm. (Hematoxylin and eosin stain, medium power)
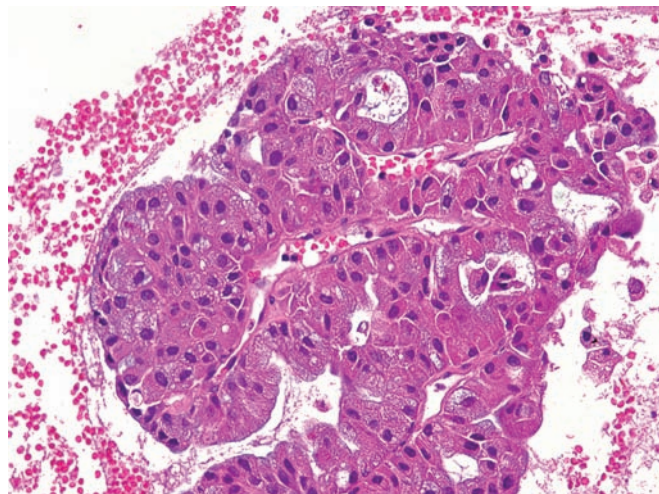
Solid-Pseudopapillary Neoplasm
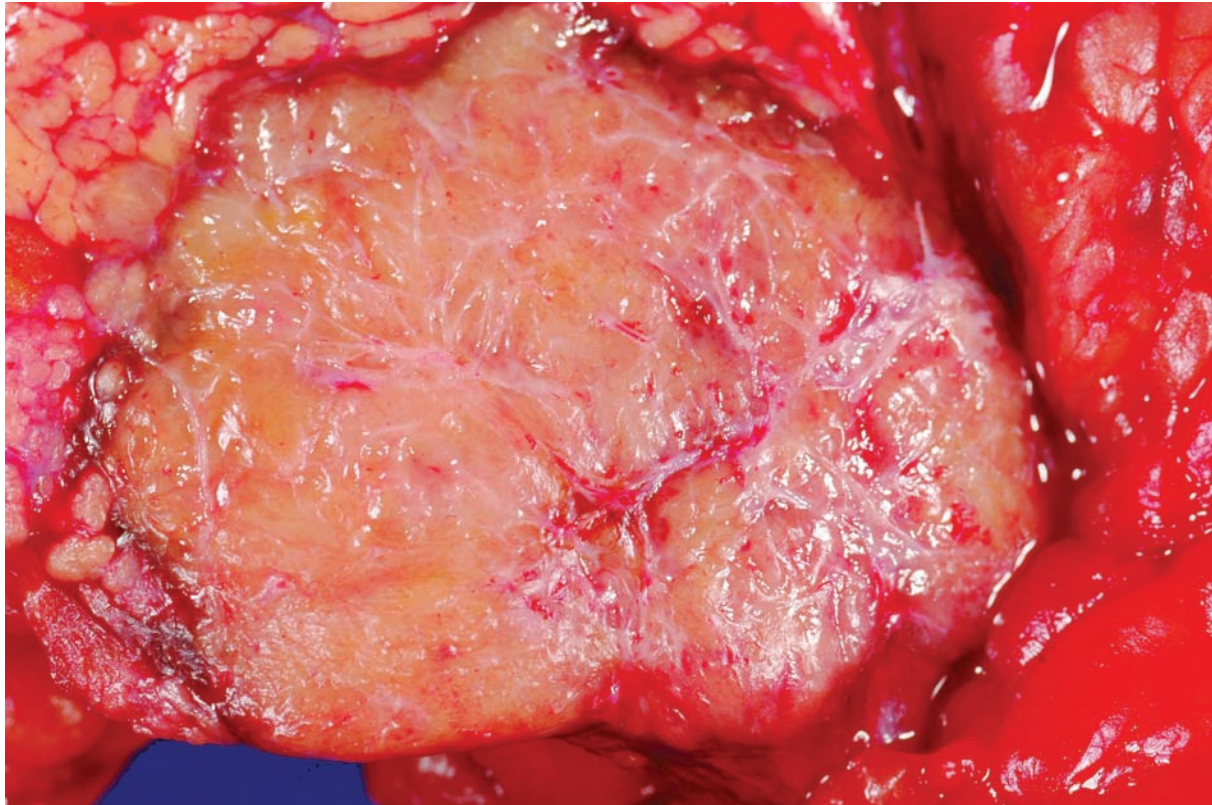
Figure 5.69 — Solid-pseudopapillary neoplasm. Smaller solid-pseudopapillary neoplasms, as in this case, are often grossly solid and yellow-tan. Larger examples tend to be more cystic. Solid-pseudopapillary neoplasms can grossly mimic a well-differentiated endocrine neoplasm. Touch preparations can be used to distinguish between these two entities, as solid-pseudopapillary neoplasms will produce a smear of loosely cohesive cells surrounding delicate branching vessels.

Solid-Pseudopapillary Neoplasm
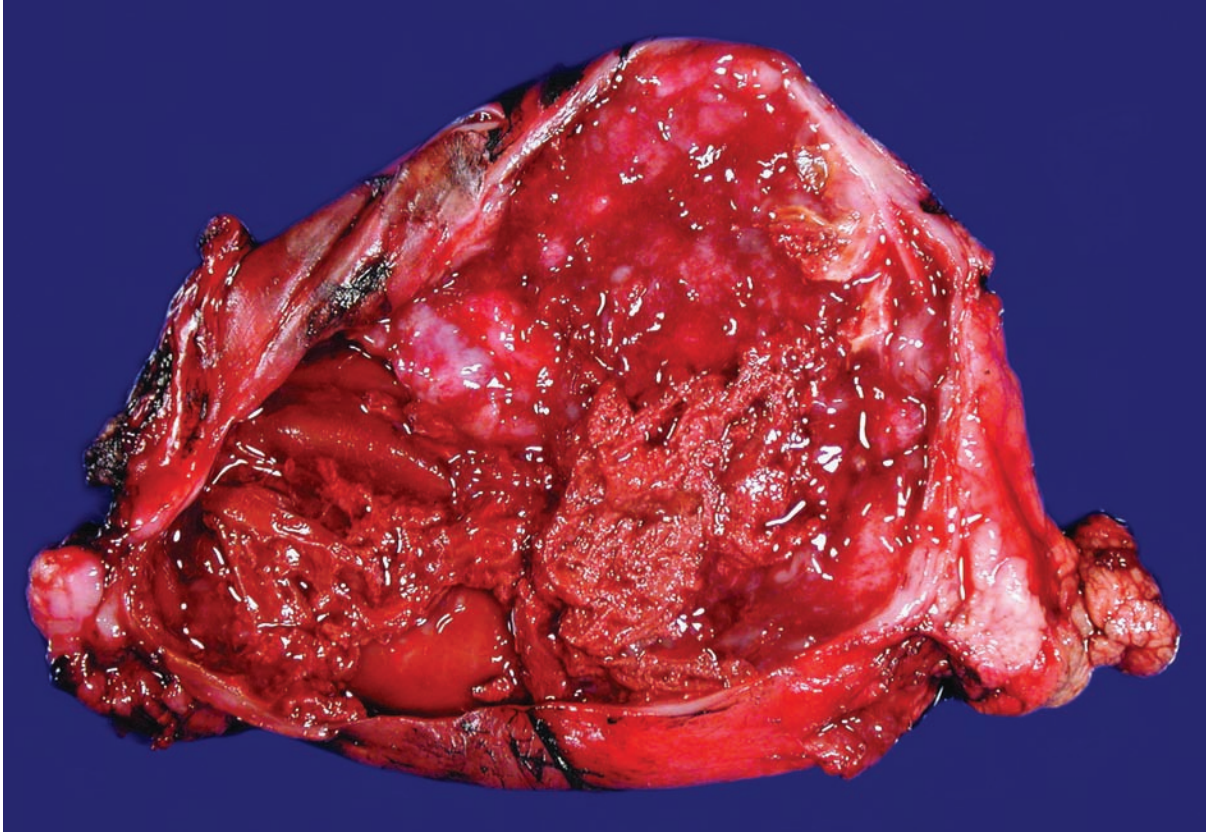
Figure 5.70 — Solid-pseudopapillary neoplasm. This mostly cystic example is filled with hemorrhagic and necrotic debris. When necrosis and cystic degeneration are extensive, the lesion can be misdiagnosed as a pseudocyst. Adequate sampling is the best way to avoid this diagnostic pitfall.

Solid-Pseudopapillary Neoplasm
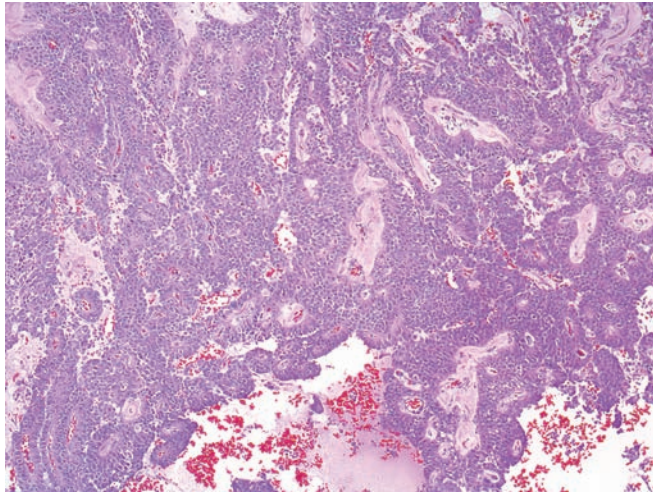
Figure 5.71 — Solid-pseudopapillary neoplasm. Poorly cohesive cells surround delicate blood vessels. The spaces contain necrotic debris and blood. These features are often pronounced on touch preparations. The well-differentiated endocrine neoplasm tops the differential diagnosis. These two entities are best distinguished by immunolabeling. (Hematoxylin and eosin stain, low power).
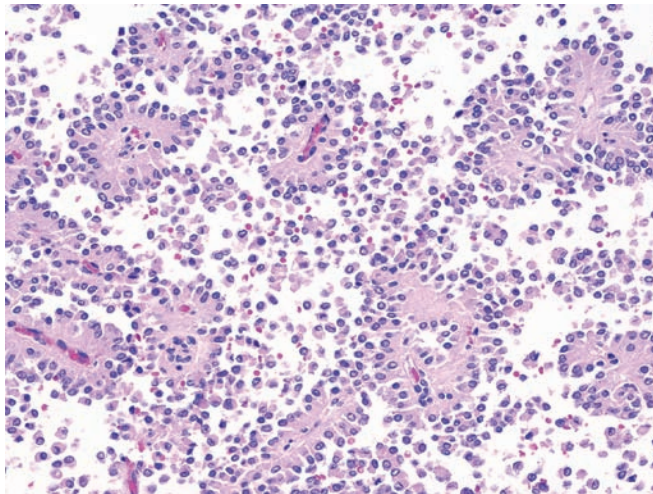
Figure 5.72 — Solid-pseudopapillary neoplasm. Numerous papillary-like structures comprised of monotonous neoplastic cells surrounding delicate fibrovascular cores. Few discohesive cells are seen as well. (Hematoxylin and eosin stain, low power)
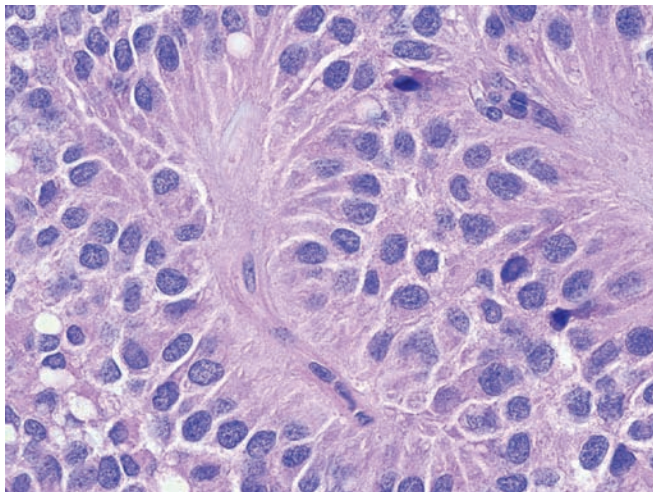
Figure 5.73 — Solid-pseudopapillary neoplasm. Poorly cohesive cells surround small delicate blood vessels. The cytoplasm is eosinophilic to amphophilic, and the nuclei are uniform. (Hematoxylin and eosin stain, high power)

Solid-Pseudopapillary Neoplasm

Figure 5.74 — Solid-pseudopapillary neoplasm.
Although usually very well-demarcated, solid-pseudo-papillary neoplasms, as can be observed here, often extend into the adjacent pancreatic parenchyma. When they do, the neoplastic cells seem to gently intermingle with the preexisting nonneoplastic cells. (Hematoxylin and eosin stain, high power)
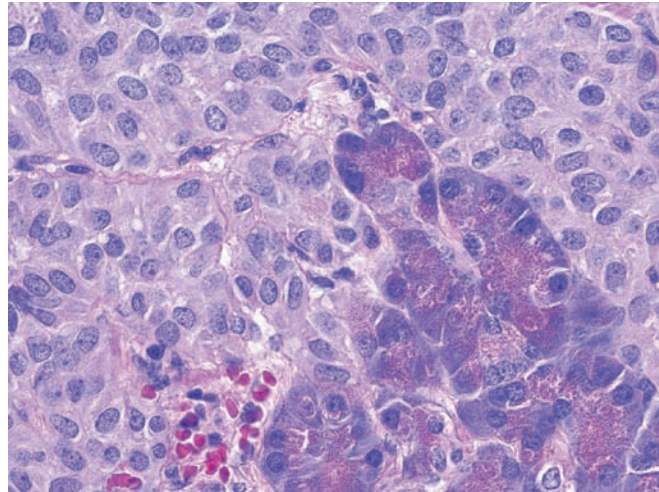
Figure 5.75 — Solid-pseudopapillary neoplasm. The eosinophilic globules seen towards the center of this image are characteristic of this entity. These globules label with antibodies to α1-antitrypsin. The focal cytoplasmic clearing that is also present in this example can be extensive. (Hematoxylin and eosin stain, high power)
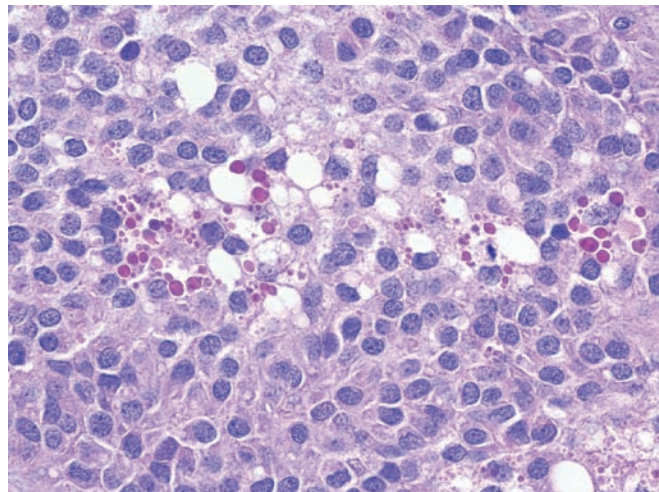
Figure 5.76 — Solid-pseudopapillary neoplasm.
Cholesterol crystals with associated giant cell reaction are depicted. A collection of foam cells is present in the lower left-hand corner. (Hematoxylin and eosin stain, low power)
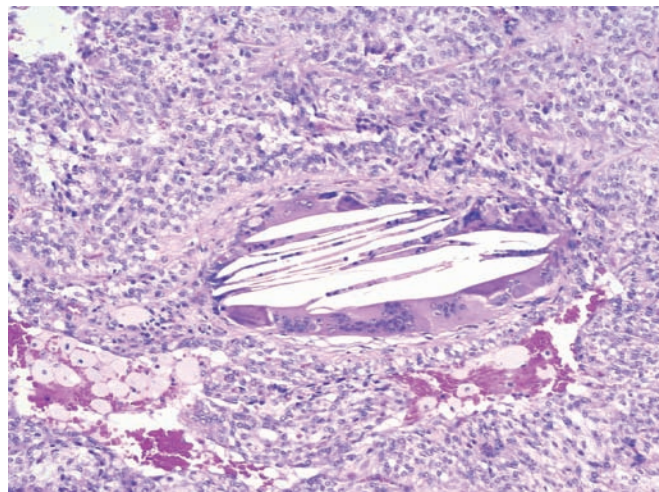
Solid-Pseudopapillary Neoplasm
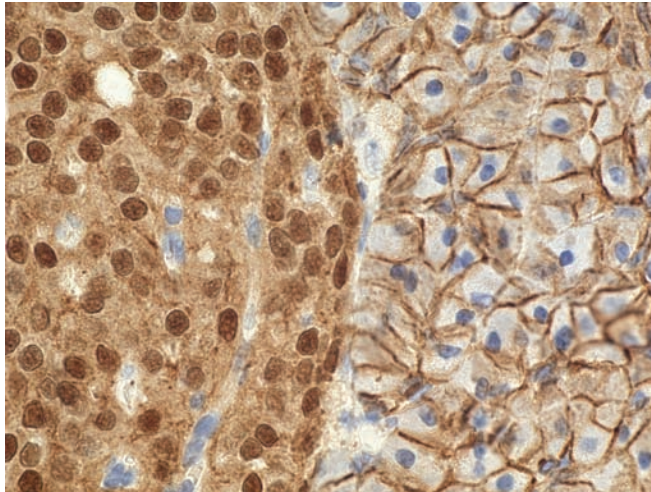
Figure 5.77 — Solid-pseudopapillary neoplasm. The cell membranes of nonneoplastic cells (right) label with antibodies to β-catenin, while the neoplastic cells (left) have an abnormal nuclear pattern of labeling. A panel of immunomarkers including chromogranin, synaptophysin, and β-catenin can be used to distinguish between a solid-pseudo-papillary neoplasm and a well-differentiated endocrine neoplasm. (Immunolabeling for β-catenin, high power)
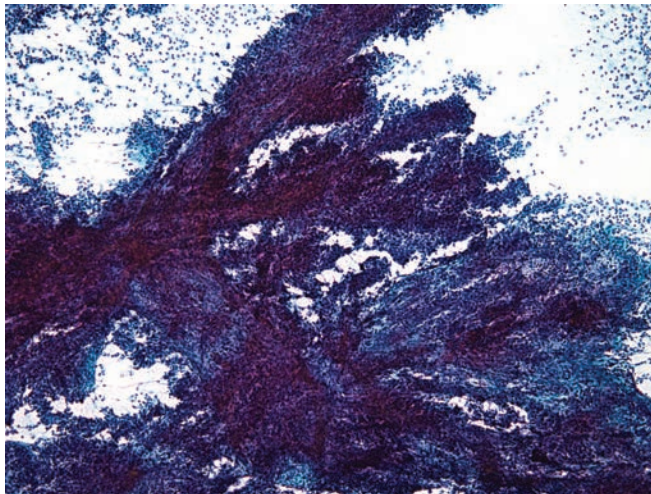
Figure 5.78 — Solid-pseudopapillary neoplasm. A large hypercellular tissue fragment with well-formed papillary architecture is seen. Numerous single cells are also seen in the smear background. Although this appearance is classic for a solid-psuedopapillary neoplasm, a well-differentiated endocrine neoplasm may display papillary architecture as well. (Papanicolaou stain, low power)
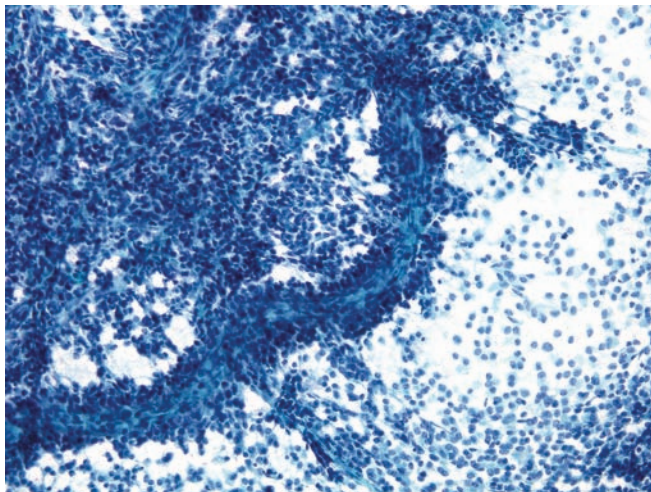
Figure 5.79 — Solid-pseudopapillary neoplasm. Three different cellular patterns are presented in this picture: a dense cellular area with traversing fine capillaries, a long delicate structure with fibrous core surrounded with uniform neoplastic cells (characteristic feature of this tumor), and single small and monotonous neoplastic cells. (Papanicolaou stain, low power)

Solid-Pseudopapillary Neoplasm

Figure 5.80 — Solid-pseudopapillary neoplasm.
This image shows a pseudopapillary structure. The neoplastic cells are relatively small and uniform with moderate amounts of delicate cytoplasm. Some cells display numerous intracytoplasmic clear vacuoles or basophilic granules. The cells tightly adhere to the vascular endothelium of the branching capillary vessels. (Diff Quik stain, medium power)
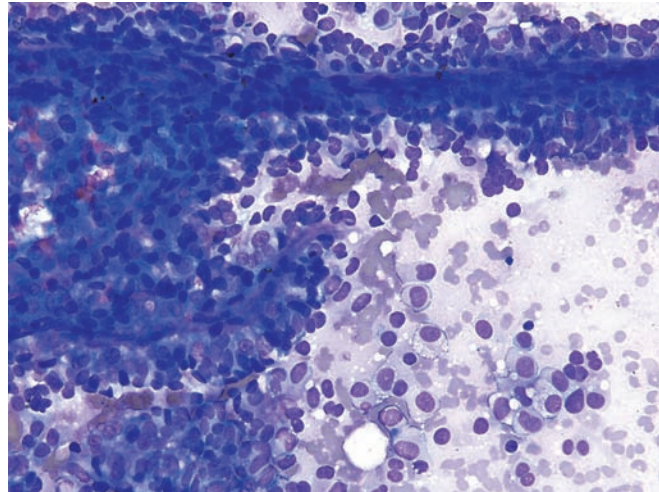
Figure 5.81 — Solid-pseudopapillary neoplasm.
Neoplastic cells intimately surround the endothelial cells of the capillary wall. The cells have uniform, round-to-oval, mildly hyperchromatic nuclei with a homogeneous chromatin pattern. A perivascular, pseudopapillary arrangement can also be seen with well-differentiated endocrine neoplasms. (Papanicolaou stain, high power)
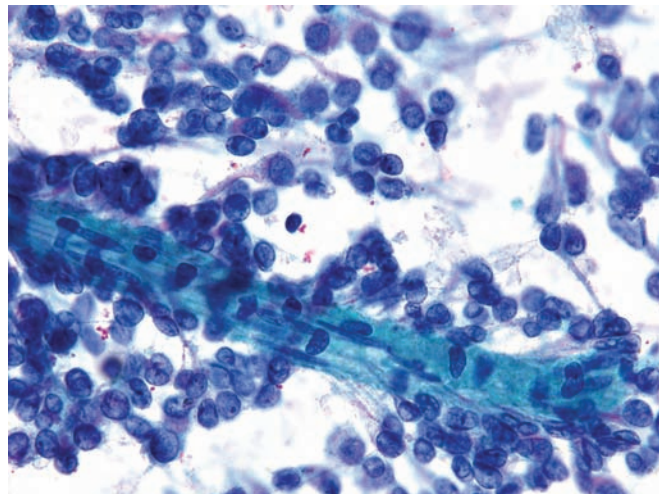
Figure 5.82 — Solid-pseudopapillary neoplasm.
Note the papillary structure similar to the previous case, and the single uniform neoplastic cells in groups and rosette-like formations. The straight, curved or branching fine wire-like capillaries with associated neoplastic cells are a highly predictive feature of a solid-psuedopapillary neoplasm on FNA. (Diff Quik, low power)
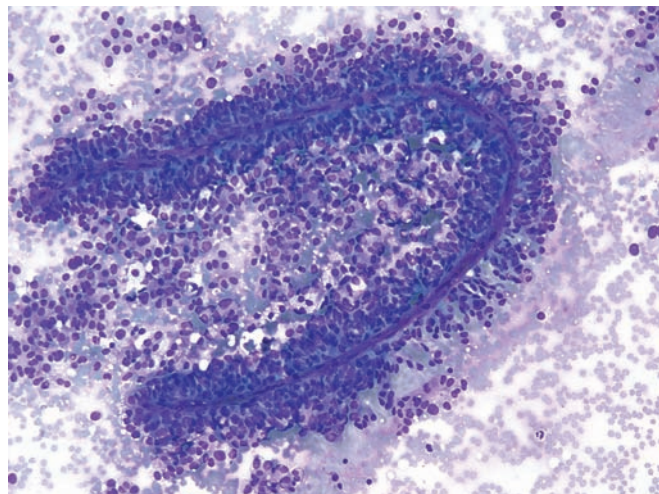
Solid-Pseudopapillary Neoplasm
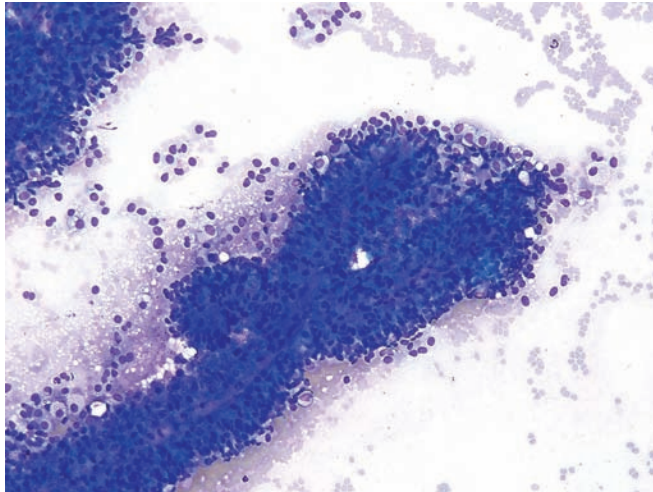
Figure 5.83 — Solid-pseudopapillary neoplasm. The image shows another papillary fragment with a fine capillary vessel in the center surrounded by neoplastic cells. (Diff Quik stain, low power)

Figure 5.84 — Solid-pseudopapillary neoplasm. Several entangled, delicate papillary structures and scattered cellular tissue fragments without a papillary architecture are seen. This phenotype is highly characteristic of this neoplasm and has been called "the Chinese character-appearance" due to the delicate branchings. (Papanicolaou stain, low power)
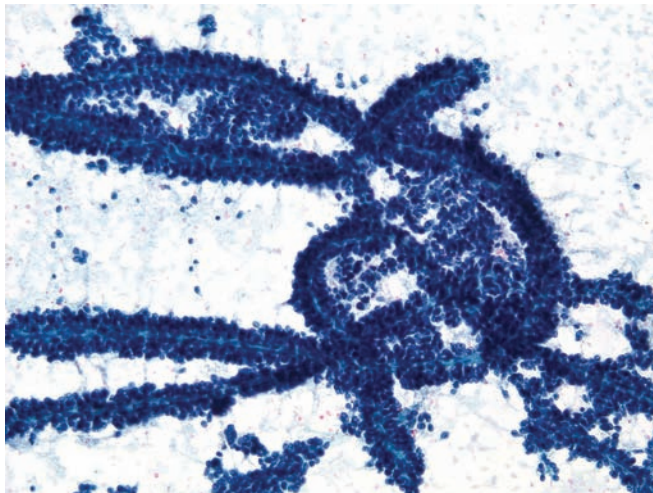
Figure 5.85 — Solid-pseudopapillary neoplasm. This case is similar to the previous example but has more complex, entangled, delicate, and slender papillary structures and solid tissue fragments of tumor. This low-power appearance is pathognomic of solid-psuedopapillary neoplasms. (Papanicolaou stain, medium power)

Solid-Pseudopapillary Neoplasm

Figure 5.86 — Solid-pseudopapillary neoplasm.
Neoplastic cells with enlarged, slightly pleomorphic nuclei surrounding a metachromatic fibrous core. This pseudorosette-like or pseudoacinar appearance can be confused with a well-differentiated endocrine neoplasm or an acinar cell carcinoma. (Diff Quik stain, high power)
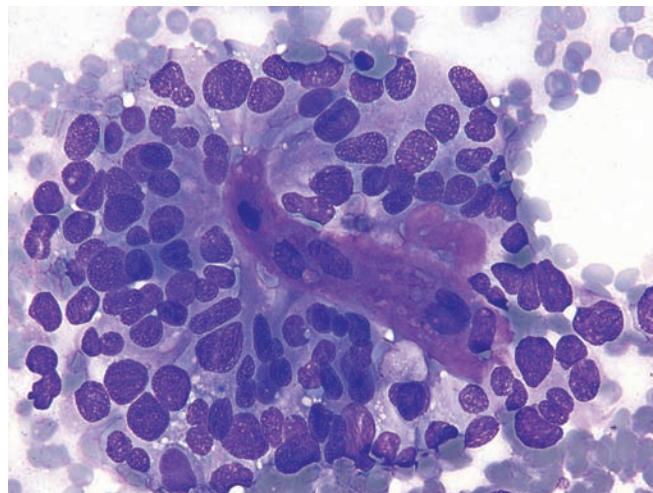
Figure 5.87 — Solid-pseudopapillary neoplasm.
Gland-like formations by the neoplastic cells with metachromatic matrix–like material in the center. The cytoplasm is delicate, ill-defined with a wispy quality. Neoplastic cells may display nuclear grooves and intra-nuclear inclusions. (Diff Quik stain, high power)
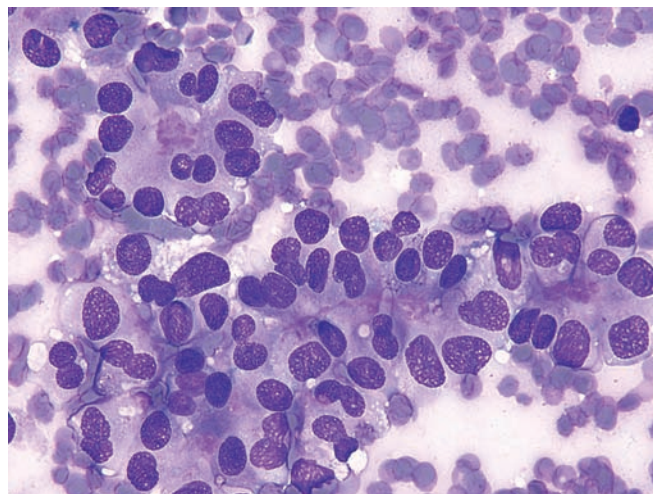
Figure 5.88 — Solid-pseudopapillary neoplasm. The neoplastic cells have uniform, round-to-ovoid, eccentrically located nuclei loosely adherent to vascular endothelium (spindled nuclei in the middle). Few cells have well-formed nuclear grooves (intranuclear pseudoinclusions may be seen in this tumor as well). A close differential diagnosis includes pancreatic endocrine neoplasm (PEN). Morphologically, this chromatin pattern is unusual for a PEN (evenly dispersed granular chromatin). Immunolabeling helps in the differential diagnosis. Solid-pseudopapillary neoplasms express CD10 and show an abnormal cytoplasmic and nuclear pattern of labeling with antibodies to β-catenin. (Papanicolaou stain, high power)
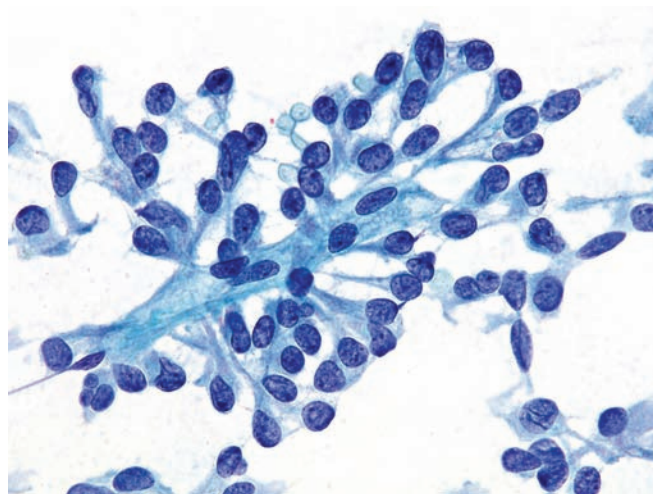
Solid-Pseudopapillary Neoplasm
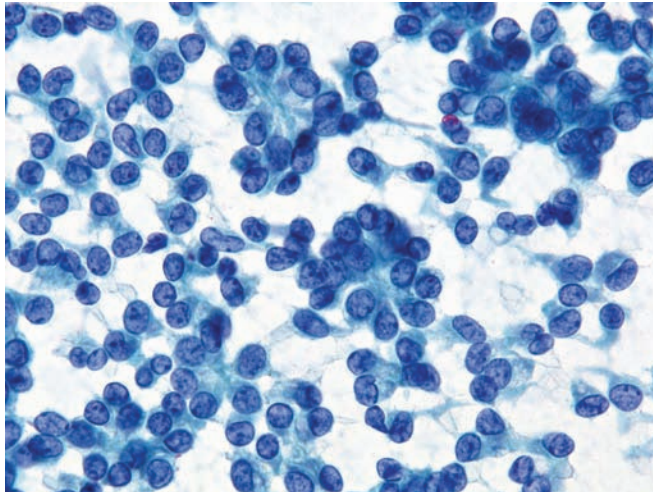
Figure 5.89 — Solid-pseudopapillary neoplasm. Acinar or rosette-like structures are often seen, creating diagnostic issues with well-differentiated pancreatic endocrine neoplasm and acinar cell carcinoma. Note the round and ovoid nuclear shapes, bland, evenly distributed pale chromatin, occasional nuclear grooves, lack of nucleoli, and fragile wispy cytoplasm devoid of granularity. (Papanicolaou stain, high power)

Acinar Cell Cystadenoma

Figure 5.90 — Acinar cell cystadenoma. This cyst is lined by cuboidal to columnar cells with basally oriented uniform nuclei and amphophilic granular cytoplasm. Collections of acinar cells with dilated lumina were present elsewhere in the cyst. The differential diagnosis includes other cystic lesions in the pancreas such as retention cysts (cuboidal to columnar cells with ductal differentiation), mucinous cystic neoplasms (columnar mucin-producing epithelium with ovarian-type stroma), intraductal papillary mucinous neoplasm (columnar mucin-producing epithelium in a large duct), and the serous cystadenoma (glycogen-rich cuboidal cells). (Hematoxylin and eosin stain, high power)
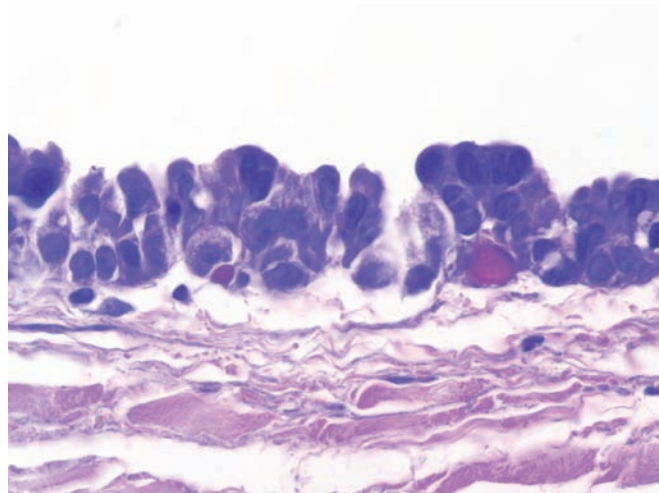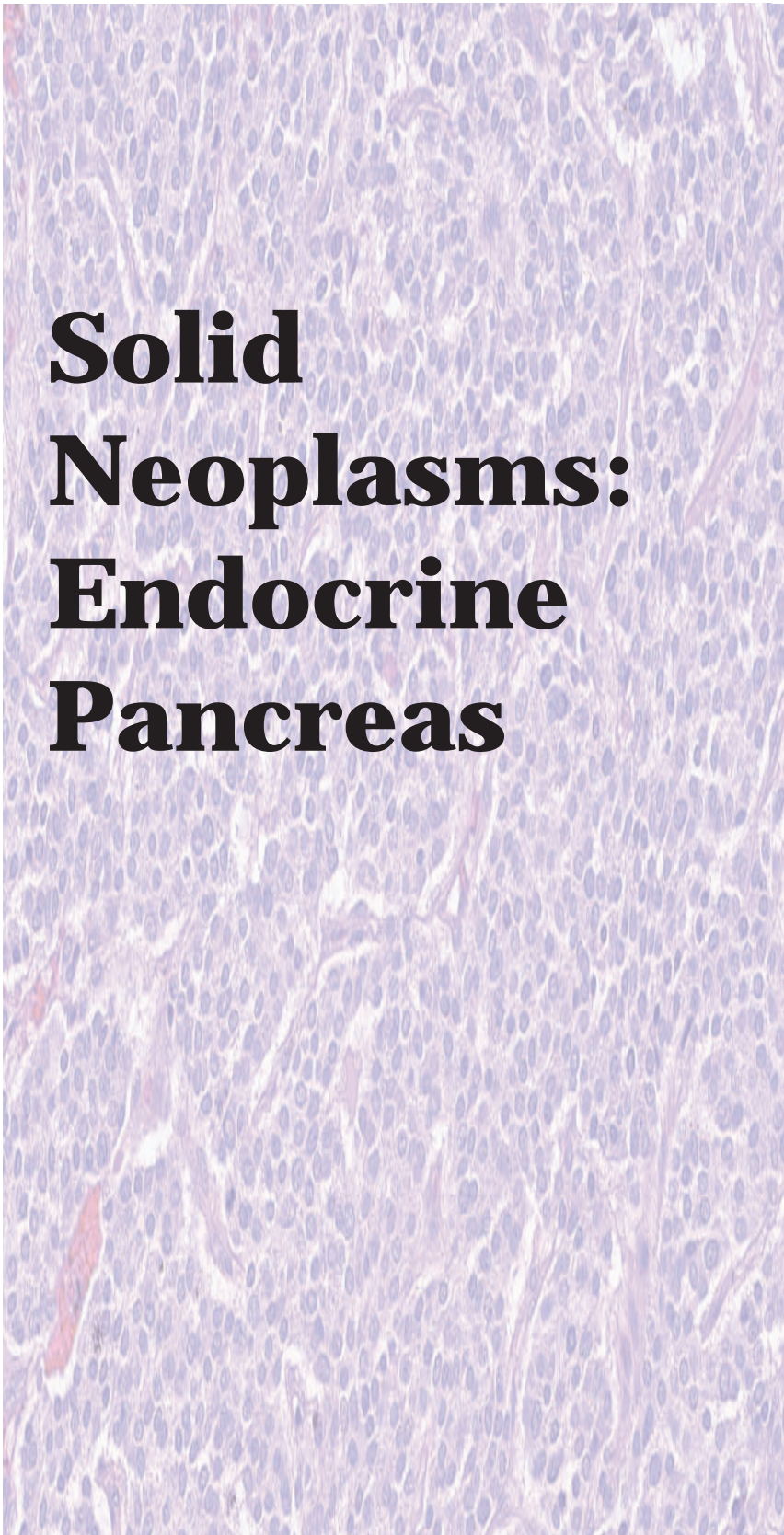
Figure 5.91 — Acinar cell cystadenoma. Immuno-labeling for trypsin demonstrates the production of exocrine pancreatic enzymes by the cells lining the cysts. Immunolabeling for trypsin, lipase, and cytokeratin 7 will be positive in most cases. Acinar cystadenocarcinoma (nuclear pleomorphism, loss of polarity, mitoses, necrosis, and tissue invasion), the malignant counterpart to the acinar cell cystadenoma, tops the differential diagnosis. (Immunolabeling for trypsin, high power)
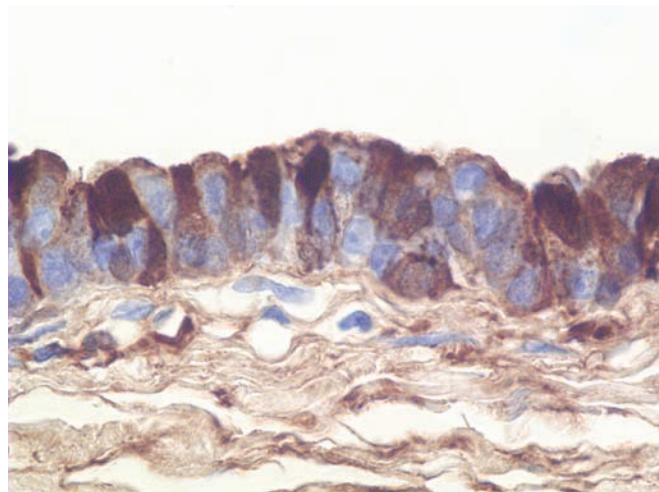
Solid Neoplasms: Endocrine Pancreas

6
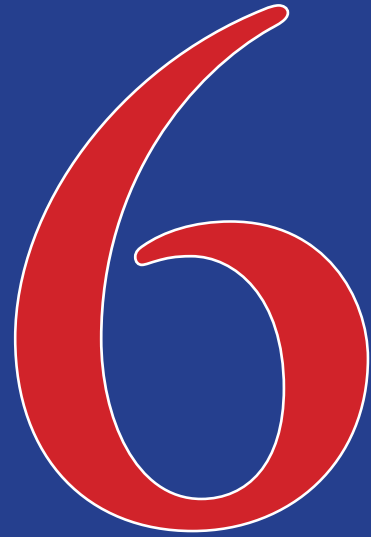
Well-Differentiated
Endocrine Neoplasm
(Islet Cell Tumor)

Poorly Differentiated
Endocrine Neoplasm
(Small Cell
Carcinoma)

Well-Differentiated Endocrine Neoplasm (Islet Cell Tumor)
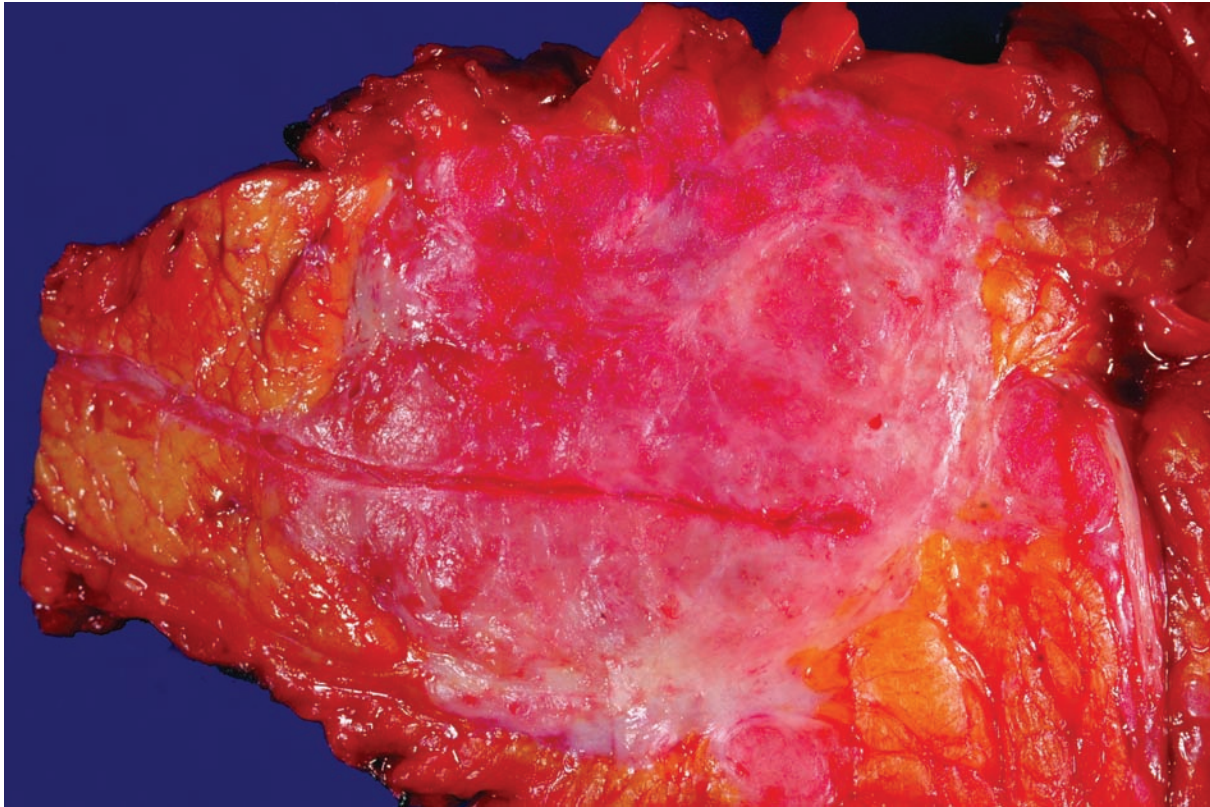
Figure 6.1 — Well-differentiated pancreatic endocrine neoplasm. This fairly well-demarcated neoplasm has surrounded and compressed the pancreatic duct, the remnant of which runs through the center of the tumor.

Well-Differentiated Endocrine Neoplasm (Islet Cell Tumor)
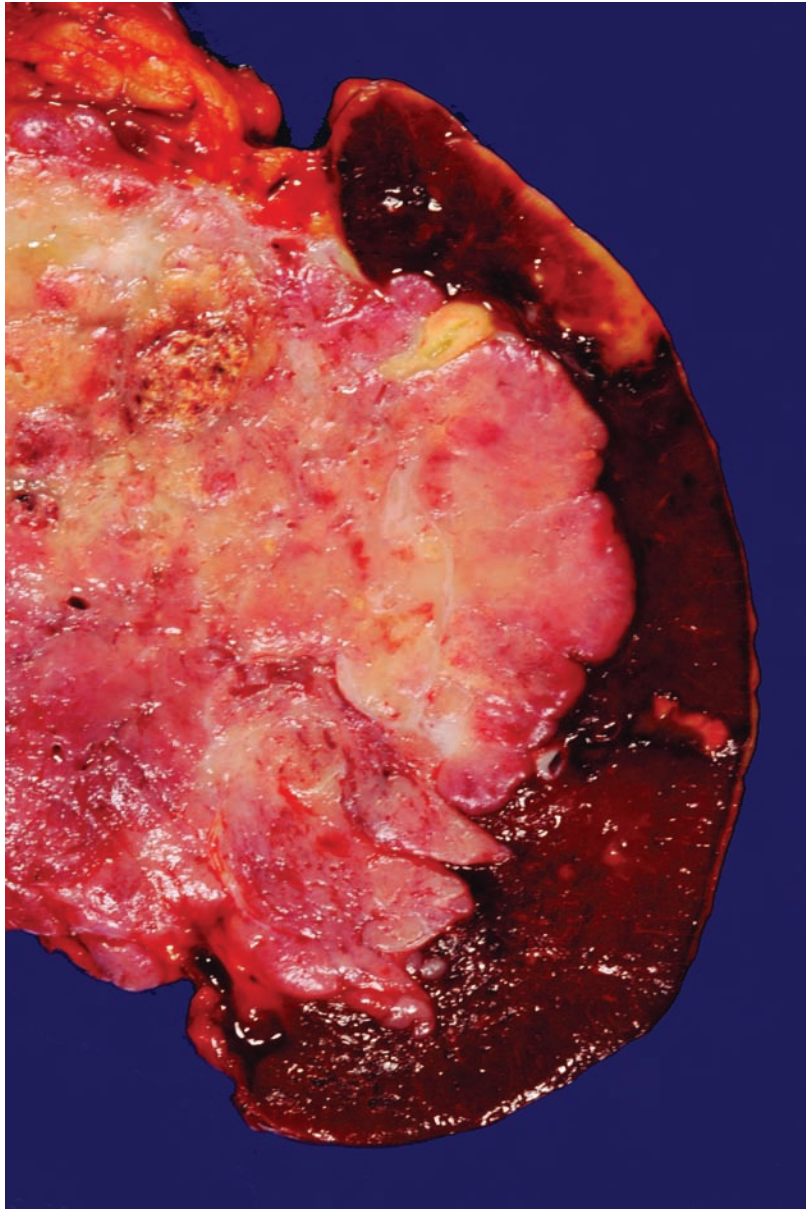
Figure 6.2 — Well-differentiated pancreatic endocrine neoplasm. This locally aggressive neoplasm has infiltrated into the spleen. Note the associated splenic infarct. Other cellular neoplasms with minimal stroma, such as acinar cell carcinoma, pancreatoblastoma, and solid-pseudopapillary neoplasm, may have a similar gross appearance and should be considered in the differential diagnosis.

Well-Differentiated Endocrine Neoplasm (Islet Cell Tumor)
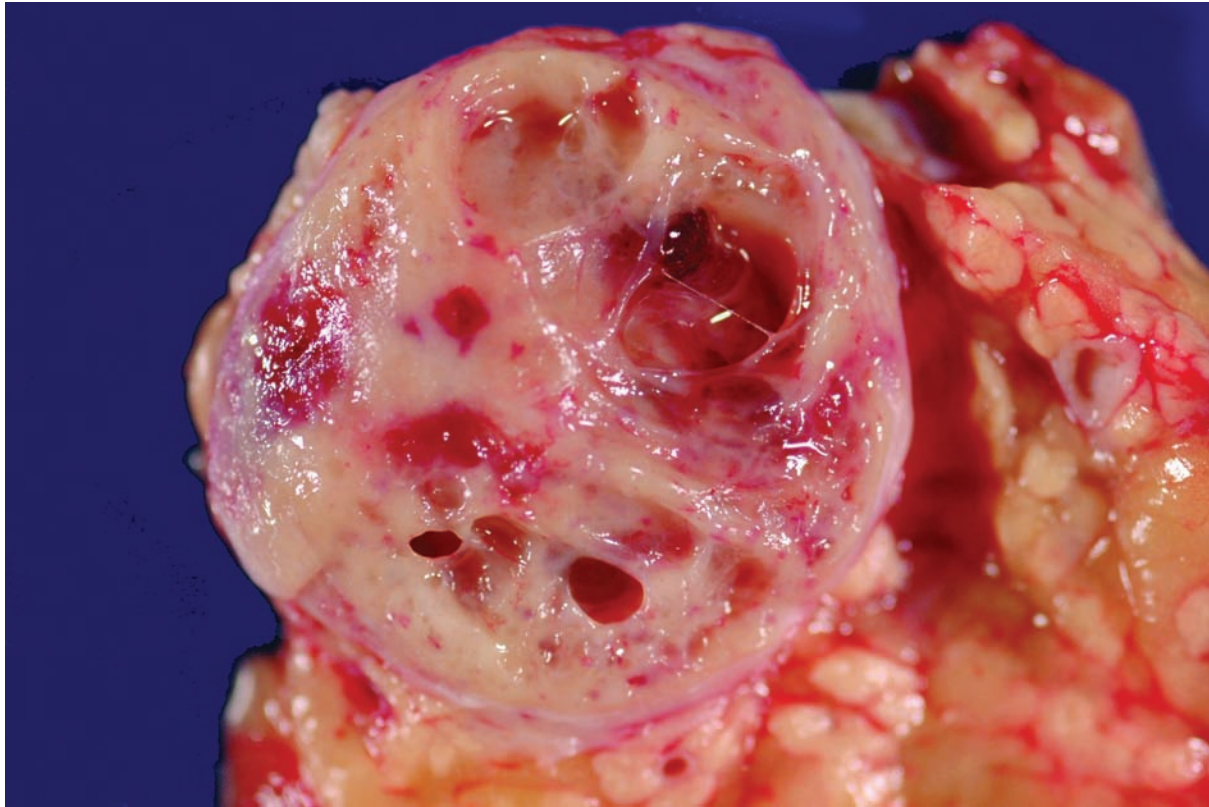
Figure 6.3 — Well-differentiated pancreatic endocrine neoplasm. Even though this neoplasm is not too large, focal cystic change is present. It can be almost impossible to distinguish grossly between a solid-pseudopapillary neoplasm and a well-differentiated pancreatic endocrine neoplasm. The cysts in the former are degenerative areas filled with necrotic debris and blood, while the spaces in a well-differentiated pancreatic endocrine neoplasm are typically filled with clear watery fluid.

Well-Differentiated Endocrine Neoplasm (Islet Cell Tumor)
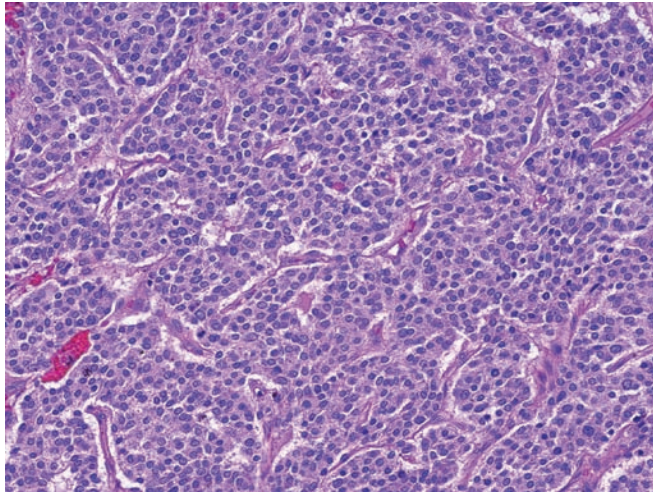
Figure 6.4 — Well-differentiated pancreatic endocrine neoplasm. The nested growth pattern of this cellular neoplasm with a rich vasculature is easily appreciated. Other cellular neoplasms of the pancreas with minimal stroma, including acinar cell carcinoma (greater pleomorphism, single prominent nucleoli), pancreatoblastoma (squamoid nests), and solid-pseudopapillary neoplasm (poorly cohesive cells), should be considered in the differential diagnosis. (Hematoxylin and eosin stain, low power)
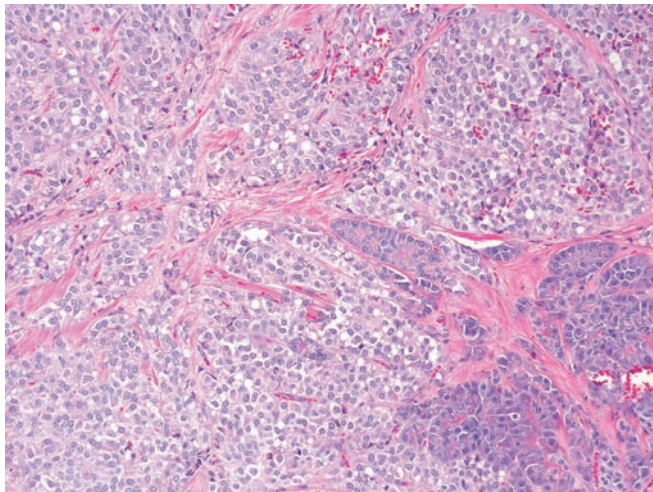
Figure 6.5 — Well-differentiated pancreatic endocrine neoplasm. Delicate fibrous cores divides the neoplastic cells into distinct lobules. Note the rich vascularity with numerous small vessels permeating the entire neoplasm. (Hematoxylin and eosin stain, low power)
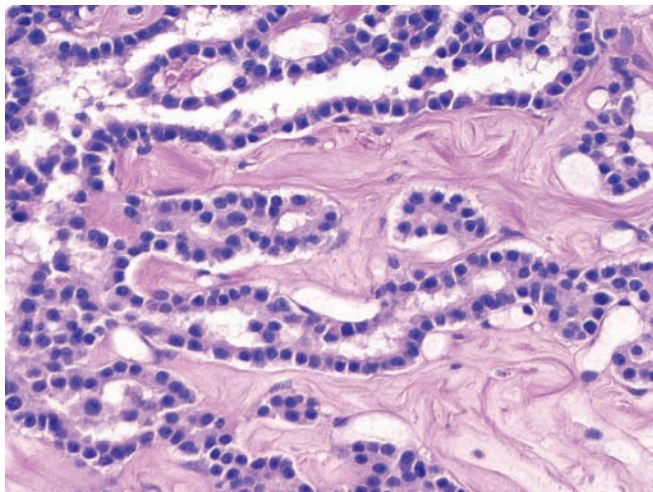
Figure 6.6 — Well-differentiated pancreatic endocrine neoplasm. Note the abundant hyalinized stroma and the formation of lumina by the neoplastic cells. Lumen formation in a well-differentiated pancreatic endocrine neoplasm can mimic an adenocarcinoma. Uniform nuclei with "salt and pepper" chromatin and the strong diffuse expression of endocrine markers such as chromogranin should suggest an endocrine neoplasm, while pleomorphism, mucin production, and the expression of cytokeratin 7 all favor an adenocarcinoma (Hematoxylin and eosin stain, medium power).

Well-Differentiated Endocrine Neoplasm (Islet Cell Tumor)

Figure 6.7 — Well-differentiated pancreatic endocrine neoplasm. Neoplastic cells with monotonous round nuclei separated by delicate fibrous stroma into well-defined lobules. Note the characteristic fine and delicate nuclear chromatin and lack of prominent nucleoli (Hematoxylin and eosin stain, low power)
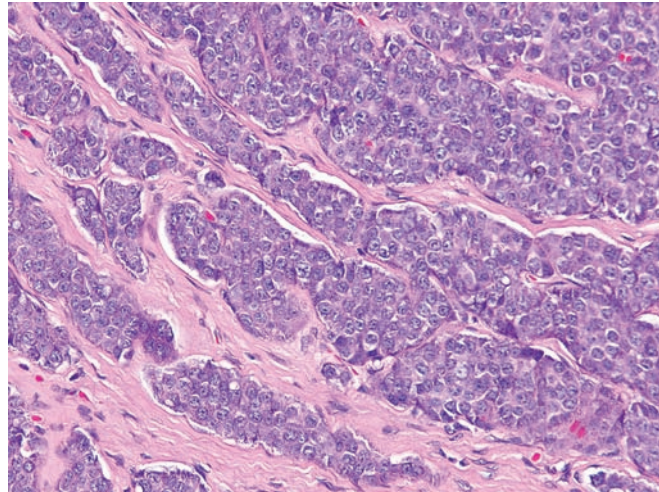
Figure 6.8 — Well-differentiated pancreatic endocrine neoplasm. The prominent trabecular pattern of growth is a clue to the diagnosis. The nuclei are relatively uniform, mitotic figures are rare, and the nuclei have the classic "salt and pepper" chromatin pattern. The nucleoli are a little more prominent in this example than is typical for a well-differentiated pancreatic endocrine neoplasm. Acinar cell carcinoma should be included in the differential diagnosis when single prominent nucleoli are present. (Hematoxylin and eosin stain, high power)
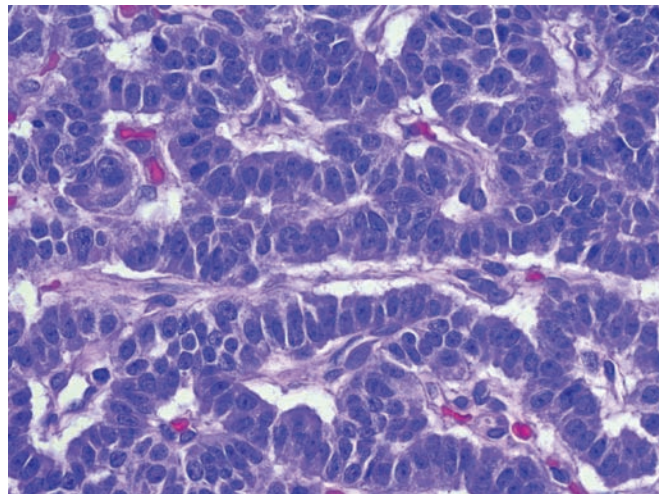
Figure 6.9 — Well-differentiated pancreatic endocrine neoplasm. This hypercellular smear contains varying sized tissue fragments and single cells. Neoplastic cells appear small and uniform and form mostly flat monolayered sheets. Differential diagnosis here includes acinar cell carcinoma and solid-pseudopapillary neoplasm. (Papanicolaou stain, low power)
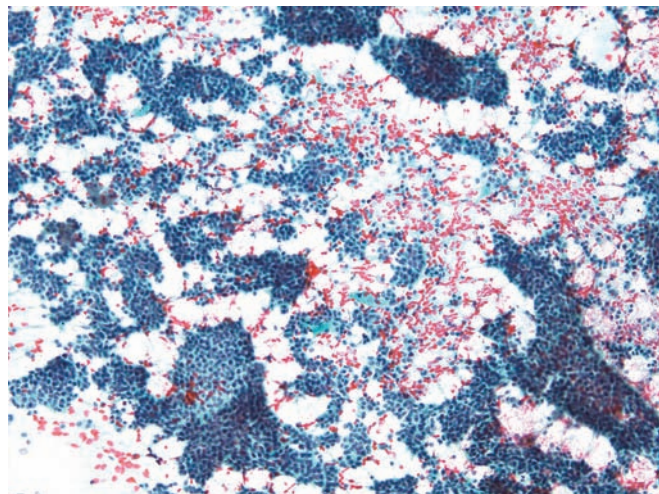
Well-Differentiated Endocrine Neoplasm (Islet Cell Tumor)
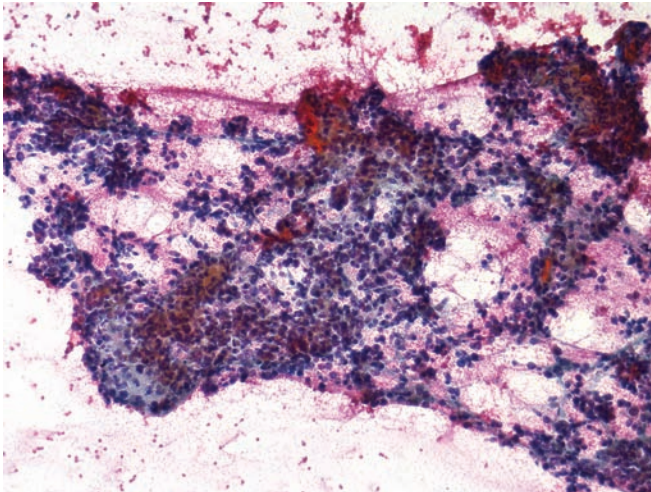
Figure 6.10 — Well-differentiated pancreatic endocrine neoplasm. Tissue fragments and loose groups of uniform small neoplastic cells are noted in a hemorrhagic background. Lack of cohesion and cellular monotony may bring up a low-grade lymphoma in the differential diagnosis. (Papanicolaou stain, low power)
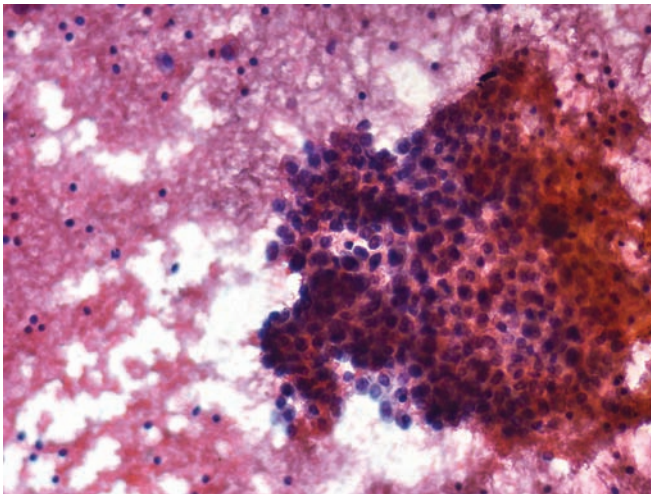
Figure 6.11 — Well-differentiated pancreatic endocrine neoplasm. A large fragment of neoplasm composed of a monotonous population of cells with uniform, round, eccentrically located nuclei and delicate cytoplasm is seen. (Papanicolaou stain, medium power)
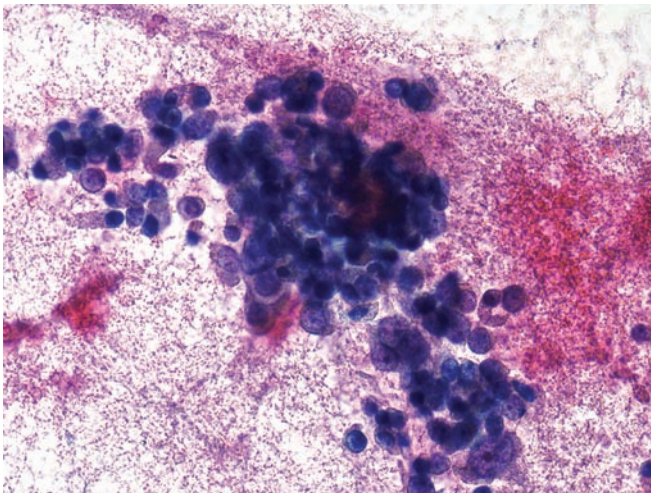
Figure 6.12 — Well-differentiated pancreatic endocrine neoplasm. Tissue fragments and groups of neoplastic cells are seen in a hemorrhagic background. Unlike typical endocrine features, the neoplastic cells have large nuclei, open chromatin, and occasional prominent nucleoli. Focal areas with anisonucleosis, such as this one, may be seen in endocrine neoplasms. (Papanicolaou stain, high power)

Well-Differentiated Endocrine Neoplasm (Islet Cell Tumor)

Figure 6.13 — Well-differentiated pancreatic endocrine neoplasm (touch imprint from resected tumor). The neoplasm displays uniform bare nuclei with slightly speckled chromatin and inconspicuous nucleoli. Focal nuclear crush artifact is seen, which is dependent on the physical force applied at the time of slide smearing. (Hematoxylin and eosin stain, low and medium power)
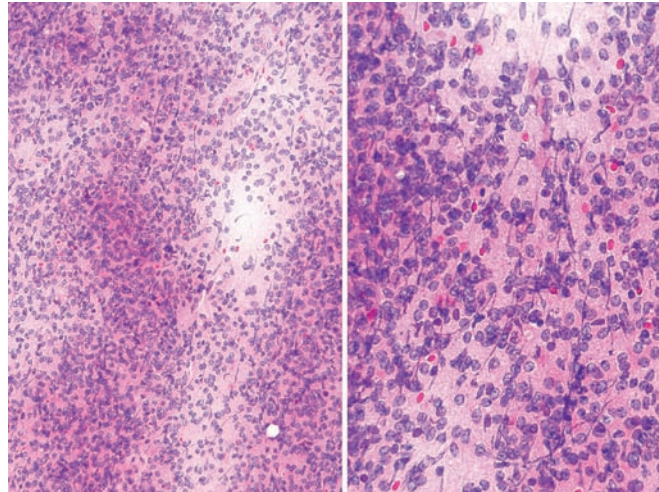
Figure 6.14 — Well-differentiated pancreatic endocrine neoplasm (touch imprint from resected tumor). This shows features similar to Figure 6.13. Due to the dispersed single cell pattern and the presence of numerous naked nuclei mimicking lymphocytes, the differential diagnosis includes a low-grade non-Hodgkin lymphoma. (Diff Quik stain, low and medium power)
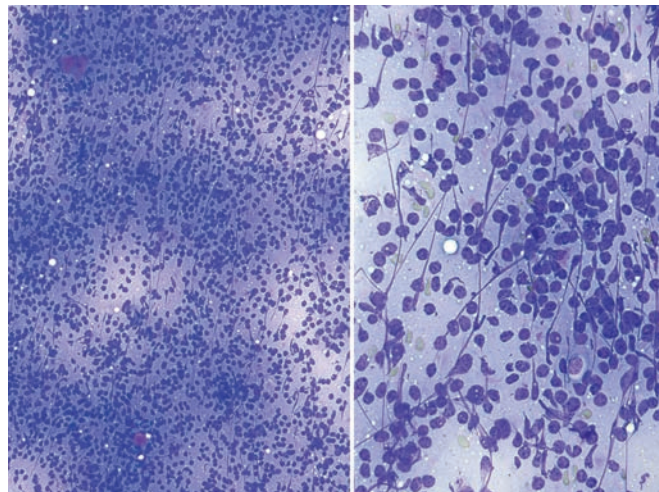
Figure 6.15 — Well-differentiated pancreatic endocrine neoplasm (touch imprint from resected tumor). Cytomorphologic features similar to the previous cases are observed. All neoplastic cells are stripped of their cytoplasm. This phenotypic appearance would be difficult to differentiate from a low-grade lymphoma. (Diff Quik stain, high power)
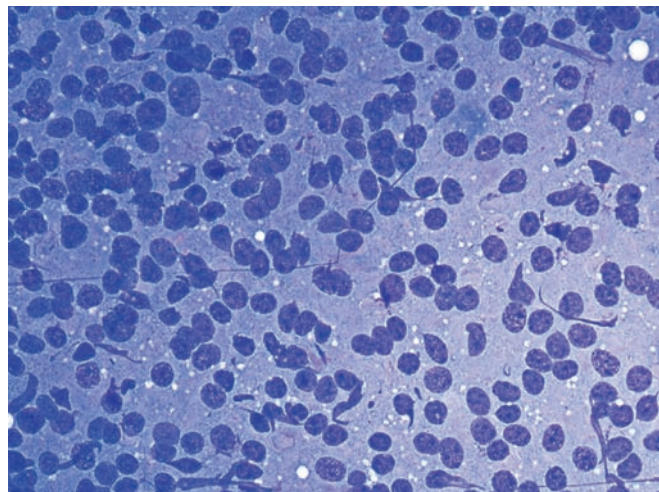
Well-Differentiated Endocrine Neoplasm (Islet Cell Tumor)
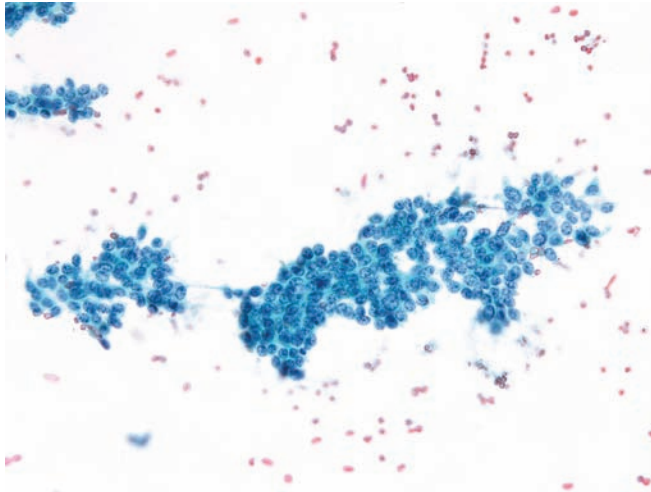
Figure 6.16 — Well-differentiated pancreatic endocrine neoplasm. Neoplastic cells form loosely cohesive fragments. The cells have uniform round or ovoid nuclei with focal crowding and overlapping. The chromatin texture is characteristically speckled or "checker board-like." The cytoplasm is fragile and wispy, scant or ill defined. (Papanicolaou stain, low power)
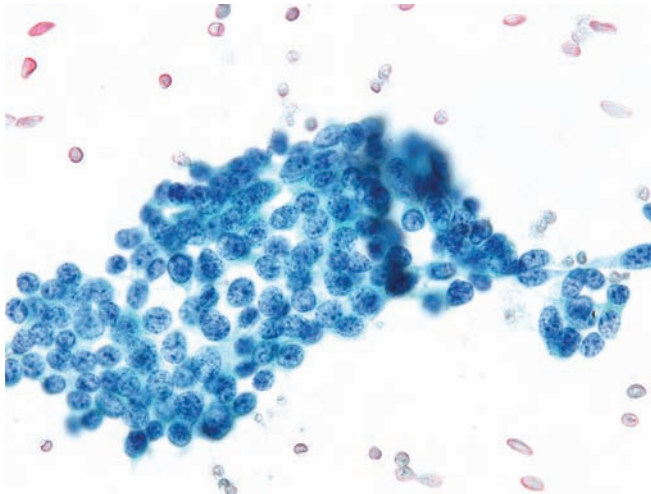
Figure 6.17 — Well-differentiated pancreatic endocrine neoplasm. Neoplastic cells similar to those in the previous image are present. Note the even granular or speckled chromatin pattern and absence of prominent nucleoli. This chromatin pattern helps in distinguishing these cells from other primary pancreatic neoplasms. (Papanicolaou stain, high power)
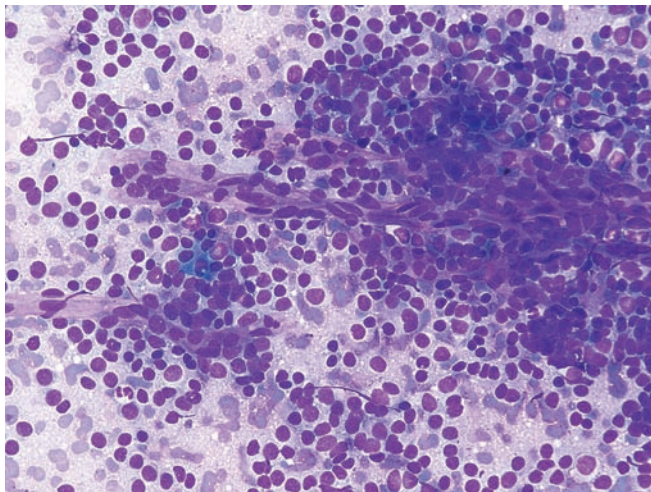
Figure 6.18 — Well-differentiated pancreatic endocrine neoplasm. This shows a hypercellular smear composed of predominantly single cells with monotonous, small-to-intermediate sized, round-to-ovoid nuclei and indistinct cytoplasmic borders. A traversing capillary vessel tightly surrounded by neoplastic cells is seen. These are hypervascular lesions—a feature extremely helpful in the radiologic identification at the time of clinical presentation. (Diff Quik stain, medium power)

Well-Differentiated Endocrine Neoplasm (Islet Cell Tumor)

Figure 6.19 — Well-differentiated pancreatic endocrine neoplasm. A group of loosely cohesive neoplastic cells is depicted. The nuclei are large and generally round, and some have partially folded corners, causing irregular shapes. The cells in the crowded areas appear to have high N/C ratios, but cells at the margins of the group have moderate amounts of cytoplasm and eccentrically located nuclei. Relatively small cell size and monotony are the key cytomorphologic features in this tumor. (Papanicolaou stain, high power)
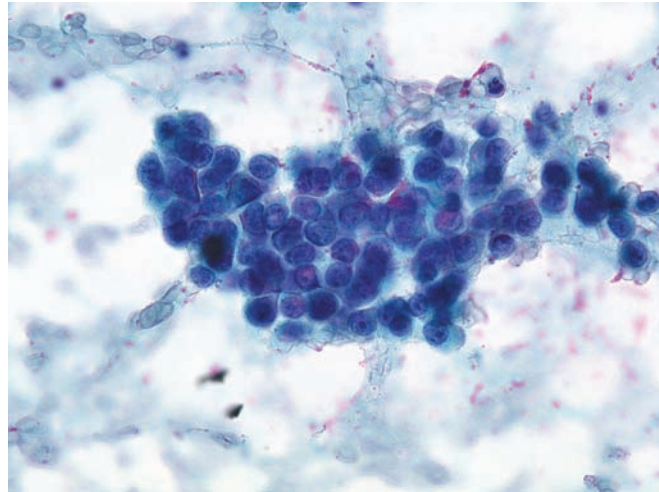
Figure 6.20 — Well-differentiated pancreatic endocrine neoplasm. These neoplastic cells have densely granular and faintly basophilic cytoplasm, which is focally replaced with clear fine vacuoles (left). Round-to-oval uniform nuclei illustrate the characteristic speckled nuclear chromatin (right). (Diff Quik and Papanicolaou stains, high power)
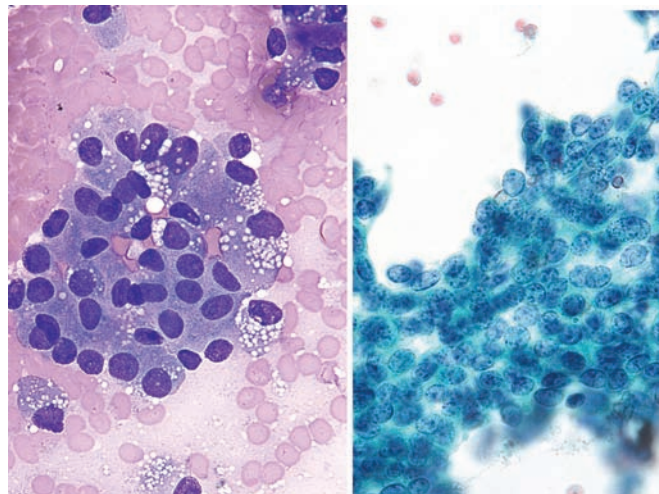
Figure 6.21 — Well-differentiated pancreatic endocrine neoplasm. Note the loose cluster of neoplastic cells with eccentrically placed "plasmacytoid," round-to-oval uniform nuclei. Occasional cells are binucleated, with few showing cytoplasmic vacuolization. (Diff Quik stain, medium power)
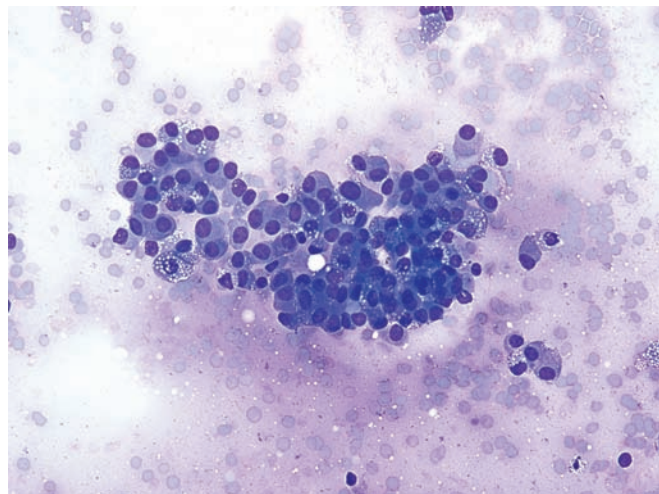
Well-Differentiated Endocrine Neoplasm (Islet Cell Tumor)
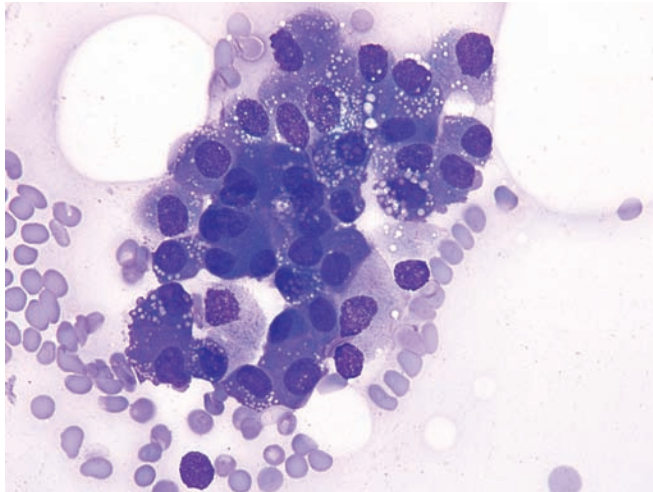
Figure 6.22 — Well-differentiated pancreatic endocrine neoplasm. Cells similar to the ones in Figure 6.21 are present. Note the nuclei with evenly distributed granular chromatin, lack of nucleoli and densely granular basophilic cytoplasm. A close differential diagnosis here would be with acinar cell carcinoma. Cases like this often need a thorough immunolabeling for a definitive interpretation. (Diff Quik stain, high power)
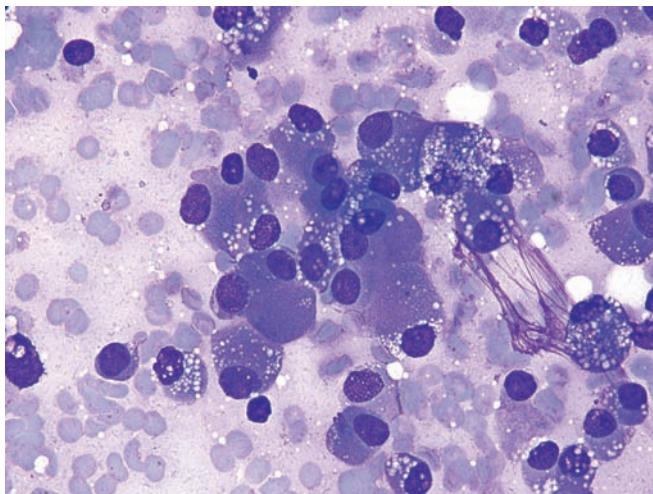
Figure 6.23 — Well-differentiated pancreatic endocrine neoplasm. Neoplastic cells with relatively abundant, densely granular cytoplasm dominate the field. Nuclei are eccentrically placed or "plasmacy-toid" in appearance. Few cells show binucleation. An acinar cell carcinoma should be carefully excluded in such cases. (Diff Quik stain, high power)
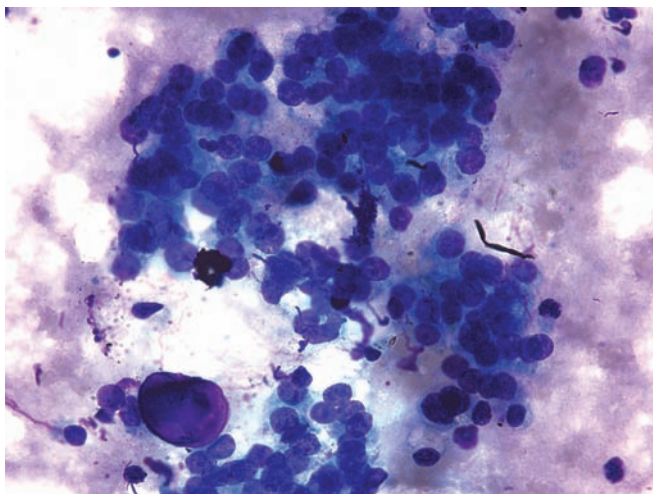
Figure 6.24 — Well-differentiated pancreatic endocrine neoplasm. Neoplastic cells associated with a well-formed psammoma body are seen. This finding is unusual in an aspirate of this neoplasm, however, when observed strongly favors a well-differentiated endocrine neoplasm, particularly an insulinoma or a somatostatinoma. (Diff Quik stain, medum power)

Well-Differentiated Endocrine Neoplasm (Islet Cell Tumor)

Figure 6.25 — Well-differentiated pancreatic endocrine neoplasm. This shows a psammoma body from a case in which only scant cellular evidence of a well-differentiated pancreatic endocrine neoplasm was present. Isolated psammoma bodies are extremely rare in pancreatic FNA. However, when present, should raise the possibility of an endocrine neoplasm. (Diff Quik stain, high power)
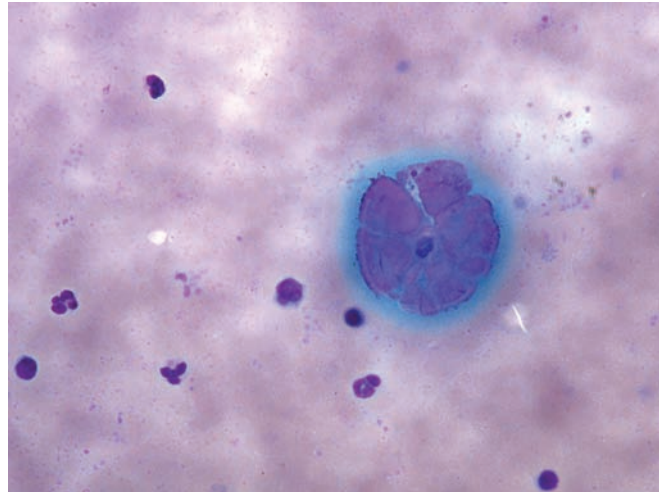
Figure 6.26 — Well-differentiated pancreatic endocrine neoplasm. Hypercellular smear composed of dispersed, uniform, single neoplastic cells is depicted. The tumor typically shows abundant cellularity on aspiration due to the stroma-poor nature of the lesion. Few cells also exhibit fine cytoplasmic vacuolization. (Diff Quik stain, low power)
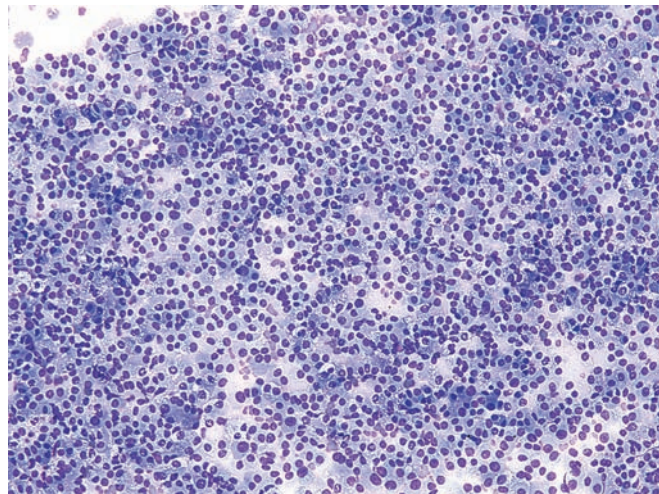
Figure 6.27 — Well-differentiated pancreatic endocrine neoplasm. Cellular smear composed of uniformly dispersed neoplastic cells is seen. The cells have round-to-ovoid eccentrically placed "plasmacytoid" nuclei with even chromatin patterns and occasional small nucleoli. The neoplastic cells display characteristic finely vacuolated cytoplasm, which may represent lipid droplets. (Diff Quik stain, high power)
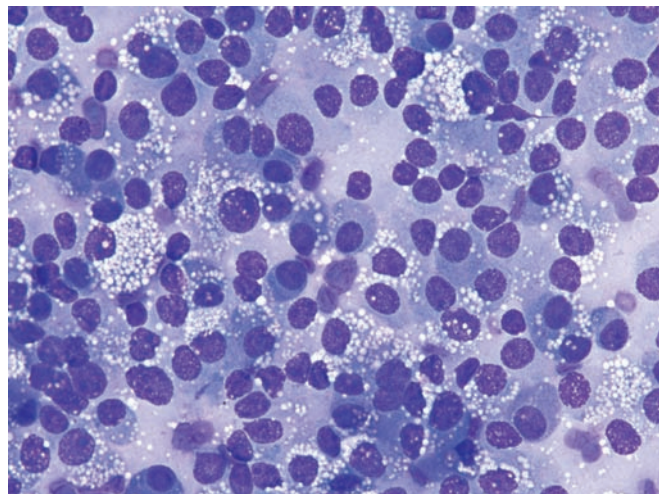
Well-Differentiated Endocrine Neoplasm (Islet Cell Tumor)
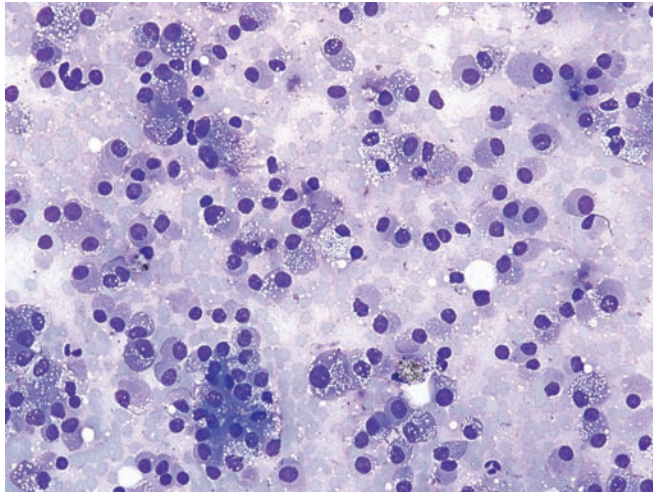
Figure 6.28 — Well-differentiated pancreatic endocrine neoplasm. Neoplastic cells are present with features similar to Figure 6.27. Cells have eccentrically located round nuclei and finely vacuolated or solid well-defined cytoplasm. One tight group of cells may represent a tissue fragment. (Diff Quik stain, medium power)
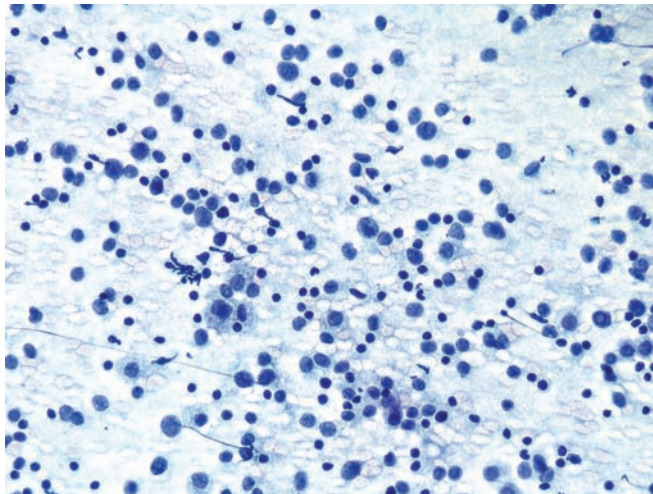
Figure 6.29 — Well-differentiated pancreatic endocrine neoplasm. This example illustrates almost all single, dispersed neoplastic cells with mostly bare nuclei. Some cells display delicate and fragile cytoplasm. Numerous lymphocytes admixed with neoplastic cells are also present. Background has a characteristic foamy or granular appearance. (Papanicolaou stain, low power)
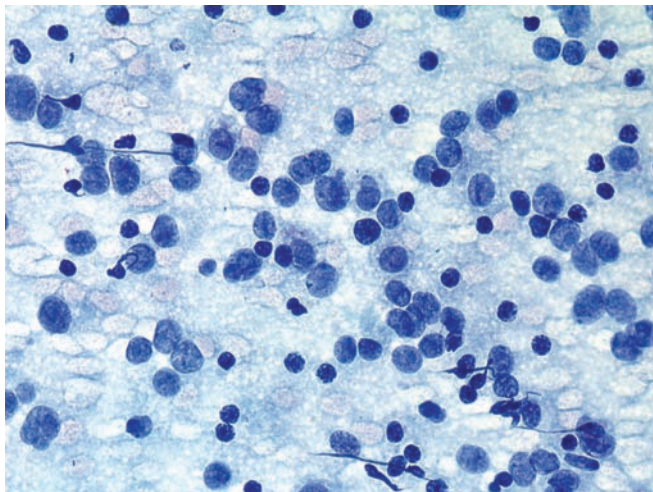
Figure 6.30 — Well-differentiated pancreatic endocrine neoplasm. Features are similar to Figure 6.29, showing monotonous nuclei with evenly granular chromatin, lacking nucleoli. A low-grade non-Hodgkin lymphoma would be in the differential diagnosis.(Papanicolaou stain, high power)

Well-Differentiated Endocrine Neoplasm (Islet Cell Tumor)

Figure 6.31 — Well-differentiated pancreatic endocrine neoplasm. Neoplastic cells are present with eccentrically located single or double nuclei with granular chromatin, admixed with lymphocytes. Cells have moderate to large amounts of finely vacuolated cytoplasm simulating histiocytes. (Papanicolaou stain, high power)
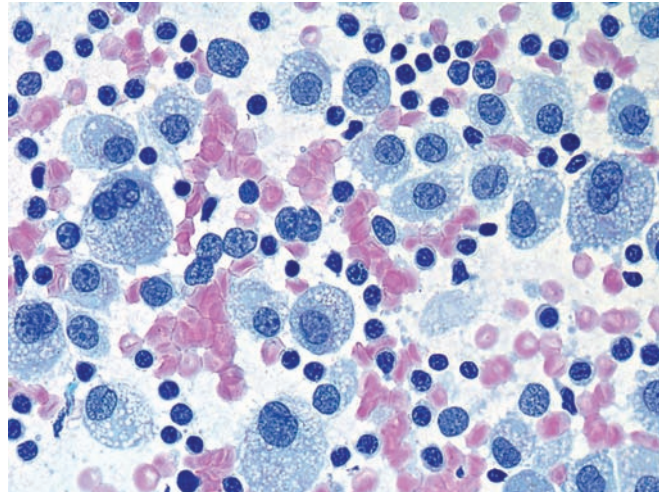
Figure 6.32 — Well-differentiated pancreatic endocrine neoplasm. Hypercellular smear composed of numerous small to medium-sized fragments of neoplastic cells. The cells have monotonous, round-to-ovoid, eccentrically located nuclei and moderate amounts of cytoplasm. Tissue fragments and rosette-like forms composed of loosely arranged, uniform neoplastic cells are present. This pattern is characteristic of a well-differentiated pancreatic endocrine neoplasm (islet cell tumor). (Diff Quik stain, low power)
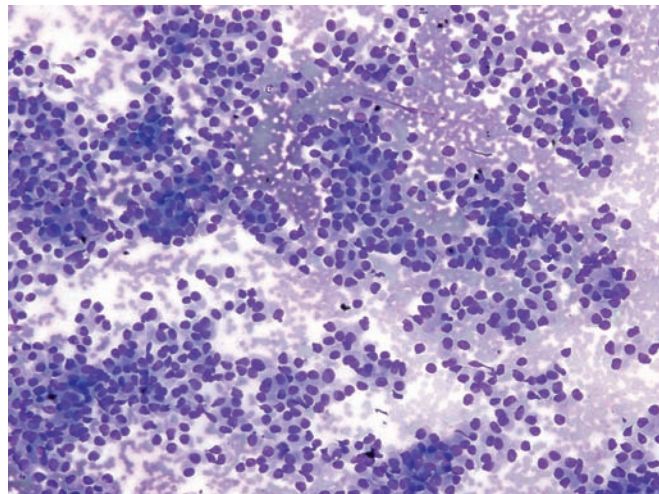
Figure 6.33 — Well-differentiated pancreatic endocrine neoplasm. A few hypercellular crowded tissue fragments are present with overlapping nuclei. The neoplastic cells appear to have high N/C ratios and uniform hyperchromatic nuclei. A few nuclei exhibit molding, a feature not typically seen in this tumor. Nuclear molding is classically observed in high-grade endocrine tumors (small cell carcinoma). A well-formed rosette is seen at 9 o'clock. (Diff Quik stain, medium power)
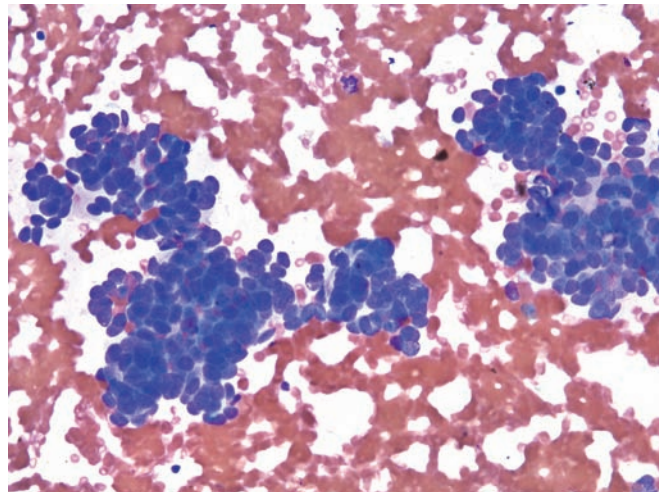
Well-Differentiated Endocrine Neoplasm (Islet Cell Tumor)
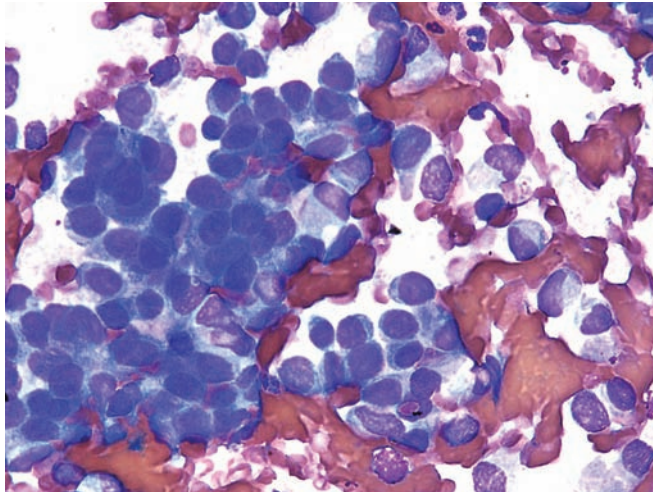
Figure 6.34 — Well-differentiated pancreatic endocrine neoplasm. Tissue fragments, groups, and single neoplastic cells highlight this field. Some of the single cells have high N/C ratios. One rosette or gland-like formation is present at 12 o'clock. Absence of prominent nucleoli favors a well-differentiated pancreatic endocrine neoplasm as opposed to an adenocarcinoma, a close differential diagnosis in this particular example. (Diff Quik stain, high power)
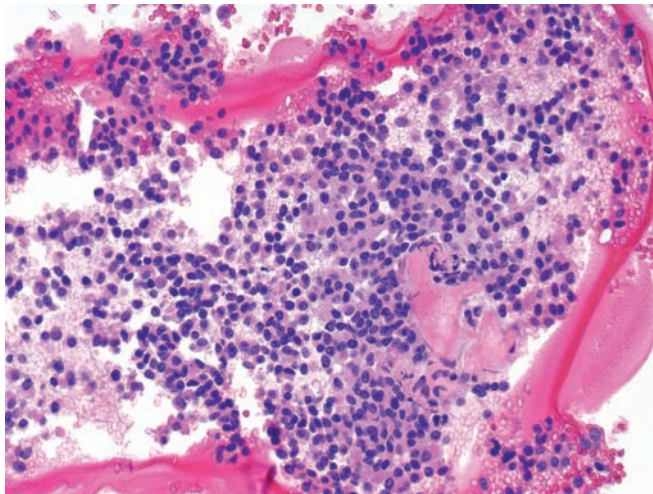
Figure 6.35 — Well-differentiated pancreatic endocrine neoplasm (cell block section). These uniform appearing neoplastic cells have round nuclei, speckled chromatin, and pale pink cytoplasm. An acinar cell carcinoma should be considered in the differential diagnosis. (Hematoxylin and eosin stain, low power)
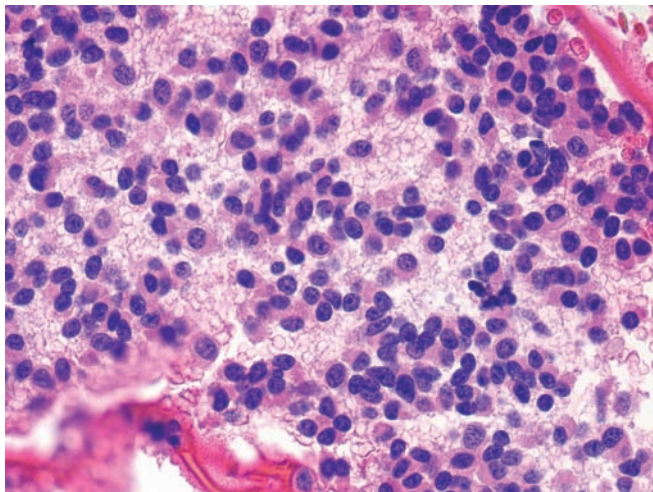
Figure 6.36 — Well-differentiated pancreatic endocrine neoplasm (cell block section). Note the dispersed neoplastic cells with round or ovoid eccentrically located nuclei showing bland chromatin pattern and moderate amounts of eosinophilic cytoplasm. Cell blocks are extremely important in such cases and provide excellent results when confirmatory immunolabeling is preformed. (Hematoxylin & eosin stain, high power)

Well-Differentiated Endocrine Neoplasm (Islet Cell Tumor)

Figure 6.37 — Well-differentiated pancreatic endocrine neoplasm (cell block section). Immunolabeling with neuroendocrine markers displays strong and diffuse reaction of the neoplastic cells for chromogranin. (Immunolabeling, low power)
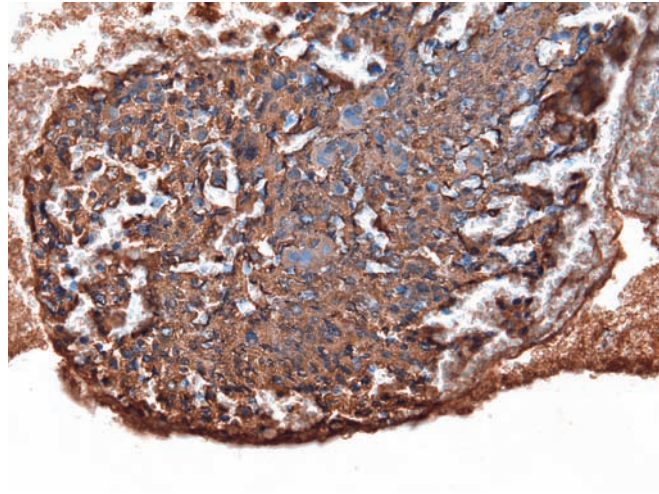
Figure 6.38 — Well-differentiated pancreatic endocrine neoplasm (cell block section). Synaptoplysin immunolabeling is characteristically strong in the neoplastic cells. (Immunolabeling, medium power)
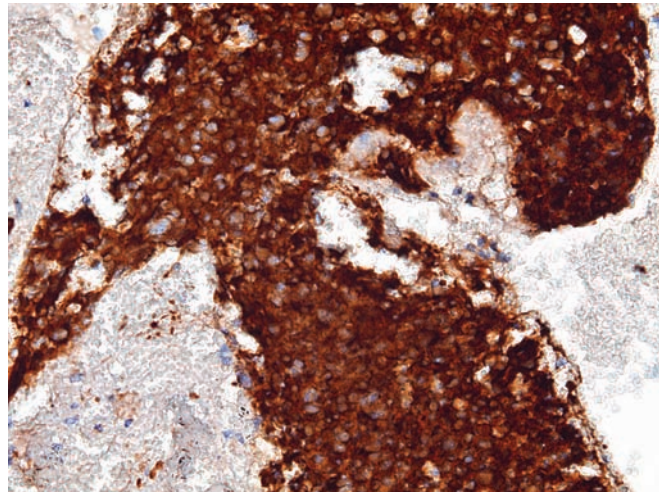
Poorly-Differentiated Endocrine Neoplasm (Small Cell Carcinoma)
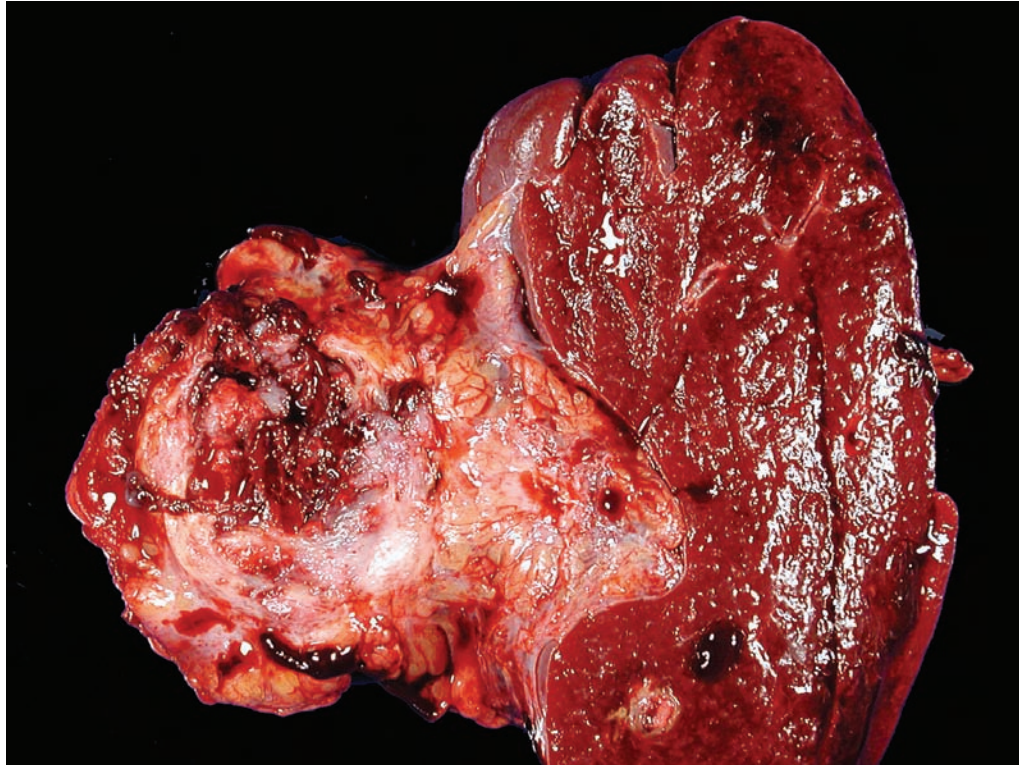
Figure 6.39 — Small cell carcinoma. This neoplasm forms a large hemorrhagic mass in the tail of the pancreas. Most small cell carcinomas in the pancreas are metastases from a lung primary. Extrapancreatic primaries should therefore be ruled out before establishing a small cell carcinoma primary to the pancreas.

Poorly-Differentiated Endocrine Neoplasm (Small Cell Carcinoma)

Figure 6.40 — Small cell carcinoma. This extremely aggressive carcinoma is composed of pleomorphic cells with a high nuclear-to-cytoplasmic ratio, minimal cytoplasm, and a high mitotic rate. The nuclei are remarkable for nuclear molding, fine chromatin, and inconspicuous nucleoli. Small cell carcinomas are distinguished from well-differentiated endocrine neoplasms by their high proliferation rate (more than 10 mitoses per 10 high power fields), fine chromatin, and nuclear molding. (Hematoxylin and eosin stain, high power)
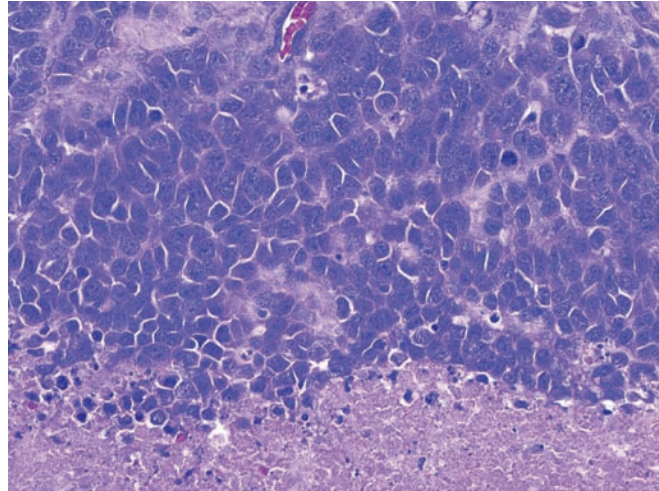
Figure 6.41 — Small cell carcinoma. Immunolabeling for CD56 highlights the endocrine differentiation of this neoplasm. Antibodies to synaptophysin and chromogranin focally label most cases, while Ki67 will label the majority of the cells reflecting the extraordinary proliferation rate of these neoplasms. (Immunolabeling for CD56, high power)
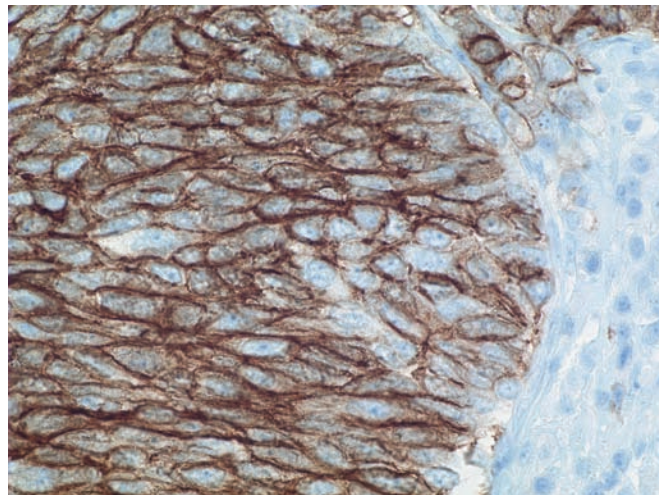
Poorly-Differentiated Endocrine Neoplasm (Small Cell Carcinoma)
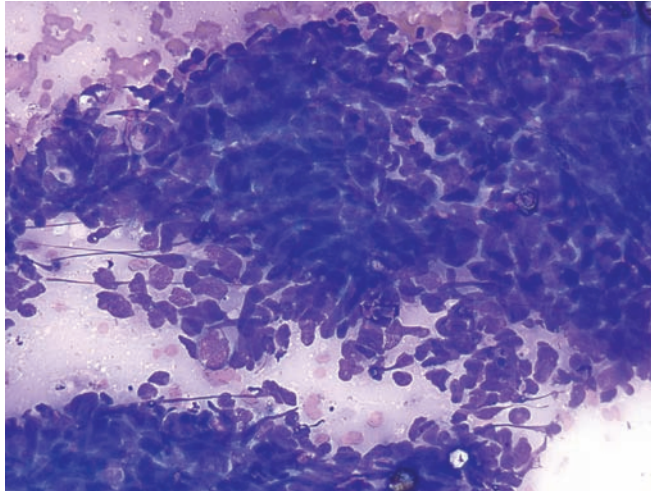
Figure 6.42 — Small cell carcinoma. This hypercellular smear is comprised of small, undifferentiated neoplastic cells with high N/C ratio, nuclear molding, and crush artifact. Nuclei are oval shaped with often pointy edges—"oat cell-like." A morphologic distinction from a lung small cell carcinoma is not possible, and the diagnosis of a primary small cell carcinoma is only made after careful clinico-radiologic exclusion of other primary sites. (Diff Quik stain, medium power)
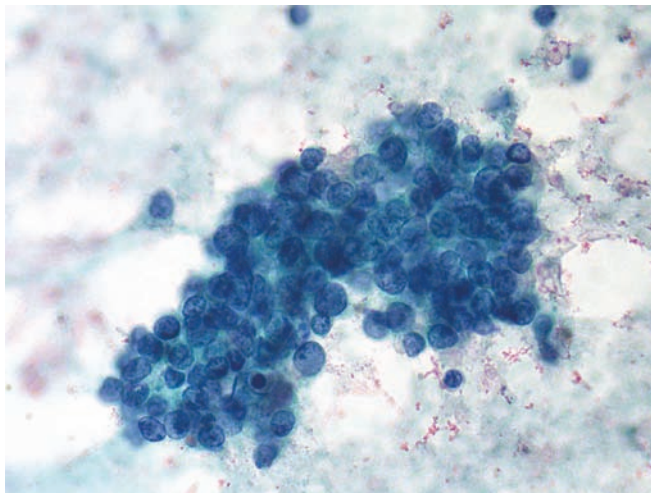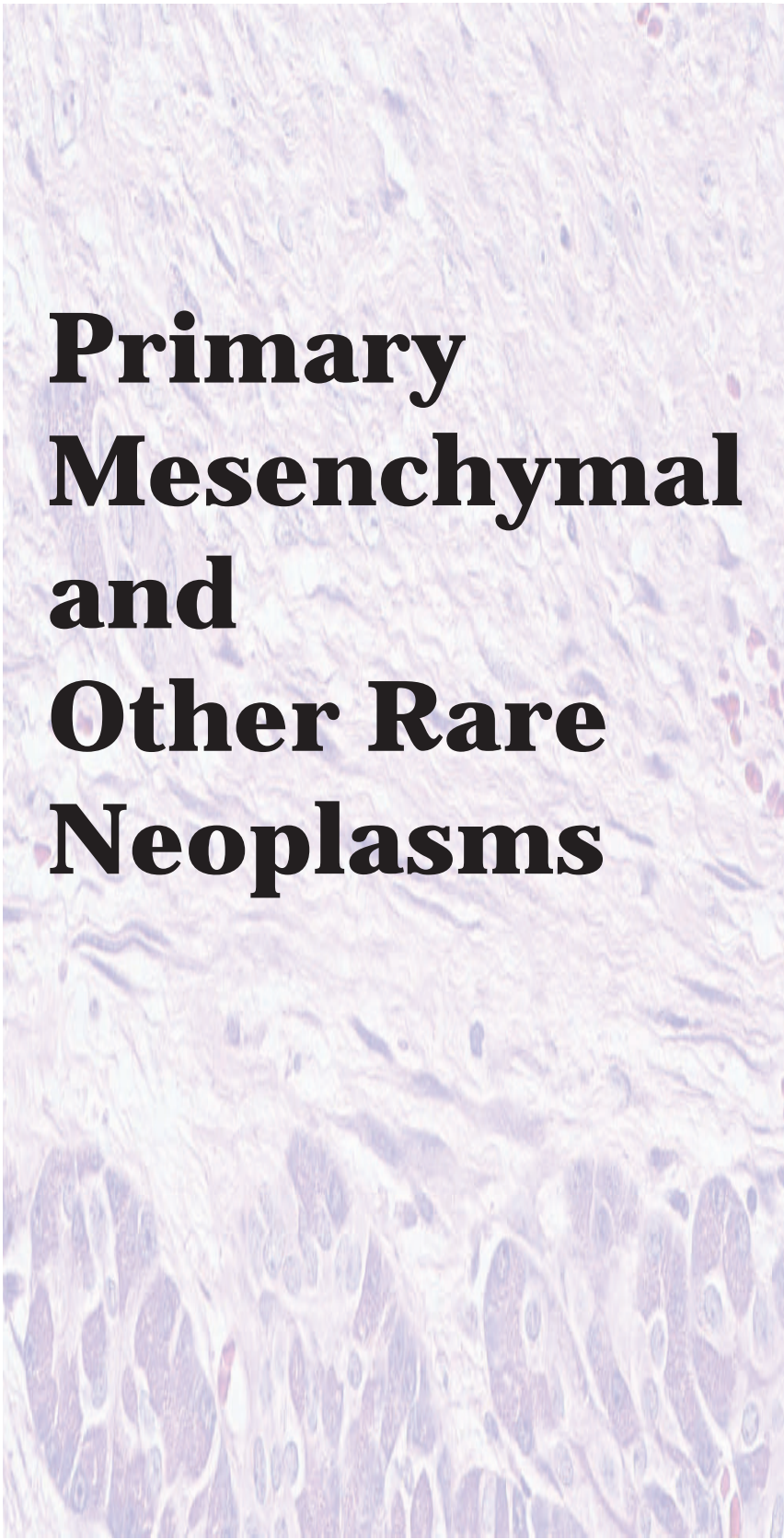
Figure 6.43 — Small cell carcinoma. A tissue fragment of relatively small neoplastic cells having extremely scant cytoplasm and apparent nuclear molding is present. Nuclei have a finely granular or "salt and pepper-like" chromatin pattern. A lymphoma is often in the differential diagnosis, but the cellular clustering and the chromatin pattern clearly favor small cell carcinoma. (Papanicolaou stain, high power)

Primary Mesenchymal and Other Rare Neoplasms

7

Fibromatosis (desmoid tumor)

Lymphangioma

Paraganglioma

Fibromatosis (desmoid tumor)

Figure 7.1 — Fibromatosis (desmoid tumor) involving the pancreas. This mesenchymal neoplasm is composed of spindle-shaped cells admixed with abundant fibrous stroma. Note how the spindle cells surround preexisting acinar structures. Mesenchymal neoplasms, such as fibromatosis, lymphangioma, schwannoma, granular cell tumor, inflammatory myofibroblastic tumor, solitary fibrous tumor, and sarcoma, can rarely involve the pancreas. In general, the behavior of these neoplasms parallels the behavior of extrapancreatic cases. (Hematoxylin and eosin stain, high power)
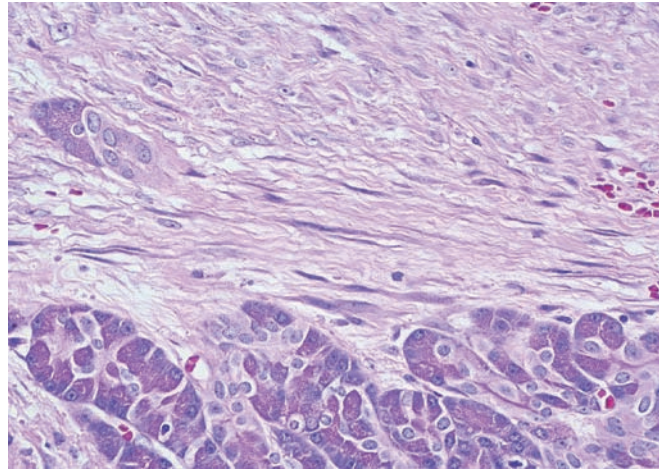
Figure 7.2 — Fibromatosis (desmoid tumor) involving the pancreas. A fragment of hypercellular dense fibrous tissue containing spindled cells is seen. The cells have crowded, fusiform nuclei with tapering ends, lacking palisading or any distinct architecture. (Diff Quik stain, medium power)
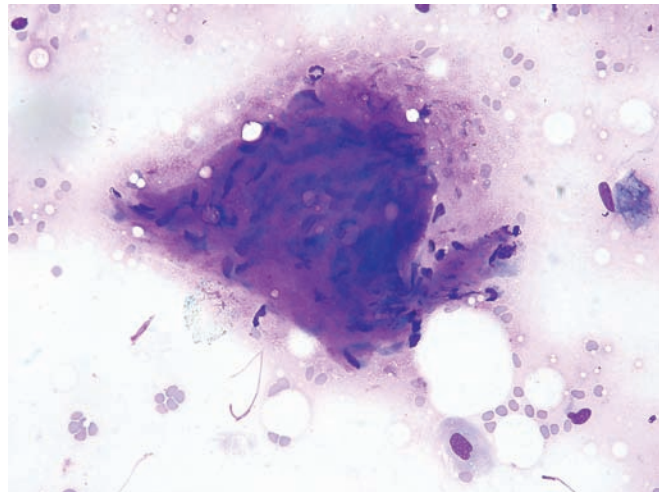
Figure 7.3 — Fibromatosis (desmoid tumor) involving the pancreas. Cells show bipolar tailing of basophilic cytoplasm and large ovoid nuclei with conspicuous nucleoli and are loosely embedded in a myxomatous stroma. A number of metastatic spindle-cell neoplasms (mostly nerve sheath or smooth muscle type) would be in the differential diagnosis. (Diff Quik stain, high power)
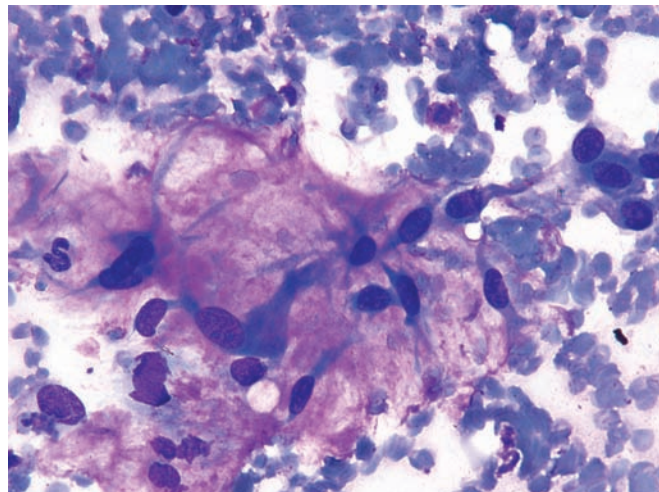
Lymphangioma
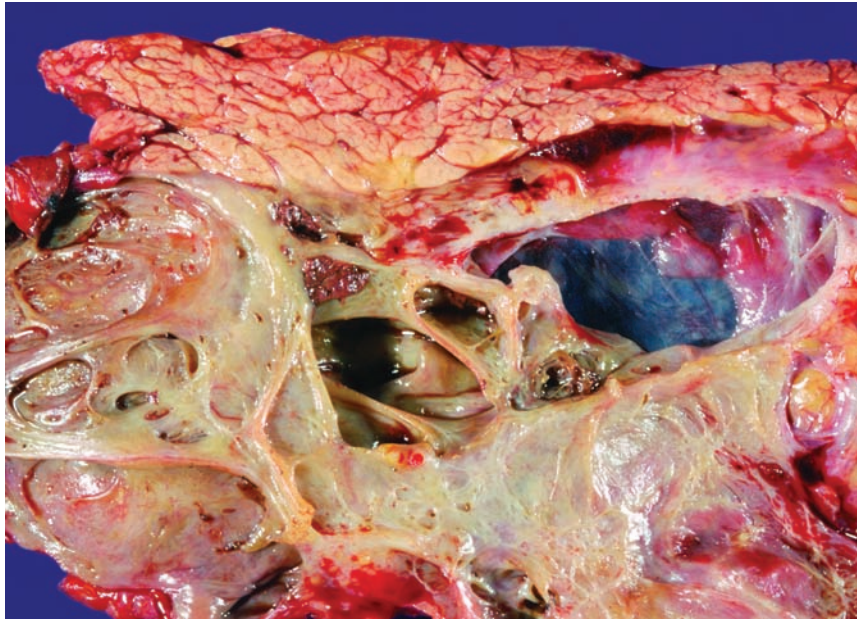
Figure 7.4 — Lymphangioma. This large cystic mass was filled with watery straw-colored fluid. The cysts have a smooth lining and thin walls. Oligocystic serous cystadenomas can have a similar appearance; the distinction between these lesions is made histologically. Serous cystadenomas are lined by cuboidal epithelial cells, while lymphangiomas are lined by flattened endothelial cells.
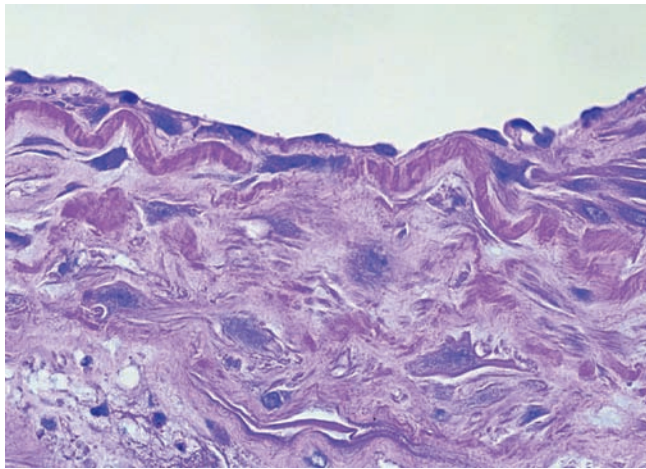
Figure 7.5 — Lymphangioma. The cysts (top) are lined by a flat layer of endothelial cells. If present, stromal lymphoid nests can provide a clue to the diagnosis. The epithelial cells lining serous cystadenomas can sometimes be focally flattened. These two entities can be distinguished by immunolabeling. The endothelial differentiation of lymphangiomas can be confirmed by immunolabeling for CD31, while serous neoplasms will express cytokeratin. (Hematoxylin and eosin stain, high power)
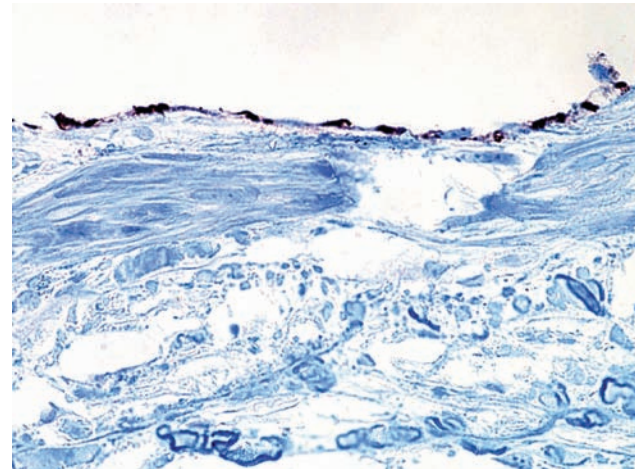
Figure 7.6 — Lymphangioma. Immunolabeling for CD31 highlights the lymphatic endothelial cells. Lymphangiomas can be distinguished from hemangiomas by immunolabeling for D2-40, CD31, and CD34. Lymphangiomas express CD31 and D2-40, while hemangiomas express CD34. (Immunolabeling for CD31, high power)

Paraganglioma

Figure 7.7 — Paraganglioma. Primary paraganglioma of the pancreas is extremely rare and may create diagnostic issues in unsuspected cases. This case displays a hypercellular smear composed of cells with monotonous round, ovoid, or spindle-shaped nuclei, which are bare or surrounded by pale cytoplasm with indistinct borders. Two dense aggregates/fragments of more epithelioid cells with organoid patterns are seen. The larger aggregate has a capillary crossing the center and is surrounded by pale metachromatic matrix. A close differential diagnosis in this case includes a well-differentiated pancreatic endocrine neoplasm and metastatic sarcomas (such as gastrointestinal stromal tumor). (Diff Quik stain, low power)
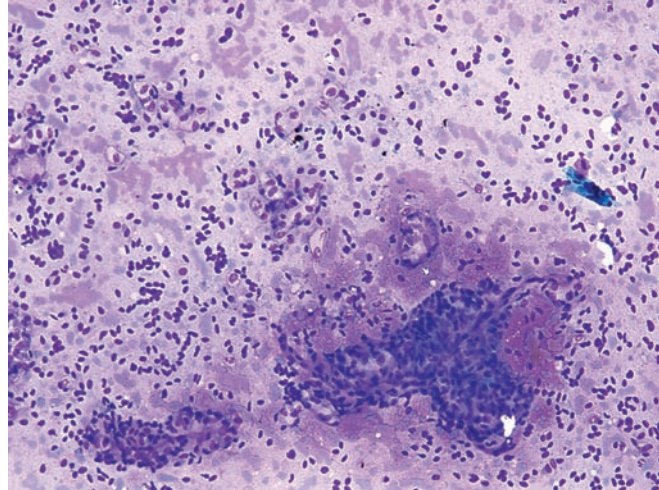
Figure 7.8 — Paraganglioma. The biphasic appearance of the tumor is best seen here with fragments of neoplastic cells with granular, densely staining cytoplasm in a background of bare nuclei and cells with pale cytoplasm. This pattern resembles the "zellballen" seen in tissue sections of this neoplasm. (Diff Quik stain, low power)
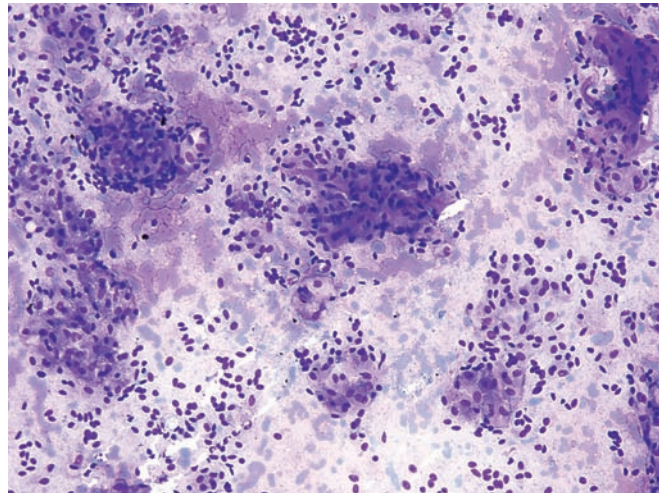
Figure 7.9 — Paraganglioma. This hypercellular smear displays monotonous neoplastic cells with oval to spindled nuclei dispersed in a single-cell discohesive pattern. Neoplastic cells show small nucleoli with a densely granular smear background (Papanicolaou stain, medium power)
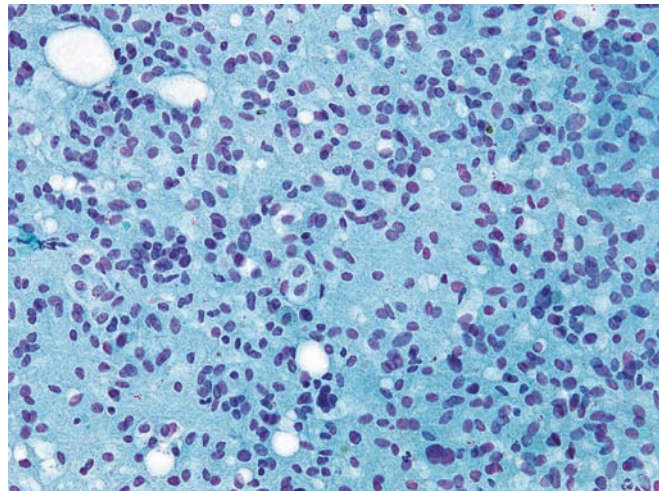
Paraganglioma
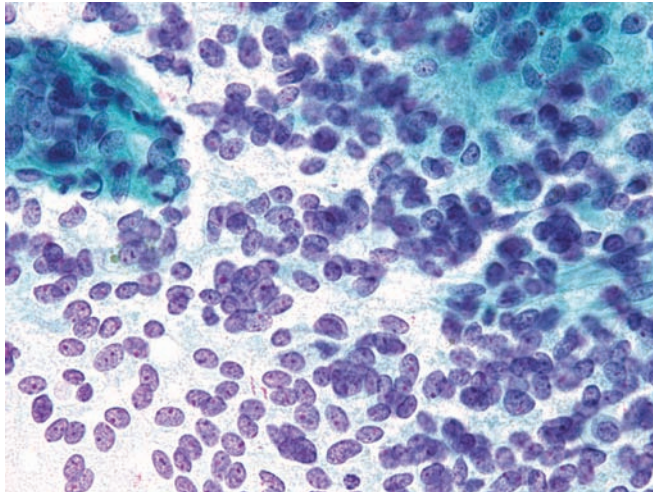
Figure 7.10 — Paraganglioma. Hypercellular smear composed of neoplastic cells with bare uniform plump spindled or ovoid nuclei and ill-defined cytoplasm is highlighted in this photograph. Several nuclei display small red nucleoli. Focal rosette-like arrangements are seen. (Papanicolaou stain, high power)
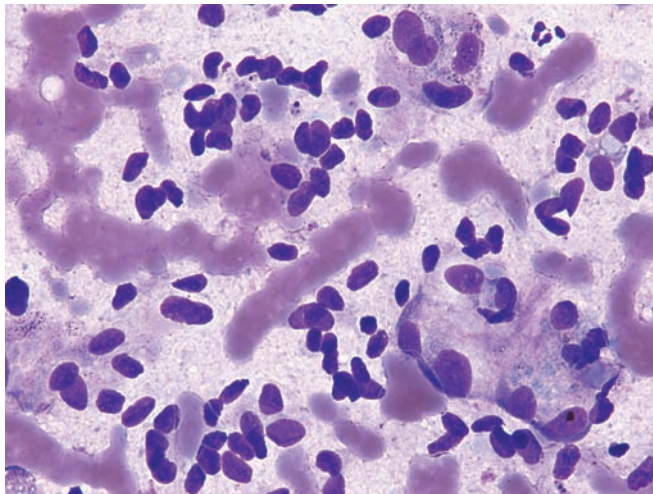
Figure 7.11 — Paraganglioma. A large population of bare, spindled nuclei is highlighted here with bland chromatin patterns and small nucleoli. Some cells have plump ovoid nuclei with abundant pale and wispy cytoplasm (Diff Quik stain, high power)
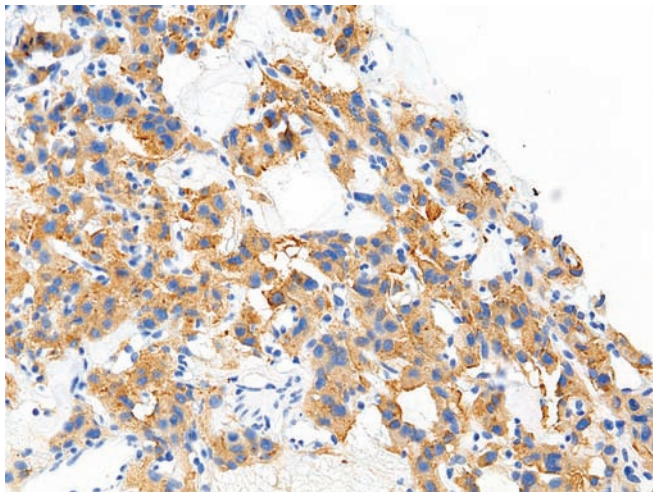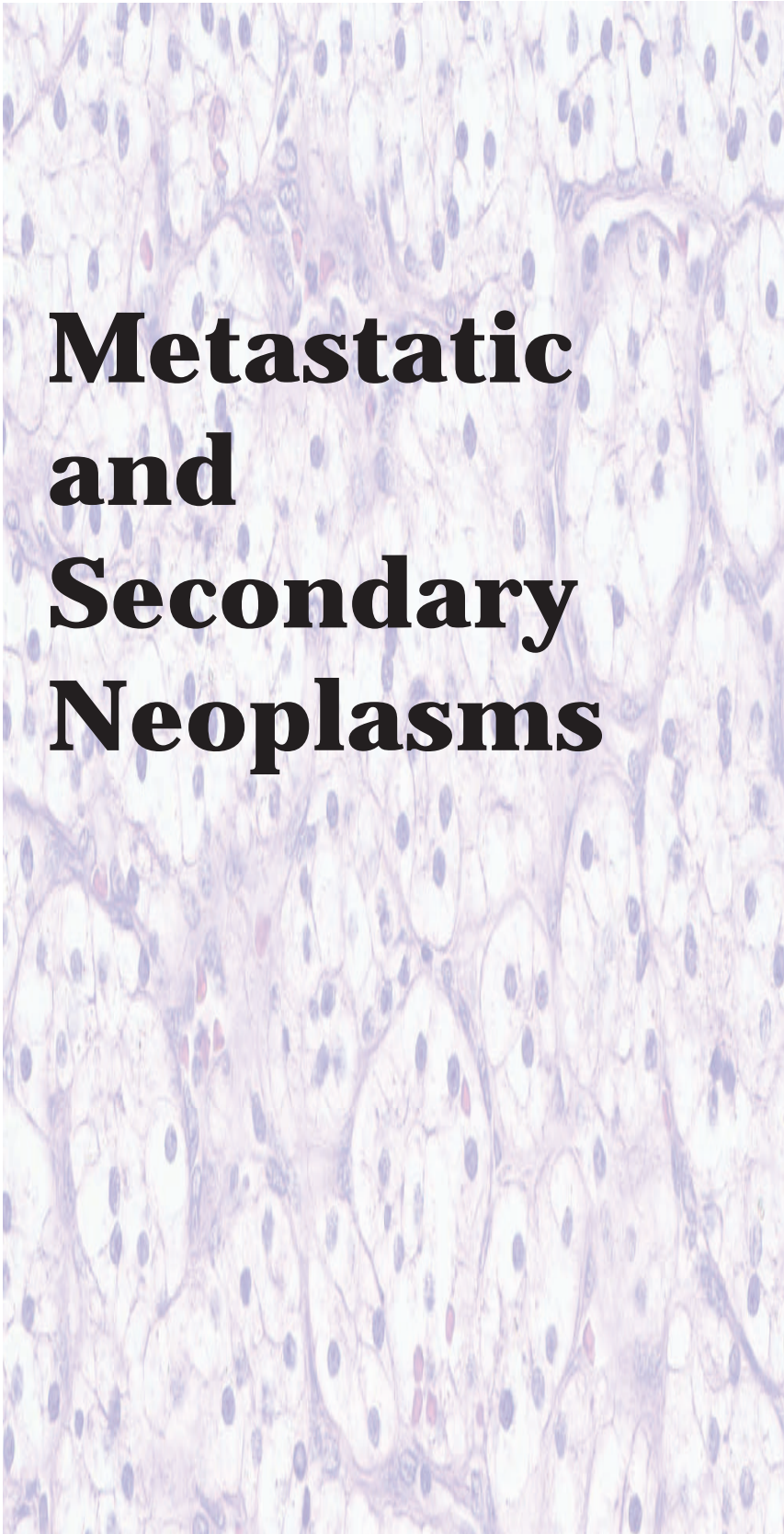
Figure 7.12 — Paraganglioma – (cell block section). Neoplastic cells are strongly reactive with antibodies to synaptophysin. The cytoplasm of the cells is more clearly demonstrated here than in the Diff Quik and Papanicolaou stains. (Immunolabeling with synaptophysin, low power)

Metastatic and Secondary Neoplasms
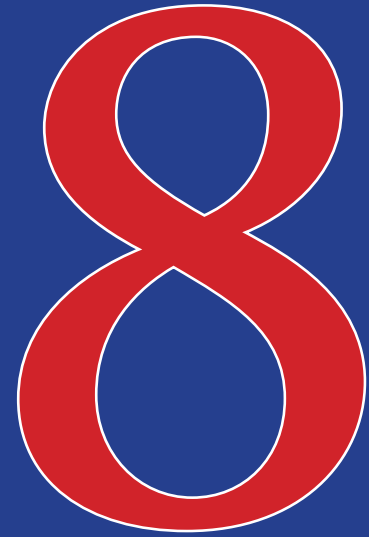
8

Carcinomas Metastatic to the Pancreas
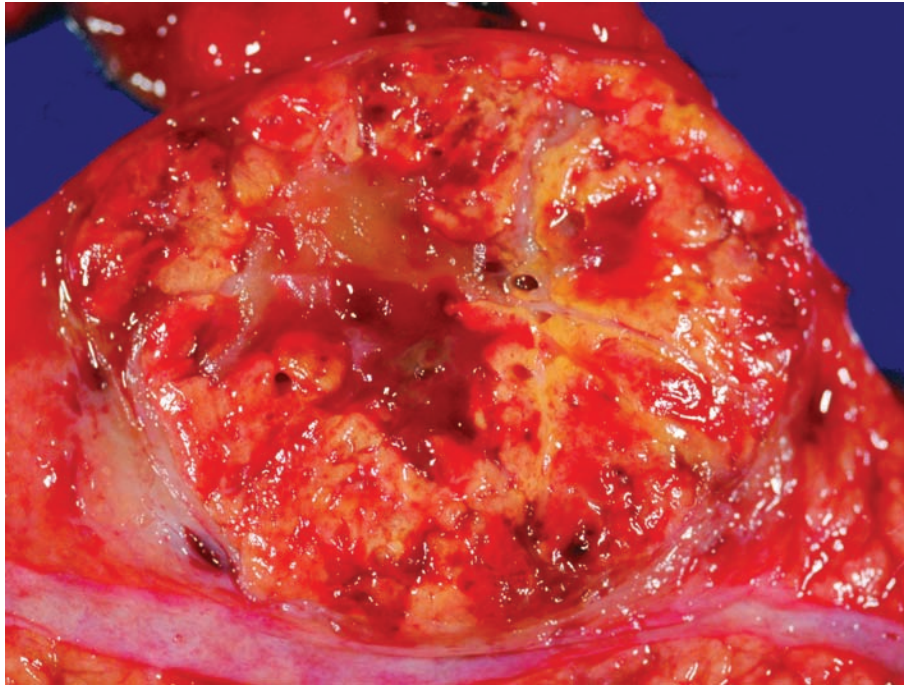
Figure 8.1 — Metastatic renal cell carcinoma. This bright yellow-orange mass distorts the pancreatic duct, which runs along the bottom of the image. Malignancies that metastasize to the pancreas include melanoma as well as carcinomas of the lung, kidney, breast, and colon. Metastases to the pancreas should be considered in the differential diagnosis of neoplasms with morphologic appearances that are not typical of a pancreatic primary.

Figure 8.2 — Metastatic renal cell carcinoma. This richly vascular neoplasm is composed of large polygonal cells with abundant clear cytoplasm. Well-differentiated pancreatic endocrine neoplasm (strongly and diffusely chromogranin and synaptophysin positive) and solid serous neoplasm (uniform small round nuclei, abundant intracytoplasmic glycogen) should be considered in the differential diagnosis. (Hematoxylin and eosin stain, high power)
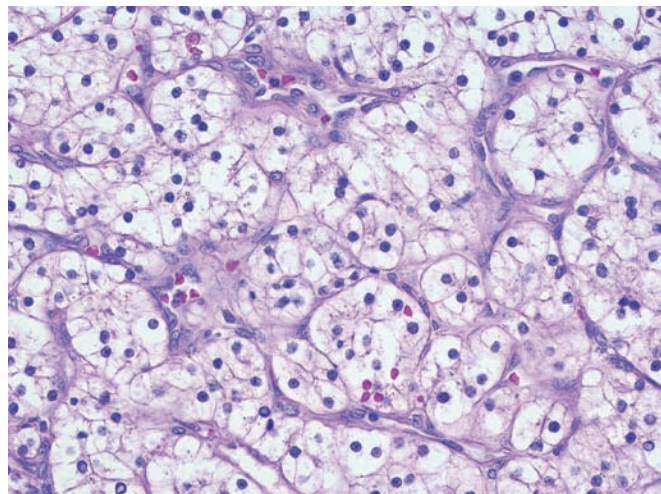
Carcinomas Metastatic to the Pancreas
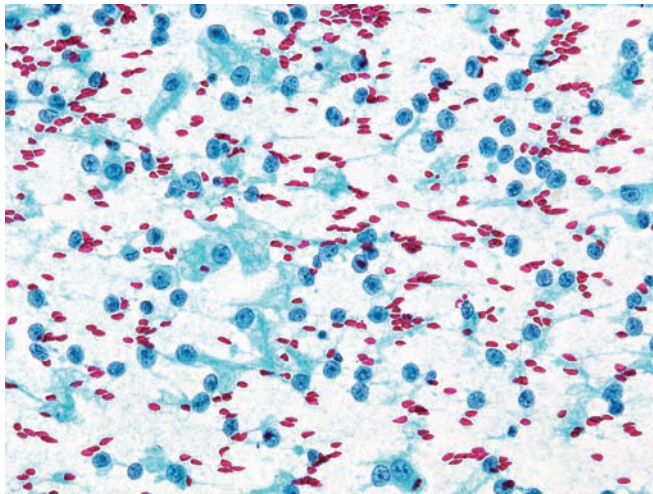
Figure 8.3 — Metastatic renal cell carcinoma. A dispersed population of large round nuclei with prominent nucleoli is noted. Most nuclei have lost their cytoplasm. Clear cell neoplasms tend to lose their delicate cytoplasm when smeared onto glass slides. Although these findings alone are not diagnostic, in patients with suspected or documented renal tumor they most likely represent metastatic renal cell carcinoma. The other tumor with similar cytomorphology in the pancreas would be an acinar cell carcinoma. (Papanicolaou stain, medium power)
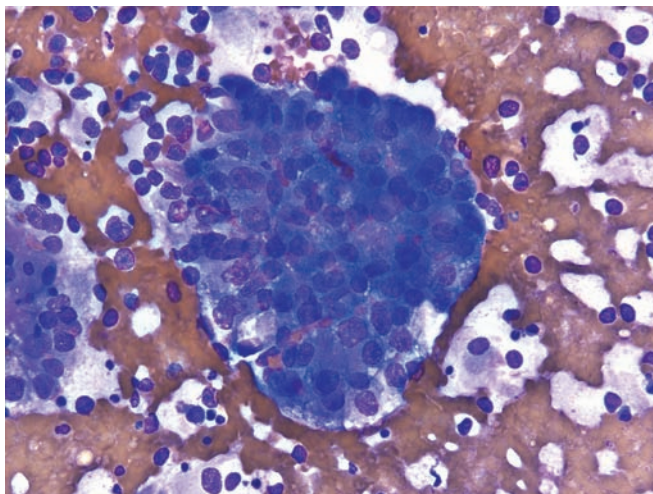
Figure 8.4 — Metastatic renal cell carcinoma. A cellular tissue fragment comprised of cells with large nuclei, prominent nucleoli, and fragile basophilic cytoplasm is present. Few cells show finely vacuolated cytoplasm. Numerous naked nuclei are seen in the smear background. (Diff Quik stain, high power)
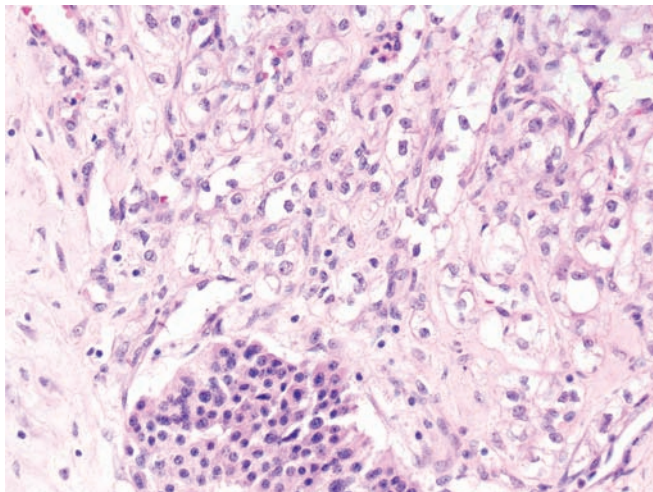
Figure 8.5 — Metastatic renal cell carcinoma (cell block section). Carcinoma with clear cell features is seen adjacent to an uninvolved islet of Langerhans at 6 o'clock. Renal cell carcinoma is well known to cause delayed metastasis to the pancreas and should always be included in the differential diagnosis of clear cell lesions of the pancreas. (Hematoxylin and eosin stain, low power)

Carcinomas Metastatic to the Pancreas

Figure 8.6 — Metastatic squamous cell carcinoma (laryngeal primary). Seen here are several neoplastic keratinized squamous cells in a background of tumor necrosis and inflammatory cells. Note the sharply angulated hyperchromatic nucleus of the neoplastic cell (12 o' clock). The differential diagnosis would include a primary adenosquamous cell carcinoma of the pancreas. (Papanicolaou stain, low power)
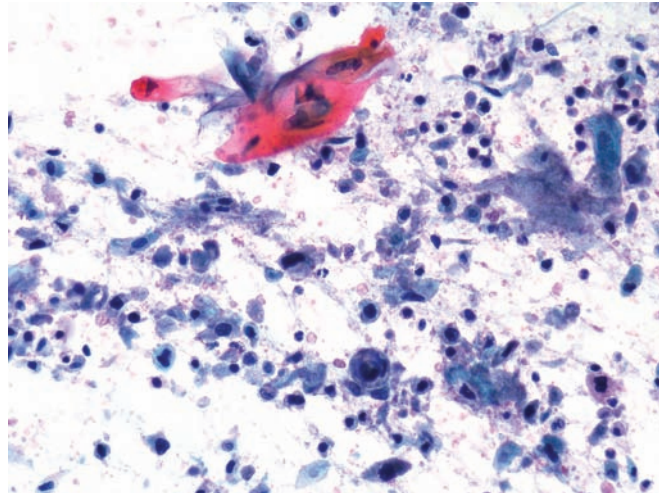
Figure 8.7 — Metastatic small cell carcinoma (lung primary). This cellular specimen is composed of monotonous small neoplastic cells singly and in tight aggregates. Most nuclei appear to be naked. Nuclear molding, at times forming columns, is seen. In an adult patient, the differential diagnoses include non-Hodgkin lymphoma, primary small cell carcinoma and metastatic small cell carcinoma. The presence of nuclear molding excludes lymphoma; but in air-dried material artifactual molding may occur. Papanicolaou-stained material is better for determining nuclear molding and observing neuroendocrine chromatin pattern. Immunolabeling with antibodies to TTF-1 may be helpful in supporting a lung origin (however, a large percentage of primary small cell carcinomas of the pancreas may immunoexpress TTF-1 as well). (Diff Quik stain, medium power)
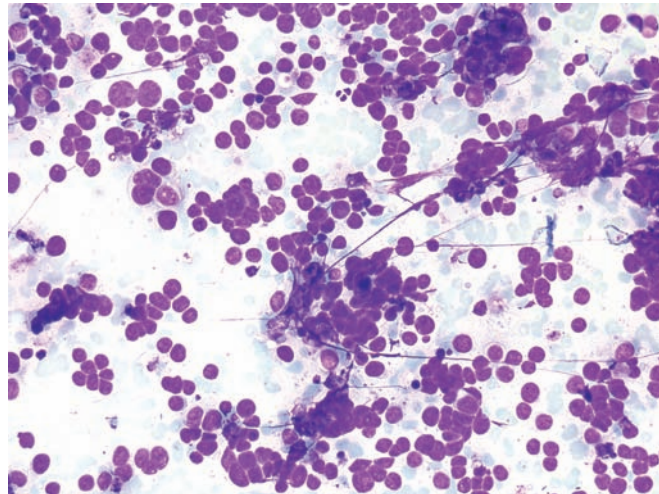
Carcinomas Metastatic to the Pancreas
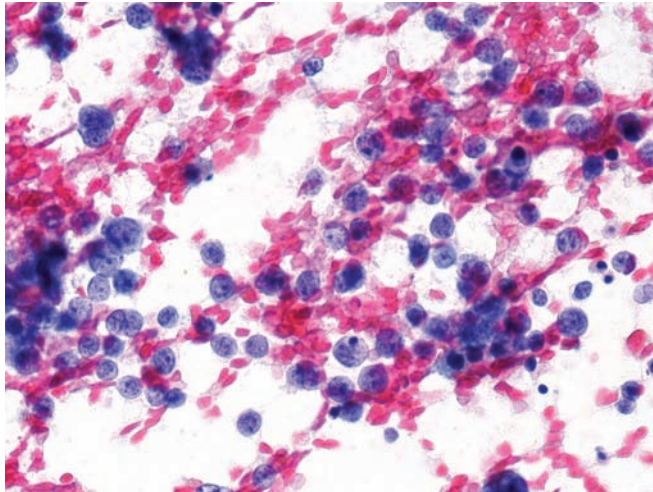
Figure 8.8 — Metastatic small cell carcinoma (lung primary). Predominantly bare nuclei are highlighted here. Note the finely stippled chromatin pattern and inconspicuous nucleoli. A few karyorrhectic nuclei are seen as well. (Papanicolaou stain, high power)
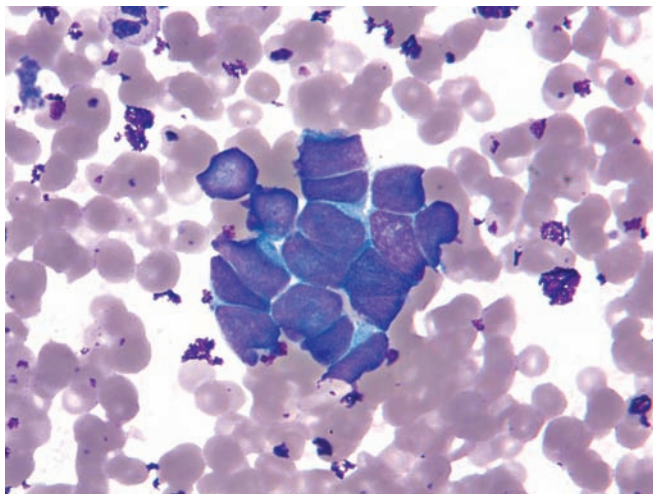
Figure 8.9 — Metastatic Merkel cell carcinoma. Neoplastic cells with extremely high N/C ratios are noted. The pleomorphic nuclei display tight nuclear molding. A cytomorphologic distinction with a primary or metastatic small cell carcinoma (such as from the lung) cannot be made in such cases. (Diff Quik stain, high power)
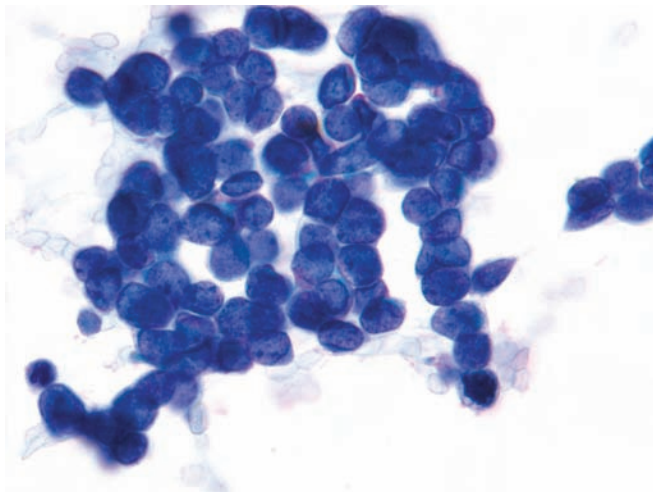
Figure 8.10 — Metastatic Merkel cell carcinoma. This shows relatively small neoplastic cells (compared with a neutrophil at 7 o'clock) with extremely high N/C ratios, evenly distributed, finely granular chromatin with occasional chromocenters, forming columns and rosette-like structures. Cytomorphology is indistinguishable from a small cell carcinoma. Both tumors react to neuroendocrine markers, but CK20 is positive (in a "dot-like" pattern) and CK7 is negative in a Merkel cell carcinoma. Small cell carcinoma typically shows the reverse reaction with CK7 and CK20. (Papanicolaou stain, high power)

Sarcomas Metastatic to the Pancreas

Figure 8.11 — Metastatic gastrointestinal stromal tumor. This cellular specimen is composed of thick groups and single atypical spindled cells. Individual nuclei have a slender elongated appearance "Cuban cigars" with undulating borders—"nerve sheath-like." Few cells are embedded in thick myxoid stroma. Differential diagnosis will include other spindle cell lesions such as of neural and smooth muscle origin. (Diff Quik stain, low power)
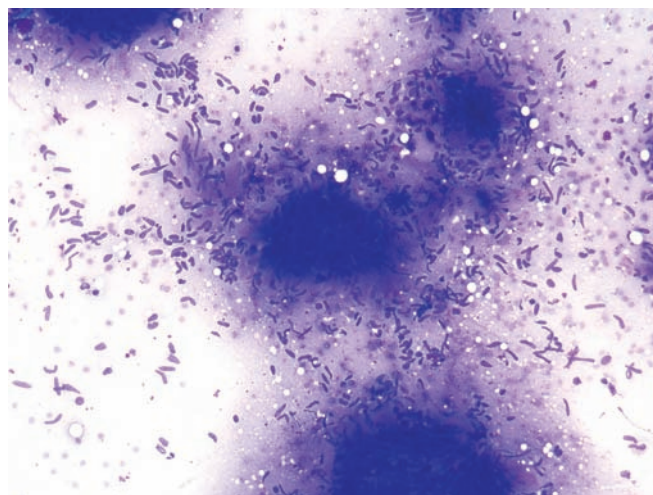
Figure 8.12 — Metastatic gastrointestinal stromal tumor. Mixture of thick, elongated (spindle-shaped), and ovoid nuclei in a myxomatous and metachromatic background dominate the field. Note the varying shapes (straight to curved) of the elongated nuclei. (Diff Quik stain, high power)
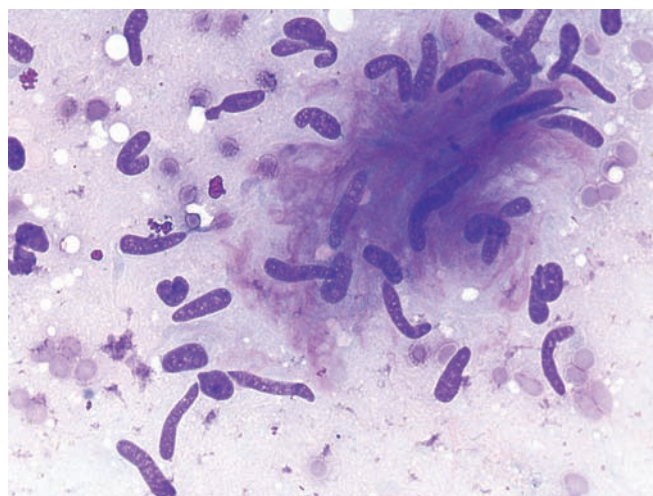
Figure 8.13 — Metastatic gastrointestinal stromal tumor. Similar to the previous figure, this hypercellular tissue fragment is comprised of atypical spindle cells in a collagenous background. The elongated nuclei display focal palisading resembling a nerve sheath tumor. (Papanicolaou stain, high power)
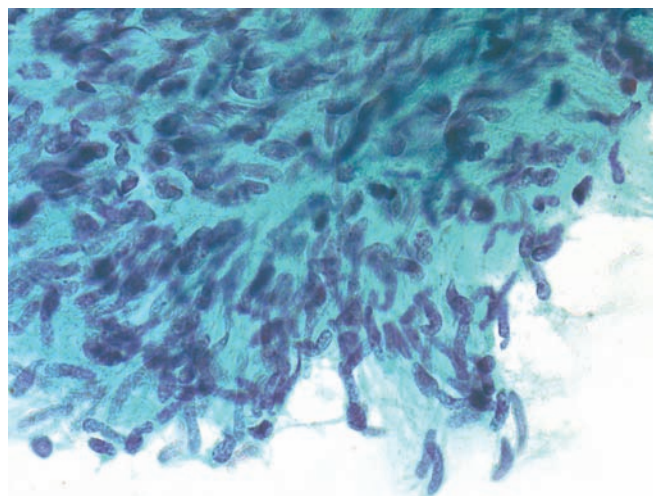
Sarcomas Metastatic to the Pancreas
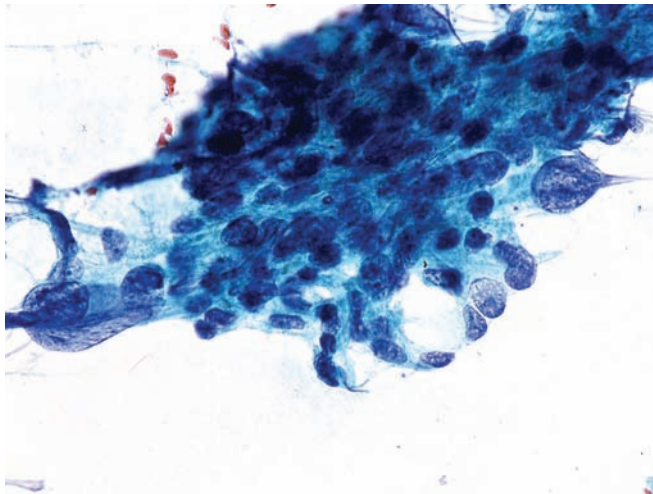
Figure 8.14 — Metastatic high-grade leiomyosarcoma. The neoplasm forms a cellular tissue fragment with both highly pleomorphic epithelioid and spindle cell features. These cells have lost all phenotypic resemblance to smooth muscle cells. A diagnosis of leiomyosarcoma can only be made in this case in light of the previous history of this sarcoma and immunoreaction to smooth muscle markers. (Papanicolaou stain, high power)
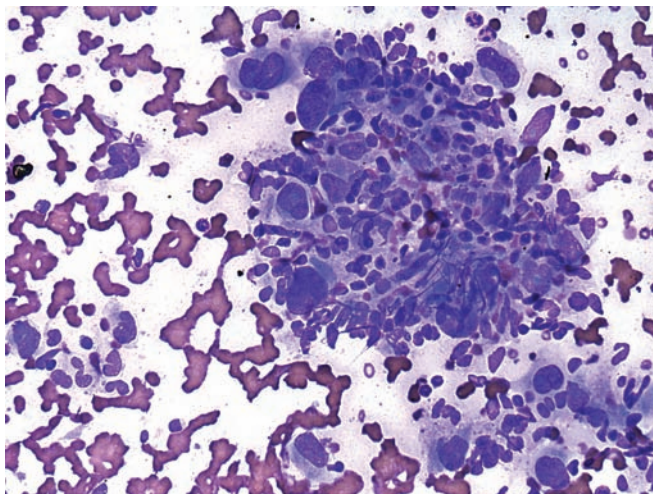
Figure 8.15 — Metastatic malignant fibrous histiocytoma. Malignant cells are present with pleomorphic markedly enlarged single, double, or multiple nuclei. Numerous spindled cells are seen as well. The cytomorphologic appearance is nonspecific, and the diagnosis is dependent on the patient's previous history of this sarcoma. (Diff Quik stain, high power)
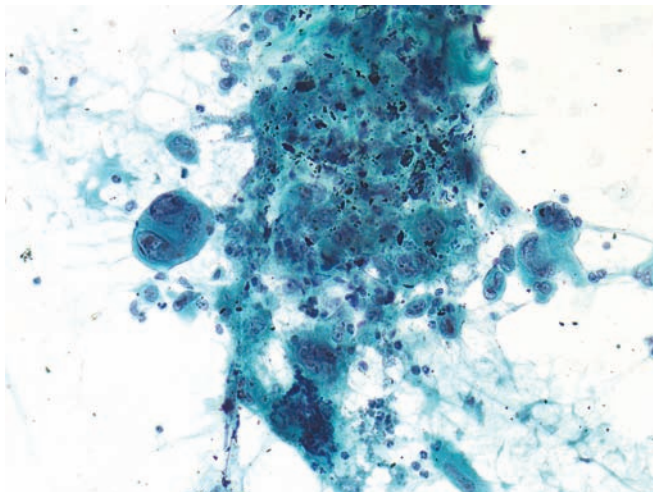
Figure 8.16 — Metastatic malignant fibrous histiocytoma. Note the multinucleated giant cells with pleomorphic nuclei and macronucleoli. Once again, an accurate diagnosis requires knowledge of the patient's previous history. (Papanicolaou stain, high power)

Sarcomas Metastatic to the Pancreas

Figure 8.17 — Metastatic embryonal rhabdomyosacoma. Primitive small round blue cells are present with hyperchromatic nuclei, inconspicuous nucleoli, and extremely high N/C ratios. The history of a previous known embryonal rhabdomyosacoma is extremely valuable in this case. Differential diagnosis includes other small, round blue cell tumors, pancreatic endocrine neoplasm, and malignant non-Hodgkin lymphoma. (Papanicolaou stain, high power)
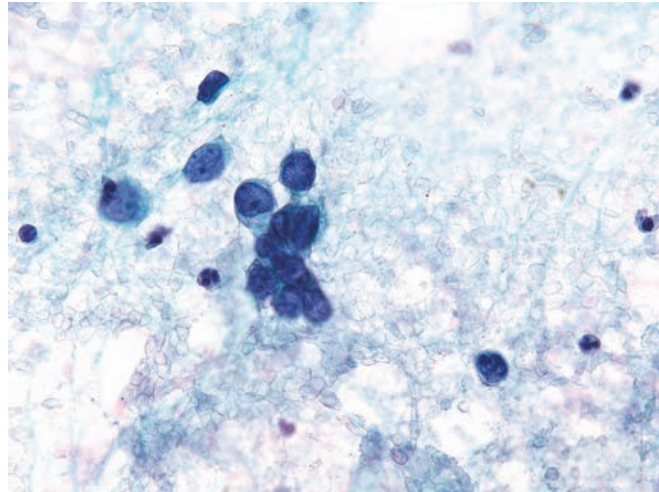
Other Neoplasms Metastatic to the Pancreas
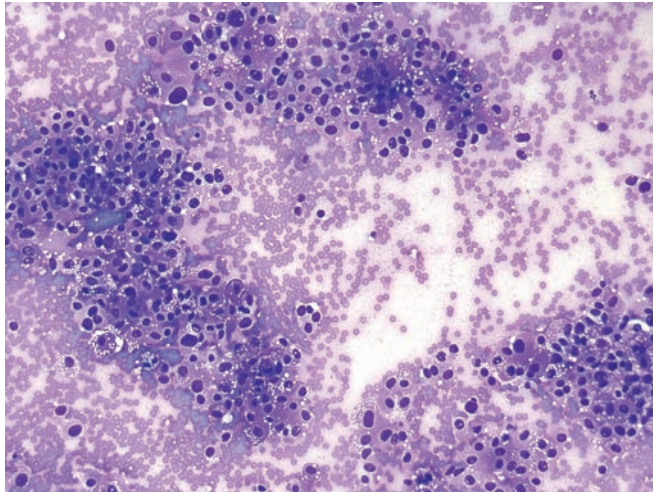
Figure 8.18 — Metastatic pheochromocytoma. Loose aggregates of neoplastic cells are present with varying sized nuclei and amphophilic cytoplasm. The majority of the cells contain well-formed multiple small vacuoles. A few multinucleated cells are also present. Differential diagnosis includes a well-differentiated pancreatic endocrine neoplasm, acinar cell carcinoma, and metastasis from an adrenal cortical carcinoma, renal cell carcinoma, or malignant melanoma. (Diff Quik stain, low power)
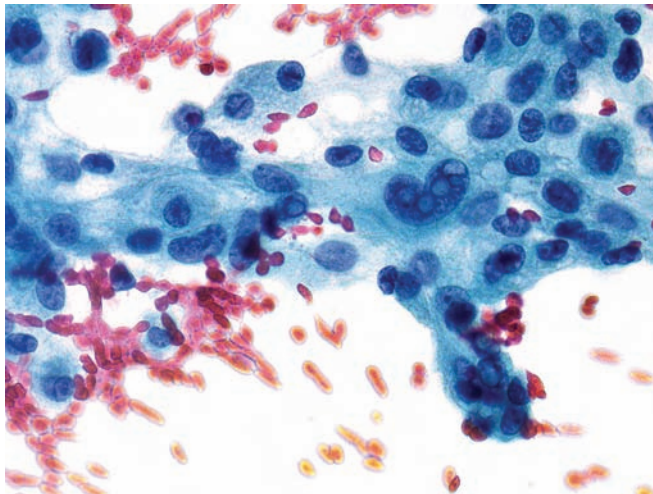
Figure 8.19 — Metastatic pheochromocytoma. A tissue fragment of loosely arranged neoplastic cells is present. There is moderate variation in nuclear size and shape. Nuclei of several cells has single or multiple intranuclear pseudoinclusions. The majority of the neoplastic cells have multiple small vacuoles which are more clearly seen in the Diff-Quik stain. All neoplasms mentioned in the differential diagnosis previously may have intranuclear pseudoinclusions. (Papanicolaou stain, high power)
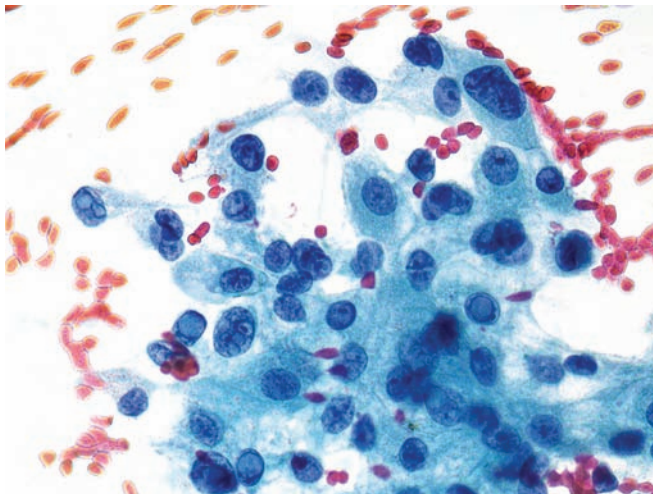
Figure 8.20 — Metastatic pheochromocytoma. The cytomorphologic features are similar to those seen in the previous figure. Frequent large single or multiple, intranuclear pseudoinclusions are present. The cells have delicate wispy cytoplasm with some nuclei displaying prominent nucleoli. Most nuclei are round or ovoid, with the exception of one large cell with a markedly enlarged, irregular shaped, hyperchromatic nucleus. (Papanicolaou stain, high power)

Other Neoplasms Metastatic to the Pancreas
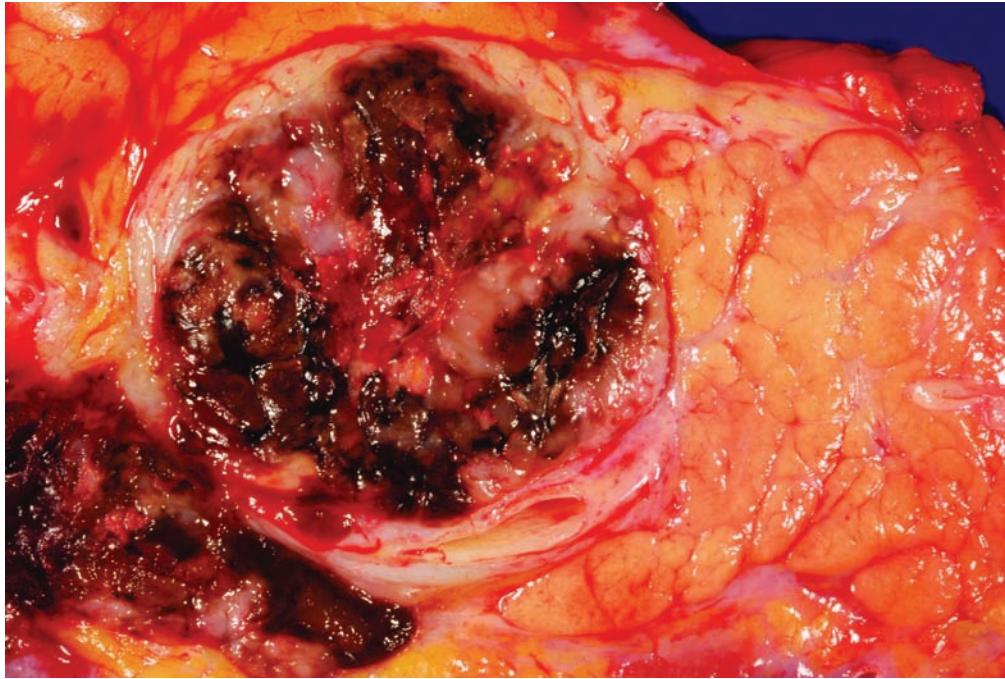
Figure 8.21 — **Metastatic melanoma.** In this case several nodules were noted, and on cross section many were black-brown as is typical of melanoma. Rarely endocrine neoplasms of the pancreas can have a black appearance, most likely from the accumulation of lipofuscin.

Figure 8.22 — **Metastatic melanoma.** The metastasis forms a well-demarcated mass (left). The neoplastic cells are "big pink cells" with enlarged pleomorphic nuclei, which contain single prominent nucleoli. The nucleoli in acinar cell carcinomas can also be prominent, and, in the absence of pigment, the distinction between melanoma and acinar cell carcinoma often has to be made immunohistochemically. (Hematoxylin and eosin, high power)
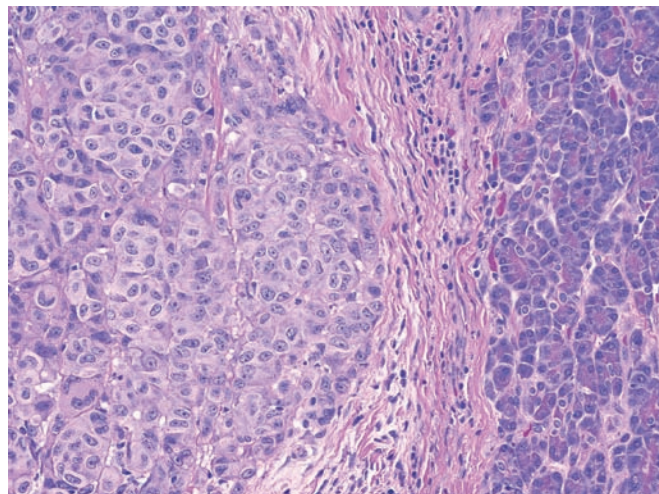
Other Neoplasms Metastatic to the Pancreas
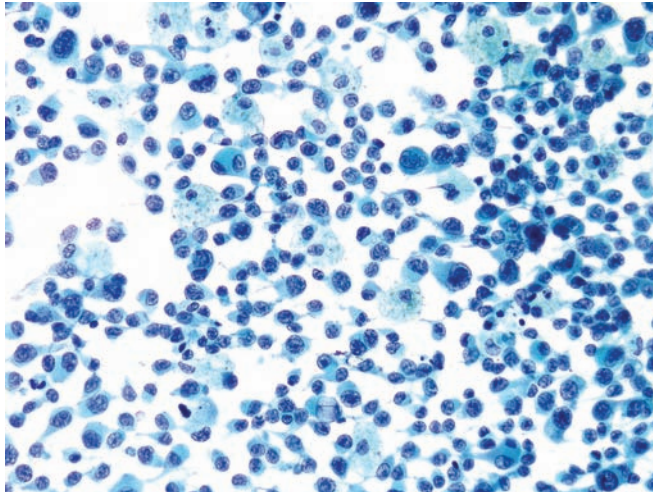
Figure 8.23 — Metastatic melanoma. An almost entirely single-cell population composed of neoplastic cells with eccentrically located, single or double nuclei is seen. The amount of cytoplasm varies, but one common feature is unipolar tailing out of the cytoplasm. This feature, however, can be seen in poorly differentiated or anaplastic carcinomas and in nonepithelial neoplasms, such as anaplastic lymphoma, rhabdomyosarcoma, and rhabdoid tumor. Binucleated cells with nuclei which are peripherally located and opposite each other ("bug-eye") have been described in melanomas. Although this feature is more commonly seen in melanomas, it is not specific and can be seen in other poorly differentiated malignant neoplasms. (Papanicolaou stain, low power)
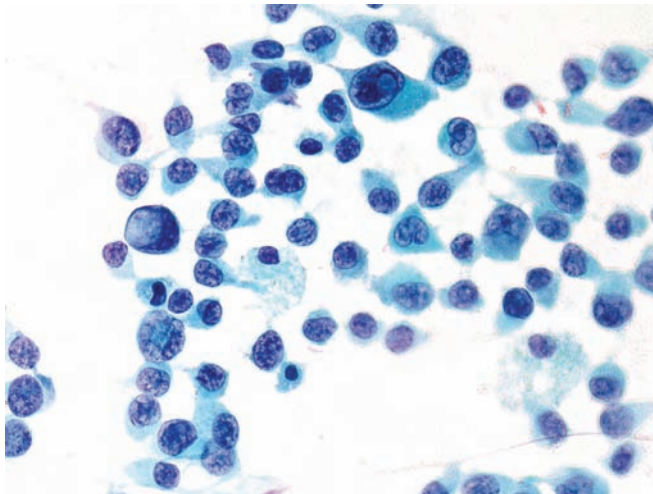
Figure 8.24 — Metastatic melanoma. The neoplastic cells are similar to those seen in the previous figure. They are pleomorphic with varying N/C ratios and occasional tapering cytoplasmic tails. Several cells have markedly enlarged nuclei containing intranuclear pseudoinclusions. (Papanicolaou stain, high power)
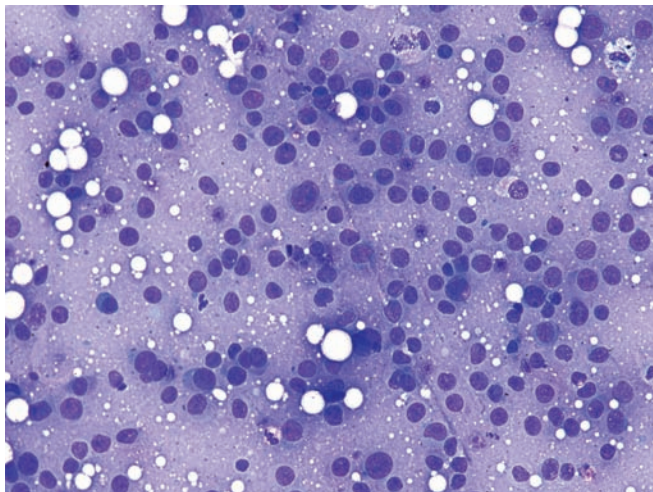
Figure 8.25 — Metastatic melanoma. Single neoplastic cells with large round or ovoid nuclei, prominent nucleoli and ill-defined cytoplasm are present. Differential diagnosis in this case would include a non-Hodgkin lymphoma. (Diff Quik stain, medium power)

Other Neoplasms Metastatic to the Pancreas

Figure 8.26 — Metastatic melanoma. Under high power, in addition to the single neoplastic cells there are two cohesive tumor cell groups, which appear to be tissue fragments. Most neoplastic cells have prominent nucleoli. The differential diagnosis includes poorly-differentiated ductal adenocarcinoma and an acinar cell carcinoma. (Diff Quik stain, high power)
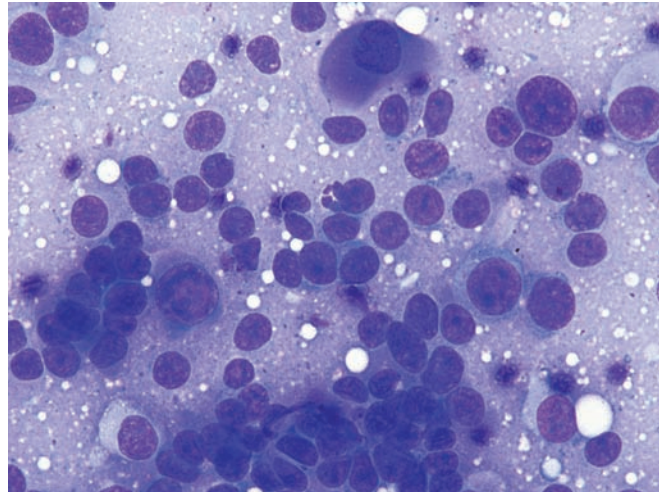
Figure 8.27 — Metastatic melanoma. Note the prominent anisonucleosis and well-formed intra-nuclear pseudoinclusions. One cell has scant brown intracytoplasmic pigment (10 o'clock) suggestive of melanin. (Papanicolaou stain, high power)
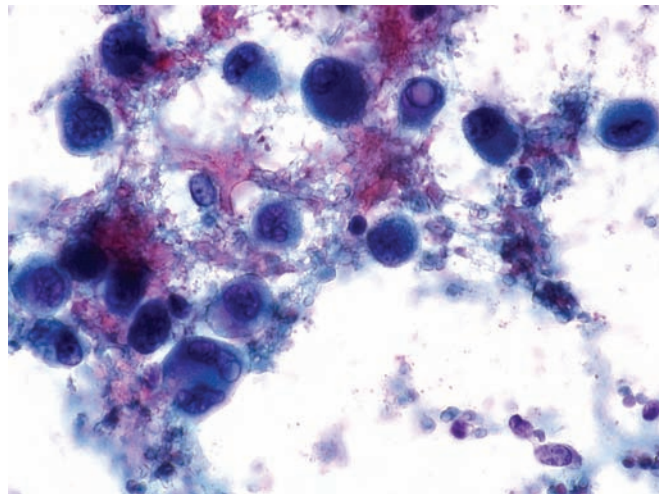
Figure 8.28 — Metastatic melanoma. Pleomorphic cells are present with tail-like elongations of the cyto-plasm. One cell has an intranuclear pseudoinclusion. These features are considered extremely helpful in the cytologic interpretation of melanoma. (Papanicolaou stain, high power)
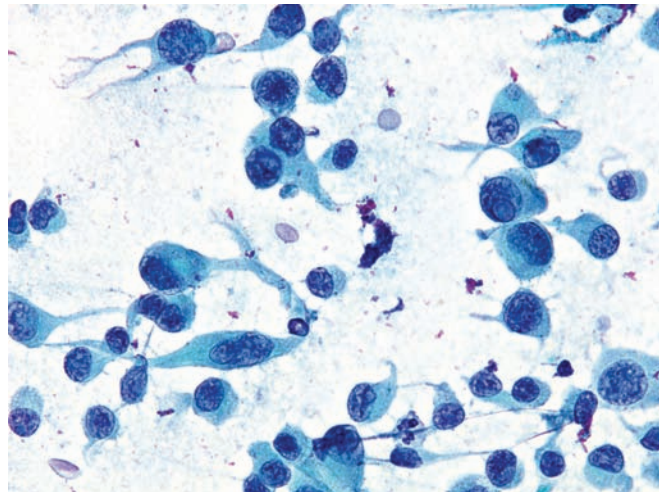
Malignant Lymphomas
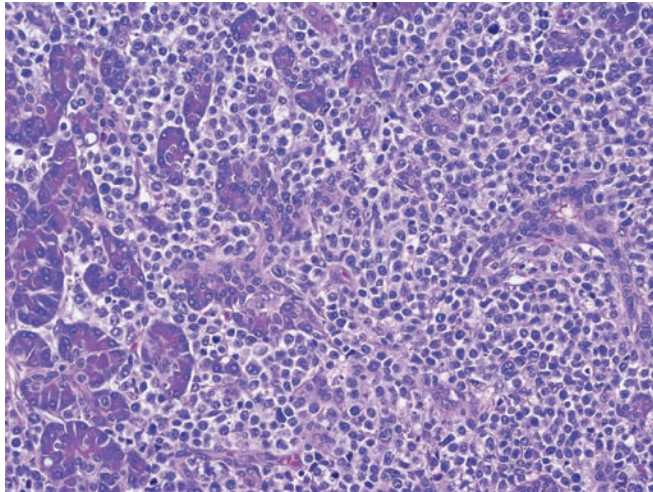
Figure 8.29 — Malignant lymphoma. The noncohesive neoplastic cells intermingle with preexisting ducts and acini. Immunophenotyping established lymphoid differentiation and monoclonality in this case. Lymphoplasmacytic sclerosing pancreatitis should be included in the differential diagnosis, but lymphoplasmacytic sclerosing pancreatitis has a duct-centric and mixed inflammatory cell infiltrate, not the diffuse monomorphic one observed here. (Hematoxylin and eosin, high power)
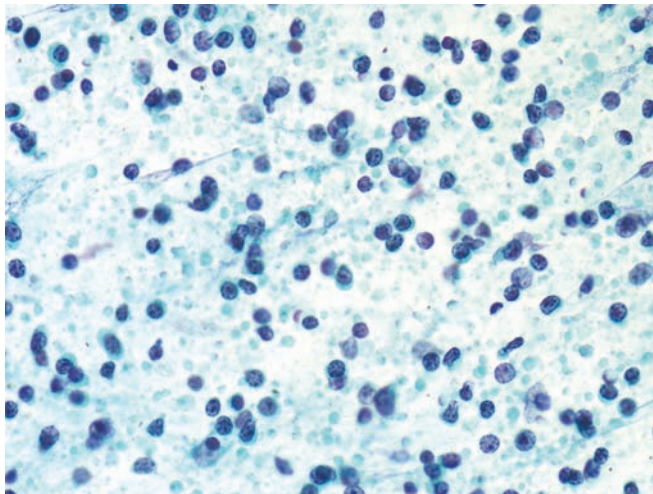
Figure 8.30 — Non-Hodgkin lymphoma. This cellular specimen is composed of single round cells with mostly naked nuclei and conspicuous nucleoli. Numerous so-called "lymphoglandular bodies" are also present. Flow cytometry is needed to establish monoclonality and to determine the specific phenotype of the malignant lymphocytes. On-site interpretation of FNA in such cases ensures specimen adequacy and triage for flow cytometric analysis. Differential diagnosis would include a well-differentiated pancreatic endocrine neoplasm (Papanicolaou stain, low power)
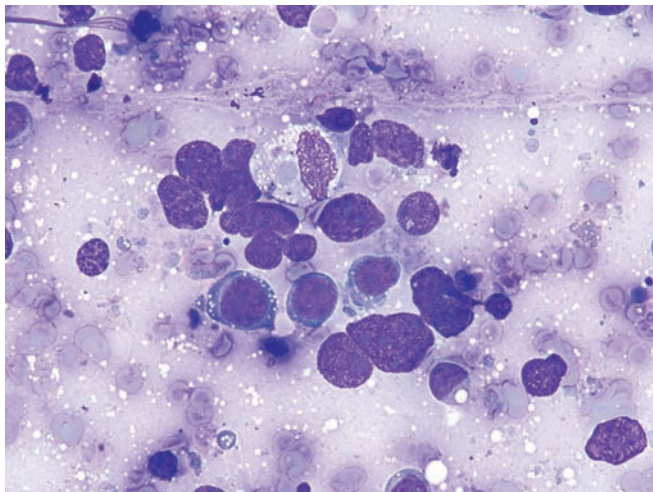
Figure 8.31 — Non-Hodgkin lymphoma. Note the single cells and tight groups of atypical cells with high N/C ratios and prominent nucleoli. Two of the single cells have fine cytoplasmic vacuoles, which suggest Burkitt-type phenotype. However, cytoplasmic vacuoles in an air-dried, Diff Quik stained smear can be artifactual and should be interpreted with caution. (Diff Quik stain, high power)

Malignant Lymphomas

Figure 8.32 — Non-Hodgkin lymphoma. Single cells are present with large bare nuclei, prominent nucleoli, and high N/C ratios. Marked irregularity of the nuclear envelope is clearly seen in most nuclei. Cytomorphology in this case suggests an aggressive phenotype. (Papanicolaou stain, high power)
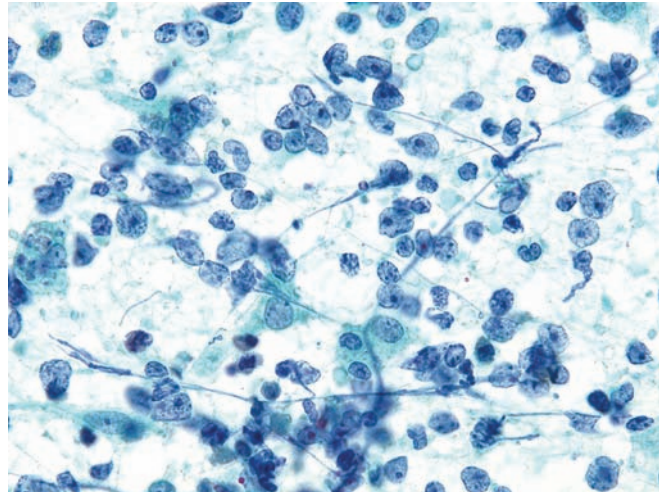
Figure 8.33 — Non-Hodgkin lymphoma. Cellular smear composed of large atypical nuclei with prominent nucleoli in small groups or single forms is seen. Cytoplasm is not visible in most of the cells. Some nuclei have irregular borders. Smear background suggests cellular necrosis. (Papanicolaou stain, high power)
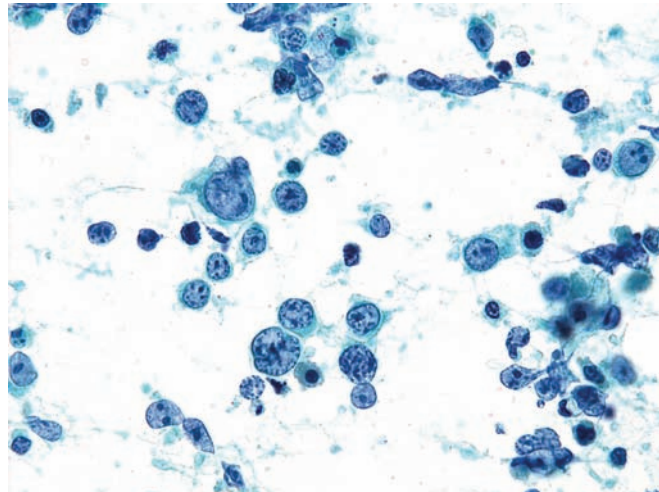
Figure 8.34 — Plasma cell neoplasm. Atypical single cells with eccentrically-placed round nuclei can be seen. Differential diagnosis includes well-differentiated pancreatic endocrine neoplasm. Ancillary techniques, i.e., flow cytometric analysis and immunolabeling, are needed for definitive diagnosis. (Diff Quik stain, high power)
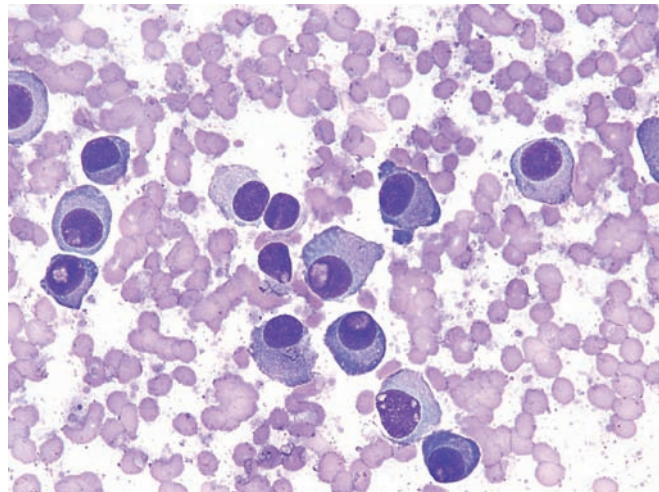
Malignant Lymphomas
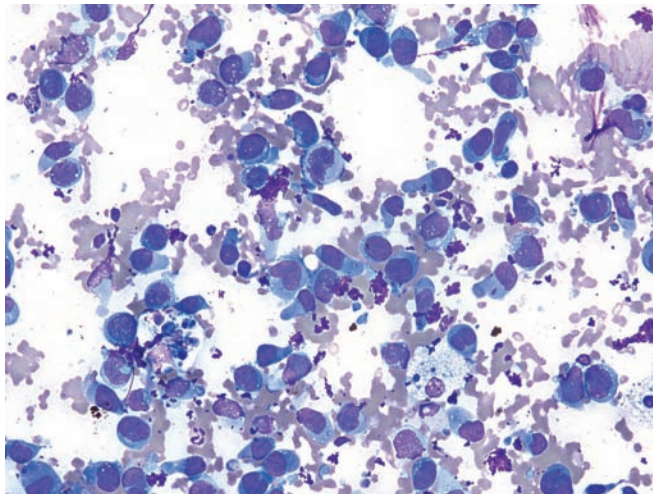
Figure 8.35 — Ki-1 lymphoma (anaplastic lymphoma). Pleomorphic large single cells, most with eccentrically located nuclei, some with high N/C ratio dominate this specimen. Cells are large (compared to a normal lymphocyte) and contain relatively abundant pale blue cytoplasm. Nuclear karyorrhexis and mitoses are also seen. (Diff Quik stain, medium power)
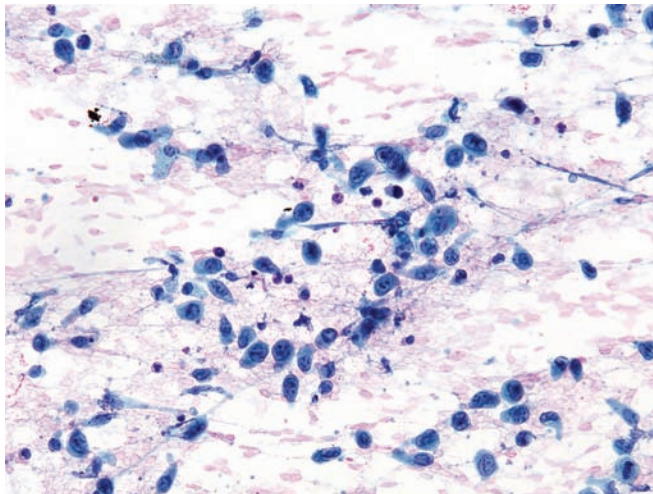
Figure 8.36 — Ki-1 lymphoma (anaplastic lymphoma). Note the pleomorphic cells with varying size and shape of cytoplasm, large round or ovoid nuclei with slightly irregular nuclear borders, and prominent nucleoli. Rare multinucleated cells are also present. Differential diagnosis includes a poorly differentiated carcinoma and malignant melanoma. (Papanicolaou stain, low power)
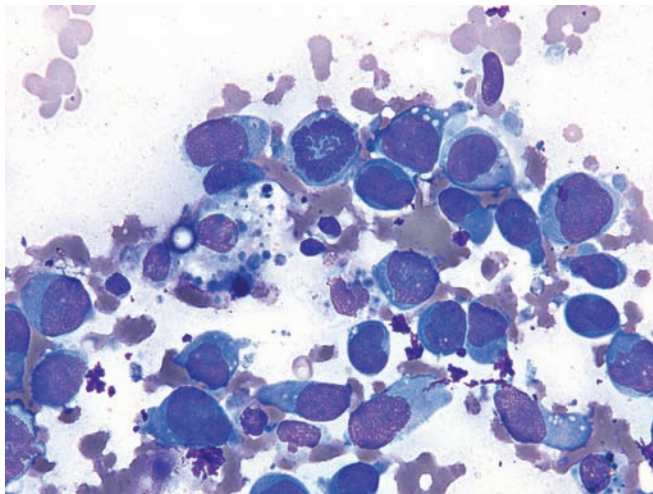
Figure 8.37 — Ki-1 lymphoma (anaplastic lymphoma). The cells have large nuclei with prominent nucleoli. An atypical mitosis is present. Note that in many of the neoplastic cells the cytoplasm is tightly wrapped around the nucleus and extends out from the opposite pole. This is one of the most reliable features of malignancy in cytopathologic material. (Diff Quik stain, high power)

Malignant Lymphomas

Figure 8.38 — Ki-1 lymphoma (anaplastic lymphoma). This high-power view demonstrates the large pleomorphic neoplastic cells. Many of the cells have high N/C ratios, irregular distribution of chromatin, and irregular nuclear borders. The characteristic "horseshoe-shaped" or "wreath-like" nuclear forms were not seen in this case. The cytomorphology seen in this case is diagnostic for an undifferentiated malignant neoplasm. Major differential diagnoses in this location include undifferentiated (anaplastic) carcinoma of the pancreas and metastatic neoplasms (e.g., malignant melanoma, metastatic poorly differentiated carcinoma). (Papanicolaou stain, high power)
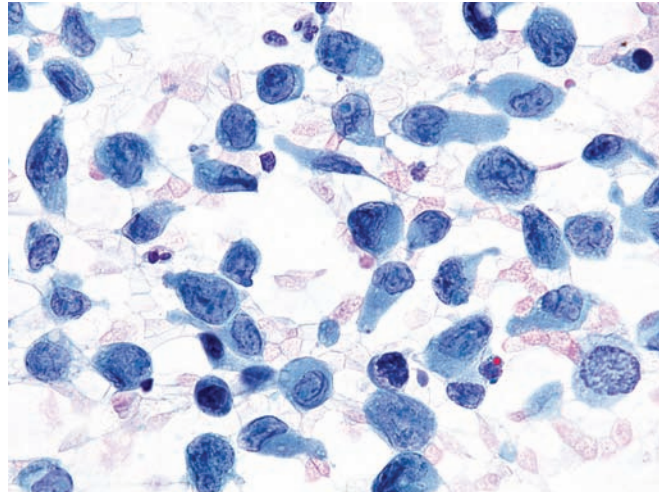
Figure 8.39 — Ki-1 lymphoma (anaplastic lymphoma) (cell block section). Immunoperoxidase labeling for Alk-1 is strongly positive, supporting the diagnosis. (Alk-1 immunolabeling, medium power)
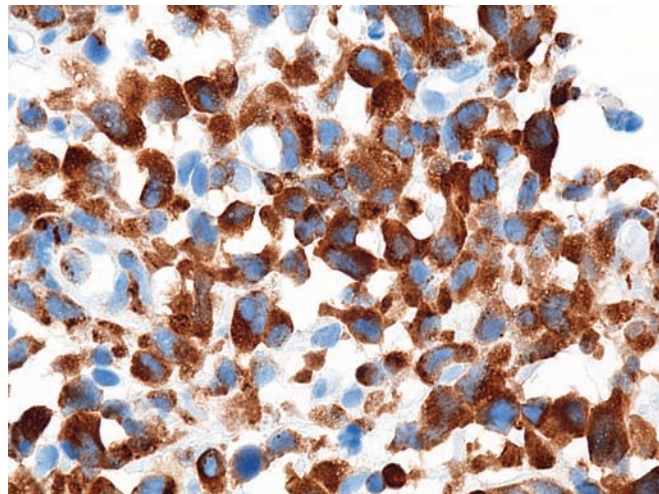
Figure 8.40 — Ki-1 lymphoma (Anaplastic lymphoma) (cell block section). Immunolabeling for CD30 is also strongly positive, which also supports the diagnosis of a Ki-1 lymphoma. (Ki-1 immunolabeling, low power)

Index

ATLAS OF

PANCREATIC CYTOPATHOLOGY

WITH HISTOPATHOLOGIC CORRELATIONS

"Although there are other excellent references available on the topic I do not know of any that will better fulfill the needs of both pathologists who are experienced with pancreatic cytopathology and those who are new to the field."
— *Thomas A. Bonfiglio, M.D., Professor, Pathology and Laboratory Medicine, University of Rochester Medical Center*

This new atlas presents a comprehensive and integrated approach to diagnostic cytopathology that is critical to improving the detection and recognition of pancreatic masses.

Written by recognized experts in the field, *Atlas of Pancreatic Cytopathology with Histopathologic Correlations* includes:

- Extensive high-resolution color images including cytopathologic, histopathologic and radiologic features of pancreatic disease
- Detailed descriptions cover classic features, diagnostic clues and potential pitfalls

This invaluable reference will be a resource for every practitioner involved in the diagnosis of pancreatic disease, including the seasoned cytopathologist, general and surgical pathologists, pathology trainees, and cytotechnologists, in avoiding potential pitfalls and obtaining an accurate diagnosis of this very complex and challenging diagnostic area of medicine.

A Look Inside the Book's Contents

- Normal Pancreas and Fine Needle Aspiration Contaminants
- Radiologic Characteristics of Pancreatic Disease
- Non-neoplastic Lesions
- Solid Neoplasms: Exocrine Pancreas
- Cystic Neoplasms
- Neoplasms: Endocrine Pancreas
- Primary Mesenchymal and Other Rare Neoplasms
- Metastatic and Secondary Neoplasms

Syed Z. Ali, MD, Associate Professor of Pathology and Radiology, Johns Hopkins Hospital in Baltimore, Maryland, USA

Yener S. Erozan, MD, Professor of Pathology, Johns Hopkins Hospital in Baltimore, Maryland, USA

Ralph H. Hruban, MD, Professor of Pathology and Oncology, Johns Hopkins Hospital in Baltimore, Maryland, USA